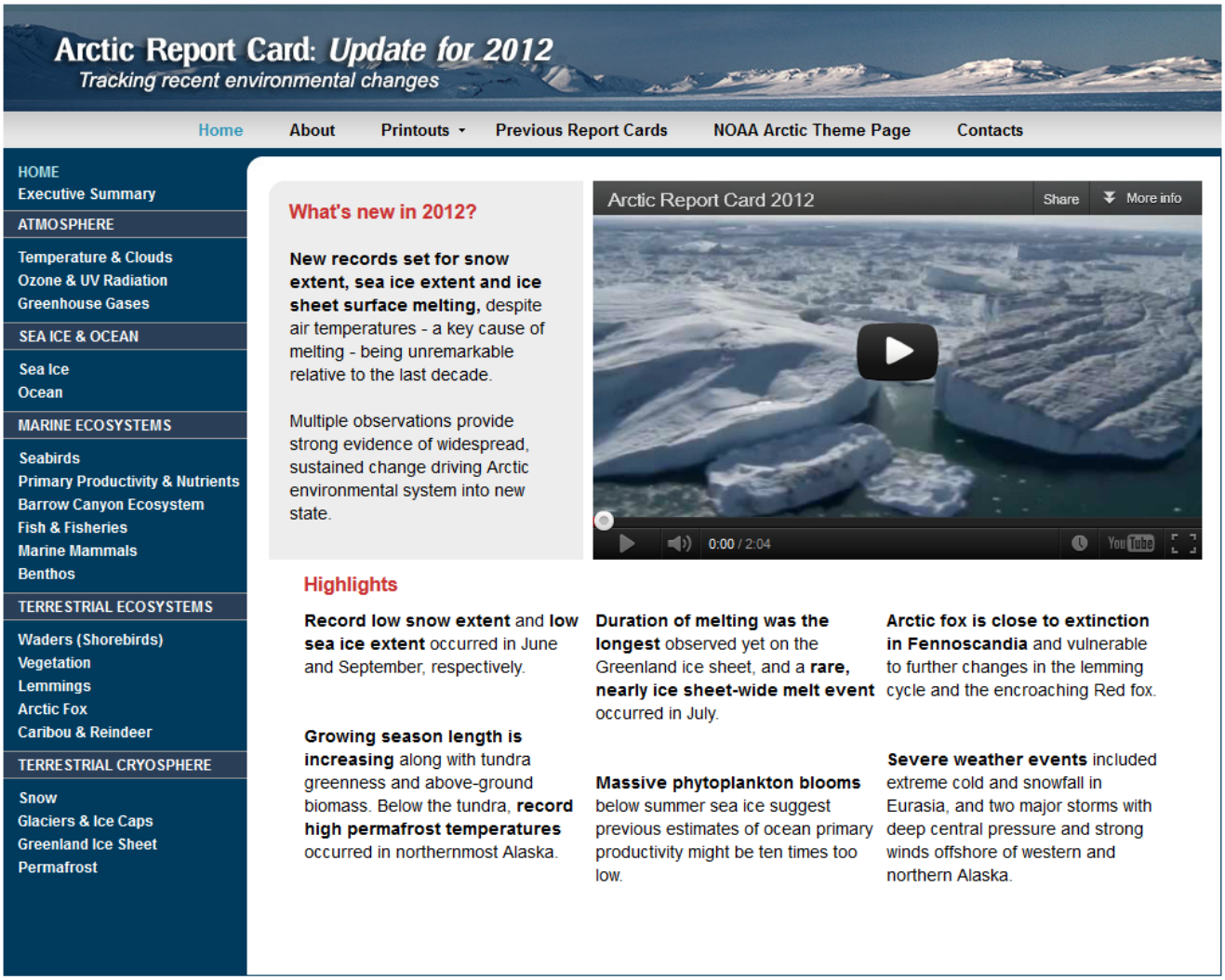

December 2012

www.arctic.noaa.gov/reportcard

Citing the complete report:
Jeffries, M. O., J. A. Richter-Menge and J. E. Overland, Eds., 2012: Arctic Report Card 2012, http://www.arctic.noaa.gov/reportcard.

Citing an essay (example):
Derksen, C. and R. Brown, 2012: Snow [in Arctic Report Card 2012], http://www.arctic.noaa.gov/reportcard.

Table of Contents

Authors and Affiliations

A. Angerbjörn, Department of Zoology, Stockholm University

K.R. Arrigo, Department of Environmental Earth System Science, Stanford University, Stanford, CA, USA

I. Ashik, Arctic and Antarctic Research Institute, St. Petersburg, Russia

C. Ashjian, Woods Hole Oceanographic Institution, Woods Hole, MA, USA

P.S.A. Beck, Woods Hole Research Center, Falmouth, MA, USA

G. Bernhard, Biospherical Instruments, San Diego, CA

D. Berteaux, Département de Biologie, Université du Québec à Rimouski

A. Beszczynska-Moeller, Alfred Wegener Institute, Bremerhaven, Germany

U.S. Bhatt, Geophysical Institute, University of Alaska Fairbanks, Fairbanks, AK, USA

P. Bieniek, Geophysical Institute, University of Alaska Fairbanks, Fairbanks, AK, USA

D. Blok, Center for Permafrost, University of Copenhagen, Copenhagen, Denmark

B. Bluhm, Institute of Marine Science, University of Alaska Fairbanks, Fairbanks, AK, USA

J.E. Box, Byrd Polar Research Center, The Ohio State University, Columbus, OH, USA

R. Brown, Climate Research Division, Environment Canada

S. Brown, Manomet Center for Conservation Sciences, Plymouth, MA, USA

L. Bruhwiler, NOAA, Earth System Research Laboratory (ESRL), Global Monitoring Division, Boulder, CO, USA

D. Burgess, Geological Survey of Canada, National Glaciology Program

T.V. Callaghan, Department of Animal and Plant Sciences, University of Sheffield, Sheffield, UK

J. Cappelen, Danish Meteorological Institute, Copenhagen, Denmark

E. Carmack, Institute of Ocean Sciences, Sidney, Canada

C. Chen, Byrd Polar Research Center, The Ohio State University, Columbus, OH, USA

H.H. Christiansen, Geology Department, University Centre in Svalbard, UNIS, Norway and Institute of Geography and Geology, University of Copenhagen, Denmark

J. Comiso, Cryospheric Sciences Branch, NASA Goddard Space Flight Center, Greenbelt, MD, USA

L. Cooper, University of Maryland Center for Environmental Science, Solomons, MD, USA

D. Decker, Byrd Polar Research Center, The Ohio State University, Columbus, OH, USA

C. Derksen, Climate Research Division, Environment Canada

E. Dlugokencky, NOAA, Earth System Research Laboratory (ESRL), Global Monitoring Division, Boulder, CO, USA

D.S. Drozdov, Earth Cryosphere Institute, Tyumen, Russia

D. Ehrich, Department of Arctic and Marine Biology, University of Tromsø, Norway

H.E. Epstein, Department of Environmental Sciences, University of Virginia, Charlottesville, VA, USA

X. Fettweis, Department of Geography, University of Liège, Liège, Belgium

V. Fioletov, Environment Canada, Toronto, Ontario, Canada

B.C. Forbes, Arctic Centre, University of Lapland, Rovaniemi, Finland

K.E. Frey, Graduate School of Geography, Clark University, Worcester, MA, USA

I. Frolov, Arctic and Antarctic Research Institute, St. Petersburg, Russia

G. Gauthier, Department of Biology, Laval University, Canada

M.-L. Geai, University of Alberta, Department of Earth and Atmospheric Sciences

S. Gerland, Norwegian Polar Institute, Fram Centre,Tromsø Norway

S.J. Goetz, Woods Hole Research Center, Falmouth, MA, USA

J. Grebmeier, University of Maryland Center for Environmental Science, Solomons, MD, USA

J.-U. Grooß, Forschungszentrum Jülich, Jülich, Germany

A. Gunn, 368 Roland Road, Salt Spring Island, BC, Canada V8K 1V1

E. Hanna, Department of Geography, University of Sheffield, UK

J. He, Polar Research Institute of China, Shanghai, People's Republic of China

A. Heikkilä, Finnish Meteorological Institute, Helsinki, Finland

G.H.R. Henry, Department of Geography, University of British Columbia, Vancouver, BC, Canada

A.B. Hollowed, Alaska Fisheries Science Center, National Marine Fisheries Service, National Oceanic and Atmospheric Administration, 7600 Sand Point Way NE, Seattle, WA 98115

R.A. Ims, Department of Arctic and Marine Biology, University of Tromsø, Norway

R. Ingvaldsen, Institute of Marine Research, Bergen, Norway

M. Itoh, Japan Agency for Marine-Earth Science and Technology (JAMSTEC), Yokosuka, Japan

J. Jackson, Applied Physics Laboratory, University of Washington, Seattle, USA

G.J. Jia, Institute of Atmospheric Physics, Chinese Academy of Sciences, Beijing, China

B. Johnsen, Norwegian Radiation Protection Authority, Østerås, Norway

N.J. Karnovsky, Department of Biology, Pomona College, Claremont, CA, USA

Y. Kawaguchi, Japan Agency for Marine-Earth Science and Technology, Tokyo, Japan

M. Kedra, University of Maryland Center for Environmental Science, Solomons, MD, USA

J. Key, Center for Satellite Applications and Research, NOAA/NESDIS, Madison, WI, USA

A.L. Kholodov, Geophysical Institute, University of Alaska Fairbanks, Fairbanks, Alaska, USA

T. Kikuchi, Japan Agency for Marine-Earth Science and Technology (JAMSTEC), Yokosuka, Japan

B.-M. Kim, Korea Polar Research Institute, PO Box 32, Incheon, Korea

S.-J. Kim, Korea Polar Research Institute, PO Box 32, Incheon, Korea

N.T. Knudsen, Department of Geology, Aarhus University, Aarhus, Denmark

T. Koskela, Finnish Meteorological Institute, Helsinki, Finland

R. Krishfield, Woods Hole Oceanographic Institution, Woods Hole, MA, USA

K.J. Kuletz, U.S. Fish and Wildlife Service, Anchorage, AK, USA

K.L. Laidre, Polar Science Center, Applied Physics Laboratory University of Washington, Seattle, WA, USA

K. Lakkala, Finnish Meteorological Institute, Arctic Research Centre, Sodankylä, Finland

R. Lanctot, U. S. Fish & Wildlife Service, Division of Migratory Bird Management, Anchorage, AK, USA

Y. Liu, Cooperative Institute for Meteorological Satellite Studies, University of Wisconsin, Madison, WI, USA

H. Loeng, Institute of Marine Research, Bergen, Norway

M.M. Loranty, Department of Geography, Colgate University, Hamilton, NY, USA

C. Lund Myhre, Norwegian Institute for Air Research, Kjeller, Norway

G. Manney, Jet Propulsion Laboratory, California Institute of Technology, Pasadena, CA; New Mexico Institute of Mining and Technology, Socorro, NM

S.S. Marchenko, Geophysical Institute, University of Alaska Fairbanks, Fairbanks, Alaska, USA

F. McLaughlin, Institute of Ocean Sciences, Sidney, Canada

W. Meier, National Snow and Ice Data Center, University of Colorado, Boulder, CO, USA

S. Moore, NOAA/Fisheries, Office of Science & Technology, Seattle, WA, USA

T. Mote, Department of Geography, University of Georgia, Athens, Georgia, USA

R. Müller, Forschungszentrum Jülich, Jülich, Germany

I.H. Myers-Smith, Department of Geography, University of British Columbia, Vancouver, BC, Canada

J. Nelson, Institute of Ocean Sciences, Dept. Fisheries and Oceans, Sidney, BC, Canada

S. Nishino, Japan Agency for Marine-Earth Science and Technology, Tokyo, Japan

N.G. Oberman, MIRECO Mining Company, Syktyvkar, Russia

J. Overland, Pacific Marine Environmental Laboratory, NOAA, Seattle, WA, USA

D. Perovich, ERDC - CRREL, 72 Lyme Road, Hanover, NH, USA; Thayer School of Engineering, Dartmouth College, Hanover, NH, USA

R. Pickart, Woods Hole Oceanographic Institution, Woods Hole, MA, USA

J. Pinzon, Biospheric Science Branch, NASA Goddard Space Flight Center, Greenbelt, MD, USA

A. Proshutinsky, Woods Hole Oceanographic Institution, Woods Hole, MA, USA

B. Rabe, Alfred Wegener Institute, Bremerhaven, Germany

M.K. Raynolds, Institute of Arctic Biology, University of Alaska Fairbanks, Fairbanks, AK, USA

D.G. Reid, Wildlife Conservation Society, Whitehorse, Canada

M. Rex, Alfred Wegener Institute for Polar and Marine Research, Potsdam, Germany

J. Richter-Menge, ERDC - CRREL, 72 Lyme Road, Hanover, NH, USA

A.V. Rocha, Department of Biological Sciences, University of Notre Dame, Notre Dame, IN, USA

V.E. Romanovsky, Geophysical Institute, University of Alaska Fairbanks, Fairbanks, Alaska, USA

B. Rudels, Finish Institute of Marine Research, Helsinki, Finland

D. Russell, Yukon College, Box 10038 Whitehorse YT, Canada Y1A 7A1

U. Schauer, Alfred Wegener Institute, Bremerhaven, Germany

N.M. Schmidt, Department of Biosciences - Arctic Environment, Aarhus University, Denmark

I. Semiletov, International Arctic Research Center, University of Alaska Fairbanks, Fairbanks, USA

N. Shakhova, International Arctic Research Center, University of Alaska Fairbanks, Fairbanks, USA

M. Sharp, University of Alberta, Department of Earth and Atmospheric Sciences

G.R. Shaver, The Ecosystems Center, Marine Biological Laboratory, Woods Hole, MA, USA

N.I. Shiklomanov, Department of Geography, George Washington University, Washington, DC, USA

K. Shimada, Tokyo University of Marine Science and Technology, Tokyo, Japan

M.F. Sigler, Alaska Fisheries Science Center, National Marine Fisheries Service, National Oceanic and Atmospheric Administration, 17109 Point Lena Loop Road, Juneau, AK 99801

S.L. Smith, Geological Survey of Canada, Natural Resources Canada, Ottawa, Ontario, Canada

V. Sokolov, Arctic and Antarctic Research Institute, St. Petersburg, Russia

M. Steele,Applied Physics Laboratory, University of Washington, Seattle, USA

K. Steffen, Swiss Federal Research Institute WSL, Birmensdorf, Switzerland

D.A. Streletskiy, Department of Geography, George Washington University, Washington, DC, USA

E. Syroechkovskiy, BirdsRussia, Moscow, Russia

M. Tedesco, City College of New York, New York, NY, USA

M.-L. Timmermans, Yale University, New Haven, USA

J. Toole, Woods Hole Oceanographic Institution, Woods Hole, MA, USA

M. Tschudi, Aerospace Engineering Sciences, University of Colorado, Boulder, CO, USA

C.J. Tucker, Biospheric Science Branch, NASA Goddard Space Flight Center, Greenbelt, MD, USA

C.E. Tweedie, Department of Biology, University of Texas - El Paso, El Paso, TX, USA

S. Vagle, Institute of Ocean Sciences, Dept. Fisheries and Oceans, Sidney, BC, Canada

R.S.W. van de Wal, Institute for Marine and Atmospheric Research Utrecht, Utrecht University, Utrecht, The Netherlands

J. Wahr, CIRES, University of Colorado, Boulder, CO, USA

D.A. Walker, Institute of Arctic Biology, University of Alaska Fairbanks, Fairbanks, AK, USA

J. Walsh, International Arctic Research Center, University of Alaska Fairbanks, Fairbanks, AK, USA

M. Wang, Joint Institute for the Study of the Atmosphere and Ocean, University of Washington, Seattle, WA, USA

P.J. Webber, Department of Plant Biology, Michigan State University, East Lancing, MI, USA

T. Weingartner, University of Alaska Fairbanks, Fairbanks, USA

J.M. Welker, Department of Biological Sciences, University of Alaska Anchorage, Anchorage, AK, USA

W.J. Williams, Institute of Ocean Sciences, Fisheries and Oceans Canada, Sidney, BC, Canada

G. Wolken, Alaska Division of Geological & Geophysical Surveys

R. Woodgate, Applied Physics Laboratory, University of Washington, Seattle, USA

M. Yamamoto-Kawai, Tokyo University of Marine Science and Technology, Tokyo, Japan

H. Zeng, Institute of Atmospheric Physics, Chinese Academy of Sciences, Beijing, China

S. Zimmermann, Institute of Ocean Sciences, Sidney, Canada

C. Zöckler, UNEP World Conservation Monitoring Centre, Cambridge, UK

Executive Summary

November 27, 2012

Overview

The Arctic Report Card (www.arctic.noaa.gov/reportcard/) considers a wide range of environmental observations throughout the Arctic, and is updated annually. A major finding of the Report Card 2012 is that numerous record-setting melting events occurred, even though, with the exception of a few limited episodes, Arctic-wide it was an unremarkable year, relative to the previous decade, for a primary driver of melting - surface air temperatures. From October 2011 through August 2012, positive (warm) temperature anomalies were relatively small over the central Arctic compared to conditions in recent years (2003-2010). Yet, in spite of these moderate conditions, new records were set for sea ice extent, terrestrial snow extent, melting at the surface of the Greenland ice sheet, and permafrost temperature.

Large changes in multiple indicators are affecting climate and ecosystems, and, combined, these changes provide strong evidence of the momentum that has developed in the Arctic environmental system due to the impacts of a persistent warming trend that began over 30 years ago. A major source of this momentum is the fact that changes in the sea ice cover, snow cover, glaciers and Greenland ice sheet all conspire to reduce the overall surface reflectivity of the region in the summer, when the sun is ever-present. In other words, bright, white surfaces that reflect summer sunlight are being replaced by darker surfaces, e.g., ocean and land, which absorb sunlight. These conditions increase the capacity to store heat within the Arctic system, which enables more melting - a positive feedback. Thus, we arrive at the conclusion that it is very likely that major changes will continue to occur in the Arctic in years to come, particularly in the face of projections that indicate continued global warming.

A second key point in Report Card 2012 is that changes in the Arctic marine environment are affecting the foundation of the food web in both the terrestrial and marine ecosystems. While more difficult to discern, there are also observations that confirm the inevitable impacts these changes have on a wide range of higher-trophic Arctic and migratory species. Motivated by these linkages and the record-setting environmental changes in the Arctic region, a number of new programs are underway to more effectively measure, monitor and document changes in the marine and terrestrial ecosystems.

Highlights for 2012

During 2012, a number of record or near-record events occurred in relation to the Arctic terrestrial snow cover. Snow cover duration was the second shortest on record and new minima were set for snow cover extent in May over Eurasia and in June (when snow still covers most of the Arctic region) over the Northern Hemisphere. The rate of loss of June snow cover extent between 1979 and 2012 (the period of satellite observation) set a new record of -17.6%/decade, relative to the 1979-2000 mean. Also on land, new record high temperatures at 20 m depth were measured at most permafrost observatories on the North Slope of Alaska and in the Brooks Range, Alaska, where measurements began in the late 1970s.

In Greenland, surface melting on the ice sheet set new records, with melting in some locations lasting up to ~2 months longer than the average (1979-2011) and melting being detected by satellite instruments over ~97 % of the surface in July. Albedo (reflectivity) estimated from

satellite measurements (2000-2012) and in-situ measured mass losses at high elevations also set new records in Greenland.

Sea ice extent in September 2012 reached the lowest observed in the satellite record (1979-present), with a related continued decline in the extent of thick multi-year ice that forms in the central Arctic Basin. This record was set despite a relatively high maximum sea-ice extent in March 2012, which was due to extensive ice in the Bering Sea. March to September 2012 showed the largest seasonal decline in sea ice between the maximum and minimum extents during the satellite record. August 2012 was a period of exceptionally rapid ice loss, with accelerated decline during an intense storm in early August in the East Siberian and Chukchi seas. Illustrating the close connection between the timing and extent of the summer sea ice retreat and sea-surface ocean temperatures, a strong cold anomaly was evident in August in the Chukchi Sea due to the persistence sea ice in this area even as the main body of the pack ice retreated northward.

Observations of the Arctic marine ecosystem provide further evidence of linkages between sea ice conditions and primary productivity, with impacts on the abundance and composition of phytoplankton communities. For instance, new satellite remote sensing observations show the near ubiquity of ice-edge blooms throughout the Arctic and the importance of seasonal sea ice variability in regulating primary production. These results suggest that previous estimates of annual primary production in waters where these under-ice blooms develop may be about ten times too low. At a higher trophic level, seabird phenology, diet, physiology, foraging behavior and survival rates have changed in response to higher water temperatures, which affect prey species.

Changes in the terrestrial ecosystem are exemplified by vegetation and mammals. The tundra continues to become more green and in some locations above-ground plant biomass has increased by as much as 26% since 1982. The length of the growing season increased throughout much of the Arctic, e.g., by ~30 days in Eurasia, between 2000 and 2010. There is evidence that the lemming population cycle is decaying, i.e., the time between population peaks is increasing, and the amplitude of the cycle is collapsing to relatively low population densities.

One species most directly affected by lemming population dynamics is the Arctic fox, which depends on them as a primary food source. In Europe, the Arctic fox population has declined to near extinction due to failure to recover from over-harvesting at the start of the 20th Century and the recent absence of lemming peaks. In contrast, the Arctic fox is abundant in North America. However, in both regions, the larger Red fox has been expanding northward, leading to increased competition with the Arctic fox for resources.

Acknowledgements

The preparation of Arctic Report Card 2012 was directed by a U.S. inter-agency editorial team of representatives from NOAA, the Cold Regions Research and Engineering Laboratory and the Office of Naval Research. The 20 essays in Report Card 2012, representing the collective effort of an international team of 141 researchers in 15 countries, are based on published and ongoing scientific research. Independent, peer-review of the scientific content of the Report Card was facilitated by the Arctic Monitoring and Assessment (AMAP) Program of the Arctic Council. The Circumpolar Biodiversity Monitoring Program (CBMP), the cornerstone program of the Conservation of Arctic Flora and Fauna (CAFF) Working Group of the Arctic Council, was instrumental in soliciting essays in the ecosystem sections of the Report Card. The Arctic

Report Card is supported by the NOAA Climate Program Office through the Arctic Research Program.

Atmosphere Summary

Section Coordinator: James Overland

NOAA Pacific Marine Environmental Laboratory, Seattle, WA, USA

December 3, 2012

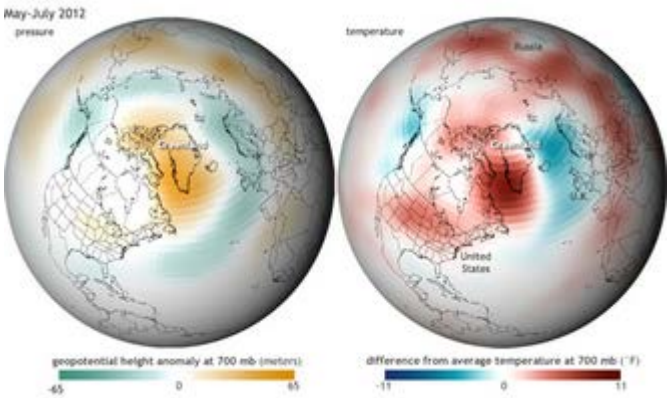

Extended high pressure over southern Greenland (left) caused anomalously high air temperatures (right) and extensive melting at the surface of the ice sheet (see essay on *Greenland Ice Sheet*). Large version available from NOAA Climate.gov.

October 2011 through August 2012 was a departure from typical atmospheric conditions of recent years (2003-2010) in that warm temperature anomalies were relatively small over the central Arctic relative to the late 20th Century. Similarly, cloud cover in 2012 was average compared to the period 2001-2010. Stratospheric ozone concentrations during spring 2012 were also within normal ranges and considerably lower than those in spring 2011, when unprecedented chemical ozone losses occurred. Air sampling sites in the Arctic continue to measure rising greenhouse gas concentrations from worldwide human sources, and indicate that there is, as yet, no direct atmospheric evidence that Arctic emissions of CH_4 or the net balance of C from CO_2 are changing.

Notable weather activity in fall 2011 and winter 2012 occurred in the sub-Arctic due to a strong positive North Atlantic Oscillation (NAO) Index, which promoted westerly winds in the northern North Atlantic Ocean region and warm temperatures in western Eurasia and the Kara Sea. Further east, in the Siberian sub-Arctic, unusually cold winter conditions caused many fatalities. Though 2012 saw a new record summer minimum sea ice extent for the satellite period starting in 1979, the atmospheric forcing conditions were very different than those during the previous record retreat of 2007. In 2012, southerly winds in early June and a major storm in August in the East Siberian and Chukchi seas enhanced sea ice retreat, whereas a persistent warm and windy pattern was responsible for more rapid sea ice melt than normal in 2007. Also noteworthy in 2012 was NAO-related high sea level pressure over Greenland in early summer, a feature of the last six years that has promoted greater than expected mass loss from Greenland and Canadian Arctic glaciers and reduced snow cover in North America.

Air Temperature, Atmospheric Circulation and Clouds

J. Overland[1], J. Key[2], B.-M. Kim[3], S.-J. Kim[3], Y. Liu[4], J. Walsh[5], M. Wang[6], U. Bhatt[7]

[1]Pacific Marine Environmental Laboratory, NOAA, Seattle, WA, USA
[2]Center for Satellite Applications and Research, NOAA/NESDIS, Madison, WI, USA
[3]Korea Polar Research Institute, PO Box 32, Incheon, Korea
[4]Cooperative Institute for Meteorological Satellite Studies, University of Wisconsin, Madison, WI, USA
[5]International Arctic Research Center, University of Alaska Fairbanks, Fairbanks, AK, USA
[6]Joint Institute for the Study of the Atmosphere and Ocean, University of Washington, Seattle, WA, USA
[7]Geophysical Institute, University of Alaska Fairbanks, Fairbanks, AK, USA

November 7, 2011

Highlights

- October 2011 through August 2012 was a departure from typical atmospheric conditions of recent years (2003-2010), in that temperature anomalies were small over the central Arctic. Most of the notable weather activity in fall and winter occurred in the sub-Arctic due to a strong positive North Atlantic Oscillation. Summer 2012 was dominated by low sea level pressure.
- Three severe weather events included (1) unusual cold in late January to early February 2012 across Eurasia, and (2) two record storms characterized by deep central pressure and strong winds near western Alaska in November 2011 and north of Alaska in August 2012.

Mean Annual Surface Air Temperature

In contrast to the years 2003 through 2010, which had substantial positive temperature anomalies in the central Arctic, the period October 2011-August 2012 showed positive temperature anomalies in the sub-Arctic rather than over the central Arctic Ocean (**Fig. 1.1**).

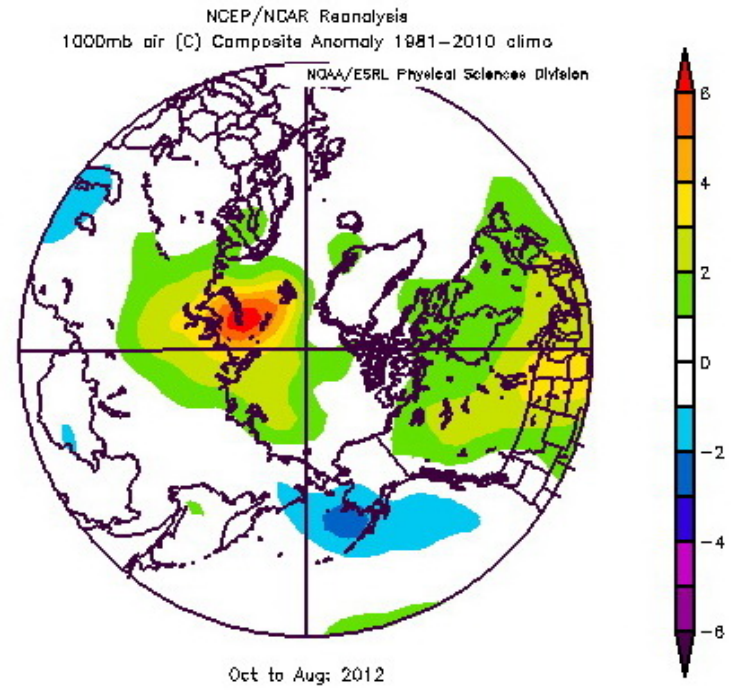

Fig. 1.1. Annual average (October 2011 through August 2012) near-surface air temperature anomalies relative to the period 1981-2010. Data are from NOAA/ESRL, Boulder, CO: http://www.esrl.noaa.gov/psd/.

Over a longer time interval, the annual mean surface air temperature over Arctic land areas has experienced an overall warming of about +2ºC since the mid-1960s (**Fig. 1.2**). In 2011, the annual mean air temperature was slightly warmer than in 2009 and 2010. The cooler temperatures in 2009 and 2010 reflected cold continents in winter, while Eurasia had warmer temperatures in spring 2011. The annual mean surface temperature for 2012 is not available, as the year was incomplete at the time of writing.

Positive temperature anomalies were seen everywhere across the central Arctic for the first decade in 21st century (2001-2011) relative to a 1971-2000 baseline period at the end of the 20th Century (**Fig. 1.3**). This temperature pattern is a manifestation of "Arctic Amplification", which is characterized by temperature increases 1.5°C greater than (more than double) the increases at lower latitudes (Overland et al., 2011; Stroeve et al., 2012).

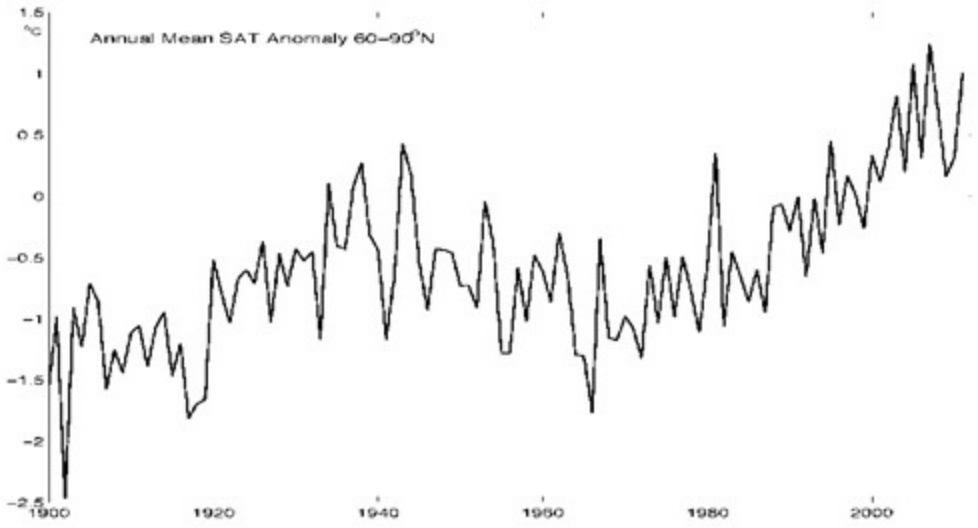

Fig. 1.2. Arctic-wide annual average surface air temperature (SAT) anomalies for the period 1900-2011 relative to the 1981-2010 mean value, based on land stations north of 60°N. Data are from the CRUTEM3v dataset at www.cru.uea.ac.uk/cru/data/temperature/. Note: this curve includes neither marine observations nor 2012 data, as the year was incomplete at the time of writing.

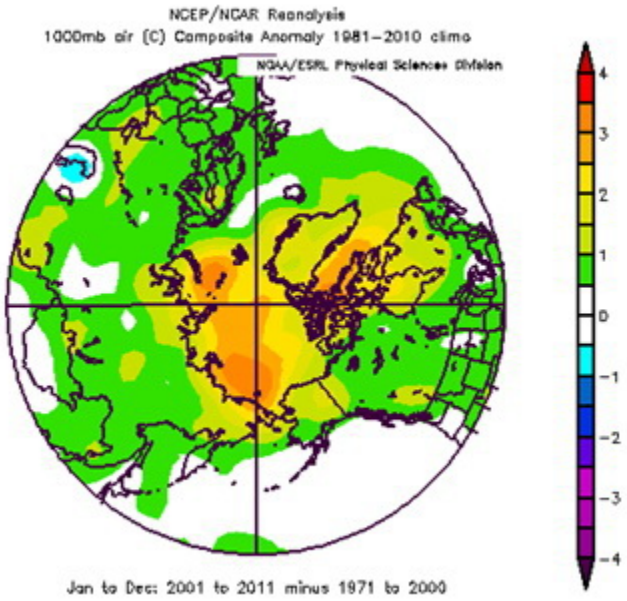

Fig. 1.3. Annual average near-surface air temperature anomalies for the first decade of the 21st century (2001-11) relative to the baseline period of 1971-2000. Data are from NOAA/ESRL, Boulder, CO: http://www.esrl.noaa.gov/psd/.

Seasonal Air Temperatures

Consistent with the annual average temperatures (**Fig. 1.1**), each seasonal anomaly distribution for near-surface temperatures shows departures primarily in the sub-Arctic (**Fig. 1.4**). Fall 2011 and winter 2012 were characterized by a positive North Atlantic Oscillation (NAO). This promotes the warm temperature anomaly over the Barents and Kara Seas, which are downstream of the stronger winds and lower pressures of the Icelandic low pressure center. This is unlike the Warm Arctic/Cold Continents pattern associated with a negative Arctic Oscillation (AO) climate pattern over the central Arctic (see previous Report Cards), which dominated the previous two falls and winters (2009-10 and 2010-11).

In contrast to the positive NAO in fall 2011 and winter 2012, spring and summer 2012 had a very negative NAO, with significant consequences for snow cover duration and extent (see the *Snow* essay) and melting on the Greenland Ice Sheet (see the *Greenland Ice Sheet* essay). Spring 2012 also saw the early formation of the Arctic Dipole (AD) pattern (**Fig. 1.5**) with high pressure on the North American side of the Arctic and low pressure on the Siberian side. In the previous five years this has not occurred until June (Overland et al., 2012). The dipole pattern supported increased winds across the Arctic and warmer temperature anomalies over the East Siberian Sea and western Greenland (**Fig. 1.4c**). In summer 2012 an unusual low pressure, centered on the Pacific Arctic sector, was a new feature of central Arctic weather relative to the last decade (**Fig. 1.6**).

Also noteworthy in **Fig. 1.6** is the high sea level pressure over Greenland, which has been a feature of early summer for the last six years. Higher pressures over Greenland and their influence on Arctic and subarctic wind patterns, a so called blocking pattern, suggests physical connections between it and reduced Arctic sea ice in the summer, loss of Greenland and Canadian Arctic glacier ice, reduced North American snow cover in May and June, and potentially extremes in mid-latitude weather (Overland et al., 2012). See the essays on *Sea Ice*, *Glaciers and Ice Caps*, *Greenland Ice Sheet* and *Snow* for further information on those topics.

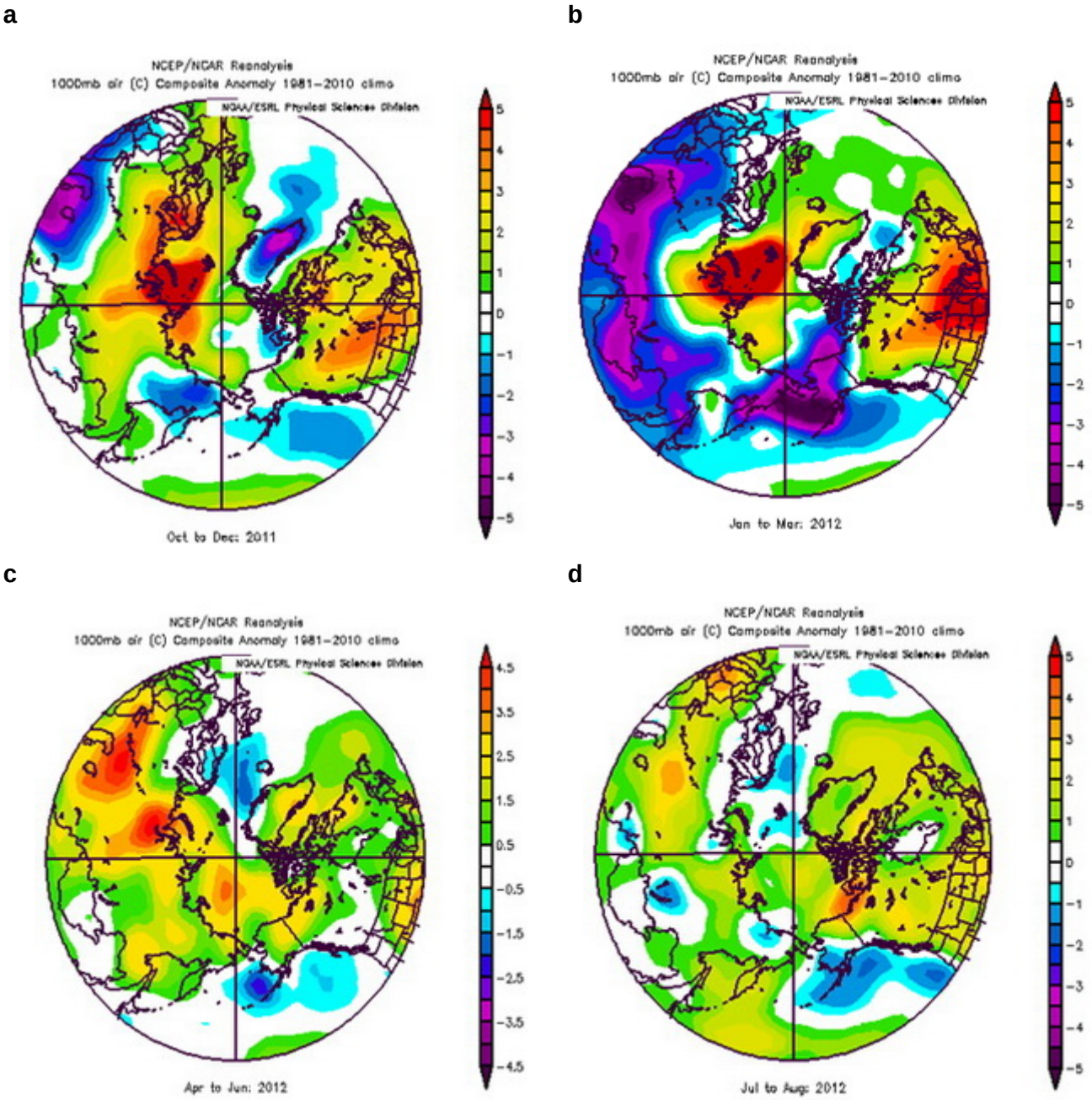

Fig. 1.4. Seasonal anomaly patterns for near surface air temperatures in 2012 relative to the baseline period 1981-2010. Fall 2011, (a), winter 2012 (b). spring 2012 (c) and summer 2012 (d). Data are from NOAA/ESRL, Boulder, CO: http://www.esrl.noaa.gov/psd/.

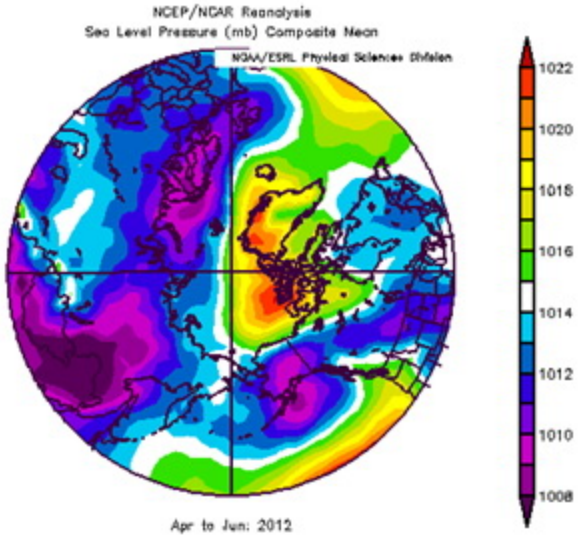

Fig. 1.5. Sea level pressure field for April through June 2012 showing the Arctic Dipole (AD) pattern with high pressure on the North American side of the Arctic and low pressure on the Siberian side. Data are from NOAA/ESRL, Boulder, CO: http://www.esrl.noaa.gov/psd/.

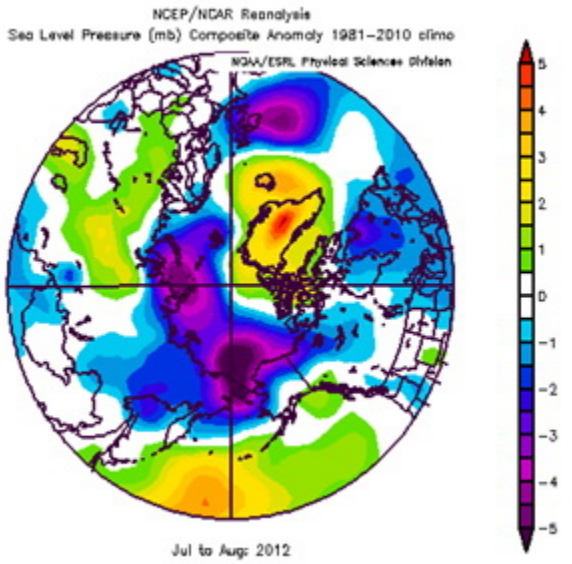

Fig. 1.6. In summer 2012 an extensive low sea level pressure anomaly was centered on the Pacific Arctic sector while high pressure remained over Greenland. Data are from NOAA/ESRL, Boulder, CO: http://www.esrl.noaa.gov/psd/.

Severe Weather

The period late 2011 through summer 2012 was notable for three severe weather events.

The Bering Sea storm of November 2011, one of the most powerful extra-tropical cyclones on record to affect Alaska, caused extensive coastal flooding. Moving northeastward from its

origins in the western Pacific Ocean, the storm deepened by 25 hPa in the 24 hours ending November 8, when its central pressure of 945 hPa was comparable to that of a Category 3 hurricane. The storm's forward speed exceeded 100 km/hour as it approached Alaska and turned northward, passing just offshore of Alaska's western coast, then through the Bering Strait and into the Chukchi Sea. Wind gusts of 144 km/hour and 151 km/hour were recorded on the western Seward Peninsula and Little Diomede Island, respectively.

In late January-early February 2012, a warm center occurred over the Kara and Laptev Seas and broader, severe cold anomalies occurred over the northern Eurasian sub-Arctic during a brief period of negative AO (**Fig. 1.4b**). North America and Eurasia exhibited a sharp contrast in surface temperature anomalies. The United States experienced its fourth warmest winter since national records began in 1895, whereas extremely low temperatures occurred across parts of the Eurasian continent during January 24th-February 14th. This was Europe's worst cold spell in at least 26 years, and >650 people died as a result of the frigid conditions in Russia, Ukraine and Poland. A significant amount of snow fell across the affected areas, resulting in the third largest February snow cover extent (Source: NOAA National Climatic Data Center, State of the Climate: Global Analysis for February 2012, published online March 2012, http://www.ncdc.noaa.gov/sotc/global/2012/2). These observations suggest that a negative AO can favor the development of cold weather over Europe and warm weather over North America.

In August 2012, a storm of exceptional intensity affected the Arctic Ocean north of Alaska. The central pressure of 965 hPa made this system one of the strongest August storms to have affected the Arctic Ocean in the past several decades. The storm likely had a significant impact on ocean mixing due to the already reduced sea ice cover, but this remains to be fully evaluated. The storm did have a significant impact on the further retreat of the pack ice, as illustrated in the *Sea Ice* essay (**Fig. 2.5**).

Cloud Cover

Unlike 2011, when Arctic cloud cover was somewhat higher than normal in winter and lower in the summer, Arctic cloud cover in 2012 was, overall, average when compared to the period 2001-2010. However, there were significant monthly anomalies that warrant closer examination, as the spatial patterns varied in important ways on the regional scale.

While clouds influence the surface energy budget, they also respond to changes in the ice cover (Liu et al., 2012). As in recent years, positive cloud cover anomalies (more cloud) over the Arctic Ocean correspond to negative sea ice anomalies (less ice). This was particularly evident in the winter months in the Barents and Kara seas region, and in the summer months from the East Siberian Sea to the Beaufort Sea. An example for February is shown in **Figs. 1.7a and b**. The reader is referred to the *Sea Ice* essay for information on Arctic-wide sea ice anomalies during the period 1979-2012.

Large-scale advection of heat and moisture and the frequency of synoptic scale systems also influence cloud cover (Liu et al., 2007). Positive cloud anomalies over northern Russia and the

Kara Sea in the 2011-2012 winter months correspond to southerly flow on the western side of an anticyclonic pattern, while negative cloud anomalies over Siberia are found on the eastern side of the same pattern (**Figs. 1.7 c and d**). Positive cloud anomalies over the Chukchi Sea in June (not shown) also appear to be related more to changes in circulation than to changes in sea ice extent. These patterns are also seen in the surface temperature fields (**Figs. 1.4b, and c**).

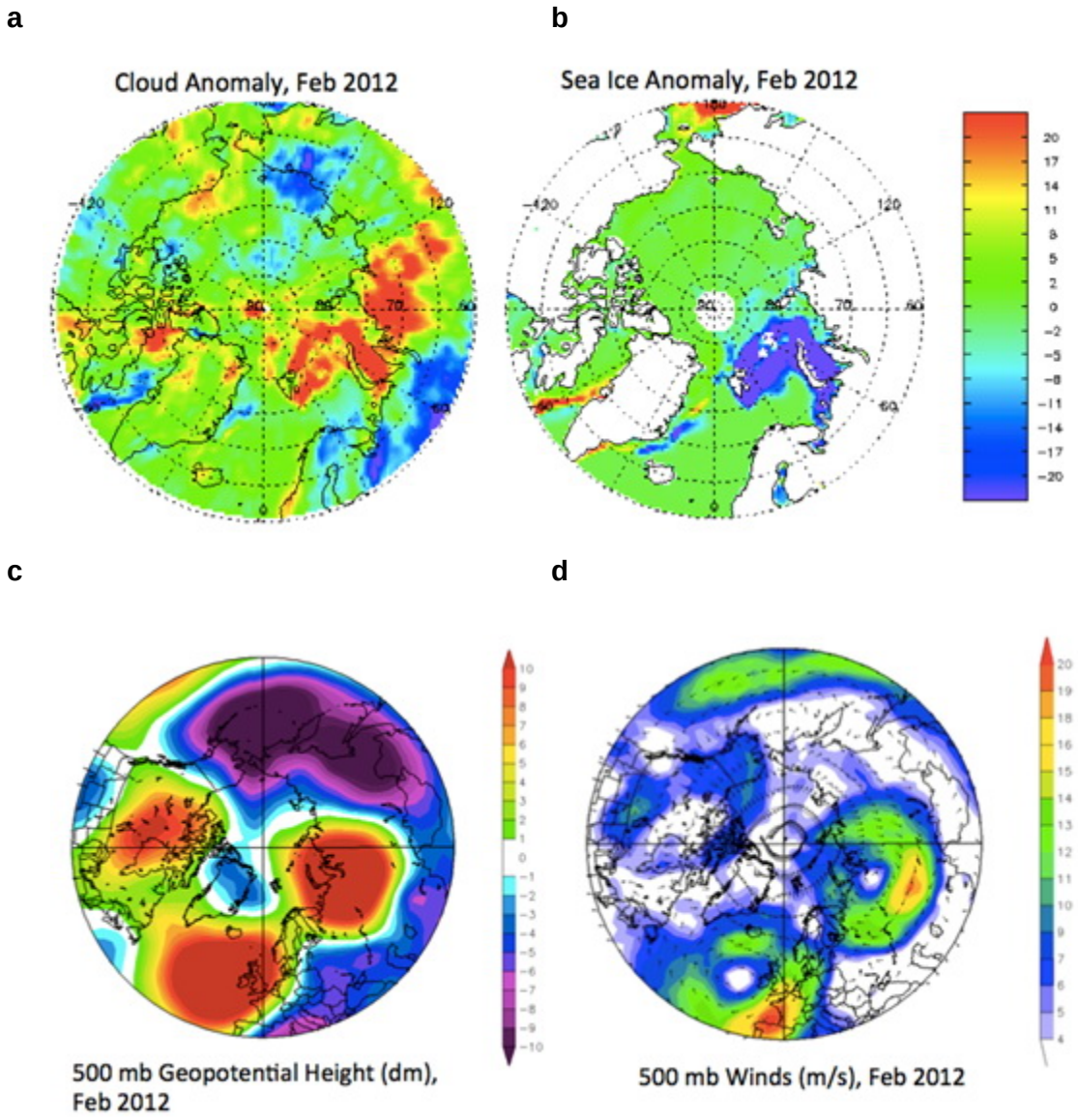

Fig. 1.7. Cloud cover (a) and sea ice concentration (b) anomalies (in %) in February 2012 relative to the corresponding monthly means for the period 2002-2010. Data are from the Moderate Resolution Imaging Spectroradiometer (MODIS) on the Aqua satellite. Corresponding 500 mb geopotential height (c) and 500 mb wind field (right) anomalies in February 2012 are from NCEP.

References

Liu, Y., J. R. Key, Z. Liu, X. Wang and S. J. Vavrus. 2012. A cloudier Arctic expected with diminishing sea ice. *Geophys. Res. Lett.*, 39, L05705, doi:10.1029/2012GL051251.

Liu, Y., J. Key, J. Francis and X. Wang. 2007. Possible causes of decreasing cloud cover in the Arctic winter, 1982-2000. *Geophys. Res. Lett.*, 34, L14705, doi:10.1029/2007GL030042.

Overland, J. E., J. A. Francis, E. Hanna and M. Wang. 2012. The recent shift in early summer arctic atmospheric circulation. *Geophys. Res. Lett.*, doi: 10.1029/2012GL053268. [In press].

Overland, J. E., K. R. Wood and M. Wang. 2011. Warm Arctic-cold continents: Impacts of the newly open Arctic Sea. *Polar Res.*, 30, 15787, doi: 10.3402/polar.v30i0.15787.

Stroeve, J. C., M. C. Serreze, M. M. Holland, J. E. Kay, J. Maslanik and A. P. Barrett. 2012. The Arctic's rapidly shrinking sea ice cover: a research synthesis. *Climatic Change*, doi 10.1007/s10584-011-0101-1.

Ozone and UV Radiation

G. Bernhard[1], G. Manney[2,3], V. Fioletov[4], J.-U. Grooß[5], A. Heikkilä[6], B. Johnsen[7], T. Koskela[6], K. Lakkala[8], R. Müller[5], C. Lund Myhre[9], M. Rex[10]

[1]Biospherical Instruments, San Diego, CA
[2]Jet Propulsion Laboratory, California Institute of Technology, Pasadena, CA
[3]New Mexico Institute of Mining and Technology, Socorro, NM
[4]Environment Canada, Toronto, Ontario, Canada
[5]Forschungszentrum Jülich, Jülich, Germany
[6]Finnish Meteorological Institute, Helsinki, Finland
[7]Norwegian Radiation Protection Authority, Østerås, Norway
[8]Finnish Meteorological Institute, Arctic Research Centre, Sodankylä, Finland
[9]Norwegian Institute for Air Research, Kjeller, Norway
[10]Alfred Wegener Institute for Polar and Marine Research, Potsdam, Germany

November 7, 2012

Highlights

- Temperatures in the Arctic stratosphere in early December 2011 were among the lowest on record. Strong dynamical activity in late December 2011 and January 2012 caused the temperature to rise rapidly and led to conditions unfavorable to sustaining chemical ozone loss.
- Ozone concentrations in the Arctic stratosphere and UV radiation levels at Arctic and sub-Arctic locations during the spring of 2012 were generally within the range of values observed during the first decade of this century.
- Below-average ozone concentrations at several sites in southern Scandinavia led to increases in the UV Index of about 12% during January, February and March of 2012.

Introduction

Ozone molecules in the Earth's atmosphere greatly attenuate the part of the Sun's ultraviolet (UV) radiation that is harmful to life. Reductions in the atmospheric ozone amount will always lead to increased UV levels, but other factors such as the height of the Sun above the horizon, cloud cover and aerosols also play important roles. This essay compares ozone and UV radiation measurements performed in the Arctic in 2012 with historical records.

Ozone observations

Stratospheric ozone concentrations measured during the spring of 2012 in the Arctic were, by and large, within the typical range observed during the first decade of this century. The 2012 ozone levels were considerably higher than those in the spring of 2011, when unprecedented chemical ozone losses occurred (Manney et al., 2011). The minimum total ozone column[1] for March 2012, averaged over the "equivalent latitude[2]" band 63°-90° N, was 372 Dobson Units (DU[3]). The 2011 record-low was 302 DU (**Fig. 1.8**). The average for 2000-2010 is 359 DU, 13 DU below the value for 2012.

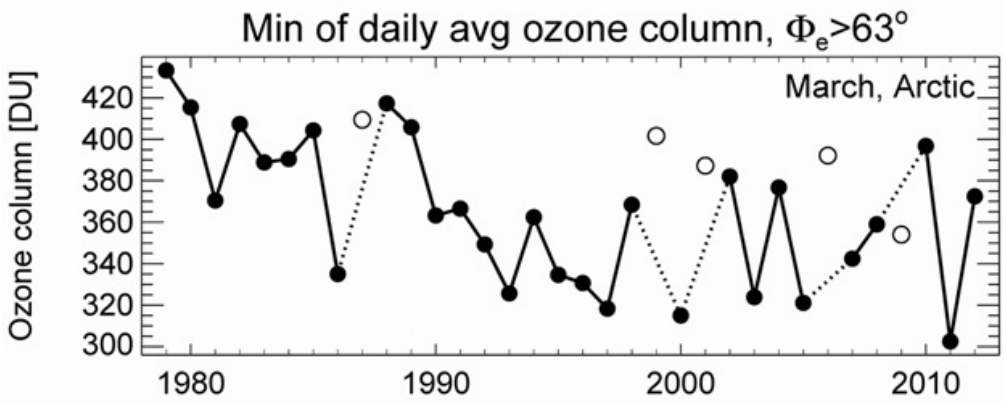

Fig. 1.8. Time series of minimum total ozone for March in the Arctic, calculated as the minimum of daily average column ozone poleward of 63° equivalent latitude. Winters in which the vortex broke up before March (1987, 1999, 2001, 2006, and 2009) are shown as circles. Polar ozone in those years was relatively high because of mixing with air from lower latitudes. Figure adapted from Müller et al. (2008), updated using Version 2.8 of the combined total column ozone database produced by Bodeker Scientific, available at http://www.bodekerscientific.com/data/total-column-ozone.

The monthly mean total ozone columns for February through May 2012 are compared with baseline data from the 1978-1988 period in **Fig. 1.9**. During February, total ozone was more than 30% below the baseline value at Svalbard. Regions with monthly mean ozone levels 10% and more below the historical reference encompassed the North Pole, the North Sea, northern Siberia, northern Greenland, Scandinavia, Iceland, the British Isles, Denmark, the Netherlands and northern Germany. Above-average ozone levels were observed over the Aleutian Islands in the north Pacific Ocean. In March, the area with total ozone 10% below the baseline was centered on the North Sea and extended towards southern Scandinavia, the British Isles, France and central Europe. Much of eastern Canada, the eastern United States and southern Alaska were also affected by below-average total ozone columns. In April, Arctic regions with lower-than-normal ozone included the northern part of Canada (Victoria Island) and southern Greenland. Extended areas with large deviations from the historical measurements were not observed in the Arctic during May and through the summer.

The above discussion refers to monthly mean values. Departures from the baseline (either up or down) were larger for individual days. For certain regions and days, the ozone layer was 30% thinner than the long term mean. Deviations exceeding -35% were observed in the southwestern part of Russia as late as the second half of April. Deviations above the reference tended to be smaller in magnitude and less frequent.

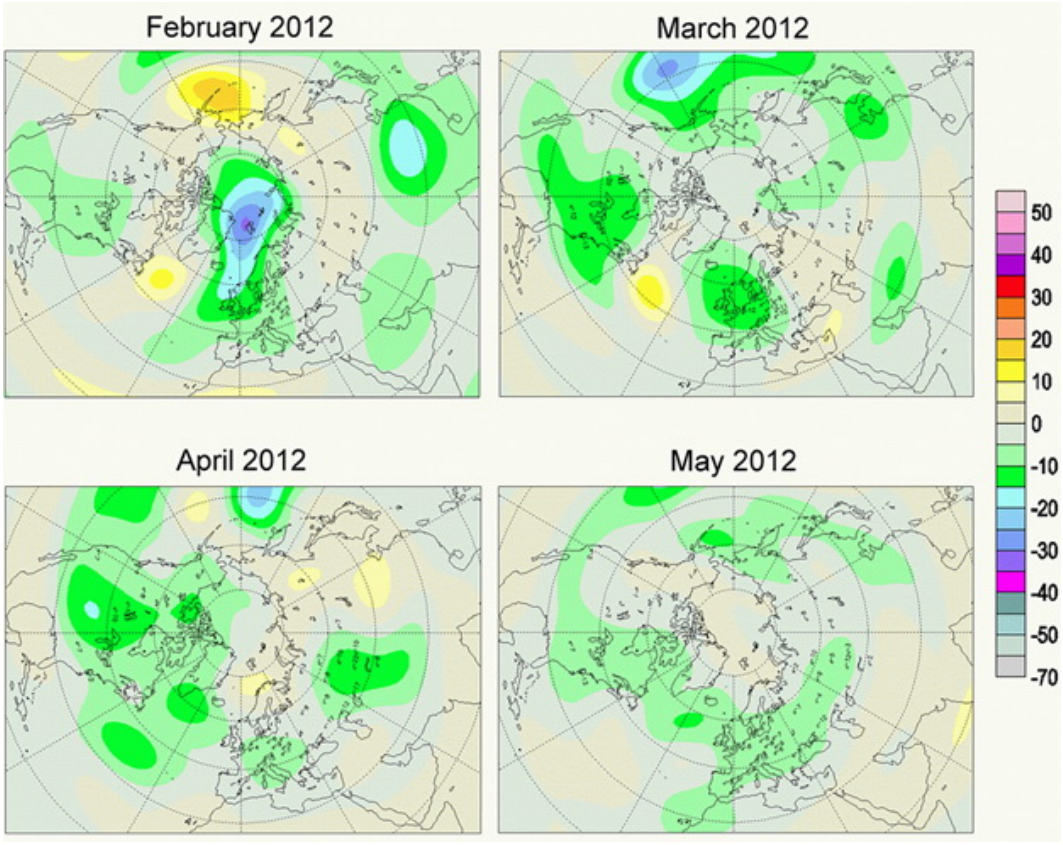

Fig. 1.9. Deviation (%) of monthly average total ozone for February, March, April and May 2012 from the 1978-1988 level. Maps were provided by Environment Canada and are available at http://es-ee.tor.ec.gc.ca/cgi-bin/selectMap. The 2012 data are based on ground-based measurements and space-based - OMI (Ozone Monitoring Instrument) and GOME-2 (Global Ozone Monitoring Experiment-2) - data. NOAA Stratosphere Monitoring Ozone Blended Analysis (SMOBA) data were used for the polar night area in February. Reference data for 1978-1988 were estimated using Total Ozone Mapping Spectrometer (TOMS) observations available at http://ozoneaq.gsfc.nasa.gov/nimbus7Ozone.md.

The distribution of total ozone column over the Arctic on 3 April of the years 1981 (a year with a long-lasting and cold Arctic vortex, and relatively low stratospheric chlorine concentrations), 2002 (long-lasting warm vortex, high total chlorine loading), 2011 (long-lasting cold vortex, high chlorine), and 2012 (warm vortex, high chlorine) are illustrated in **Fig. 1.10**. The figure emphasizes that chemical ozone loss resulting from chlorine activation is most effective in years when there is a long-lasting, cold vortex, such as 2011. Years with a warm vortex, such as 2002 and 2012, result in little ozone loss.

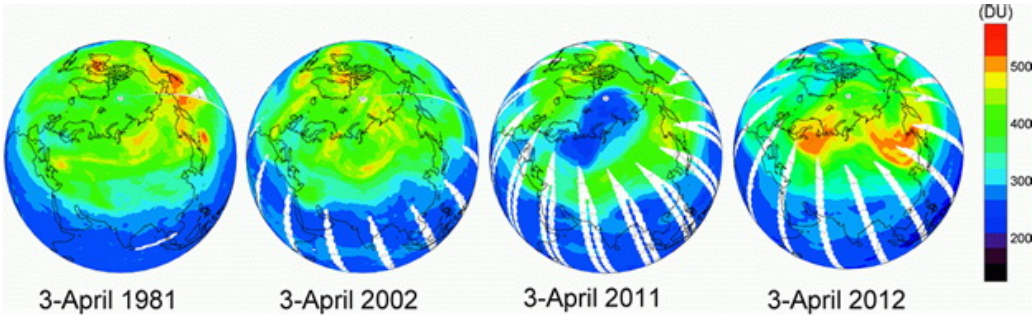

Fig. 1.10. Comparison of total ozone column measured by satellites on 3 April 1981, 2002, 2011, and 2012. Data are from the TOMS aboard the Nimbus-7 (1981) and Earth Probe (2002) satellites, and the OMI aboard the Aura spacecraft (2011 and 2012).

Chemical ozone loss

Arctic stratospheric temperatures in December 2011 were among the lowest on record but rose to near average temperatures after strong dynamical activity in late December. Low temperatures facilitate the formation of polar stratospheric clouds (PSC), which provide surfaces for heterogeneous reactions (i.e., reactions between gases and liquid or solid matter) that activate stratospheric chlorine. The activated chlorine, in turn, destroys ozone rapidly in catalytic cycles. Sudden stratospheric warming in January 2012 halted PSC formation and hence the activation of chlorine, and led to conditions that were unfavorable to sustaining chemical ozone loss. The temporal evolution of several parameters which are crucial for stratospheric ozone chemistry are illustrated in the following with data from the Microwave Limb Sounder (MLS) on the Aura satellite (**Fig 1.11**).

Temperatures below the threshold temperature for PSC occurrence and chlorine activation of about 196 K (-77°C) existed locally until late January 2012 (**Fig. 1.11a**). When PSCs are formed, gas-phase nitric acid (HNO3) molecules occurring in the stratosphere are partly converted to solid particles such as nitric acid dihydrate (NAD), which then activate chlorine. The formation of PSCs at the beginning of the 2011/2012 winter is indicated by the large decrease of gaseous nitric acid in early December 2011 (**Fig. 1.11b**). The conversion of chlorine from inactive "reservoir chemicals" such as hydrogen chloride (HCl) to active forms such as chlorine monoxide (ClO) commenced at about the same time and is indicated by the decrease in HCl (**Fig. 1.11c**) and the increase in ClO (**Fig. 1.11d**). Of note, active chlorine in the form of ClO occurs only in sunlit regions of the vortex. Hence the decrease in HCl appears larger and earlier than the increase in ClO.

ClO is the primary ozone-destroying form of chlorine, so its presence is a sign for the potential for chemical ozone destruction. However, the catalytic cycles that enable ClO to destroy large amounts of ozone also require sunlight. So, even with chlorine activated, ozone destruction is typically small in January when much of the Arctic is still dark. The small drop in ozone in late January 2012 indicated in **Fig. 1.11e** suggests that a small amount of ozone was destroyed when the polar vortex was positioned so that substantial portions of it received sunlight.

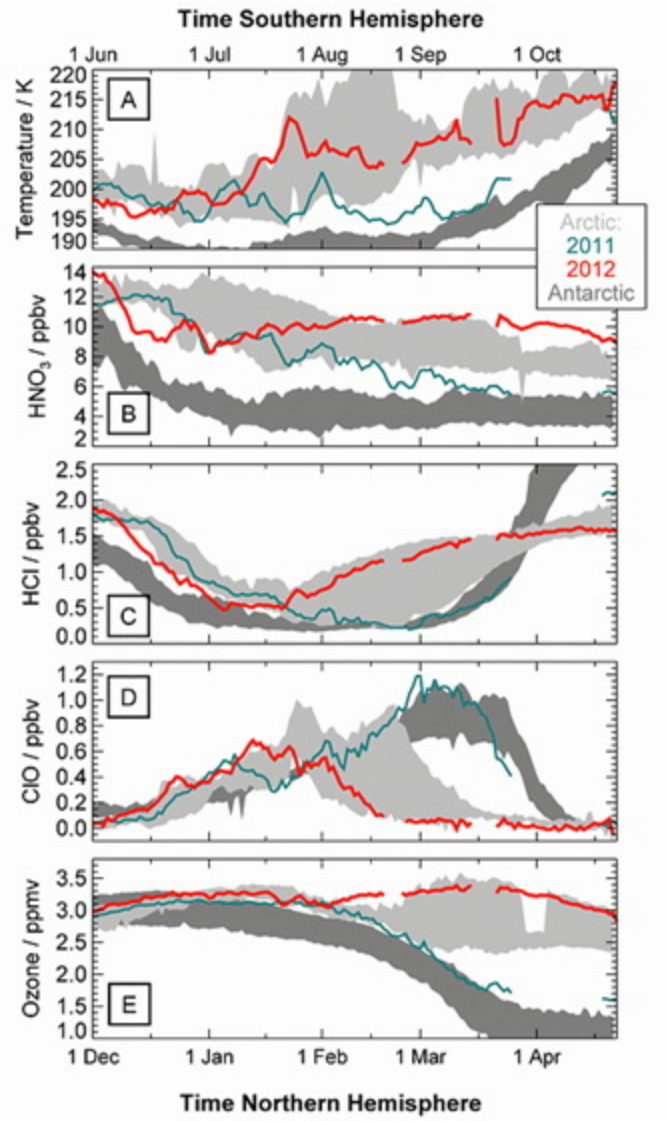

Fig. 1.11. Averages of high latitude stratospheric temperatures (panel A), nitric acid (HNO_3; panel B), hydrogen chloride (HCl; panel C), chlorine monoxide (ClO; panel D) and ozone (panel E) derived from MLS measurements on the Aura satellite. Measurements of the 2011/2012 Arctic winter (bold red line) are compared with similar data from the 2010/2011 Arctic winter (blue-green lines) during which unprecedented chemical ozone loss had occurred. Light grey shading indicates the range of values observed in Arctic winters between 2004/2005 and 2009/2010. Dark grey shading shows the range of values for Antarctic winters from 2005 through 2011. Temperature and mixing ratios refer to the 485 K potential temperature surface (altitude of approximately 20 km, pressure of about 50 hPa) and were averaged over the polar vortex (the region of strong westerly winds in the stratosphere encircling the pole in winter, within which chemical ozone destruction occurs).

In late January, a very strong and prolonged "stratospheric sudden warming" (SSW) event resulted in temperatures rising above the threshold below which chlorine can be activated, and chlorine was thus converted back to inactive forms by mid-February. No further ozone

destruction occurred, and ozone increased slightly through mid-March as vertical motions transported higher ozone down from above.

SSWs are a common dynamical event in the Arctic winter, during which the strong westerly winds that encircle the polar vortex reverse to easterly and polar stratospheric temperatures rise abruptly, sometimes increasing by more than 30 K over 2-3 days. Such events have historically occurred on average about once every two winters, but are irregular, with periods of many years without one occurring (e.g., in most of the 1990s) and other periods such as the past decade having many more than average. The contrast between the meteorological conditions in 2011/2012 with those in 2010/2011 highlights the large range of interannual variability in Arctic winter conditions, and hence in Arctic ozone loss.

UV Radiation

UV levels measured at Arctic terrestrial locations during the first half of 2012 were generally within the typical range of values observed during the last two decades, with notable exceptions discussed below.

Figure 1.12 compares measurements of the UV Index for 12 Arctic and sub-Arctic sites performed in 2012 and 2011 with historical measurements. The UV Index is a measure of the ability of UV radiation to cause erythema (sunburn) in human skin. It is calculated by weighting UV spectra with the CIE action spectrum for erythema (McKinlay and Diffey, 1987) and multiplying the result by 40 m^2/W. Changes in the UV Index tend to anti-correlate with changes in total ozone. This can be seen by comparing the center panels of **Fig. 1.12**, which show UV Index measurements of 2011 and 2012 relative to the climatological average, with the bottom panels, which show a similar analysis for total ozone. The anti-correlation is most obvious for periods not affected by clouds.

Closer inspection of **Fig. 1.12** reveals that total ozone at the southern Scandinavian sites (last row of **Fig. 1.12**) was significantly below the long-term mean for much of January, February and March 2012, consistent with the ozone maps shown in **Fig. 1.9**. On average, ozone was reduced by 16% over Trondheim, 11% over Finse, 6% over Jokioinen and 10% over Østerås. These reductions led to increases of the UV Index by 11% at Finse and 13% at Østerås. UV levels at Trondheim and Jokioinen were not notably affected, likely because of the dominance of cloud effects. While it is unusual that total ozone remains below the climatological average for three consecutive months, reductions for individual days remained, by and large, within historical limits.

Total ozone at Barrow, Alaska, was 257 DU on 9 June 2012 and 267 DU on 10 June 2012. The long-term mean for the two days is 345 DU and the standard deviation of the year-to-year variability is 23 DU. Thus, total ozone on these two days was 3.8 and 3.4 standard deviations below the climatology. Satellite images (e.g., http://www.temis.nl/protocols/o3field/o3month_omi.php?Year=2012&Month=06&View=np) indicate that the low-ozone event was caused by advection of ozone-poor air from lower latitudes originating from above the United States. The transport of ozone-poor air from lower to

higher latitudes is well documented (e.g., Bojkov and Balis, 2001), but advection from sub-tropical to polar latitudes is less common. As a consequence of low ozone, the UV Index at Barrow on 10 June 2012 was 40% above the mean value for this day.

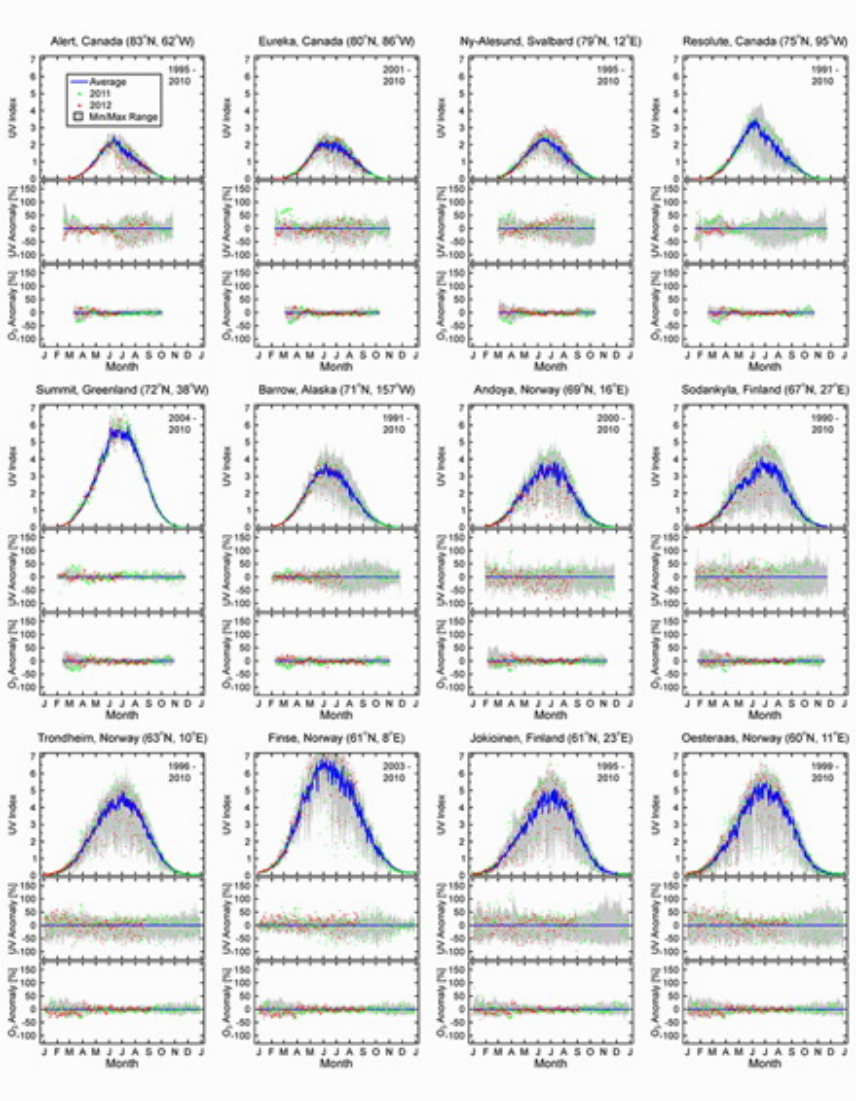

Fig. 1.12. Seasonal variation of the UV Index for 12 Arctic and sub-Arctic sites measured by ground-based radiometers. Data are based on the daily maximum UV Index for all sites but Alert, Eureka and Resolute, which use the UV Index averaged over the period of two hours centered at solar noon. The upper panel for each site compares the climatological average (blue line) with the measurements in 2011 (green dots) and 2012 (red dots), and historical minima and maxima (shaded range). The latter were calculated from measurements during the periods indicated in the top-right corner of the panel. The center panel shows the anomaly in the UV Index, calculated as the percentage departure from the climatological average. The bottom panel shows a similar anomaly analysis for total ozone derived from measurements by the following satellites: TOMS/Nimbus7 (1991-1992), TOMS/Meteor3 (1993-1994), TOMS/EarthProbe (1996-2004) and OMI (2005-2012). The shaded range for the ozone data set is based on data for 1991-2010 (1996-2010 for Trondheim and Finse). Ozone data are available at http://ozoneaq.gsfc.nasa.gov/ and http://avdc.gsfc.nasa.gov/index.php?site=1593048672&id=28.

Figure 1.12 also highlights measurements made in 2011. The abnormally low stratospheric ozone concentrations in spring of that year (see Arctic Report Card 2011) led to large increases in UV radiation during March and April. These increases were considerably larger than any enhancement observed in 2012.

In addition to atmospheric ozone concentrations, UV radiation is affected by the height of the Sun above the horizon, clouds, aerosols (liquid and solid particles suspended in air), the reflectivity of the surface (high, when snow or ice covered), and other factors (Weatherhead et al., 2005). The main driver of the annual cycle is the solar elevation. Sites closest to the North Pole (Alert, Eureka and Ny-Alesund in **Fig. 1.12**) have the smallest peak radiation, with UV Index remaining below 4 all year. Although UV Indices below 5 are considered "low" or "moderate" (WHO, 2002), people involved in certain outdoor activities may receive higher-than-expected UV doses if their faces and eyes are oriented perpendicular to the low Sun or if they are exposed to UV radiation reflected off snow.

Clouds lead to a large variability in UV levels on time scales from minutes to days, but their effect is largely reduced when the ground is covered by fresh snow (Bernhard et al., 2008). Measurements at Barrow, and to a lesser extent at Alert and Eureka, show a large asymmetry between spring (low variability) and fall (high variability) because the surface at these sites is covered by snow until about June and free of snow thereafter until the beginning of winter. During summer and fall, the variability introduced by clouds is substantially larger than that related to ozone variations (compare shaded ranges in center and bottom panels of **Fig. 1.12**).

Footnotes

[1]Total ozone column is the height of a hypothetical layer that would result if all ozone molecules in a vertical column above the Earth's surface were brought to standard pressure (1013.25 hPa) and temperature (273.15 K).

[2]Equivalent latitude is a latitude-like coordinate aligned with the polar vortex (Butchart and Remsberg, 1986).

[3]Dobson Unit, the standard unit for measuring the total ozone column. 1 DU equals a column height of 0.01 mm and corresponds to 2.69×10^{16} molecules / cm^2.

References

Bernhard, G., C. R. Booth and J. C. Ehramjian. 2008. Comparison of UV irradiance measurements at Summit, Greenland; Barrow, Alaska; and South Pole, Antarctica. *Atmos. Chem. Phys.*, 8, 4799-4810. Available at: http://www.atmos-chem-phys.net/8/4799/2008/acp-8-4799-2008.html.

Bojkov, R. D. and D. S. Balis. 2001. Characteristics of episodes with extremely low ozone values in the northern middle latitudes 1957-2000. *Ann. Geophys.*, 19, 797-807. Available at: http://www.ann-geophys.net/19/797/2001/angeo-19-797-2001.html.

Butchart, N. and E. E. Remsberg. 1986. The area of the stratospheric polar vortex as a diagnostic for tracer transport on an isentropic surface. *J. Atmos. Sci.*, 43, 1319-1339.

Manney, G. L., M. L. Santee, M. Rex., N. J. Livesey, M. C. Pitts, P. Veefkind, E. R. Nash, I. Wohltmann, R. Lehmann, L. Froidevaux, L. R. Poole, M. R. Schoeberl, D. P. Haffner, J. Davies, V. Dorokhov, H. Gernandt, B. Johnson, R. Kivi, E. Kyrö, N. Larsen, P. F. Levelt, A. Makshtas, C. T. McElroy, H. Nakajima, M. C. Parrondo, D. W. Tarasick, P. von der Gathen, K. A. Walker and N. S. Zinoviev. 2011. Unprecedented Arctic ozone loss in 2011 echoed the Antarctic ozone hole. *Nature*, 478, 469-475. Available at: http://www.nature.com/nature/journal/v478/n7370/full/nature10556.html.

McKinlay, A. F. and B. L. Diffey. 1987. A reference action spectrum for ultraviolet induced erythema in human skin. *CIE Res. Note*, 6(1), 17- 22.

Müller, R., J.-U. Grooß, C. Lemmen, D. Heinze, M. Dameris and G. Bodeker. 2008. Simple measures of ozone depletion in the polar stratosphere. *Atmos. Chem. Phys.*, 8, 251-264. Available at: http://www.atmos-chem-phys.org/8/251/2008/acp-8-251-2008.pdf.

Rex, M., R. J. Salawitch, P. von der Gathen, N. R. P. Harris, M. P. Chipperfield and B. Naujokat. 2004. Arctic ozone loss and climate change. *Geophys. Res. Lett.*, 31, L04116, doi:10.1029/2003GL018844.

Weatherhead B., A. Tanskanen and A. Stevermer. 2005. Ozone and Ultraviolet Radiation, Chapter 5 in *Arctic Climate Impact Assessment*, 1042 pp, Cambridge University Press, New York. Available at: http://www.acia.uaf.edu/PDFs/ACIA_Science_Chapters_Final/ACIA_Ch05_Final.pdf.

WHO. 2002. Global Solar UV Index: A Practical Guide, 28 pp., published by World Health Organization (WHO), World Meteorological Organization (WMO), United Nations Environment Programme (UNEP) and the International Commission on Non-Ionizing Radiation Protection (ICNIRP), WHO, Geneva, Switzerland, ISBN 9241590076. Available at: http://www.who.int/uv/publications/en/GlobalUVI.pdf.

Carbon Dioxide (CO_2) and Methane (CH_4)

L. Bruhwiler and E. Dlugokencky

NOAA, Earth System Research Laboratory (ESRL)
Global Monitoring Division, Boulder, CO, USA

November 11, 2012

Highlights

- Global increases in greenhouse gases from human sources continue.
- NOAA ESRL weekly air samples from multiple Arctic sites (north of 53°N) show that, as yet, there is no direct atmospheric evidence that either Arctic emissions of CH_4, or the net balance of C from CO_2, are changing.

Carbon dioxide (CO_2) and methane (CH_4) are the two largest contributors to radiative forcing by long-lived greenhouse gases, accounting for about 82% of the total (2.32 out of 2.84 W m^{-2} in 2011; see: http://www.esrl.noaa.gov/gmd/aggi/). Both these greenhouse gases have long atmospheric residence times; the residence time of CH_4 is about a decade due to photochemical loss (Forster et al., 2007), and for CO_2, whose loss from the atmosphere is controlled by many processes with different time scales, it is much longer (Tans, 2010). CO_2 released in the past and future decade will remain a global warming driver for most of the century. CH_4 is a potent greenhouse gas; it causes about 25 times more warming over 100 years than emission of an equal mass of CO_2 (Forster et al. 2007).

The topmost 3 m of ice-rich permafrost is estimated to hold an amount of carbon about equal to the carbon in known coal reserves, ~1000 PgC (where 1 Petagram (Pg) = 10^{15} g) (Tarnocai et al., 2009). If Arctic permafrost thaws, then the carbon stored in Arctic soils will decay and be emitted to the atmosphere as some combination of CO_2 and CH_4. If Arctic soils remain water-saturated, a larger fraction of carbon will be emitted as CH_4 as a result of anaerobic microbial activity. On the other hand, if Arctic soils drain as permafrost thaws, a larger proportion of carbon will be emitted as CO_2. Currently, the Arctic is thought to be a small sink for atmospheric CO_2 (McGuire et al., 2009). Model studies that attempt to describe permafrost dynamics as the atmospheric warms in the future suggest that even with a more productive Arctic biosphere capable of taking up more carbon, the Arctic will become a net source of carbon sometime in the first half of the 21st Century (e.g. Schaefer et al., 2011).

Shallow Arctic sea sediments, especially offshore of Siberia, are thought to be rich in organic matter that may be emitted to the atmosphere as the seawater temperature increases. In addition, ice hydrates deep within the Arctic sea shelf sediments may destabilize due to warmer water temperatures and release methane to the atmosphere. Currently, the amount of CH_4 emitted to the atmosphere by these processes is thought to be about one third of that emitted from wetlands in the Arctic tundra (Shakova et al., 2010; McGuire et al., 2012); however, the sparseness of atmospheric observations makes this difficult to confirm.

It is important to monitor Arctic greenhouse gases as they have great potential to influence global climate through positive feedbacks. Consequently, NOAA ESRL currently measures

atmospheric CO_2 and CH_4 weekly in air samples from 6 Arctic sites (north of 53°N, **Table 1.1**). This is down from 8 sites in 2011; sites in the Baltic Sea and Station M in the North Atlantic were discontinued due to budget cuts.

Table 1.1. NOAA ESRL measures CO_2 and CH_4 in air samples taken at these eight sites. All are classified as Arctic, i.e., north of 53°N. The BAL and STM sites were discontinued in 2011.

Site	Latitude (°N)	Longitude (°)*
ALT: Alert, Nunavut, Canada	82.45	-62.51
BAL: Baltic Sea, Poland	55.35	17.22
BRW: Barrow, Alaska, USA	71.32	-156.61
CBA: Cold Bay, Alaska, USA	55.21	-162.72
ICE: Storhofdi, Vestmannaeyjar, Iceland	63.40	-20.29
STM: Ocean Station M, Norway	66.00	2.00
SUM: Summit, Greenland	72.58	-38.48
ZEP: Ny Ålesund, Svalbard, Norway	78.90	11.88

*Positive and negative values are east and west of the Greenwich meridian, respectively.

Figures 1.13 and **1.14** show time series of CO_2 and CH_4 at polar northern latitudes (53 to 90°N) averaged over all NOAA network sites. Both species show large annual cycles related to summertime uptake by the land biosphere in the case of CO_2 and emissions from wetlands and other biogenic sources in the case of CH_4. Note that uptake of CO_2 and biogenic emissions of methane are largest in the warm months, so the seasonal cycles are approximately out of phase. Over many years, the behavior of CO_2 is dominated by a positive trend related to fossil fuel combustion that occurs mostly in the populated mid-latitudes. The recent upward trend in CH_4 is thought to be related mainly to growth of natural emissions in the tropics after a prolonged period of lower-than-average precipitation (Dlugokencky et al., 2009; Bousquet et al., 2011).

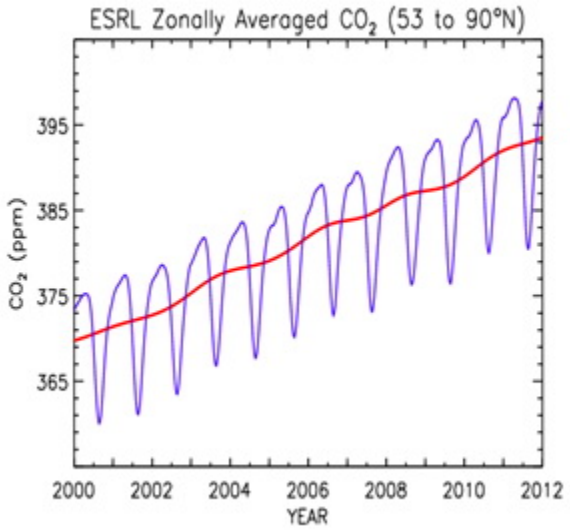

Fig. 1.13. Zonal mean abundance of CO_2 in parts per million (ppm) for the northern and polar region (53° to 90°N, PNH) determined from the NOAA ESRL global cooperative air sampling network. Data are available at http://www.esrl.noaa.gov/gmd/dv/iadv/.

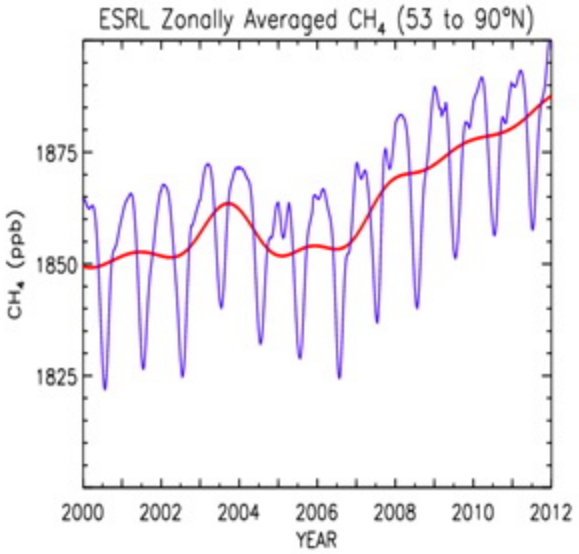

Fig. 1.14. Zonal mean abundance of CH_4 in parts per billion (ppb) for the polar northern (53° to 90°N, PNH) region determined from the NOAA ESRL global cooperative air sampling network. Data are available at http://www.esrl.noaa.gov/gmd/dv/iadv/.

Figure 1.15. shows the inter-polar difference of CH_4 (IPD, defined as the difference in zonally-averaged CH_4 annual mean abundances for polar zones covering 53° to 90° in each hemisphere). The IPD is a potential indicator of changes in Arctic CH_4 emissions because there are no significant sources in southern polar latitudes, and trends in mid-latitude sources are transported to high latitudes of both hemispheres; therefore, trends in IPD mainly reflect changes in Arctic emissions (e.g., Dlugokencky at al., 2003). No upward trend in IPD is seen for CH_4 since the 1990s, suggesting that Arctic emissions have not been increasing in recent years.

The economic collapse of the former Soviet Union from 1991 to 1992 shows the sensitivity of IPD to changing emissions of CH_4. During this period, high northern latitude emissions are estimated to have decreased by ~10 Tg CH_4 yr^{-1} (where 1 Teragram (Tg) = 10^{12} g), and IPD decreased by ~10 ppb [parts per billion]) (Dlugokencky et al., 2003), but has not recovered. As yet, multi-decadal observations of atmospheric CH_4 do not suggest that Arctic emissions are not increasing rapidly. Trends in CO_2 emission or uptake are difficult to detect because the global budget is dominated by the global increase due to fossil fuels. However, given the large inter-annual variability, trends in emissions of both species that are too small to be detected by the atmospheric network over several decades cannot be ruled out.

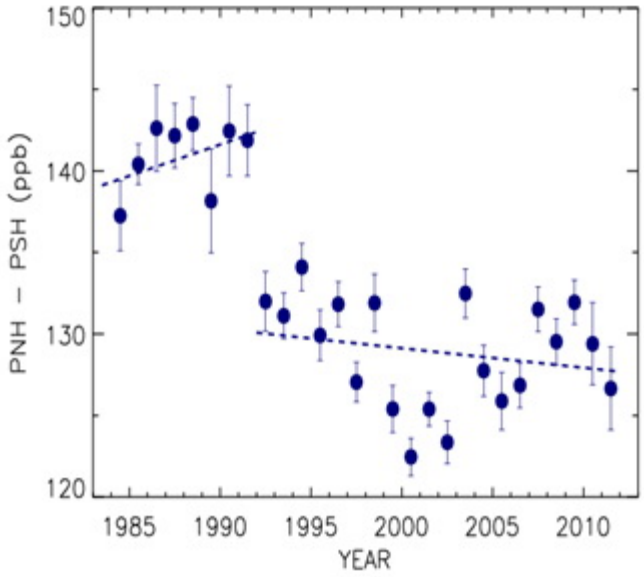

Fig. 1.15. Inter-polar difference (IPD) in annual mean abundance of CH_4 in parts per billion (ppb) for polar northern (53° to 90°N, PNH) and polar southern (53° to 90°S, PSH) regions determined from the NOAA ESRL global cooperative air sampling network. The trend lines (broken lines) emphasize the change in Arctic emissions that occurred in the early 1990s, possibly related to changes in anthropogenic emissions in the former Soviet Union. Data are available at http://www.esrl.noaa.gov/gmd/dv/iadv/.

References

Bousquet, P., B. Ringeval, I. Pison, E. J. Dlugokencky, E.-G. Brunke, C. Carouge, F. Chevallier, A. Fortems-Cheiney, C. Frankenberg, D. A. Hauglustaine, P. B. Krummel, R. L. Langenfelds, M. Ramonet, M. Schmidt, L. P. Steele, S. Szopa, C. Yver, N. Viovy and P. Ciais. 2011. Source attribution of the changes in atmospheric methane for 2006-2008. *Atmos. Chem. Phys.*, 11, 3689-3700, doi:10.5194/acp-11-3689-2011.

Dlugokencky, E. J., S. Houweling, L. Bruhwiler, K. A. Masarie, P. M. Lang, J. B. Miller and P. P. Tans. 2003. Atmospheric methane levels off: Temporary pause or a new steady-state? *Geophys. Res. Lett.*, 30, 1992, doi:10.1029/2003GL018126.

Dlugokencky E.J., L. Bruhwiler, J. W. C. White, L. K. Emmons, P. C. Novelli, S. A. Montzka, K. A. Masarie, P. M. Lang, A. M. Crotwell, J. B. Miller and L. V. Gatti. 2009. Observational

constraints on recent increases in the atmospheric CH_4 burden. *Geophys. Res. Lett.*, 36, L18803, doi:10.1029/2009GL039780.

Forster, P., V. Ramaswamy, P. Artaxo, T. Berntsen, R. Betts, D.W. Fahey, J. Haywood, J. Lean, D.C. Lowe, G. Myhre, J. Nganga, R. Prinn, G. Raga, M. Schulz and R. Van Dorland. 2007. Changes in Atmospheric Constituents and in Radiative Forcing. In *Climate Change 2007: The Physical Science Basis. Contribution of Working Group I to the Fourth Assessment Report of the Intergovernmental Panel on Climate Change*, S. Solomon, D. Qin, M. Manning, Z. Chen, M. Marquis, K. B. Averyt, M. Tignor and H. L. Miller (eds.), Cambridge University Press, Cambridge, UK and New York, NY, USA.

McGuire, D. A., L. G. Anderson, T. R. Christensen, S. Dallimore, L. Guo, D. J. Hayes, M. Heimann, T. D. Lorenson, R. W. Macdonald and N. Roulet. 2009. Sensitivity of the carbon cycle in the Arctic to climate change. *Ecol. Monogr.*, 79(4), 523-555.

McGuire, D. A., T. R. Christensen, D. Hayes, A. Heroult, E. Euskirchen, J. S. Kimball, C. Koven, P. Lafleur, P. A. Miller, W. Oechel, P. Peylin, M. Williams and Y. Yi. 2012. An assessment of the carbon balance of Arctic tundra: Comparisons among observations, process models and atmospheric inversions. *Biogeosci*., 9, 3185-3204, doi:10.5194/bg-9-3185-2012.

Schaefer, K., T. Zhang, L. Brujwiler and A. P. Barrett. 2011. Amount and timing of permafrost carbon release in response to climate warming. *Tellus*, 63(2), 165-180, doi: 10.1111/j.1600-0889.2011.00527.x.

Shakhova, N, I. Semiletov, A. Salyuk, V. Yusupov, D. Kosmach and Ö. Gustafsson. 2010. Extensive methane venting to the atmosphere from sediments of the East Siberian Arctic shelf. *Science*, 327, 1246-1250, doi:10.1126/science.1182221.

Tans, P. 2009. An accounting of the observed increase in oceanic and atmospheric CO_2 and an outlook for the future. *Oceanogr.*, 22(4), 26-35.

Tarnocai, C., J. G. Canadell, E. A. G. Schuur, P. Kuhry, G. Mazhitova and S. Zimov. 2009. Soil organic carbon pools in the northern circumpolar permafrost region. *Global Biogeochem. Cycles*, 23, GB2023, doi:10.1029/2008GB003327.

Sea Ice and Ocean Summary

Section Coordinator: Mary-Louise Timmermans

Yale University, New Haven, USA

November 15, 2012

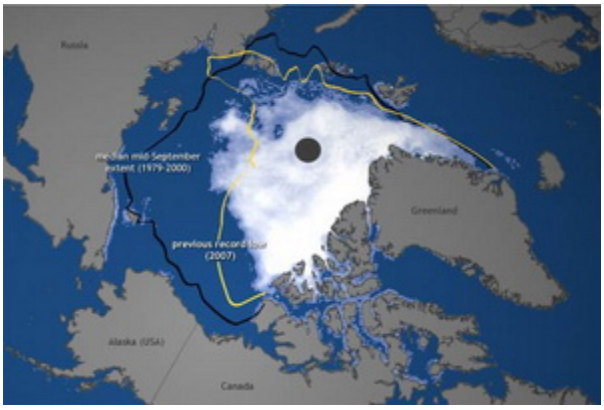

Arctic sea ice extent on Sept 16, 2012 (new record low). Black line is historical median extent in mid-Sept and yellow line is previous record low in 2007. Large version available from NOAA Climate.gov.

Sea ice extent in September 2012 reached the lowest observed in the satellite record (1979-present). A related decline in the extent of the relatively thick multi-year ice, which forms in the central Arctic Basin, continued. The record low minimum extent occurred despite a relatively high maximum sea-ice extent in March 2012, which reflected extensive ice in the Bering Sea (Pacific Arctic). March to September 2012 showed the largest decline in sea ice between the maximum and minimum extents during the satellite record. August 2012 was a period of exceptionally rapid ice loss, with accelerated decline during an intense storm in early August in the East Siberian and Chukchi seas (Pacific Arctic). Ice retreated significantly around the perimeter of the ice pack, in contrast to the preceding two summers when a tongue of older ice in the East Siberian Sea persisted through the summer. While most Arctic boundary regions displayed anomalously warm sea-surface ocean temperatures in 2012 as a result of increased solar absorption into the upper ocean in large open-water regions, a strong cold anomaly was evident in August in the Chukchi Sea. This appears to have been related to the persistence of sea ice in this area even as the main body of the pack ice retreated northward. Relatively high freshwater and heat contents, with values comparable to 2011, persisted in the Beaufort Gyre in 2012. Pacific Water volume flux continued to increase, with flow through the Bering Strait in 2011 being about 50% higher than in 2001. The 2011 Bering Strait heat flux was comparable to the previous record high in 2007. The large-scale wind-driven sea ice and ocean circulation was anticyclonic (clockwise) in the Canadian sector of the Arctic between September 2011 and August 2012, while cyclonic circulation in the marginal seas drove intensified sea ice and surface water flow from the Kara and Laptev seas northward and then out of the Arctic Ocean via Fram Strait (Atlantic Arctic). Sustained sea-level rise, resulting from a combination of ocean surface warming and wind-driven dynamics, was observed through 2011.

Sea Ice

D. Perovich[1,2], W. Meier[3], M. Tschudi[4], S. Gerland[5], J. Richter-Menge[1]

[1]ERDC - CRREL, 72 Lyme Road, Hanover, NH, USA
[2]Thayer School of Engineering, Dartmouth College, Hanover, NH, USA
[3]National Snow and Ice Data Center, University of Colorado, Boulder, CO, USA
[4]Aerospace Engineering Sciences, University of Colorado, Boulder, CO, USA
[5]Norwegian Polar Institute, Fram Centre,Tromsø Norway

December 3, 2012

Highlights

- Record minimum Arctic sea ice extent occurred in September 2012; The lowest observed during the satellite record (1979-present) and 49% below the 1979-2000 average minimum.
- 2012 had the largest loss of ice between the March maximum and September minimum extents during the satellite record.
- The extent of multi-year ice continued to decrease.
- A severe storm in August accelerated ice loss in the Pacific Arctic.

Sea ice extent

Sea ice extent is used to describe the state of the Arctic sea ice cover. There is an accurate record of extent since 1979, determined from satellite-based passive microwave instruments. There are two months each year that are of particular interest: September, at the end of summer, when the ice reaches its annual minimum extent, and March, at the end of winter, when the ice is at its maximum extent. Ice extent in March 2012 and September 2012 are illustrated in **Fig. 2.1**.

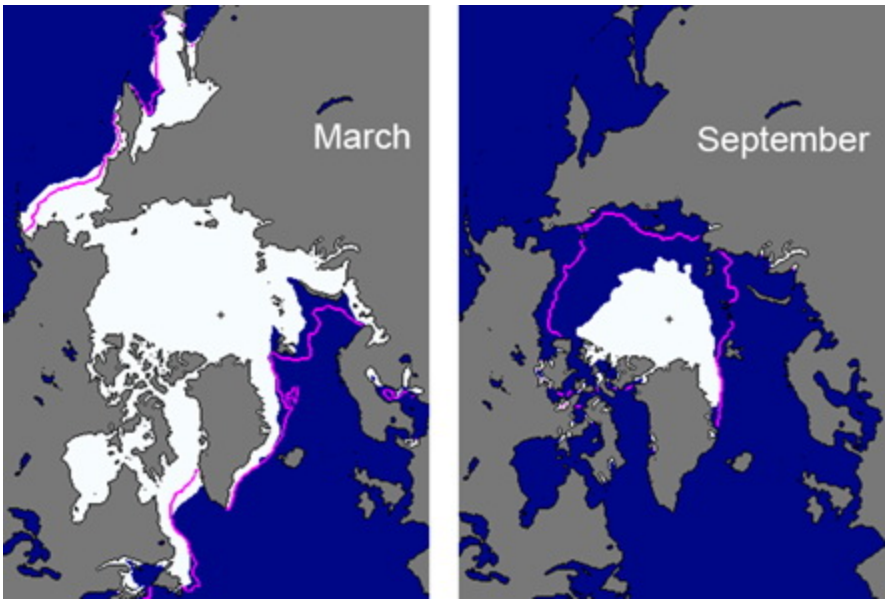

Fig. 2.1. Sea ice extent in March 2012 (left) and September 2012 (right), illustrating the respective monthly averages during the winter maximum and summer minimum extents. The magenta line indicates the median maximum and minimum ice extents in March and September, respectively, during the period 1979-2000. Maps are from the National Snow and Ice Data Center Sea Ice Index: nsidc.org/data/seaice_index.

Based on estimates produced by the National Snow and Ice Data Center, on September 16, 2012 the sea ice cover reached its minimum extent for the year of 3.41 million km^2. This was the lowest in the satellite record; 18% lower than in 2007, when the previous record of 4.17 million km^2 was recorded (**Fig. 2.2**). Overall, this year's minimum was 3.29 million km^2 (49%) below the 1979-2000 average minimum of 6.71 million km^2. The last six years, 2007-2012, have the six lowest minimum extents since satellite observations began in 1979.

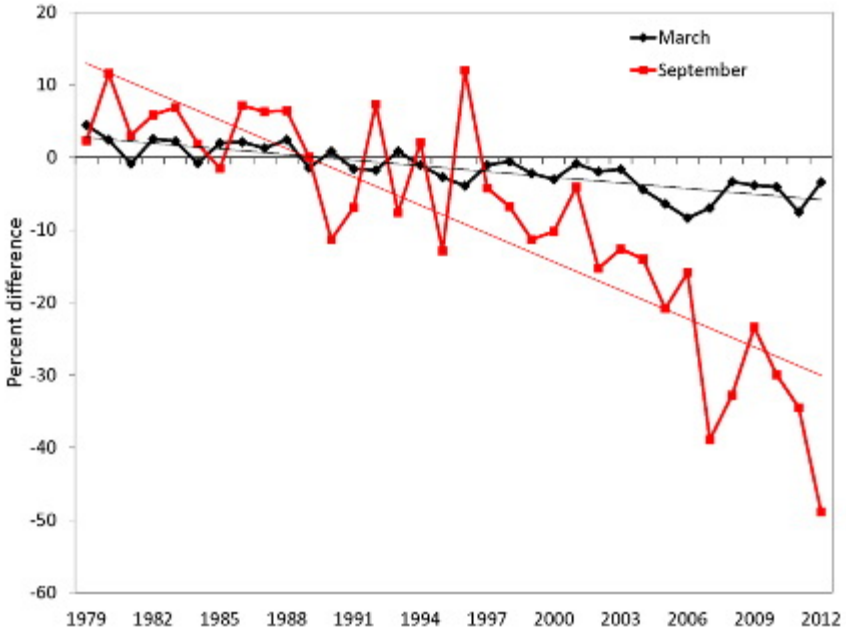

Fig. 2.2. Time series of ice extent anomalies in March (the month of ice extent maximum) and September (the month of ice extent minimum). The anomaly value for each year is the difference (in %) in ice extent relative to the mean values for the period 1979-2000. The thin black and red lines are least squares linear regression lines with slopes indicating ice losses of -2.6% and -13.0% per decade in March and September, respectively.

In March 2012 ice extent reached a maximum value of 15.24 million km^2 (**Fig. 2.2**), 4% below the 1979-2000 average. This was the highest maximum in 9 years, but 2004-2012 has the nine lowest maximum extents since 1979. The relatively high maximum extent in March 2012 was due to conditions in the Bering Sea, where ice extent was at or near record levels throughout the winter and spring.

After reaching maximum extent, the seasonal decline began slowly, particularly in the Bering Sea, and around mid-April, extent was close to the 1979-2000 average for the time of year. However, soon after that the decline accelerated and was faster than normal through much of the summer. August 2012 was a period of particularly rapid ice loss, in part due to a storm that passed through the region at the beginning of the month (see below, and the *Air Temperature, Atmospheric Circulation and Clouds* essay). Overall, 11.83 million km^2 of ice was lost between the maximum and minimum extents. This is the largest seasonal decline in the record and 1 million km^2 more than in any previous year.

Sea ice extent is decreasing in all months and virtually all regions (the exception being the Bering Sea during winter). The September monthly average trend is now -91,600 km^2 per year, or -13.0 % per decade relative to the 1979-2000 average (**Fig. 2.2**). The magnitude of the trend has increased every year since 2001. Trends are smaller during March, but still decreasing and statistically significant. The March trend is -2.6% per decade (**Fig. 2.2**).

Average ice extents for each month are presented in **Fig. 2.3**. Three time periods are compared; the reference period 1979-2000, 2001 to 2006, and the last six years (2007-2012) beginning with the previous record minimum of 2007. The 1979-2000 period has the largest ice extent for every month, with the greatest difference between the time periods occurring in September. Comparing the two 21st Century periods shows that ice extent is similar in winter and spring, but summer values are significantly lower in 2007-2012.

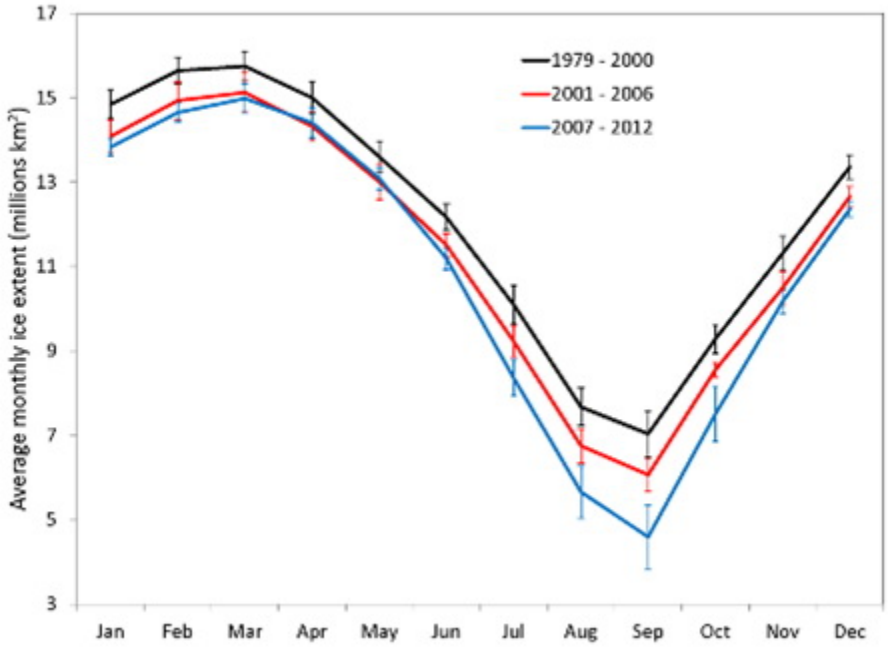

Fig. 2.3. Mean monthly sea ice extent for the reference period 1979-2000 (thick black line) and for the 2001-2006 (red line) and 2007-2012 (blue line). The vertical bars represent one standard deviation about the mean value for each month.

Spatial distribution of sea ice

In 2007 persistent winds through the summer, created by an Arctic dipole circulation pattern (see Fig. A3 in Arctic Report Card 2007, and **Fig. 1.5** in the *Air Temperature, Atmospheric Circulation and Clouds* essay), resulted in a compact ice cover and an ice edge far to the north on the Pacific side of the Arctic. However, the circulation also pushed ice onto the coast in the Laptev Sea, completely blocking the Northern Sea Route. In the years since 2007, the pattern of ice loss has varied, but a tongue of older ice in the East Siberian Sea has persisted through the summer. This tongue was particularly evident in 2010 and 2011. In 2012 that tongue of ice mostly melted away, aided by the August storm, and ice retreated significantly around the entire perimeter of the ice pack (**Fig. 2.1**, right panel). This includes the Atlantic side, north of Svalbard, where extents had been near normal in recent years. Overall, compared to 2007 there was more ice this year in the central Arctic north of the Bering Strait, but less ice nearly everywhere else.

Age of the ice

The age of the ice is another key descriptor of the state of the sea ice cover. Older ice tends to be thicker and thus more resilient to changes in atmospheric and oceanic forcing than younger ice. The age of the ice is determined using satellite observations and drifting buoy records to track ice parcels over several years (Tschudi et al., 2010). This method has been used to provide a record of ice age since the early 1980s (**Fig. 2.4**). The distribution of ice of different ages illustrates the extensive loss in recent years of the older ice types (Maslanik et al., 2011). Analysis of the time series of areal coverage by age category indicates the continued recent loss of the oldest ice types, which accelerated starting in 2005 (Maslanik et al., 2011). For the month of March, older ice (4 years and older) has decreased from 26% of the ice cover in 1988 to 19% in 2005 and to 7% in 2012. This represents a loss of 1.71 million km^2 since 2005. In March 1988, 58% of the ice pack was composed of first-year ice (ice that has not survived a melt season). In March 2012, first-year ice dominated the pack (75%). Younger ice is typically thinner than older ice (e.g., Maslanik et al., 2007), so the current ice pack is likely thinner on average than it was in 1988. Note that, from March 2011 to March 2012, much of the three-year-old ice north of the Canadian Archipelago survived the melt season, resulting in an increase in four-year-old ice in March 2012 (5%, compared to 2% in March 2011). This increase was directly associated with a reduction in the fraction of three-year-old ice, which decreased from 9 to 7%.

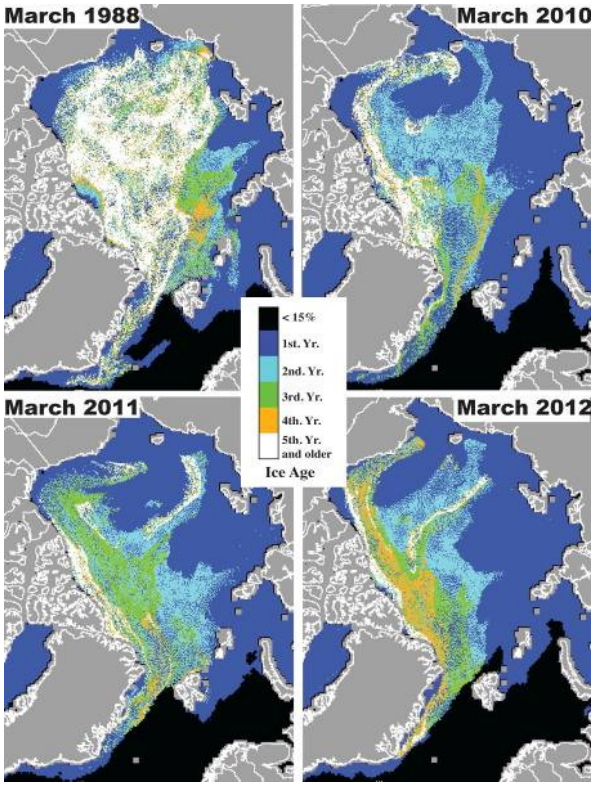

Fig. 2.4. Sea ice age in the first week of March 1988, 2010, 2011 and 2012, determined using satellite observations and drifting buoy records to track the movement of ice floes. Figure courtesy of J. Maslanik and M. Tschudi.

Impact of an August Storm

A severe storm in the Chukchi and East Siberian seas in early August 2012 (**Fig. 2.5**) accelerated ice loss and helped to quickly remove ice from the region (also see the essay on *Air Temperature, Atmospheric Circulation and Clouds*). As **Fig. 2.4** indicates, most of this region was covered by first year ice. The storm blew the ice southward into warmer water, where satellite observations indicated that it melted in a few weeks (**Fig. 2.5**). As the ice melted and diverged, ice concentration quickly fell below the detection limit of passive microwave sensors, though small amounts of ice were observed for a couple of weeks afterwards by operational ice analysts using other imagery.

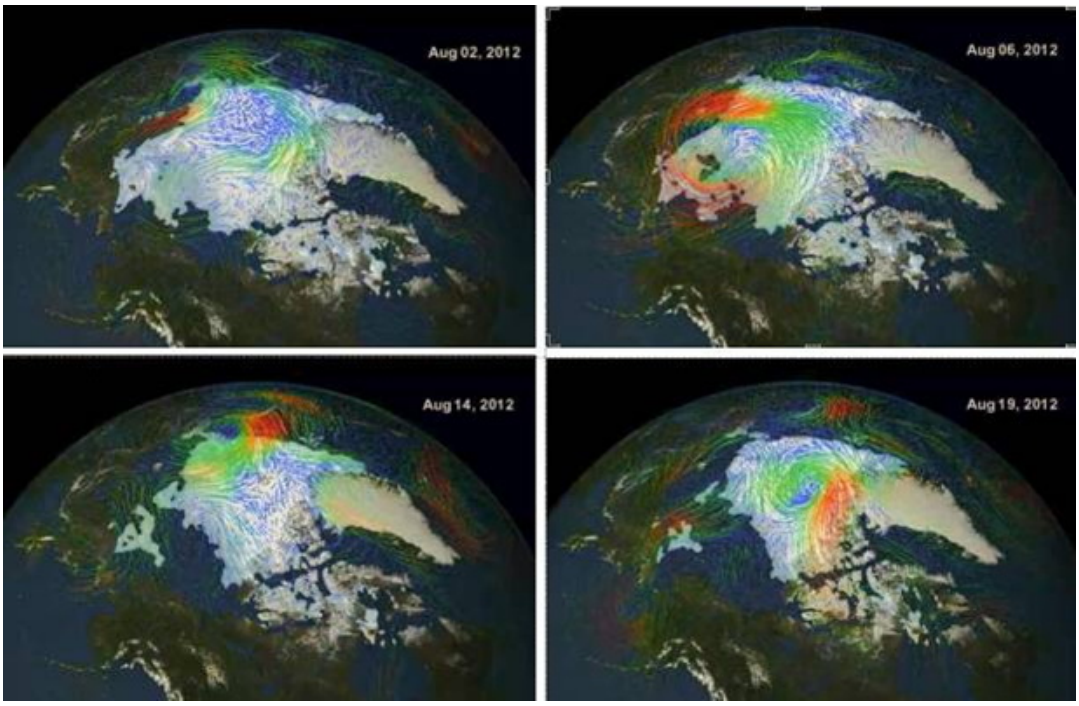

Fig. 2.5. Storm-induced breakup and melt of sea ice in the Western Arctic. The sequence illustrates breakup of ice and movement of ice southward into warmer water. Credit: NASA.

References

Maslanik J. A., C. Fowler, J. Stroeve, S. Drobot, J. Zwally, D. Yi and W. Emery. 2007. A younger, thinner Arctic ice cover: Increased potential for rapid, extensive sea-ice loss. *Geophys. Res. Lett.*, 34, L24501, doi:10.1029/2007GL032043.

Maslanik, J., J. Stroeve, C. Fowler and W. Emery. 2011. Distribution and trends in Arctic sea ice age through spring 2011. *Geophys. Res. Lett.*, 38, L13502, doi:10.1029/2011GL047735.

Tschudi, M. A., Fowler, C., Maslanik and J. A., Stroeve. 2010. Tracking the movement and changing surface characteristics of Arctic sea ice. *IEEE J. Selected Topics in Earth Obs. and Rem. Sens.*, 10.1109/JSTARS.2010.2048305.

Ocean

M.-L. Timmermans[1], A. Proshutinsky[2], I. Ashik[3], A. Beszczynska-Moeller[4], E. Carmack[5], I. Frolov[3], R. Ingvaldsen[6], M. Itoh[7], J. Jackson[11], Y. Kawaguchi[7], T. Kikuchi[7], R. Krishfield[2], F. McLaughlin[5], H. Loeng[6], S. Nishino[7], R. Pickart[2], B. Rabe[4], B. Rudels[8], I. Semiletov[9], U. Schauer[4], N. Shakhova[9], K. Shimada[10], V. Sokolov[3], M. Steele[11], J. Toole[2], T. Weingartner[12], W. Williams[5], R. Woodgate[11], M. Yamamoto-Kawai[10], S. Zimmermann[5]

[1]Yale University, New Haven, USA
[2]Woods Hole Oceanographic Institution, Woods Hole, MA, USA
[3]Arctic and Antarctic Research Institute, St. Petersburg, Russia
[4]Alfred Wegener Institute, Bremerhaven, Germany
[5]Institute of Ocean Sciences, Sidney, Canada
[6]Institute of Marine Research, Bergen, Norway
[7]Japan Agency for Marine-Earth Science and Technology, Tokyo, Japan
[8]Finish Institute of Marine Research, Helsinki, Finland
[9]International Arctic Research Center, University of Alaska Fairbanks, Fairbanks, USA
[10]Tokyo University of Marine Science and Technology, Tokyo, Japan
[11]Applied Physics Laboratory, University of Washington, Seattle, USA
[12] University of Alaska Fairbanks, Fairbanks, USA

November 24, 2012

Highlights

- The 2011 annual wind-driven circulation regime was anticyclonic, supporting continued high volumes of freshwater in the Beaufort Gyre region and consistent with a 2012 shift of the Beaufort Gyre freshwater center to the west.
- Sea surface temperatures in summer continue to be anomalously warm at the ice-free margins, while upper ocean temperature and salinity show significant interannual variability with no clear trends.
- Oceanic fluxes of volume and heat through the Bering Strait increased by ~50% between 2001 and 2011.
- Sea level exhibits decadal variability with a reduced correlation to sea level atmospheric pressure since the late 1990s.

Wind driven circulation

Sea ice and ocean surface layer circulation are closely coupled and primarily wind-driven (e.g. Proshutinsky and Johnson, 1997). The Proshutinsky and Johnson model is an effective tool to represent ice and upper-ocean velocities across the entire Arctic. Comparisons between model ice drift and daily-averaged buoy velocities for 39 Ice-Tethered Profilers drifting in different parts of the Arctic basin between 2004 and 2010 indicate average correlation coefficients (r values) between simulated and observed velocity components are 0.8, with no significant regional or temporal differences within the Arctic basin (see Timmermans et al., 2011).

In 2011 the annual simulated wind-driven ice and surface ocean circulation assimilated from satellite and drifting buoy data was anticyclonic (**Fig. 2.6**) with a well-organized clockwise Beaufort Gyre (BG) over the entire Canada Basin. To examine this in context with the most recent wind-driven circulation, we compare the average circulation pattern for September 2011-August 2012 to the average over the preceding 12 months (**Fig. 2.7**).

September 2010-August 2011. The overall sense of the ice and surface ocean circulation during September 2010-August 2011 was similar to the 2011 average (**Fig. 2.6**). Sea ice and surface freshwater transport through Fram Strait originated from the Laptev Sea and in a strong eastward current off northern Greenland. Surface waters from the Laptev Sea were also partly swept into the enlarged BG but flow was directed primarily towards Fram Strait. Near-surface waters and sea ice from the Chukchi and East Siberian Seas were driven westward by winds (**Figs. 2.6 and 2.7** [left panel]).

September 2011-August 2012. The wind-driven anticyclonic BG circulation between September 2011 and August 2012 was weaker than the average over the preceding 12 months. In 2011-2012, the somewhat weaker wind stress curl over the BG does not appear to have affected freshwater accumulation by Ekman transport, i.e., in 2012 there was no evidence of reduced freshwater in the BG (**Fig. 2.11**). However, the circulation patterns are consistent with the slight shift of the BG freshwater center to the west in 2011-2012. That same year, cyclonic circulation was intensified over the Norwegian, Barents and Kara seas, and partially over the Laptev Sea. This drove intensified sea ice and surface water flow from the Kara and Laptev seas northward and then out of the Arctic Ocean via Fram Strait. This wind driving forced earlier ice-free conditions in these regions, and therefore increased solar absorption into the upper ocean (see **Fig. 2.9** and discussion). In the Beaufort and Chukchi seas, unusually strong westward winds (see **Fig. 1.6** in the *Air Temperature, Atmospheric Circulation and Clouds* essay) resulted in delayed ice loss from the Chukchi Sea and accumulation of sea ice in the vicinity of Wrangel Island, where some ice persisted through the end of summer (see the *Sea Ice* essay for more information on ice conditions in 2012). Surface-ocean temperatures in August were subsequently relatively cool in these regions (see **Fig. 2.9** and discussion).

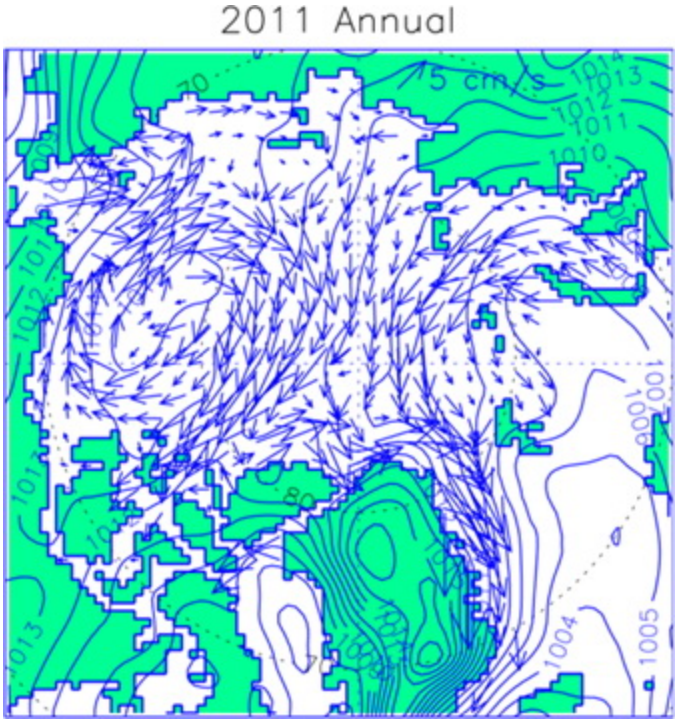

Fig. 2.6. Annual simulated wind-driven ice motion (arrows) and observed sea level atmospheric pressure (hPa, solid lines) for 2011. Results are from a 2D coupled ice-ocean model (Proshutinsky and Johnson, 1997, 2011) forced by wind stresses derived from NCEP/NCAR reanalysis 6-hourly sea level pressure fields.

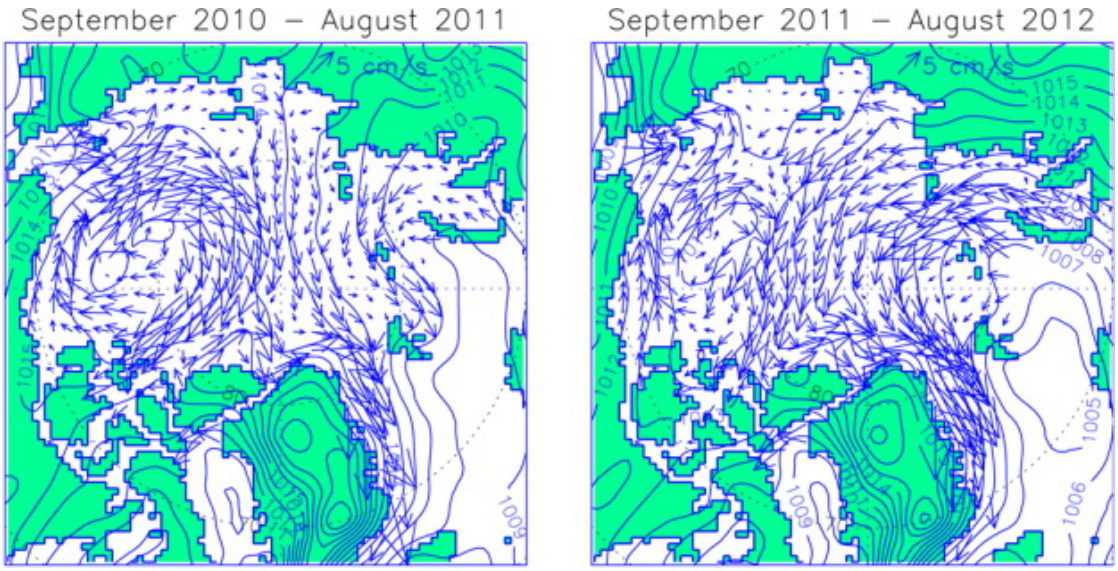

Fig. 2.7. As in Fig. 2.6, but panels indicate the simulated mean wind-driven ice motion for September to August (left: 2010-2011, right: 2011-2012).

Wind-driven circulation in August. Ice drift patterns in summer are critical to summer sea ice conditions and upper-ocean properties, and influence ice conditions over the following seasons. When strong anticyclonic ice drift prevails in the summer (as in 2007), significant volumes of sea

ice can be pushed out of the Arctic Ocean leaving vast areas of open water which can accumulate heat from direct solar radiation and delay autumn freeze up. By contrast, under cyclonic atmospheric forcing (as in 2009), sea ice outflow via Fram Strait can be reduced (**Fig. 2.8**). In these summers with more sea ice, less heat is accumulated in the upper ocean, allowing earlier autumn freeze-up. While the average wind-driven circulation in August over the years 1948 to 2012 is cyclonic (not shown), the August mean wind-driven ice and surface-ocean circulation since 2007 shows significant interannual variability (**Fig. 2.8**). Cyclonic circulation persisted in August 2008, 2009 and 2012, although with weaker Fram Strait outflows in 2008 and 2009.

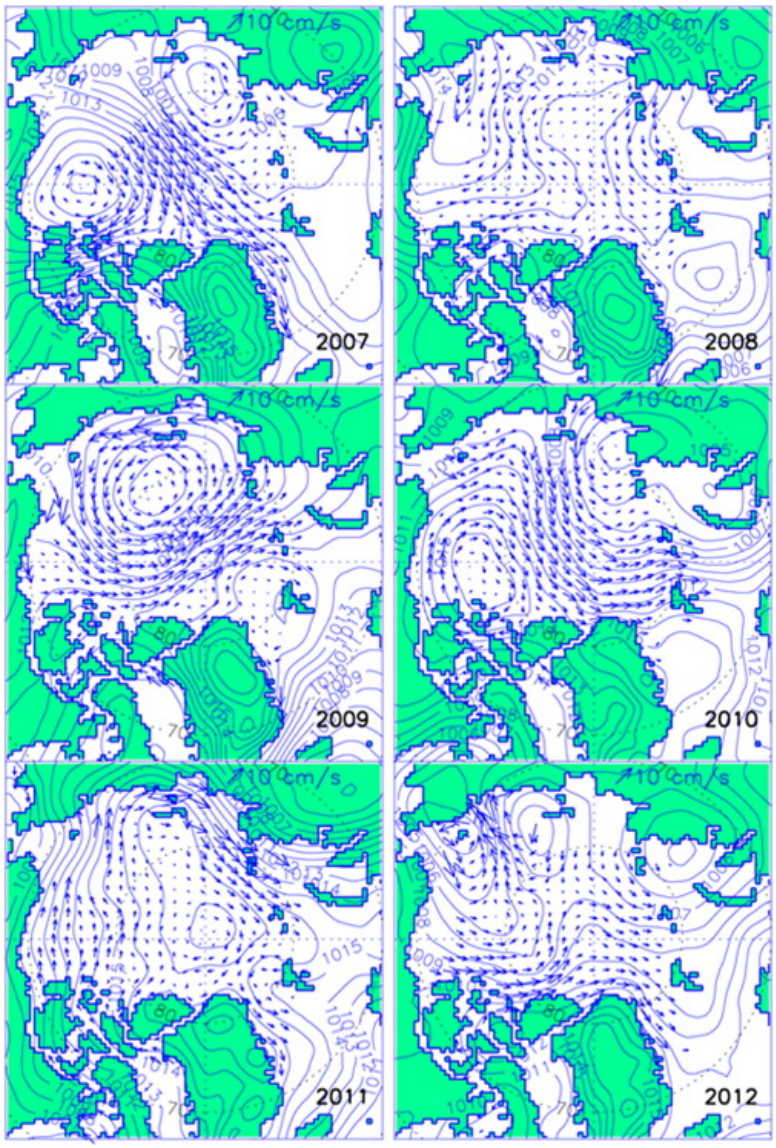

Fig. 2.8. As in Fig. 2.6, but showing simulated monthly mean wind-driven ice motion vectors for regions where ice concentration was >30% on 15 August each year. Sea-ice concentration data are NOAA_OI_SST_V2 data available at the NOAA/OAR/ESRL PSD Web site: http://www.esrl.noaa.gov/psd/.

Ocean Temperature and Salinity

Upper-ocean temperature. Mean sea surface temperature (SST) anomalies in August 2012, relative to the August mean of 1982-2006, were more than 2ºC higher in parts of the Beaufort, Laptev and Kara seas (**Fig. 2.9**). This excess heat, derived from solar radiation, can be stored below a strong summer halocline as a Near Surface Temperature Maximum (NSTM). Jackson et al. (2012) analyzed upper-ocean properties in the Canadian Basin through 2010 to demonstrate that the NSTM loses heat to the surface layer throughout winter, contributing to the surface-ocean heat budget year round.

While most Arctic boundary regions displayed anomalously warm SST in 2012, a strong cold anomaly was evident in the Chukchi Sea. This appears to be related to the unusual sea ice extent pattern, and in particular the persistence of sea ice in this area even as the main ice pack retreated northward (see the *Sea Ice* essay for more information on ice conditions in 2012). Further, a storm during the first week of August (see the essay on *Air Temperature, Atmospheric Circulation and Clouds*) caused rapid degradation of this southern ice patch (see **Fig. 2.5** in the *Sea Ice* essay) and produced very cool SSTs, which persisted for at least a week. Preliminary analysis of *in situ* UpTempO buoy data from this area (http://psc.apl.washington.edu/UpTempO) indicates that SST returned to warmer values with further ice loss and solar absorption, and possibly some contribution from sub-surface heat mixed upward.

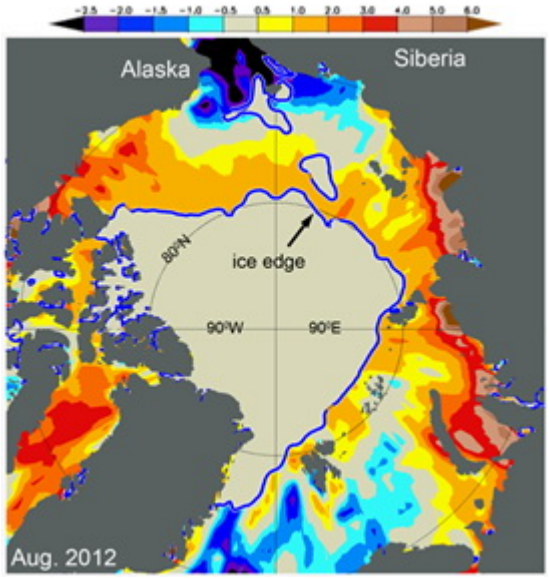

Fig. 2.9. Sea-surface temperature (SST) anomalies in August 2012 relative to the August mean of 1982-2006. The anomalies are derived from satellite data according to Reynolds et al. (2007). The August mean ice edge (blue line) is also shown.

Upper-ocean salinity. Relative to the 1970s Environmental Working Group (EWG) climatology, the major upper-ocean salinity differences in 2011 (**Fig. 2.10**) are saltier central Nansen and

Amundsen basins and a fresher Canada Basin, with the maximum freshwater anomaly centered in the BG. Another key feature of the upper ocean salinity, relative to climatology, is that the upper ocean is generally saltier around the southern boundary of the Canada Basin due to intensified upwelling at the basin boundaries associated with the large-scale wind-driven circulation in 2011 (**Figs. 2.6 and 2.7**). This circulation pattern shifted the position of the upper-ocean front between saltier waters of the Eurasian Basin and fresher Canada Basin waters. The magnitude of salinity difference from climatology is <1 in the Barents Sea, much smaller than in regions of the central Arctic basins. Upper-ocean salinity in 2011 is fresher than the 1970s climatology on the south side of the Barents Sea Opening (BSO) and to the east of Svalbard, while areas of the central Barents Sea and to the north of Svalbard exhibit higher salinity.

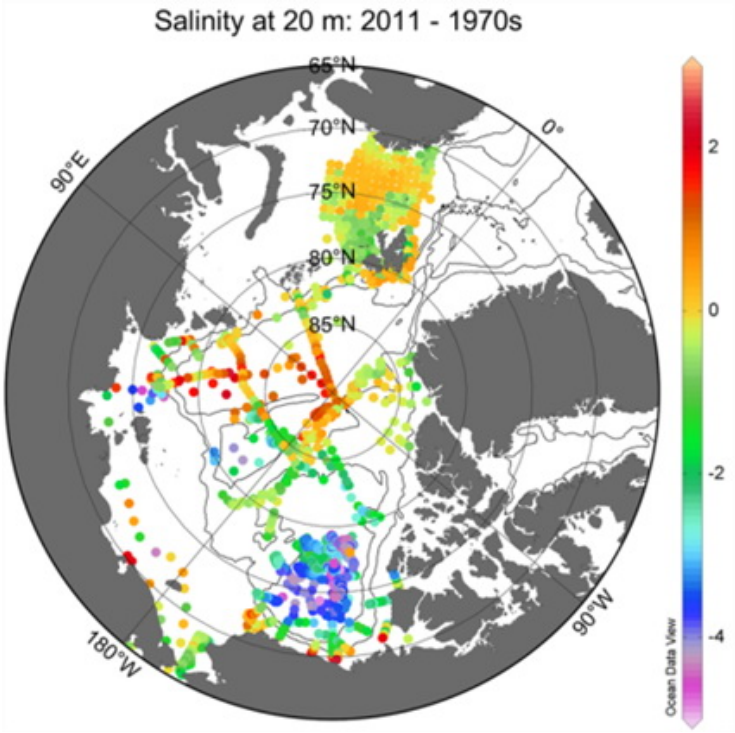

Fig. 2.10. Anomalies of salinity at 20 m depth in 2011 relative to 1970s climatology (see Fig. O.3, Proshutinsky et al. in Arctic Report Card 2011). Contour lines show the 500 m and 2500 m isobaths.

Beaufort Gyre freshwater and heat content. Arctic Ocean freshwater is concentrated in the BG of the Canada Basin, which has accumulated more than 5000 km^3 of freshwater during 2003 to 2012. This is a gain of approximately 25% (update to Proshutinsky et al., 2009) relative to climatology of the 1970s. This strong freshwater accumulation trend in the Beaufort Gyre is linked to an increase in strength over the past decade of the large-scale anticyclonic wind forcing (Proshutinsky et al., 2009; Proshutinsky and Johnson, 1997, updated). Shifts in major freshwater pathways also influence BG freshwater (Morison et al., 2012), while freshwater transported offshore during storms in the southern Beaufort Sea can also account for a significant fraction of the observed year-to-year variability in freshwater content of the BG (Pickart et al., 2012).

In 2012, the BG freshwater content was comparable to that in 2011, with preliminary estimates for the 2012 summer average freshwater content over the Beaufort Gyre region (relative to a salinity of 34.8) of 22.6 m (cf. the 2011 summer average: 21.9 m) (**Fig. 2.11**, right panels). In 2012, the freshwater center appears to have shifted to the northwest, consistent with the large-scale wind forcing (**Fig. 2.7**, right panel). The BG heat content in 2012 also remained roughly comparable to 2011 conditions, with about 25% more heat on average in the summer compared to 1970s values (**Fig. 2.11**, left panels). As further hydrographic data become available from the 2012 field season, heat and freshwater content in the boundary regions in particular will be better constrained.

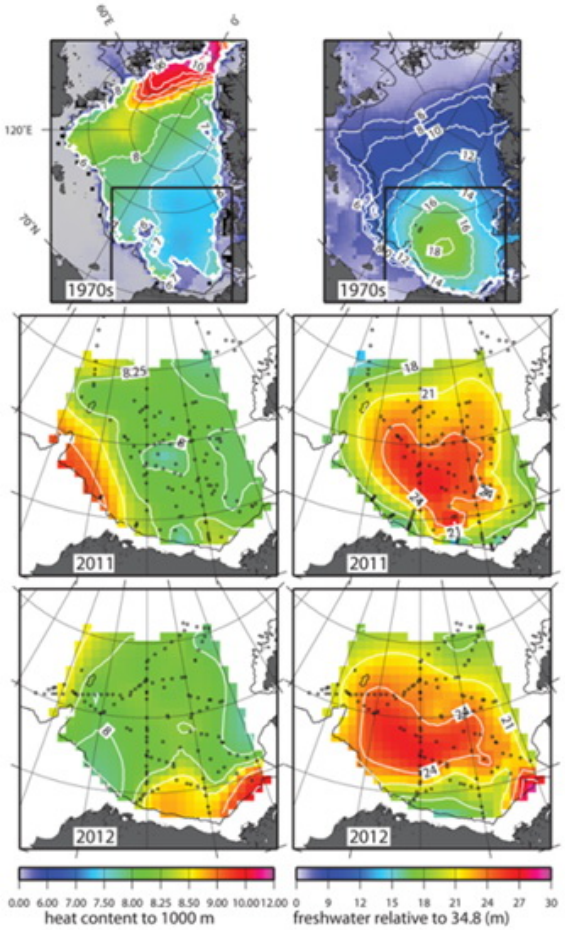

Fig. 2.11. Summer heat content (1×10^9 J m^{-2}) and freshwater content (m). Heat content is calculated relative to freezing temperature in the upper 1000 m of the water column. Freshwater content is calculated relative to a reference salinity of 34.8. The top row shows heat and freshwater content in the Arctic Ocean based on 1970s climatology (Timokhov and Tanis, 1997, 1998). The center and bottom rows show heat and freshwater content in the Beaufort Gyre (the region shown by the black boxes in the top row) based on hydrographic surveys (black dots depict hydrographic station locations) in 2011 and 2012, respectively; data are from the Beaufort Gyre Observing System (BGOS)/Joint Ocean Ice Studies (JOIS) expedition, http://www.whoi.edu/beaufortgyre/.

The Atlantic Water Layer. Warm water of North Atlantic origin, residing at depths below the Arctic halocline, is characterized by temperatures >0°C and salinities >34.5. In 2011, maximum Atlantic Water (AW) Layer temperature anomalies (relative to 1970s climatology) were generally highest on the Eurasian side of the Lomonosov Ridge, with maximum anomalies >2°C in Fram Strait (**Fig. 2.12**). Warming was less pronounced in the Canada Basin than in the Eurasian Basin. There was little to no temperature anomaly (<0.1°C) at the southeast boundary of the Canada Basin nor in the basin boundary regions adjacent to Greenland and the Canadian Archipelago. Atlantic Water temperatures are cooler now than in the 1970s in the vicinity of Nares Strait.

AW properties in the Arctic are regulated by the Atlantic water inflow through Fram Strait and via the BSO. The warmest AW temperatures in Fram Strait were observed in 2006, with a return of maximum temperatures to the long-term mean (2.7°C) by summer 2010 (**Fig. 2.13**). In summer 2011, the mean temperature remained close to that observed in 2010. In 2011 an anomalously warm and saline southward flow of AW was observed in western Fram Strait (not shown), possibly indicating that the warm AW anomaly, which had entered the Arctic Ocean in 2006, returned to Fram Strait after completing a loop in the Eurasian Basin. AW temperatures in the BSO were also maximal in 2006, and declined through 2011. The largest volume fluxes of AW through the BSO were measured in winter 2006, and were relatively low in the following years to 2011, although with strong seasonal variability; the lowest volume fluxes were observed in the spring and summer months.

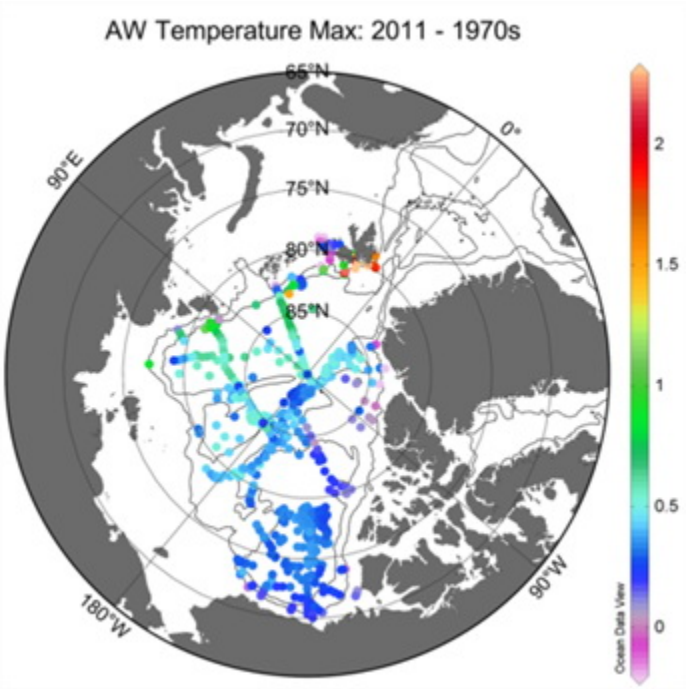

Fig. 2.12. Atlantic Water Layer temperature maximum anomalies in 2011 relative to 1970s climatology (see Fig. O.6, Proshutinsky et al., 2011). Contour lines show the 500 m and 2500 m isobaths.

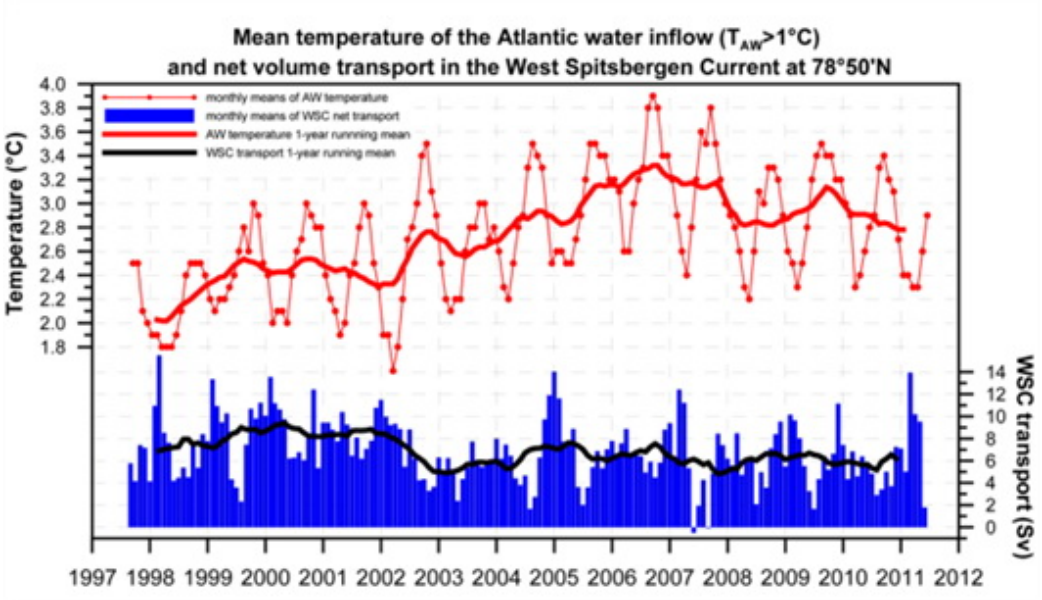

Fig. 2.13. Atlantic water (defined here as having temperatures >1°C) mean temperature and the volume inflow in the West Spitsbergen Current (WSC), northern Fram Strait, measured by a mooring array at 78°50'N maintained since 1997 by the Norwegian Polar Institute and the Alfred Wegener Institute for Polar and Marine Research.

The Pacific Water Layer. The Pacific Water Layer (PWL) in the Arctic originates from the Bering Strait inflow and resides in the Canada Basin at depths between about 50 and 150 m. PWL properties and circulation patterns depend significantly on the prevailing winds, which tended to drive Pacific waters north and westward (**Figs. 2.6 and 2.7**) in 2011. Excessively high Pacific Water (PW) temperatures (warmer than 6°C) were observed on the Chukchi shelf/slope, Northwind Ridge region in September 2010 (during the R/V Mirai expedition; Kawaguchi et al., 2012) and later in winter 2010/2011 measured by Ice-Tethered Profilers. Data from Ice-Tethered Profilers that sampled in the central Canada Basin during 2004-2012 indicate no clear trend in PW maximum temperatures (in the salinity range 29-33) over this time. There is significant interannual variability in both the salinity and temperature of PW in the central basin (temperature changes by as much as 1°C), with warming in recent years broadly congruent with freshening and the warmest temperatures observed in 2007 and 2010.

The properties of the PW inflow through the Bering Strait are measured by year-round in situ moorings, giving some information from 1990 and good coverage from 1999 to present. Recent results from these moorings (Woodgate et al., in press) show that the 2011 flow through the strait is ~1.1 Sv, significantly greater than the generally accepted climatological value of ~0.8 Sv (Roach et al., 1995), almost 50% more than the 2001 value of ~0.7 Sv (Woodgate et al., 2006), and comparable to previous high flow years of 2007 and 2004 (Woodgate et al., 2010).

The 2011 Bering Strait heat flux (~5×10^{20} J relative to -1.9°C, the freezing point of Bering Strait waters) is comparable with the previous record high in 2007. This high heat flux is due to increased flow and warming of the lower layers of the water column in the strait. Interannual change in these lower layer temperatures does not correspond to interannual change in satellite

sea surface temperatures (SSTs) in the region (Woodgate et al., in press). A preliminary estimate of the freshwater flux through the strait relative to a salinity of 34.8 (Woodgate et al., in press) suggests the 2011 annual mean is 3000-3500 km^3, roughly 50% greater than 2001 and 2005 values; interannual variability of the freshwater flux appears to be larger than the interannual variability in the other major freshwater sources to the Arctic (rivers and net precipitation). The ~50% increase in oceanic fluxes through the Bering Strait between 2001 and 2011 is mostly due to an increase in the far-field pressure head forcing of the flow (Woodgate et al., in press).

Sea Level

In 2011, sea level (SL) along the Siberian coast increased relative to previous years (**Fig. 2.14**). This caused an increase, to 2.66 ± 0.41 mm yr^{-1}, in the estimated rate of SL rise since 1954 after correction for glacial isostatic adjustment (Proshutinsky et al., 2004). Until the late 1990s, sea level atmospheric pressure accounted for more than 30% of variability in SL (Proshutinsky et al., 2004) due to the inverse barometer effect. In contrast, from 1997 to 2011, mean SL has generally increased while sea level atmospheric pressure has remained stable. The tendency toward SL rise in this period may be due to steric effects associated with a reduction of sea ice and ocean surface warming (Henry et al., 2012). After 2008, SL decreased to a minimum in 2010 and then increased in 2011. These variable changes likely result from a combination of many forcing factors. One important factor is associated with Ekman transport directed toward coastlines; in 2011, Ekman transport drove positive sea level anomalies along the Siberian coast.

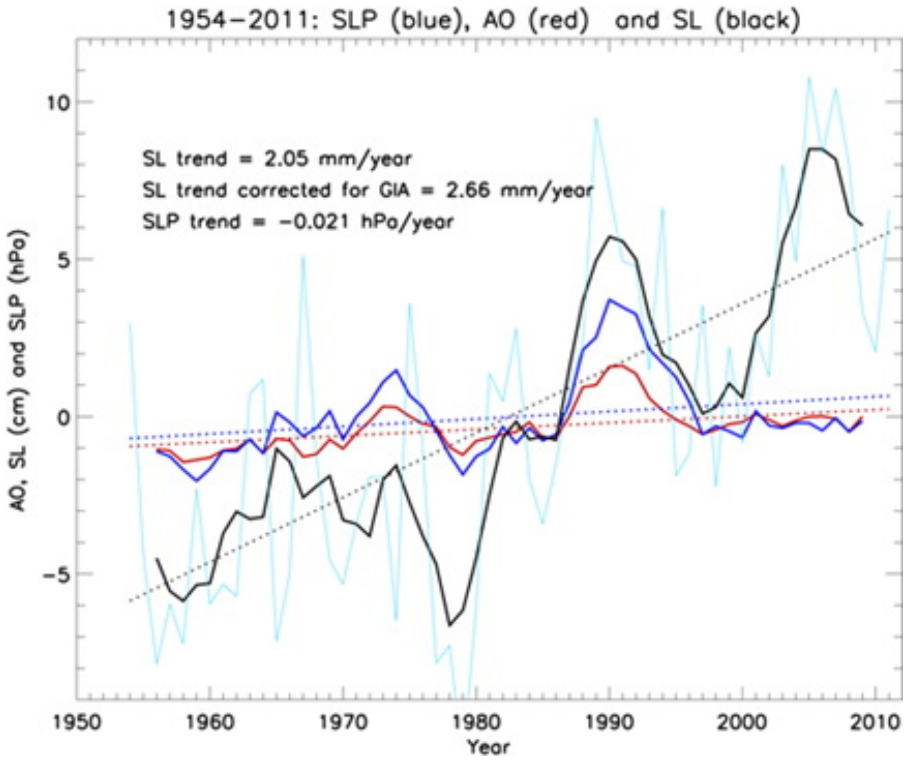

Fig. 2.14. Five-year running mean time series of: annual mean sea level (SL) at nine tide gauge stations located along the coasts of the Kara, Laptev, East Siberian and Chukchi seas (black line; the light blue line shows the annual average); anomalies of the annual mean Arctic Oscillation index (AO, Thompson and Wallace, 1998) multiplied by 3 for easier comparison with other factors (red line); sea surface atmospheric pressure (sea level pressure, SLP) at the North Pole (from NCAR-NCEP reanalysis data) multiplied by -1 to show the inverse barometer effect (dark blue line). Dotted lines depict trends for SL (black), AO (red) and SLP (blue).

References

Henry, O., P. Prandi, W. Llovel, A. Cazenave, S. Jevrejeva, D. Stammer, B. Meyssignac and N. Koldunov. 2012. Tide gauge-based sea level variations since 1950 along the Norwegian and Russian coasts of the Arctic Ocean: Contribution of the steric and mass components. *J. Geophys. Res.*, 117, C06023, doi:10.1029/2011JC007706.

Jackson, J.M., W.J. Williams and E.C. Carmack. 2012. Winter sea-ice melt in the Canada Basin, Arctic Ocean. *Geophys. Res. Lett.*, 39, L03603, doi:10.1029/2011GL050219.

Kawaguchi, Y., M. Itoh and S. Nishino. 2012. Detailed survey of a large baroclinic eddy with extremely high temperatures in the Western Canada Basin. *Deep Sea Res.*, I 66, 90-102, http://dx.doi.org/10.1016/j.dsr.2012.04.006.

Morison, J., R. Kwok, C. Peralta-Ferriz, M. Alkire, I. Rigor, R. Andersen and M. Steele. 2012. Changing Arctic Ocean freshwater pathways. *Nature*, 481, 66-70.

Pickart, R.S., M. Spall and J. Mathis. 2012. Dynamics of upwelling in the Alaskan Beaufort Sea and associated shelf-basin fluxes. Submitted to *Deep Sea Res*.

Proshutinsky A., M.-L. Timmermans, I. Ashik, A. Beszczynska-Moeller, E. Carmack, I. Frolov, R. Krishfield, F. McLaughlin, J. Morison, I. Polyakov, K. Shimada, V. Sokolov, M. Steele, J. Toole and R. Woodgate. 2011. The Arctic (Ocean) [in "State of the Climate in 2010"]. *Bull. Amer. Meteor. Soc.*, 92(6), S145-S148.

Proshutinsky, A. and M. Johnson. 1997. Two circulation regimes of the wind-driven Arctic Ocean. *J. Geophys. Res.*, 102(C9 June 15), 12493-12514.

Proshutinsky, A. and M. Johnson. 2011. Arctic Ocean Oscillation Index (AOO): Interannual and decadal changes of the Arctic climate. *Geophys. Res. Abstr.*, 13, EGU2011-7850, 2011, EGU General Assembly 2011.

Proshutinsky, A., I. M. Ashik, E. N. Dvorkin, S. Hakkinen, R. A. Krishfield and W. R. Peltier. 2004. Secular sea level change in the Russian sector of the Arctic Ocean. *J. Geophys. Res.*, 109, C03042, doi:10.1029/2003JC002007.

Proshutinsky, A., R. Krishfield, M.-L. Timmermans, J. Toole, E. Carmack, F. McLaughlin, W. J. Williams, S. Zimmermann, M. Itoh and K. Shimada. 2009. Beaufort Gyre freshwater reservoir: State and variability from observations. *J. Geophys. Res.*, doi:10.1029/2008JC005104.

Reynolds, R. W., T. M Smith, C. Liu, D. B. Chelton, K. S. Casey and M. G. Schlax. 2007. Daily high-resolution-blended analyses for sea surface temperature. *J. Climate*, 20, 5473-5496.

Roach, A. T., K. Aagaard, C. H. Pease, S. A. Salo, T. Weingartner, V. Pavlov and M. Kulakov. 1995. Direct measurements of transport and water properties through the Bering Strait. *J. Geophys. Res.*, 100(C9), 18443-18457.

Thompson, D. W. J. and J. M. Wallace. 1998. The Arctic oscillation signature in the wintertime geopotential height and temperature fields. *Geophys. Res. Lett.*, 25(9), 1297-1300.

Timmermans, M.-L., A. Proshutinsky, R. A. Krishfield, D. K. Perovich, J. A. Richter-Menge, T. P. Stanton and J. M. Toole, 2011. Surface freshening in the Arctic Ocean's Eurasian Basin: An apparent consequence of recent change in the wind-driven circulation. *J. Geophys. Res.*, 116, C00D03, doi:10.1029/2011JC006975.

Timokhov, L. and F. Tanis, Eds. 1997 & 1998. Environmental Working Group Joint U.S.-Russian Atlas of the Arctic Ocean-Winter Period. Environmental Research Institute of Michigan in association with the National Snow and Ice Data Center, Arctic Climatology Project, CD-ROM.

Woodgate, R. A., K. Aagaard and T. J. Weingartner. 2006. Interannual Changes in the Bering Strait Fluxes of Volume, Heat and Freshwater between 1991 and 2004. *Geophys. Res. Lett.*, 33, L15609, doi: 10.1029/2006GL026931.

Woodgate, R. A., T. J. Weingartner and R. W. Lindsay. 2010. The 2007 Bering Strait Oceanic Heat Flux and anomalous Arctic Sea-ice Retreat. *Geophys. Res. Lett.*, 37, L01602, doi: 10.1029/2009GL041621.

Woodgate, R. A., T. J. Weingarter and R. Lindsay. In press. Observed increases in oceanic fluxes from the Pacific to the Arctic from 2001 to 2011 and their impacts on the Arctic. *Geophys. Res. Lett.*, doi:10.1029/2012GL054092.

Marine Ecosystems Summary

Section Coordinators: Sue Moore[1], Mike Gill[2]

[1]NOAA/Fisheries Office of Science and Technology, USA
[2]Canadian Wildlife Service, Environment Canada, Whitehorse, YT, Canada & CAFF/CBMP

December 3, 2012

The Marine Ecosystem section of the 2012 Arctic Report Card highlights the highly variable nature of Arctic ecosystems and provides some insight into how the marine ecosystem and the biodiversity it supports are responding to changing environmental conditions. Recent changes in the marine ecosystem, from primary and secondary productivity to responses by seabirds and some marine mammals species, are summarized in six essays. They provide a glimpse of what can only be described as profound, continuing changes in the Arctic marine ecosystem. For example, there is increased evidence of linkages between sea ice conditions and primary productivity, affecting the abundance and composition of phytoplankton communities. New satellite remote sensing observations show the near ubiquity of ice-edge blooms throughout the Arctic and the importance of seasonal sea ice variability in regulating primary production. These results suggest that previous estimates of annual primary production in waters where under-ice blooms develop may be about ten times too low. Shifts in primary and secondary production have direct impacts on benthic communities. Recent findings on temporal trends in the benthic system include: species range changes in sub-Arctic seas and on inflow shelves; changes in feeding guild composition in the deep Fram Strait; reduction of benthic biomass in the Barents and northern Bering seas; and no apparent change in infaunal biomass in the Kara Sea. Recent sea ice declines have allowed gray whales to stay longer and feed on both benthic amphipods and zooplankton in the Barrow Canyon region of northwest Alaska. Seabirds, long considered a valuable indicator of changing marine conditions, are showing changes in phenology, diet, foraging behavior and survival rates across the Arctic. Seabirds, it is believed, are responding, at least in part, to warming sea surface temperatures and concurrent changes in prey availability.

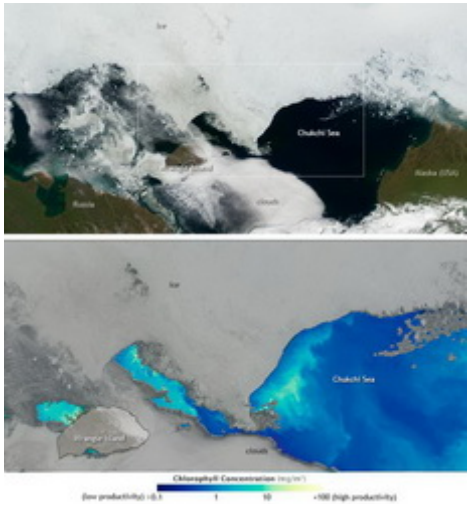

Extensive phytoplankton blooms at the sea ice edge in the Chukchi Sea seen from space in July 2011. Large version available from NOAA Climate.gov.

New programs are underway to more effectively measure, monitor and document changes in the marine ecosystem. The Distributed Biological Observatory (DBO) is an international change detection array for the identification and consistent monitoring of biophysical responses in the Pacific Arctic. One essay highlights provisional results from a production 'hotspot' in Barrow Canyon, which was investigated during the DBO pilot program. Another essay describes an international collaboration, the Arctic Biodiversity Assessment (ABA) of the Arctic Council Conservation of Arctic Flora and Fauna (CAFF) Working Group, which summarizes what is known about population sizes, trends and distributions for species that inhabit sub-Arctic and Arctic waters. During International Polar Year (2007-2009), the first coordinated, year-round sampling of underwater acoustic marine mammal habitats at two sites in the High Arctic

documented the seasonal occurrence of both Arctic and sub-Arctic species in Fram Strait (Atlantic Arctic), but only Arctic species on the Chukchi Plateau (Pacific Arctic). The Fram Strait recorders also discovered that Spitzbergen's bowhead whales were singing almost continuously through the winter, suggesting that this critically endangered population may be larger than previously thought and that Fram Strait may be an important over-wintering area for it.

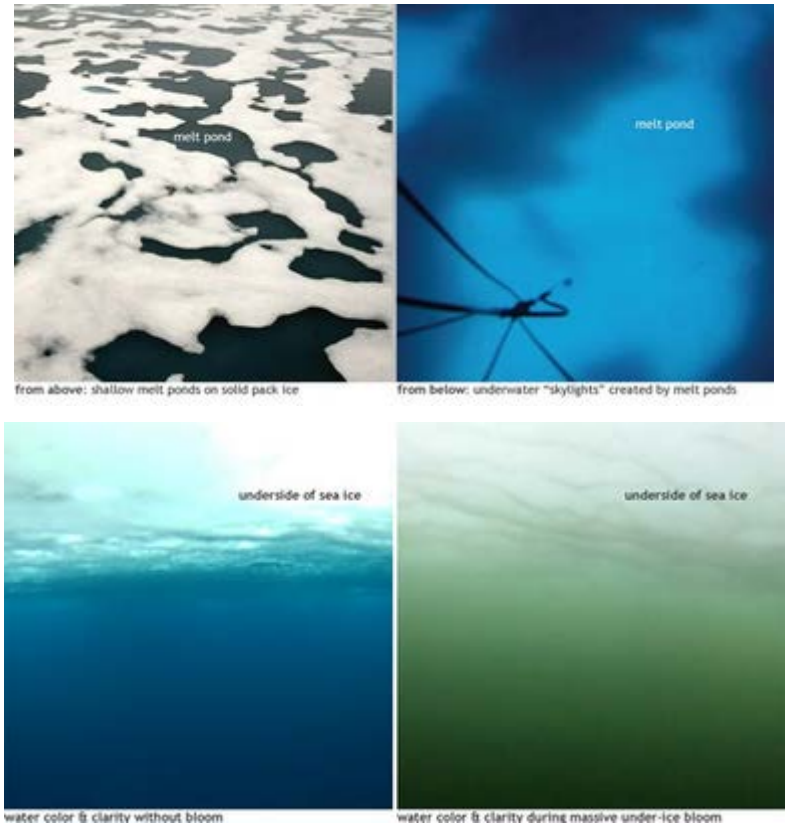

Melt ponds on the sea ice surface act as skylights (top), illuminating the underside of the ice and promoting phytoplankton blooms (bottom).

Seabirds

K.J. Kuletz[1] and N.J. Karnovsky[2]

[1]U.S. Fish and Wildlife Service, Anchorage, AK, USA
[2]Department of Biology, Pomona College, Claremont, CA, USA

November 11, 2012

Highlights

- In the Atlantic Arctic, Dovekies (Little Auks), the most abundant seabird species in the arctic, show flexibility in foraging behavior and diet that has allowed some breeding colonies to do well despite warming ocean currents that affect their prey.
- Two circumpolar species, the common murre and thick-billed murre, show long-term fluctuations in population trends at colonies in response to changes in SST (sea surface temperature). These population trends tend to be synchronous within ocean basins, but alternate between Pacific and Atlantic sectors.
- Seabirds can bring beneficial nutrients from their ocean foraging grounds to breeding sites on land, but they can also concentrate and increase deposition of harmful contaminants and mercury at inland sites.

A total of 64 marine bird species are considered 'Arctic' in that they breed in the Arctic, and additional species spend at least part of the year in Arctic waters. Of the 64 Arctic species, 20 are circumpolar, found in both the Atlantic and Pacific sectors, while 19 species breed solely in the Atlantic and 25 species solely in the Pacific (Petersen et al., in press). In the Pacific sector, Sigler et al. (2011), analyzed seabird distribution at sea and identified three major species clusters, with the north Bering Sea and Chukchi Sea birds forming one group and the central and southern Bering Sea regions another, while the Beaufort Sea birds formed a distinctly separate group. The north Bering-Chukchi region was dominated by planktivorous birds (*Aethia* auklets in the north Bering Sea and *Puffinus* shearwaters in the Chukchi Sea), whereas the Beaufort seabirds were primarily piscivorous and circumpolar in distribution.

Over the past few decades the Arctic has experienced significant warming. In response to these warming trends, seabirds have shown shifts in their phenology, diets, physiology, foraging behavior, and survival rates. In the Atlantic sector there has been increase in the flow of warmer, more saline water in the West Spitsbergen Current into the Greenland Sea and into the Arctic Ocean (Piechura and Walczowski 2009), which affects plankton and therefore the diets of seabirds that feed on them (Kwasniewski et al., 2009). See the *Ocean* essay for further information about temperature and volume flux of Atlantic Water in the Greenland Sea and Fram Strait. Seabirds that breed in the Arctic face additional challenges during the non-breeding season. For example, using geolocators, Frederiksen et al. (2012) found that black-legged kittiwakes throughout the Arctic spend winters further south in regions where they may interact with fisheries or encounter oil spills.

Dovekies (*Alle alle*, also known as the Little Auk; **Fig. 3.1**), the most abundant seabird species in the Atlantic Arctic, and possibly in the World, are planktivores that nest on rocky slopes. From 1963 to 2008, dovekies showed a trend of earlier breeding and median hatch date became

4.5±2.1 days earlier. This is likely due to earlier nest site availability because of earlier snow melt (Moe et al. 2009). In contrast, the piscivorous black-legged kittiwakes (*Rissa tridactyla*) have shown a slight trend towards later breeding, which is likely related to delays or decreases in the availability of their fish prey due to warmer sea surface temperatures (SST) and loss of sea ice (Moe et al. 2009).

Fig. 3.1. Dovekies (*Alle alle*, also known as the Little Auk) are the most abundant seabird species in the Atlantic Arctic and possibly in the World.

In the Arctic, copepods are a key prey in seabird food chains. In the Atlantic sector, increases in the flow of warm, Atlantic-derived water into the Greenland Sea have led to an increase in abundance of a smaller, low-lipid copepod, *Calanus finmarchicus*, instead of larger Arctic species (*C. glacialis* and *C. hyperboreus*) (Scott et al. 2000). While dovekies feed primarily on the large Arctic copepods (Karnovsky et al., 2003, 2010), in years with high inflow of Atlantic-derived water, they feed their chicks more of the smaller copepod species (Moline et al., 2010). Inter-colony comparisons of dovekie behavior found that dovekies make longer foraging trips when feeding in the warmer, Atlantic-derived water, where they must feed on the small copepod species, whereas at colonies where larger, high-lipid copepods are available, they spend less time searching for prey and make fewer deep dives (Welcker et al., 2009). For additional information on Atlantic Water in the Greenland Sea (Fram Strait) see the *Ocean* essay.

For dovekies, foraging conditions influence body mass and over winter survival of adult birds (Harding et al., 2011). However, despite variation in foraging conditions, dovekies have been able to maintain high reproductive success throughout the Greenland Sea (Jakubas et al., 2011; Jakubas and Wojczulanis-Jakubas, in press; Karnovsky et al., 2003, 2010; Gremillet et al., 2012; Harding et al., 2011). Continued warming, however, could result in extinction of colonies exposed to warmer Atlantic-derived water with sub-optimal prey (Karnovsky et al., 2010).

A much rarer arctic seabird that breeds in the Atlantic sector, the ivory gull (*Pagophila eburnea*), has declined by an estimated 80-90% over the past 20 years (Gilchrist and Mallory, 2005). This small gull nests in isolated nunataks (rocky outcrops among glacial icefields). Because the

declines appeared to be occurring throughout Canada and in different breeding habitats, Gilchrist and Mallory (2005) suggest that the causes of decline are related to factors associated with migration or over-wintering conditions. As with many Arctic seabird species, lack of monitoring makes it difficult to determine population trends or the factors influencing them (Petersen et al., 2008).

There have been few long-term studies at seabird colonies in the Pacific Arctic, with the exception of two sites monitored by the Alaska Maritime National Wildlife Refuge - the Cape Lisburne colony (mainland Alaska in the eastern Chukchi Sea) and Bluff colony (mainland Alaska in the northern Bering Sea, Norton Sound). Two species have been monitored at these sites since the late 1970s, the black-legged kittiwake and the common murre (*Uria aalge*). Between 1975 and 2009, kittiwake numbers have increased overall at Cape Lisburne, but their reproductive success has declined since 2004 (Dragoo et al., 2012). These contrasting trends suggest immigration to the region by prospecting birds, i.e., birds from elsewhere looking for a new place to nest. At the Bluff colony, both kittiwakes and murres have shown stable population trends, but their mean hatching dates have been earlier than the long-term (1975-2009) mean (Dragoo et al., 2012); the earlier hatch dates suggest an adaptation to earlier prey availability by both seabird species.

Two species of murres, the common murre and thick-billed murre (*U. lomvia*) are widespread and relatively abundant throughout the Arctic; consequently, they have been identified as a key species to monitor by the Circumpolar Seabird Group of CAFF (Petersen et al., 2008). In a pan-Arctic study of both murre species, data from 32 common and 21 thick-billed murre colonies were used to examine population trends and the potential influence of SST (Irons et al., 2008). The more Arctic thick-billed murre colonies increased in size when SST warmed slightly, whereas the more temperate common murre colonies increased with moderate cooling, but both species had negative trends when SST changes were extreme, regardless of direction. These patterns showed synchronous fluctuations relative to SST, with changes in trends being synchronous within ocean basins and opposite between the two basins (Pacific and Atlantic). These population trends might reflect changes in the prey base, but this remains to be determined. For more information about SST, see the *Ocean* essay.

Seabird tissues and eggs have become useful tools to monitor a wide variety of contaminants that can impact the birds themselves and serve as indicators of environmental health (e.g., Vander Pol and Becker, 2007). One example is the use of murre eggs to study atmospheric deposition of mercury in the Arctic. Variations in the isotopic composition of mercury in murre eggs (a reflection of the female bird's diet in spring) show that deposition increased with latitude and was negatively correlated with sea-ice cover (Point et al., 2011). Loss of sea-ice cover could accelerate the amount of biologically accessible methylmercury throughout the food chain (Point et al., 2011). By foraging in the ocean and returning to land-based colonies, seabirds transport beneficial nutrients to land, but they may also be responsible for transporting contaminants to inland lakes and soils. Blais et al. (2005) found that Arctic ponds near large colonies of northern fulmars (*Fulmarus glacialis*) had higher levels of persistent organic pollutants and mercury, and suggested that contaminants in seabirds could be an indicator of ecosystem health and are also a direct concern to indigenous peoples relying on traditional foods.

References

Blais, J. M., L. E. Kimpe, D. McMahon, B. E. Keatley, M. L. Mallory, M. S. V. Douglas and J. P. Smol. 2005. Arctic seabirds transport marine-derived contaminants. *Science*, 309, 445.

Dragoo, D. E., H. M. Renner and D. B. Irons. 2012. Breeding status, population trends and diets of seabirds in Alaska, 2009. U.S. Fish and Wildlife Service Report AMNWR 2012/01. Homer, Alaska.

Frederiksen, M. and thirty others. 2012. Multicolony tracking reveals the winter distribution of a pelagic seabird on an ocean basin scale. *Divers. Distrib.*, 18, 530-542.

Gilchrist, H. G. and M. L. Mallory. 2005. Declines in abundance and distribution of the Ivory Gull (*Pagophila eburnea*) in Arctic Canada. *Biological Conservation*, 121(2), 303-309.

Grémillet, D., J. Welcker, N. J. Karnovsky, W. Walkusz, M. E. Hall, J. Fort, Z. W. Brown, J. R. Speakman and A. M. A. Harding. 2012. Little auks buffer the impact of current Arctic climate change. *Mar. Ecol. Progr. Ser.*, 454, 197-206.

Harding, A. M. A., J. Welcker, H. Steen, K. Hamer, A. S. Kitaysky, J. Fort, S. L. Talbot, L. Cornick, N. J. Karnovsky, G. Gabrielsen and D. Grémillet. 2011. Adverse foraging conditions may impact body mass and survival of a High Arctic seabird. *Oecologia*, 167, 49-59.

Irons, D. B., T. Anker-Nilssen, A. J. Gaston, G. V. Byrd, K. Falk, G. Gilchrist, M. Hario, M. Hjernquist, Y. V. Krasnov, A. Mosbech, B. Olsen, A. Petersen, J. Reid, G. Robertson, H. Strom and K. D. Wohl. 2008. Magnitude of climate shift determines direction of circumpolar seabird population trends. *Glob. Change Biol.*, 14, 1455-1463.

Jakubas D. and K. Wojczulanis-Jakubas. Rates and consequences of relaying in little auks Alle alle breeding in the High Arctic - an experimental study with egg removal. *J. Avian Biol.*, in press.

Jakubas, D., M. Głuchowska, K. Wojczulanis-Jakubas, N. J. Karnovsky, L. Keslinka, D. Kidawa, W. Walkusz, R. Boehnke , M. Cisek, S. Kwaśniewski and L. Stempniewicz. 2011. Different foraging effort does not influence body condition and stress level in little auks. *Mar. Ecol. Progr. Ser.*, 432, 277-290.

Karnovsky, N. J., J. Welcker, A. M. A. Harding, Z. W. Brown, W. Walkusz, A. Cavalcanti, J. Hardin, A. Kitaysky, G. Gabrielsen and D. Grémillet. 2011. Inter-colony comparison of diving behavior of an Arctic top predator: Implications for warming in the Greenland Sea. *Mar. Ecol. Progr. Ser.*, 440, 229-240.

Karnovsky, N. J., A. Harding, W. Walkusz, S. Kwaśniewski, I. Goszczko, J. Wiktor, H. Routti, A. Bailey, L. McFadden, Z. Brown, G. Beaugrand and D. Grémillet. 2010. Foraging distributions of little auks across the Greenland Sea: Implications of present and future Arctic climate change. *Mar. Ecol. Progr. Ser.*, 415, 283-293.

Karnovsky, N. J., S. Kwaśniewski, J. M. Węsławski, W. Walkusz and A. Beszczyńska-Möller. 2003. The foraging behavior of little auks in a heterogeneous environment. *Mar. Ecol. Progr. Ser.*, 253, 289-303.

Kwasniewski, S., M. Gluchowska, W. Walkusz, N. J. Karnovsky, D. Jakubas, K. Wojczulanis-Jakubas, A. M. A. Harding, I. Goszczko, M. Cisek, A. Beszczynska-Möller, W. Walczowski, J. M. Weslawski and L. Stempniewicz. 2012. Interannual changes in zooplankton on the West

Spitsbergen Shelf in relation to hydrography and their consequences for the diet of planktivorous seabirds. *ICES J. Mar. Sci.*, 69(5), 890-901.

Moe, B., L. Stempniewicz , D. Jakubas, F. Angelier, O. Chastel, F. Dinessen, G. W. Gabrielsen, F. Hanssen, N.J. Karnovsky, B. Rønning, J. Welcker, K. Wojczulanis-Jakubas and C. Bech. 2009. Climate change and phenological responses of two seabird species breeding in the high-Arctic. *Mar. Ecol. Progr. Ser.*, 393, 235-246.

Moline, M. A., N. J. Karnovsky, Z. Brown, G. J. Divoky, T. R. Frazer, C. A. Jacoby, J. J. Torres and W. R. Fraser. 2008. High latitude changes in ice dynamics and their impact on Polar marine ecosystems. In *The Year in Ecology and Conservation Biology*, R. S. Ostfield and W. H. Schlesinger (eds.), *Ann. New York Acad. Sci.*, 1134, 267-319.

Piechura, J. and W. Walczowski. 2009. Warming of the west Spitsbergen Current and sea ice north of Svalbard. *Oceanologia*, 51(2), 147-164.

Petersen, A., D. Irons, T. Anker-Nilssen, Yu. Artukhin, R. Barrett, D. Boertmann, C. Egevang, M.V. Gavrilo, G. Gilchrist, M. Hario, M. Mallory, A. Mosbech, B. Olsen, H. Osterblom, G. Robertson and H. Strom. 2008. Framework for a Circumpolar Arctic Seabird Monitoring Network. CAFF CBMP Report no. 15. 64 pp.

Petersen, A., D. Irons, Yu. Artukhin, R. Barrett, D. Boertmann, M. V. Gavrilo, G. Gilchrist, M. Hario, K. Kampp, A. Mosbech, B. Olsen, H. Osterblom, G. Robertson and H. Strøm, 2012. Circumpolar Arctic Seabirds: Population Status and Trends. CAFF CBMP Report, in press.

Point, D., J. E. Sonke, R. D. Day, D. G. Roseneau, K. A. Hobson, S. S. Vander Pol, A. J. Moors, R. S. Pugh, O. F. X. Donard and P. R. Becker. 2011. Methylmercury photodegradation influenced by sea-ice cover in Arctic marine ecosystems. *Nature Geosci.*, 4, 188-194, doi:10.1038/ngeo1049.

Sigler, M. F., M. Renner, S. L. Danielson, L. B. Eisner, R. R. Lauth, K. J. Kuletz, E. A. Logerwell and G. L. Hunt, Jr. 2011. Fluxes, fins, and feathers: Relationships among the Bering, Chukchi, and Beaufort seas in a time of climate change. *Oceanogr.*, 24(3), 250-265.

Scott, C. L., S. Kwasniewski, S. Falk-Petersen and J. R. Sargent. 2000. Lipids and life strategies of *Calanus finmarchicus*, *Calanus glacialis* and *Calanus hyperboreus* in late autumn, Kongsfjorden, Svalbard. *Polar Biol.*, 23, 510-516.

Vander Pol, S. S. and P. R. Becker. 2007. Monitoring contaminants in seabirds: the importance of specimen banking. *Marine Ornithology* 35: 113-118.

Welcker, J., A. Harding, N. Karnovsky, H. Steen, H. Strøm and G. Gabrielsen. 2009. Flexibility in the bimodal foraging strategy of a high Arctic alcid, the little auk *Alle alle*. *J. Avian Biol.*, 40, 388-399.

Primary Productivity and Nutrient Variability

K.E. Frey[1], K.R. Arrigo[2], W.J. Williams[3]

[1]Graduate School of Geography, Clark University, Worcester, MA, USA
[2]Department of Environmental Earth System Science, Stanford University, Stanford, CA, USA
[3]Institute of Ocean Sciences, Fisheries and Oceans Canada, Sidney, BC, Canada

November 14, 2012

Highlights

- Massive phytoplankton blooms beneath a 0.8-1.3 m thick, fully consolidated (yet melt-ponded) sea ice pack were observed in the north-central Chukchi Sea in July 2011. The blooms extended >100 km into the ice pack and biomass was greatest (>1000 mg C m^{-3}) near the ice-seawater interface, with nutrient depletion to depths of 20-30 m.
- New satellite remote sensing observations show (a) the near ubiquity of ice-edge blooms across the Arctic and the importance of seasonal sea ice variability in regulating primary production, and (b) a reduction in the size structure of phytoplankton communities across the northern Bering and Chukchi seas during 2003-2010.
- A unique marine habitat containing abundant algal species in so-called "melt holes" was observed for the first time in perennial sea ice in the central Arctic Ocean.
- During the last decade, the intensification of the Beaufort Gyre has pushed the nutricline deeper, and the subsurface chlorophyll maximum that was at 45 m in 2002 has deepened to 60-65 m in 2008-2012.

Sea ice melt and breakup during spring strongly drive primary production in the Arctic Ocean and its adjacent shelf seas by enhancing light availability as well as increasing stratification and stabilization of the water column. Previous large-scale, synoptic estimates of primary production in the Arctic Ocean typically assume that phytoplankton in the water column beneath the sea ice pack is negligible. However, massive phytoplankton blooms beneath a 0.8-1.3 m thick, fully consolidated, yet melt-ponded, sea ice pack were observed in the north-central Chukchi Sea in July 2011 (Arrigo et al., 2012) (**Fig. 3.1**). These blooms, primarily consisting of pelagic diatoms of the genera *Chaetoceros*, *Thalassiosira*, and *Fragilariopsis*, indicating this was not a remnant sea ice algal bloom, extended from the ice edge to >100 km northward into the pack ice. Biomass was greatest (>1000 mg C m^{-3}) near the ice/seawater interface and was associated with large nutrient deficits in the upper 25-30 m of the water column beneath the ice (**Fig. 3.2**). Given these new observations, previous estimates of annual primary production in waters where these under-ice blooms develop may be ~10-times too low (Arrigo et al., 2012).

Although it is not clear whether these under-ice phytoplankton blooms are a new phenomenon, a shift away from snow-covered multi-year ice (typical of these areas in the 1980s) towards a thinner, more melt-ponded sea ice cover (typical of current conditions) will enhance the light transmittance (Frey et al., 2011) necessary for primary production, given the presence of sufficient nutrients. During the early 1980s, the location of these under-ice phytoplankton blooms was covered throughout the summer by thick (~3 m) multiyear ice with a deeper snow cover (0.4 m) and fewer melt ponds than the first year ice observed in July 2011. As such, the amount of light transmitted through snow-covered multi-year ice in the 1980s (<0.1% of surface

light) would have been far less than that transmitted through melt-ponded first year ice during July 2011 (13-59% of surface light) and inadequate to support the large under-ice phytoplankton blooms observed that year (Arrigo et al., 2012).

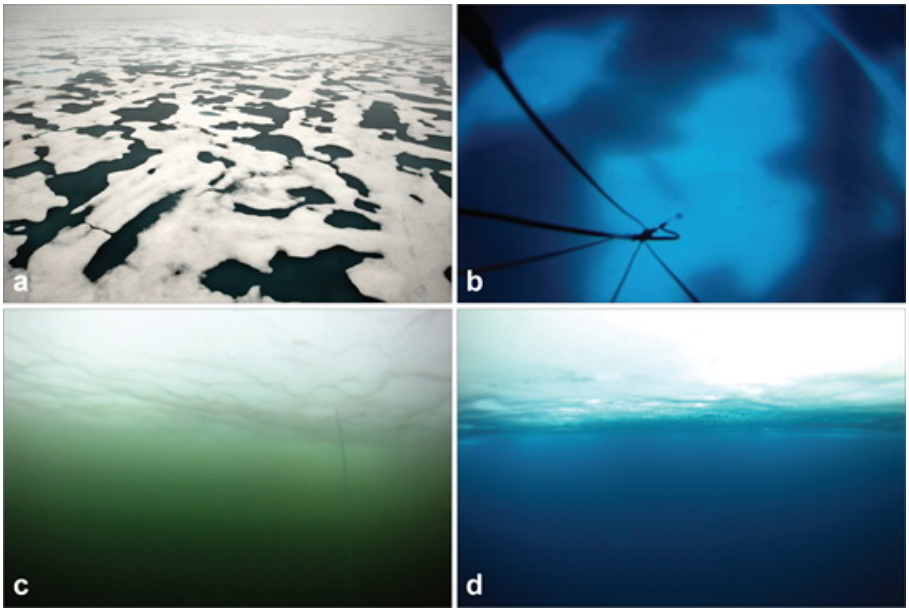

Fig. 3.1. Under-ice phytoplankton blooms observed during July 2011 in the north-central Chukchi Sea and associated: (a) aerial view of surface melt pond distributions; (b) view from ~20 m under the sea ice looking up through a melt pond; (c) massive phytoplankton bloom directly under the sea ice; and (d) non-bloom waters under sea ice further east in the Chukchi Sea. Photographs by K. Frey.

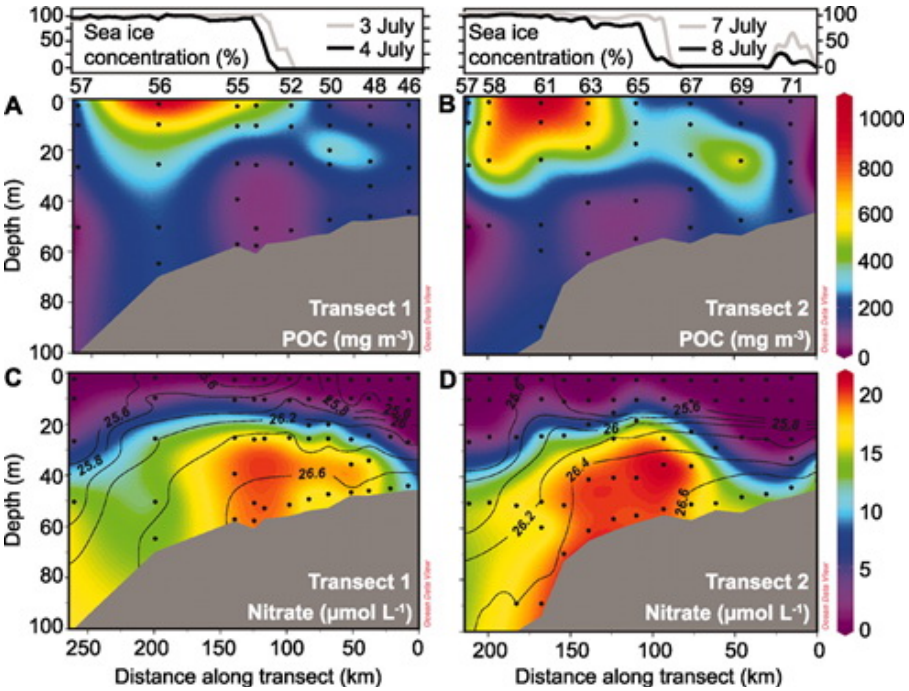

Fig. 3.2. Under-ice phytoplankton blooms observed during July 2011 along two transects in the north-central Chukchi Sea and associated measurements: (a) Particulate organic carbon (POC) and (c) nitrate from Transect 1, and (b) POC and (d) nitrate from Transect 2. From Arrigo et al. (2011).

Additional insights into Arctic Ocean primary production have been derived from satellite remote sensing observations, including information related to ice-edge blooms and size structure of phytoplankton communities. Perrete et al. (2011) show strong connections between seasonal sea ice retreat and primary production, where these near-ubiquitous ice-edge blooms across the pan-Arctic are observed in 77-89% of locations where adequate data exist. These bloom are typically observed to peak within 20 days of ice retreat and average >1 mg m^{-3} (with major blooms >10 mg m^{-3}). Ice-edge blooms are less common in areas of early sea ice melt (at lower latitudes) and their contributions to annual primary productivity rates are reduced owing to the long periods available for open-water blooms. In contrast, at higher latitudes, it is shown that primary productivity rates at the ice-edge may be 1.5-2 times greater than those in open-water conditions. In addition, Fujiwara et al. (2011) have developed a new satellite-based algorithm for deriving the size structure of phytoplankton communities across the northern Bering and Chukchi seas. Through these analyses, it is suggested that phytoplankton size is inversely related to variability in sea surface temperature. Furthermore, during the period investigated (2003-2010), the derived phytoplankton size index was shown to significantly decrease (likely related to limitations in nutrients), which is an important finding in the context of carbon turnover rates and the vertical pathways of carbon flow. For example, picoplankton-based systems, such as those observed in the Canada Basin, typically do not support large exports of biogenic carbon, neither through extraction via heterotrophic activity nor sequestration in benthic environments (Li et al., 2009).

In addition to phytoplankton primary production, sea ice algal production is also important to consider in the overall Arctic Ocean system. Sea ice primary production was recently modeled to account for up to ~40% of total primary production (depending on location) and up to ~7.5% when considering the entire Arctic region (Dupont, 2012). Furthermore, a unique marine habitat for sea ice algae in so-called "melt holes" was observed for the first time in perennial sea ice in the central Arctic Ocean (Lee et al., 2011; Lee et al., 2012). The melt holes are formed in thinning sea ice where surface melt ponds completely penetrate the ice and connect to the underlying seawater, and rarely have been investigated for their role in ecosystem productivity. These open ponds have higher nutrient concentrations than closed surface melt ponds owing to the connection with the seawater; consequently, this newly observed marine habitat contains abundant algal species (mainly *Melosira arctica*, constituting >95% of the biomass) known to be important for zooplankton consumption. Furthermore, the accumulation of these algal masses attached to refreezing ice in late summer may provide an important food supplement for higher trophic levels as the ecosystem enters winter. Lee et al. (2012) estimate that the total carbon production in melt ponds in Arctic sea ice amounts to ~2.6 Tg C yr^{-1}, which constitutes <1% of recent total production in the whole Arctic Ocean. However, this fraction may be significantly higher when only considering ice-covered portion of the Arctic Ocean. Lee et al. (2011) suggest that continued warming and decreases in sea ice extent and thickness may result in a northward extension of these open pond areas (enhancing overall primary production in these habitats), but even their ultimate potential disappearance as perennial sea ice cover becomes more scarce across the Arctic Ocean.

Important shifts in nutrient availability in recent years have also driven significant changes in primary production of Arctic Ocean waters. A subsurface chlorophyll maximum stretches across the Beaufort Gyre region of the Canada Basin in summer. It occurs at the top of the nutricline, a location that is as close to sunlight as possible while nutrients are still present (McLaughlin and Carmack, 2010). The Beaufort Gyre has intensified dramatically since 2002 owing to Ekman convergence, with a particularly large jump in the winter of 2007/2008 (see the *Ocean* essay for more information about the intensification of the Beaufort Gyre and consequences for heat and

freshwater content). This intensification has pushed the halocline down, as indicated by the deepening of the 33.1 psu isohaline (**Fig. 3.3a**). Additional melting of sea ice during this time has also resulted in lower surface salinities (**Fig. 3.3b**) and increased upper halocline stratification (**Fig. 3.3c**). The combination of a deeper halocline and stronger stratification has pushed the top of the nutricline farther away from sunlight and reduced nutrient availability, thus stressing phytoplankton at the subsurface chlorophyll maximum (McLaughlin and Carmack, 2010). The subsurface chlorophyll maximum is correspondingly deeper (**Fig. 3.3d**). Data from 2012 are similar to 2008-2010, and consistent with a slight relaxation of the Beaufort Gyre.

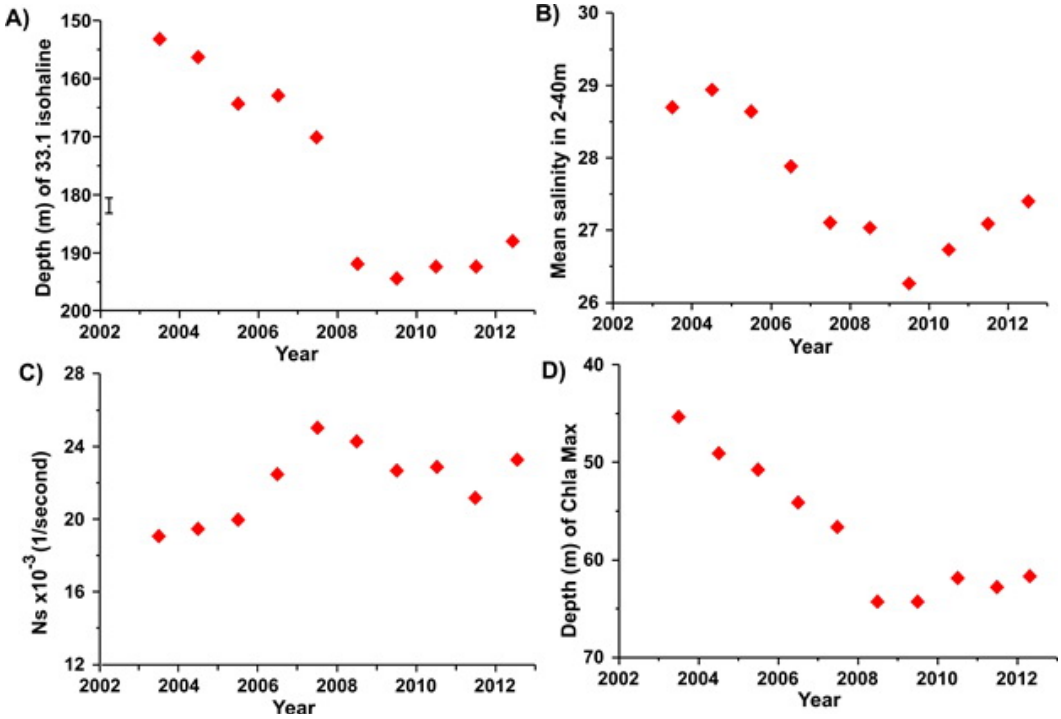

Fig. 3.3. Time series of mean near-surface properties of the Beaufort Gyre region of the Canada Basin as measured in summer (August and September) by the Joint Ocean Ice Studies expeditions aboard the *CCGS Louis S. St-Laurent* in collaboration with the Beaufort Gyre Exploration Project of the Woods Hole Oceanographic Institution. Each data point is the mean of that property for a set stations that are repeated each year in the southern Canada Basin and representative of the Beaufort Gyre (following McLaughlin and Carmack, 2010). Properties plotted are (a) depth of the 33.1 psu isohaline, (b) mean salinity over the depth range 2-40 m, (c) mean density stratification due to salinity in the depth range 5-100 m, and (d) depth of the subsurface chlorophyll maximum.

References

Arrigo, K. R., D. K. Perovich, R. S. Pickart, Z. W. Brown, G. L. van Dijken, K. E. Lowry, M. M. Mills, M. A. Palmer, W. M. Balch, F. Bahr, N. R. Bates, C. Benitez-Nelson, B. Bowler, E. Brownlee, J. K. Ehn, K. E. Frey, R. Garley, S. R. Laney, L. Lubelczyk, J. Mathis, A. Matsuoka, B. G. Mitchell, G. W. K. Moore, E. Ortega-Retuerta, S. Pal, C. M. Polashenski, R. A. Reynolds, B. Scheiber, H. M. Sosik, M. Stephens and J. H. Swift. 2012. Massive phytoplankton blooms under Arctic sea ice. *Science*, 336, 1408, doi:10.1126/science.1215065.

Dupont, F. 2012. Impact of sea-ice biology on overall primary production in a biophysical model of the pan-Arctic Ocean. *J. Geophys. Res.*, 117, C00D17, doi:10.1029/2011JC006983.

Fujiwara, A., T. Hirawake, K. Suzuki and S. I. Saitoh. 2011. Remote sensing of size structure of phytoplankton communities using optical properties of the Chukchi and Bering Sea shelf region. *Biogeosci.*, 8, 3567-3580.

Frey, K. E., D. K. Perovich and B. Light. 2011. The spatial distribution of solar radiation under a melting Arctic sea ice cover. *Geophys. Res. Lett.*, 38, L22501, doi:10.1029/2011GL049421.

Lee, S. H., C. P. McRoy, H. M. Joo, R. Gradinger, X. Cui, M. S. Yun, K.H. Chung, S. H. Kang, C. K. Kang, E. J. Choy, S. Son, E. Carmack and T. E. Whitledge. 2011. Holes in progressively thinning Arctic sea ice lead to new ice algae habitat. *Oceanography*, 24(3), 302-308, http://dx.doi.org/10.5670/oceanog.2011.81.

Lee, S. H., D. A. Stockwell, H. M. Joo, Y. B. Son, C. K. Kang and T. E. Whitledge. 2012. Phytoplankton production from melting ponds on Arctic sea ice. *J. Geophys. Res.*, 117, C04030, doi:10.1029/2011JC007717.

Li, W. K. W., F. A. McLaughlin, C. Lovejoy and E. C. Carmack. 2009. Smallest algae thrive as the Arctic Ocean freshens. *Science*, 326, 539.

Perrette, M., A. Yool, G. D. Quartly and E. E. Popova. 2011. Near-ubiquity of ice-edge blooms in the Arctic. *Biogeosci.*, 8, 515-524.

Ecosystem Observations in Barrow Canyon: A Focus for the International Distributed Biological Observatory (DBO)

J. Grebmeier[1], R. Pickart[2], C. Ashjian[2], L. Cooper[1], K. Frey[3], J. He[4], M. Itoh[5], M. Kedra[1], T. Kikuchi[5], S. Moore[6], J. Nelson[7], S. Vagle[7]

[1]University of Maryland Center for Environmental Science, Solomons, MD, USA
[2]Woods Hole Oceanographic Institution, Woods Hole, MA, USA
[3]Graduate School of Geography. Clark University, Worchester, MA, USA
[4]Polar Research Institute of China, Shanghai, People's Republic of China
[5]Japan Agency for Marine-Earth Science and Technology (JAMSTEC), Yokosuka, Japan
[6]NOAA/Fisheries, Office of Science & Technology, Seattle, WA, USA
[7]Institute of Ocean Sciences, Dept. Fisheries and Oceans, Sidney, BC, Canada

November 11, 2012

Highlights

- Since 1980, sea ice persistence in the Barrow Canyon (BC) region of the Distributed Biological Observatory (DBO) has declined by ~3 days per year.
- Heat flux during the 2010 DBO BC section was 3 times higher compared to that in 1993; heat flux was particularly high in the Alaska Coastal Water. The ACW was warmer in July 2011 than July 2010, suggesting a continued warming trend.
- Zooplankton and benthic species composition vary by water mass type in BC; total zooplankton abundance was greater in 2011 than in 2010.

Introduction

The Chukchi Sea continental shelf in the Pacific Arctic region (**Fig 3.5**) is influenced by the northward transport of nutrient-rich Pacific water via the Bering Strait (see the *Ocean* essay for more information about Pacific Water flow through the Bering Strait), which supports areas of high water column and benthic production on the southeast and northeast portions of the shelf (citations in Grebmeier, 2012). Dramatic, broad temporal and spatial variation in chlorophyll biomass in the Chukchi Sea has coincided with seasonal sea ice retreat and increases in seawater temperatures. One of the key uncertainties in this region is how the marine ecosystem will respond to seasonal shifts in the timing of sea ice retreat and/or delays in fall sea ice formation.

The Distributed Biological Observatory (DBO; **Fig. 3.5**) is being developed by an international consortium of scientists in the Pacific Arctic as a change detection array to systematically track the broad biological response to sea ice retreat and associated environmental change that is occurring (Grebmeier et al., 2010). The DBO relies on coordinated, international sampling by a network of ships from Canada, China, Korea, Japan, Russia and the United States. Specific high productivity locations in the Bering and Chukchi seas are sampled on a repeated basis as research vessels transit the Pacific sector of the Arctic. Additional measurements by satellite and moorings at the designated sites are providing important time series data to develop an

early detection system for biological and ecosystem response to climate warming. The following report highlights specific findings at the DBO Barrow Canyon site (**Fig. 3.5**).

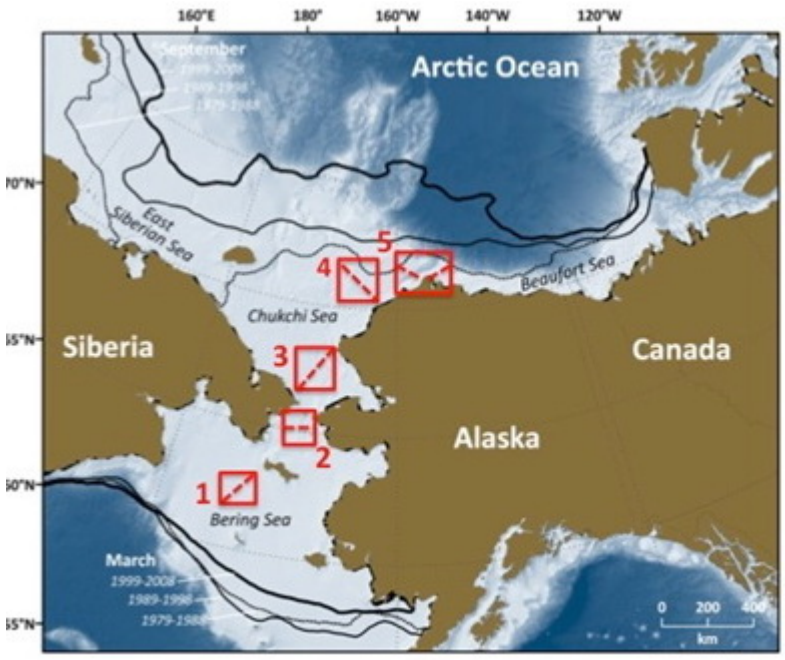

Fig. 3.5. Map of the Pacific Arctic Region showing Distributed Biological Observatory (DBO) sampling regions (numbered red boxes) and transects (broken red lines). Barrow Canyon is in box 5. Map is modified after Grebmeier et al. (2010).

Sea Ice and Hydrography

Barrow Canyon (BC) in the northeast Chukchi Sea is one of the major conduits for Pacific water into the interior Arctic Basin. Shelf-basin exchange is strongly wind-forced, which leads to upwelling in the canyon (Aagaard and Roach, 1990; Pickart et al., 2012) and along the continental slopes of the Chukchi and Beaufort seas (e.g., Nikolopoulos et al., 2009; Llinas et al., 2009). Upwelling occurs in all seasons and under ice conditions that vary between open water and 100% cover (Schulze and Pickart, 2012). Annual sea ice cover at the DBO BC site has declined dramatically during recent decades, being nearly year round in the early 1980s and declining to only ~9 months by 2009. This amounts to a reduction rate of ~2.95 days per year (Cavalieri et al., 2008), which translates into annual sea ice cover reduction of nearly three months (~88.5 days) over the past three decades. This reduction in annual sea ice persistence is due, in part, to earlier sea ice retreat in spring, but even more so because of later sea ice formation during late autumn. These dramatic shifts in sea ice cover undoubtedly have significant impacts on primary production and ecosystem function throughout the region. See the *Sea Ice* essay for a pan-Arctic perspective on the changing ice cover, and the *Arctic Ocean Primary Productivity and Nutrient Variability* essay.

As part of the DBO pilot program in 2010, six repeat high-resolution ship surveys were conducted across the canyon (**Fig. 3.6**). Total northeastward transports were between 1.0 and 1.7 Sv (Sverdrup), which consist of 0.4-1.0 Sv of warm, fresh Alaskan Coastal Water (ACW) and 0.3-0.6 Sv of cold, salty Pacific Winter Water (PWW). Measured BC transport and the local along-canyon winds are related such that, under southwesterly winds, the northeastward flow of

water through the canyon increases. The nearshore ACW supplied 9-27 TW (Tera Watts) of heat via BC into the Arctic Basin during summer 2010 (**Fig. 3.6**). This was three times larger than the heat flux measured in 1993 (Münchow and Carmack, 1997), mainly due to the higher temperature of the ACW. CTD data (not shown) reveal that the ACW was warmer in July 2011 than July 2010, suggesting a continued warming trend. Current meter sampling along the DBO BC line in July 2011, combined with salinity measurements, indicated a strong eastward flowing current. Stratification was greatest on the western side of the canyon, with higher nitrate and silicate in the deeper PWW on that side (**Fig. 3.7**). Chlorophyll *a* was relatively high in the center of the canyon, supporting the findings of the fluorescent sensor on the CTD, whereas ammonium regeneration was greatest at depth in the center of the canyon.

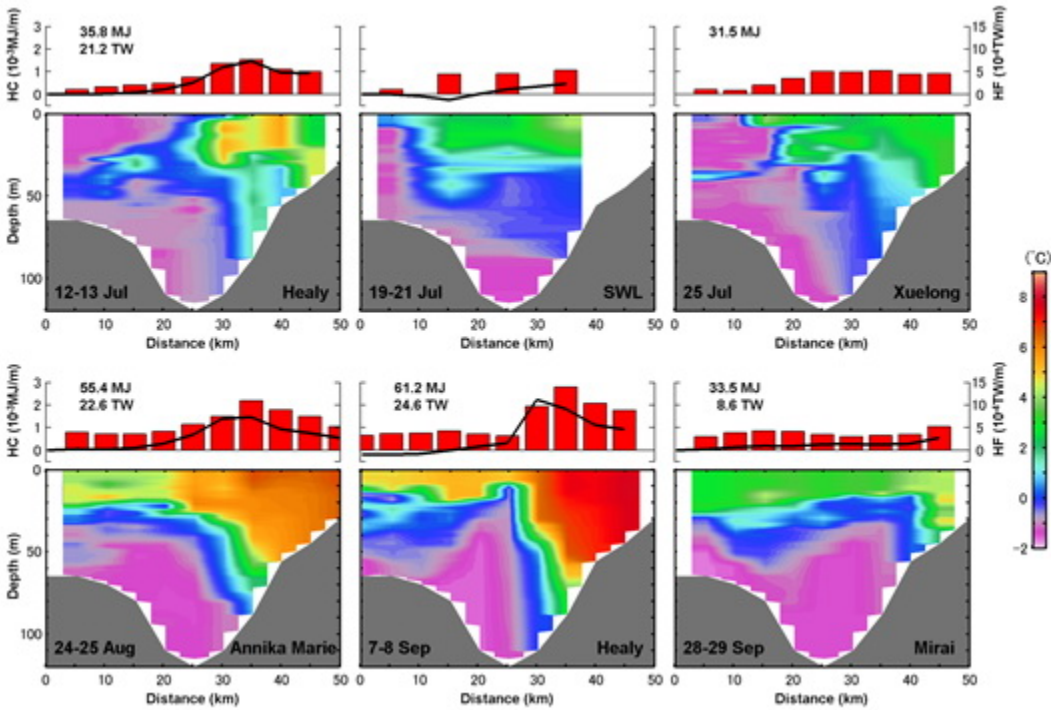

Fig. 3.6. Temperature sections (multi-colored panels, with legend at lower right), calculated heat content (HC, solid red bars) and calculated heat flux (HF, black line) across Barrow Canyon from repeat ship surveys between mid-July and late September 2010. Ship names are given in the lower right corner of each panel: Healy=USCGC Healy (USA); SWL= CCGS Sir Wilfrid Laurier (Canada); Xuelong= RV Xuelong (China); Annika Marie=RV Annika Marie (USA); Mirai=RV Mirai (Japan).

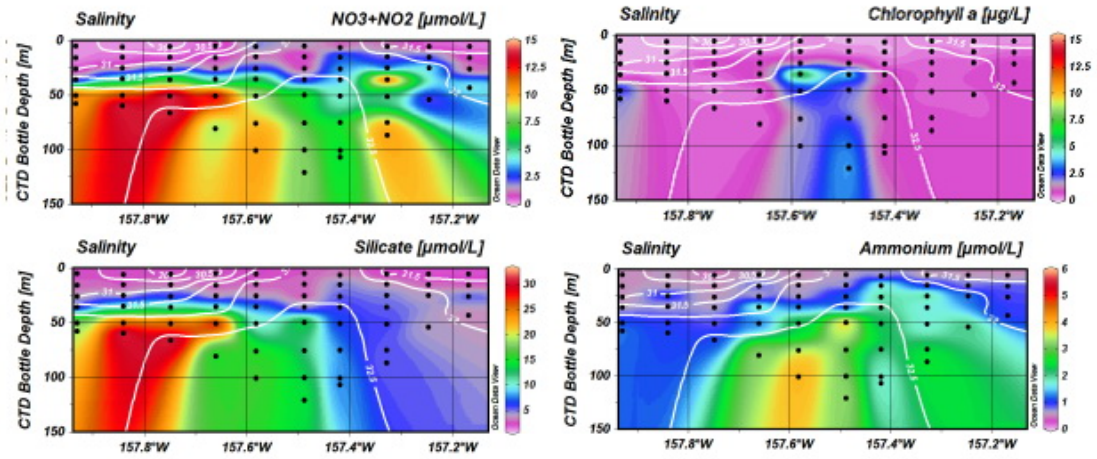

Fig. 3.7. Nutrient data (nitrate, silicate and ammonium) and chlorophyll *a* (ug/L) overlaid on salinity (white isopleths) in Barrow Canyon during the CCGS Sir Wilfrid Laurier cruise in July 2011.

Biological Measurements

The DBO stations occupied in BC during July 2010 and 2011 show regional structuring. A clear front between the arctic zooplankton community (western side) and Pacific expatriates (eastern side) was observed. During August-September, zooplankton species composition varied both within and across-stream location and water mass type as well as inter-annually, with total zooplankton abundance greater in 2011 than in 2010. The large copepod *Calanus glacialis/marshallae* was more abundant in 2010, associated with cold PWW in the west, than in 2011. Comparatively, higher abundances for the very small copepod *Oithona similis* and the small copepod *Pseudocalanus* spp. characteristic of ACW were observed in 2011. High benthic infaunal biomass, species richness and biodiversity occur in the central region of BC in the northeast Chukchi Sea (see the *Arctic Benthos* essay for additional information about the Chukchi Sea benthos and the pan-Arctic benthos). Species richness was correlated with water salinity and food quality (chlorophyll *a* and total organic carbon in the sediments). Benthic community structure and biomass indicated that the western side was dominated by surface deposit feeders (*Ennucula tenuis*) and the subsurface deposit feeding polychaete *Maldane sarsi*, with the deepest portion dominated by the suspension feeding bivalve *Mytilus* spp. Suspension feeding sea cucumbers and ascidians were closer to the shore, indicating stronger currents above these animals in the ACW. High abundance of suspension feeding amphipods (*Byblis* spp.) close to the shore provided food for gray whales.

References

Aagaard, K. and A. T. Roach, 1990. Arctic ocean-shelf exchange: Measurements in Barrow Canyon, *J. Geophys. Res.*, 95, 18,163 - 18, 175.

Cavalieri, D., C. Parkinson, P. Gloersen and H. J. Zwally. 2008. *Sea Ice Concentrations from Nimbus-7 SMMR and DMSP SSM/I Passive Microwave Data*. Boulder, Colorado USA: National Snow and Ice Data Center. Digital media.

Grebmeier, J. M. 2012. Shifting patterns of life in the Pacific Arctic and Sub-Arctic seas. *Ann. Rev. Mar. Sci.*, 4, 63-78.

Grebmeier, J. M, S. E. Moore, J. E. Overland, K. E. Frey and R. Gradinger. 2010. Biological response to recent Pacific Arctic sea ice retreats. *Eos, Trans. Amer. Geophys. Union*, 91(18), 161-162.

Münchow, A. and E. C. Carmack. 1997. Synoptic flow and density observations near an Arctic shelf break. *J. Phys. Oceanogr.*, 27, 1402-1419.

Nikolopoulos, A., R. S. Pickart, P. S. Fratantoni, K. Shimada, D. J. Torres and E. P. Jones. 2009. The western Arctic boundary current at 152ºW: Structure, variability, and transport. *Deep Sea Res. II*, 56, 1164-1181.

Pickart, R. S., M. A. Spall and J. T. Mathis. 2012. Dynamics of upwelling in the Alaskan Beaufort Sea and associated shelf-basin fluxes. *Deep Sea Res. I*, submitted.

Schulze, L. M. and R. S. Pickart. 2012. Seasonal variation of upwelling in the Alaskan Beaufort Sea. *J. Geophys. Res.*, 117, C06022, doi:10.1029/2012JC007985.

Fish and Fisheries in the Chukchi and Beaufort Seas: Projected Impacts of Climate Change

A.B. Hollowed[1] and M.F. Sigler[2]

[1]Alaska Fisheries Science Center, National Marine Fisheries Service,
National Oceanic and Atmospheric Administration, 7600 Sand Point Way NE, Seattle, WA 98115
[2]Alaska Fisheries Science Center, National Marine Fisheries Service,
National Oceanic and Atmospheric Administration, 17109 Point Lena Loop Road, Juneau, AK 99801

November 11, 2012

Highlights

- Efforts to project how shifts in environmental conditions in the Arctic Ocean will affect the distribution and abundance of marine fish have yielded different outcomes depending on the region and modeling approach.
- Current prohibitions on commercial fishing in U.S. Arctic waters provide an opportunity to design a management strategy for future fisheries that is rooted in an ecosystem approach to fisheries management.
- In support of the management strategy design, the Arctic Ecosystem integrated survey (Arctic Eis) was initiated in the northern Bering Sea and Chukchi Sea in summer 2012.

The impacts of global warming portend that U.S. Arctic (defined here as the Beaufort and Chukchi seas) marine ecosystems will experience significant change, including loss of sea ice in summer (see the *Sea Ice* essay), increased stratification (see the *Ocean* essay) and shifts in the timing and intensity of the seasonal production cycle (Slagstad et al., 2011; Wassmann et al., 2011). Several authors (Cheung et al., 2009; Hunt et al., in press; Huse and Ellingsen, 2008; Mueter et al., 2011; Sigler et al. 2011) have attempted to project how these shifts in environmental conditions will affect the distribution and abundance of marine fish in the region, with the outcomes differing depending on the region and modeling approach. Cheung et al. (2009) projected that expanding bioclimatic windows would result in increased biodiversity in the Arctic, whereas Sigler et al. (2011), projected that the shallow sill separating the northern Bering Sea and the Chukchi Sea, and the persistent presence of the cold water over the northern Bering Sea shelf (Stabeno et al., 2012), would serve as a barrier to invasions of fish species into the region. Pre-cooled water entering the Chukchi Sea from the south, and winter mixing of the Chukchi Sea as it becomes ice covered, result in water temperatures below the physiological limits of the commercially valuable fish that thrive in the southeastern Bering Sea (Hunt et al., in press). Other studies found that key life history features, including slow growth in the first year of life, fidelity to spawning grounds, limited larval dispersal and narrow food habits may impede colonization of the Arctic (Hollowed et al., submitted). Additional monitoring and research is needed to reconcile conflicting outcomes and to improve the accuracy of projected impacts of climate change on the distribution and abundance of Arctic marine fish and shellfish.

Currently, prospects for commercial fishing in the U.S. Arctic are limited by regulation. In 2009, the National Marine Fisheries Service developed an Arctic fisheries management plan (FMP) (Wilson and Ormseth, 2009). For most fish stocks within the Chukchi and Beaufort seas, stock size was insufficient to support commercial activity. For the three stocks (snow crab

Chionoecetes opilio; Arctic cod *Boreogadus saida*; and saffron cod *Eleginus gracilis*) of sufficient size to support commercial activity, additional information is needed to design sustainable harvest strategies within an ecosystem context. Further, Arctic cod and saffron cod likely would remain off limits because of their ecological importance as key prey of marine mammal and seabird predators, leaving snow crab as the only likely candidate for consideration for commercial fishing once additional information is obtained. In light of this uncertainty, the North Pacific Fishery Management Council closed the region to commercial fishing for fish stocks other than Pacific salmon and Pacific halibut (Wilson and Ormseth, 2009). Pacific salmon fisheries in the Arctic were already closed under a separate FMP. Pacific halibut (*Hippoglossus stenolepis*) fisheries in the Arctic are prohibited by the International Pacific Halibut Commission.

The existing prohibitions on commercial activity within the U.S. Arctic provide an opportunity to design a management strategy for future fisheries that is rooted in an ecosystem approach to fisheries management. In support of this long-term goal, NMFS (National Marine Fisheries Service) scientists are designing and implementing baseline surveys to gather information needed to develop age or length-based stock assessments for fish and shellfish in the Arctic (**Fig. 3.8**). Similar fish surveys are also being undertaken in the Canadian Beaufort Sea as part of the BREA (Beaufort Regional Environmental Assessment) program (Fortier, 2012; Reist, 2012).

The U.S. surveys gather oceanographic measurements, abundance, stock structure, growth, food habits and bio-energetic data to identify the mechanisms underlying fish responses to changing oceanographic conditions. These measurements will enable scientists to develop an integrated ecosystem assessment (Levin et al., 2009) that will project the present and future status of marine resources under changing climate conditions as well as potential new anthropogenic stresses emerging from increased shipping, oil and/or gas development. These ecosystem models will allow scientists to inform managers and society of the implications of different options for marine resource use in the Arctic.

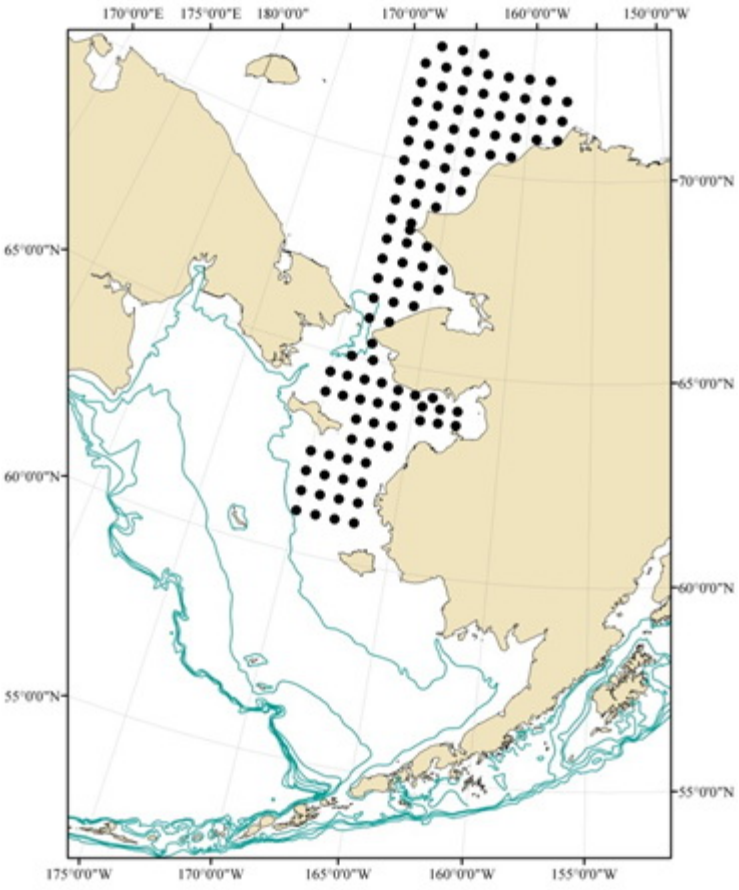

Fig. 3.8. Survey design for the Arctic Ecosystem integrated survey (Arctic Eis) during 2012-2013. These surveys are designed to develop a greater understanding of the distribution of marine fish and shellfish, seabirds and the plankton they depend upon for food in the northern Bering and Chukchi seas. The project surveys from surface to seafloor and includes diet, demography and ecosystem modeling. Collaborators include NOAA, University of Alaska Fairbanks, Bureau of Ocean Energy Management, North Slope Borough, State of Alaska and U.S. Fish & Wildlife Service.

Recent reviews of the global status of commercial fish and fisheries reveal several factors that contribute to the achievement of sustainable fisheries (Gutierrez et al., 2011). These factors include leadership, social capital and incentives as well as a commitment to the collection and assessment of high quality information on the fished populations. It is not clear how the governance structures that contribute to sustainable fisheries will work under changing climate conditions within a multinational context (Arnason, 2012). However, if at some point in the future, fish or shellfish stocks increased to a level that could sustain commercial fisheries and knowledge of the life history and population dynamics was sufficient to manage the fishery sustainably, then a comprehensive management plan would have to be developed for the region (Fluharty, 2012).

References

Arnason, R. 2012. Global warming: New challenges for the common fisheries policy? *Ocean & Coastal Management*, in press.

Cheung, W. W. L., V. W. Y. Lam, J. L. Sarmiento, K. Kearney, R. Watson and D. Pauly. 2009. Projecting global marine biodiversity impacts under climate change scenarios. *Fish and Fisheries*, 10, 235-251.

Fluharty, D. 2012. Recent developments at the federal level in ocean policymaking in the United States. *Coastal Management*, 40(2), 209-221.

Fortier, L. 2012. Active acoustic mapping of fish in the Beaufort Sea. Beaufort Regional Environmental Assessment (BREA), Aboriginal Affairs and Northern Development Canada, http://www.beaufortrea.ca/research/active-acoustic-mapping-of-fish-in-the-beaufort-sea/ (accessed 3 November, 2012).

Gutierrez, N. L., R. Hilborn and O. Defeo. 2011. Leadership, social capital and incentives promote successful fisheries. *Nature*, 470(7334), 386-389.

Hollowed, A. B., H. Loeng and B. Planque. Potential movement of fish and shellfish stocks from the Sub-Arctic to the Arctic Ocean. *Fisheries Oceanogr.*, submitted.

Hunt Jr., G. L. and fourteen others. The Barents and Chukchi seas: Comparison of two Arctic shelf ecosystems. *J. Mar. Sys.*, in press.

Huse, G. and I. Ellingsen. 2008. Capelin migrations and climate change - a modelling analysis. *Climatic Change*, 87, 177-197.

Levin, P. S., M. J. Fogarty, S. A. Murawski and D. Fluharty. 2009. Integrated ecosystem assessments: Developing the scientific basis for ecosystem-based management of the ocean. *PLoS ONE*, 7(1), 23-28.

Mueter, F. J., N. A. Bond, J. N. Ianelli and A. B. Hollowed. 2011. Expected declines in recruitment of walleye pollock (*Theragra chalcogramma*) in the eastern Bering Sea under future climate change. *ICES J. Mar. Sci.*, 68(6), 1284-1296.

Rand, K. M. and E. A. Logerwell. 2011. The first demersal trawl survey of benthic fish and invertebrates in the Beaufort Sea since the late 1970s. *Polar Biol.*, 34, 475-488.

Reist, J. 2012. Impacts of Development in the Beaufort Sea on Fish, their Habitats and Ecosystems. Beaufort Regional Environmental Assessment (BREA), Aboriginal Affairs and Northern Development Canada, http://www.beaufortrea.ca/research/impacts-of-development-in-the-beaufort-sea-on-fish-their-habitats-and-ecosystems/ (accessed 3 November, 2012).

Sigler, M. F., M. Renner, S. L. Danielson, L. B. Eisner, R. R. Lauth, K. J. Kuletz, E. A. Logerwell and G. L. Hunt, Jr. 2011. Fluxes, fins, and feathers: Relationships among the Bering, Chukchi, and Beaufort seas in a time of climate change. *Oceanogr.*, 24(3), 250-265.

Slagstad, D., I. H. Ellingsen and P. Wassmann. 2011. Evaluating primary and secondary production in an Arctic Ocean void of summer sea ice: An experimental simulation approach. *Progr. Oceanogr.*, 90(1-4), 117-131.

Stabeno, P. and eight others. 2012. A comparison of the physics of the northern and southern shelves of the eastern Bering Sea and some implications for the ecosystem. *Deep Sea Res. II*, 65-70, 14-30.

Wassmann, P., C. M. Duarte, S. Agusti and M. Sejr. 2011. Footprints of climate change in the Arctic marine ecosystem. *Glob. Change Biol.*, 17, 1235-1249.

Wilson, W. J. and O. A. Ormseth. 2009. A new management plan for Arctic waters of the United States. *Fisheries*, 34(11), 555-558.

Marine Mammals

K.L. Laidre

Polar Science Center, Applied Physics Laboratory University of Washington, Seattle, WA, USA

November 11, 2012

Highlights

- Species richness for core Arctic marine mammals is highest in three regions: Baffin Bay, Davis Strait and the Barents Sea, where nine of eleven species are present. Most other regions have seven or eight core species, while the Beaufort Sea and the Sea of Okhotsk regions have only six species.
- Two acoustic recorders in Fram Strait during the International Polar Year (2007-2009) documented critically endangered Spitzbergen bowhead whales singing almost continuously through the winter.
- In Hudson Bay, later departures of beluga from their summering grounds have been linked to warmer and more spatially more heterogeneous sea temperatures.

CAFF Arctic Biodiversity Assessment (ABA)

Arctic marine mammals are widely considered to be icons of climate change. However, no comprehensive studies have examined available data on population abundance, distribution and trends across the Arctic. In 2011, the "Arctic Biodiversity Assessment - Status and Trends" (ABA) was launched by the Arctic Council Working Group on Conservation of Arctic Flora and Fauna (CAFF) to synthesize and assess the status and trends of biological diversity in the Arctic (CAFF, in press). The report is an international collaboration among marine mammal scientists from all Arctic countries, which serves to inventory and update the status and trends of all stocks of Arctic marine mammals. The ABA summarizes what is known about population sizes, trends, and distributions for species that inhabit sub-Arctic and Arctic waters. It also discusses implications of data gaps on various species given predictions of continued sea ice loss and climate warming (see the *Sea Ice* and *Air Temperature, Atmospheric Circulation and Clouds* essays, respectively, for more information about sea ice loss and climate warming).

In total, 35 marine mammal species that inhabit or seasonally use Arctic waters were reviewed in the ABA and assessed in the context of 12 marine regions in low or high Arctic waters. Species were considered in two categories: (1) species that occur north of the Arctic Circle for most of the year and depend on the arctic ecosystem for all aspects of life (n=11 "core" Arctic marine mammals) (**Table 3.1**), and (2) selected sub-arctic species whose life histories include seasonal migration to and occupation of arctic waters, yet do not depend on the arctic ecosystem for some parts of the year (n=24 species). Authors calculated species richness (number of species present in different regions) and summarized available data on changes in distribution, population abundance estimates and available trends for marine mammals inhabiting the circumpolar Arctic. Species richness for core Arctic marine mammals is highest in 3 regions: Baffin Bay, Davis Strait, and the Barents Sea, where nine of 11 species are present (**Fig. 3.9**); most other regions have seven or eight core species, while the Beaufort Sea and the Sea of Okhotsk regions have only six species. The final CAFF ABA is due in spring 2013.

Table 3.1. List of core marine mammal species considered in the CAFF ABA.

Arctic	Narwhal	*Monodon monoceros*
	Beluga whale	*Delphinapterus leucas*
	Bowhead whale	*Balaena mysticetus*
	Ringed seal	*Phoca hispida*
	Bearded seal	*Erignathus barbatus*
	Walrus	*Odobenus rosmarus*
	Polar bear*	*Ursus maritimus*
Sub-Arctic	Spotted seal	*Phoca largha*
	Ribbon seal	*Phoca fasciata*
	Harp seal	*Pagophilus groenlandicus*
	Hooded seal	*Cystophora cristata*

*The status and trends of polar bear populations were reported in Arctic Report Card 2011 (Vongraven and Richardson, 2011).

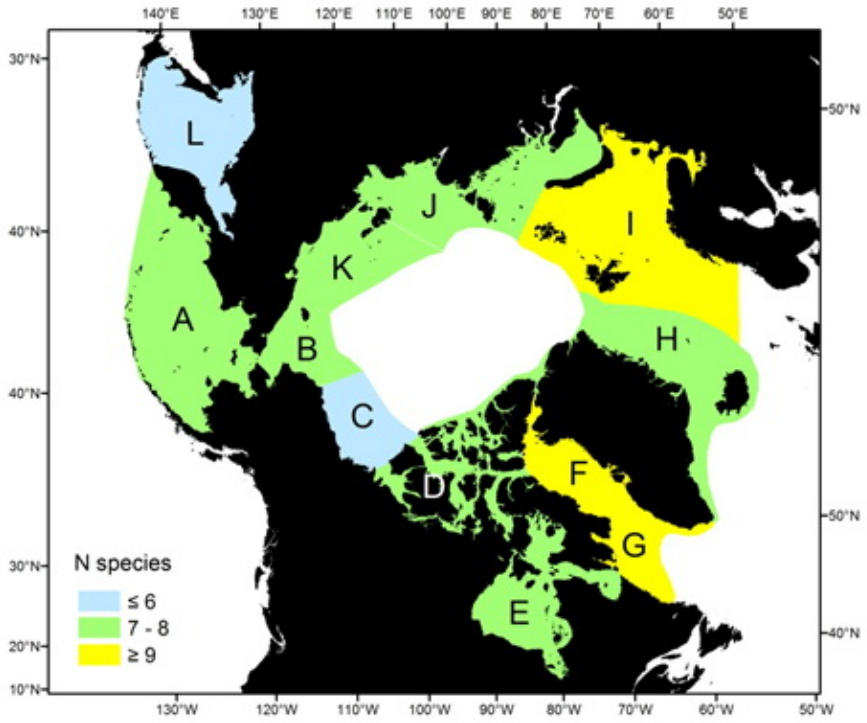

Fig. 3.9. Species richness of core marine mammals (n = 11) in high and low Arctic waters quantified for 12 regions: (A) Bering Sea, (B) Chukchi Sea, (C) Beaufort Sea, (D) Arctic Archipelago, (E) Hudson Bay and Foxe Basin, (F) Baffin Bay, (G) Davis Strait, (H) East Greenland and Iceland, (I) the Barents Sea, (J) the Laptev and Kara Seas, (K) East Siberian Sea, and (L) Okhotsk Sea. Figure from CAFF (2013).

Acoustic Ecology

Several recent studies of Arctic marine mammals using autonomous recorders have provided new information on species seasonality and acoustic environments in the Arctic. Moore et al. (2012) report on an initiative from the International Polar Year (2007-2009), when acoustic recorders were deployed on oceanographic moorings in Fram Strait and on the Chukchi Plateau. This was the first coordinated year-round sampling of underwater acoustic habitats at two sites in the High Arctic. Some aspects of water flow through Fram Strait are described in the *Ocean* essay.

Distinctly different acoustic habitats (the sounds underwater to which animals are exposed) were found at each site, with the Fram Strait being acoustically complex compared to the Chukchi Plateau. In Fram Strait, calls from bowhead whales (*Balaena mysticetus*) and a variety of toothed whales (odontocetes) were recorded year-round. Surprisingly, calls from sub-Arctic whales, including blue (*Balaenoptera musculus*) and fin whales (*B. physalus*), were recorded from June to October and August to March, respectively. At the Chukchi Plateau site, beluga (*Delphinapterus leucas*) and bowhead whale calls were recorded primarily from May to August. Ribbon seal (*Phoca fasciata*) calls were detected in October-November, and no marine mammal calls were recorded from December to February.

Differences in acoustic habitats between the two sites were related to contrasts in sea ice cover, temperature, ocean circulation patterns and contributions from anthropogenic noise sources. Stafford et al. (2012) reported on bowhead whales singing almost continuously through the winter from data from two recorders in Fram Strait, where Spitzbergen bowheads are considered to be a critically endangered population. Peak levels of song production coincided with the period of lowest water temperature, high ice concentration and almost complete darkness. Repeated call sequences and songs were detected nearly every hour from early November 2008 through late April 2009 by the western Fram Strait recorder and more than 60 unique songs were recorded from October 2008 to April 2009. The authors concluded that western Fram Strait may be a wintering ground or potential mating area for this critically endangered population of bowhead whales.

Updates on Arctic marine mammal movements and distribution relative to sea ice

Bowhead whales. Wheeler et al. (2012) used governmental, private and historical whaling location datasets on eastern Canadian Arctic (ECA) bowhead whales to create a monthly ecological niche factor analysis for the 'reduced-ice' period (June to October) to determine habitat suitability. Multiple habitat suitability models were developed to create a composite map of predicted high suitability habitat for 5 months. Six critical habitats were identified around Baffin Island, Hudson Strait and the Labrador coast, which were supported by recent scientific evidence and Inuit knowledge. The study provides resource managers with a timely tool for population recovery, conservation, and protection.

Laidre and Heide-Jørgensen (2012) used satellite telemetry to examine the movements of two co-occurring baleen whales, the bowhead whale and the humpback whale (*Megaptera novaeangliae*), in Disko Bay, west Greenland. Data were collected from tagged bowhead (n=49) and humpback whales (n=44) during the transition from sea ice breakup to open water between 2008 and 2010. The departure of bowhead whales from Disko Bay coincided almost precisely with the arrival of humpback whales, and, during a brief period of overlap, the two species used different areas and habitat. A significant trend in later spring migration departure date was found

for bowhead whales, with an approximate 2-week difference in departure between 2001 and 2010.

Beluga whales. Goetz et al. (2012) developed predictive habitat models for the endangered population of beluga whales in Cook Inlet, Alaska, using an analysis based on data from aerial surveys conducted between 1994 and 2008. Distinguishing suitable habitat is integral to the sustainability and recovery of the Cook Inlet beluga whale population. Goetz et al. found there is a greater probability of belugas being present closer to rivers with Chinook salmon runs, rivers with medium flow accumulation (assessed using quartile values of each river), tidal flats, and areas with sandy coastlines. Probability of beluga presence decreased closer to rivers with chum salmon, rivers with high flow accumulation, local communities, oil development and coastal areas with rocky substrate.

Bailleul et al. (2012) report on differences in migration timing for beluga whales in Eastern Hudson Bay (EHB) and suggest a mechanism by which environmental conditions determine habitat use and migration patterns. Later migration date departures were observed for whales in 2002 and 2003, when warmer and spatially more heterogeneous sea temperatures prevailed during summer. This was in contrast to 2004, which was the coldest summer since the 1990s. The authors suggest later departures may become more typical for beluga whales as temperatures continue to increase.

Ringed seals. Chambellant et al. (2012a) reported on differences in ringed seal pregnancy rates, percent pups, ovulation and growth in the fall harvest in Hudson Bay Canada in the 1990s and 2000s. Pregnancy rate and percent pups increased in the 2000s relative to the 1990s with no change in ovulation rate. Ringed seals grew faster and attained sexual maturity earlier in life, and the population age structure shifted to younger age classes in the 2000s. The decline of ringed seal reproductive parameters and pup survival in the 1990s may have been triggered by unusually cold winters and heavy ice conditions that prevailed in Hudson Bay in the early 1990s.

Chambellant et al. (2012b) conducted strip-transect surveys in late spring in 1995-1997, 1999-2000 and 2007-2008 to estimate distribution, density and abundance of ice-obligated ringed and bearded seals in western Hudson Bay. Ringed and bearded seal density estimates varied from 0.46 to 1.60 seals/km^2 of ice to 0.0036 to 0.0229 seals/km^2 of ice, respectively. Strong inter-annual variations were recorded in the abundance estimates of both species, with the largest abundance estimates in 1995 and the lowest in 2008 for ringed seals and in 1997 for bearded seals.

References

Bailleul, F., V. Lesage, M. Power, D. W. Doidge and M. O. Hammill. 2012. Migration phenology of beluga whales in a changing Arctic. *Climate Res.*, 53, 169-178.

CAFF. *Status and Trends in Arctic Biodiversity*. Conservation of Arctic Flora and Fauna (CAFF), Akureyri, Iceland, in press.

Chambellant, M., I. Stirling, W. A. Gough and S. H. Ferguson. 2012a. Temporal variations in Hudson Bay ringed seal (*Phoca hispida*) life-history parameters in relation to environment. *J. Mammal.*, 93, 267-281.

Chambellant, M., N. J. Lunn and S. H. Ferguson. 2012b. Temporal variation in distribution and density of ice-obligated seals in western Hudson Bay, Canada. *Polar Biol.*, online, doi:10.1007/s00300-012-1159-6.

Goetz, K. T., R. A. Montgomery, J. M. Ver Hoef, R. C. Hobbs and D. S. Johnson. 2012. Identifying essential summer habitat of the endangered beluga whale *Delphinapterus leucas* in Cook Inlet, Alaska. *Endangered Species Res.*, 16, 135-147.

Laidre, K. and M. P. Heide-Jørgensen. 2012. Spring partitioning of Disko Bay, West Greenland, by Arctic and Subarctic baleen whales. *ICES J. Marine Sci.*, doi: 10.1093/icesjms/fss095.

Moore, S. E., K. M. Stafford, et al. 2012. Comparing marine mammal acoustic habitats in Atlantic and Pacific sectors of the High Arctic: Year-long records from Fram Strait and the Chukchi Plateau. *Polar Biol.*, 35(3), 475-480.

Stafford, K.M., S.E. Moore, C. L. Berchok, Ø. Wiig, C. Lydersen, E. Hansen, D. Kalmbach and K. M. Kovacs. 2012. Spitsbergen's endangered bowhead whales sing through the polar night. *Endangered Species Res.*, 18, 95-103.

Wheeler, B., M. Gilbert and S. Rowe. 2012. Definition of critical summer and fall habitat for bowhead whales in the eastern Canadian Arctic. *Endangered Species Res.*, 17, 1-16.

Benthos

B. Bluhm

Institute of Marine Science, University of Alaska Fairbanks, Fairbanks, AK, USA

November 12, 2012

Highlights

- Recent findings on temporal trends in the benthic system include: species range changes in sub-Arctic seas and on inflow shelves; changes in feeding guild composition in the deep Fram Strait; reduction of benthic biomass in the Barents and northern Bering seas; no apparent change in infaunal biomass in the Kara Sea.
- Results from Greenland, and the northern Bering and Chukchi seas show spatial and temporal differences and variability in invertebrate growth, energy budgets and resulting biomass that are related to variation in seasonal sea ice dynamics, temperature and food supply.
- Greatly improved benthic species inventories for Iceland, Greenland and the Russian Arctic show upwards of 1000 species per region.
- Contrary to long-standing belief, terrestrial carbon significantly contributes to benthic food webs on the river-influenced Beaufort Sea shelf.

Introduction

Macrobenthic infauna (animals living within the sediments) act as long-term integrators of overlying sediment processes. They remain relatively stationary in the sediment and their community patterns are thus directly affected by export production from the overlying water column. The distribution, abundance and biomass of infauna vary by region and are related to water mass characteristics and current patterns. Larger epifaunal organisms (animals living on top of the sediment) contribute considerably to carbon remineralization, and through their mobility, to carbon distribution.

This report on the status of Arctic marine benthic communities is pan-Arctic in scope and organized by region. International members of the benthic expert group of the Arctic Council's Circumpolar Biodiversity Monitoring Program under CAFF (Conservation of Arctic Flora and Fauna) summarized new key findings in their regions. The scope of research and nature of those findings vary among regions.

Northern Bering Sea and Chukchi Sea

Bivalves, amphipods, and polychaetes dominate the infaunal biomass south of St. Lawrence Island in the northern Bering Sea, where time series data indicate a decline in overall station biomass and of specific components in recent decades (**Fig. 3.10**). Amphipods and bivalves dominate in the central region from St. Lawrence Island to Bering Strait, and bivalves and polychaetes dominate in the southern Chukchi Sea to the slope region of the Canada Basin (Bluhm and Grebmeier, 2011).

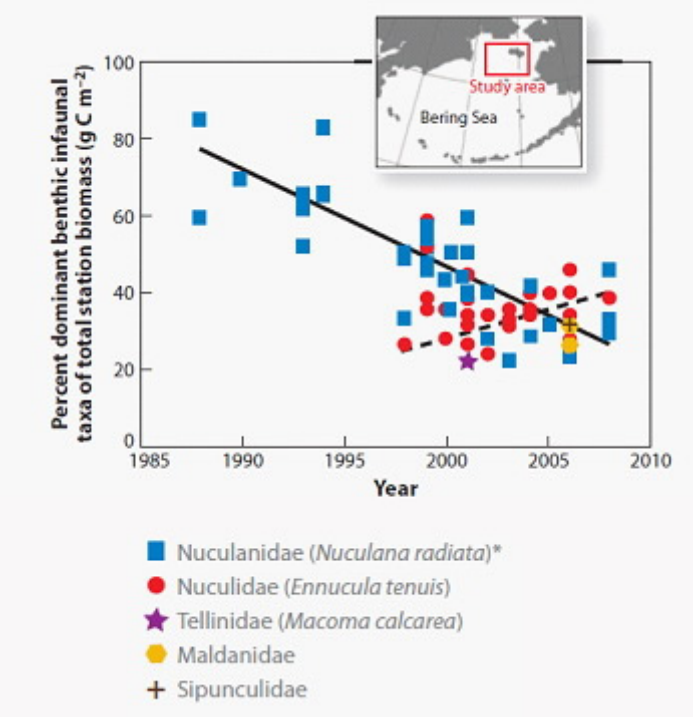

Fig. 3.10. Example of change in infaunal benthos on Arctic shelves (Grebmeier, 2012). The solid black line shows a decrease in relative contribution of the bivalve *Nuculana radiata* to total infaunal biomass south of St. Lawrence Island. The dashed black line shows an apparent, but not statistically significant, increase in *Ennucula tenuis*, a bivalve that is not a preferred prey for diving sea ducks that overwinter in the region.

The nutrient- and phytoplankton-rich water that is transported northwestward through Bering Strait (see the *Ocean* essay for a description of Pacific Water flow through the Bering Strait) is a major driver of the high benthic faunal productivity of the south-central Chukchi Sea. Macrobenthic infaunal biomass in the south-central Chukchi Sea ranges from 24 to 59 g C m^{-2} and exceeds 120 g C m^{-2} at the 'hot-spot" just northwest of Bering Strait (citations in Grebmeier, 2012). This southeastern Chukchi infaunal assemblage is dominated by tellinid and nuculid bivalves, ampeliscid and lysianassid amphipods (Grebmeier, 2012). In contrast to the very productive western side of the system, benthic communities to the east, which are strongly influenced by Alaska Coastal Water, are more patchy, variable in composition and typically of very low biomass (<10 g C m^{-2}, but occasionally ranging up to 12-23 g C m^{-2}), but are characterized by higher diversity. As this Pacific water mass flows north into the central Chukchi Sea, it becomes progressively depleted of nutrients and phytoplankton. Perhaps not surprisingly, then, infaunal biomass declines from the southern Chukchi Sea "hot-spot" to <10 g C m^{-2} in the central Chukchi Sea (Bluhm and Grebmeier, 2011: Figure 1).

Winter-transformed Bering Sea water flows through Herald Valley and Herald Trough (located in the western and central Chukchi Sea, respectively), where infaunal communities are dominated by maldanid, lumbrinerid, and nephtyid polychaetes. Bivalves and polychaetes dominate the infaunal community of the northern Chukchi Sea, where average infaunal benthic biomass is a moderate 5-15 g C m^{-2}, although recent studies indicate high benthic biomass in upper Barrow Canyon (see the essay on *Ecosystem Observations in Barrow Canyon* for information about sea ice, hydrography and biology in the Barrow Canyon region). On the upper slope (200-1000 m depth) and extending down into the Canada Basin, the benthic community becomes foraminifera-dominated, with biomasses of <5 g C m^{-2} (citations in Grebmeier, 2012).

Beaufort Sea

Both the International Polar Year and ongoing and planned fossil fuel development recently sparked several new benthic research projects in the Beaufort Sea. Studies continue, but first results confirm trends found in the 1970s when the benthos was last surveyed. Epibenthic invertebrate biomass dominates significantly over demersal fish biomass (>90% in trawl hauls versus <10%, respectively) (Rand and Logerwell, 2011), with dominant epibenthic taxa (brittle stars, other echinoderms, and crustaceans) similar to those on other Arctic shelves. Biomass generally decreased from west to east in US waters, but high variability was observed farther east as well as hot spots in the Cape Bathurst polynya. Benthic remineralization in the region increases after ice break-up, although interactions of food availability, benthic biomass and remineralization are complex and often more spatially variable than seasonally (Link et al., 2011). A new ice algal biomarker detected in a variety of benthic taxa supports previous research that suggested that ice algae contribute significantly to the nutrition of Arctic shelf benthos (Brown and Belt, 2012) (see the *Primary Productivity and Nutrient Variability* essay for further information about sea ice algal production). In the shallow coastal lagoons of the Beaufort Sea, terrestrial carbon can add substantially to the productivity of marine nearshore Arctic habitats, as reflected in terrestrial stable isotopic signatures and high prevalence of benthic omnivorous and detritivorous fauna (Dunton et al., 2012). Comparatively short-lived and fast colonizing fauna dominate the benthic community in those lagoons, where they are preyed upon by water fowl, fish and seals.

Canadian Arctic

The establishment of ecologically or biologically significant marine areas (EBSA) through application of scientific criteria as promoted by the Convention on Biological Diversity (decision IX/20) will be a baseline for sustainable use and development of the marine ecosystem in the future. Kenchington et al. (2011) used the Canadian identification criteria (uniqueness/rarity; aggregation; fitness consequences; with naturalness and resilience used to prioritize amongst sites identify possible EBSAs) based on benthic attributes for the Canadian Arctic (**Fig. 3.11**). Specifically, benthic diversity and biomass, the density of coral and sponge beds, and benthic remineralization and sediment pigment concentration were used to identify benthic EBSAs for the Hudson Bay Complex, Eastern Arctic and Western Arctic regions. High concentrations of soft corals and sponges are observed in the Hudson Strait compared to Hudson Bay. In the Eastern Arctic, the Baffin Bay-Davis Strait areas are characterized by important aggregations of sea pens, large gorgonian corals and sponges (Kenchington et al., 2010). Franklin Bay and the Prince of Wales Strait in the Canadian Arctic Archipelago were also suggested as benthic EBSAs. Benthic assemblages differ among seven regions on the Canadian Arctic shelf, with taxonomic diversity higher in eastern regions than in the central and western Canadian Archipelago. Currently known macrobenthic (infaunal) species richness in the Canadian Arctic is 992 taxa, similar to the more highly sampled Atlantic Canada (1044 taxa) and Pacific Canada (814 taxa) regions (Archambault et al., 2010). Lancaster Sound and the North Water Polynya support particularly high benthic diversity, benthic biomass and high benthic boundary fluxes. Lancaster Sound also supports important populations of Pennatulacean sea pens with the continental slope off Baffin Bay.

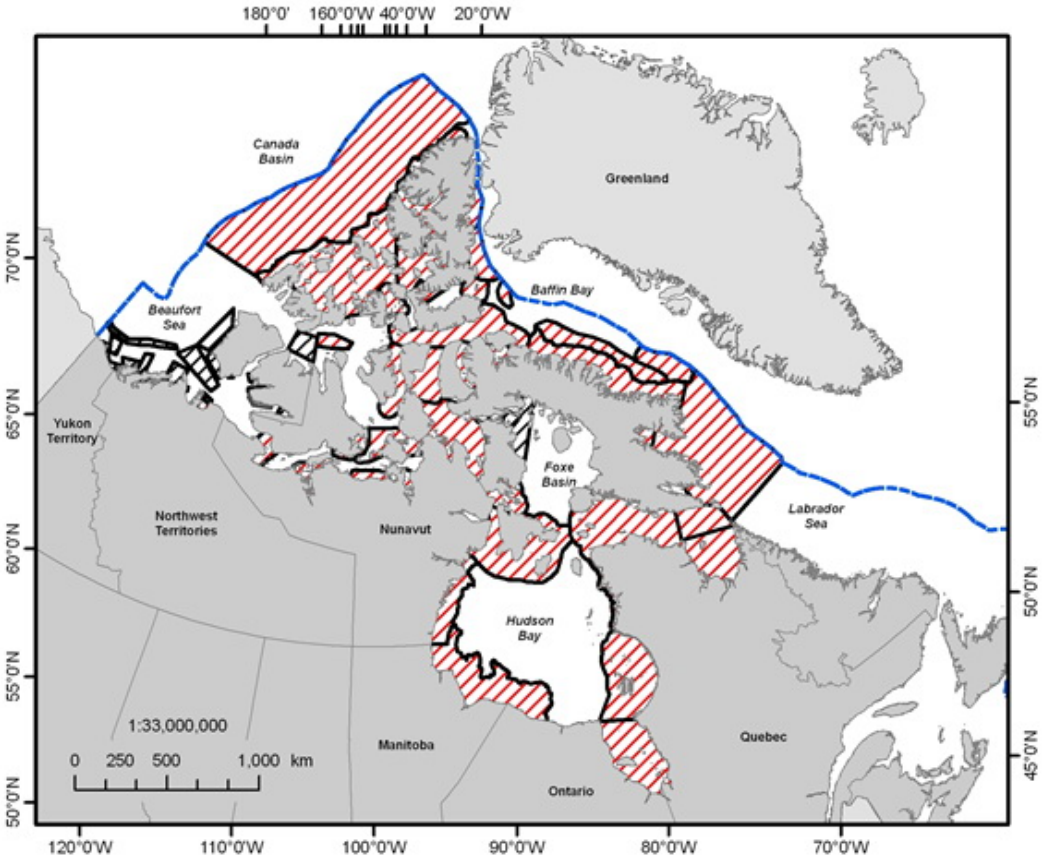

Fig. 3.11. Example for identification of Ecologically and Biologically Significant Areas (EBSAs) in the Arctic, in this case for for mega- and macrobenthos in the Canadian Arctic. From Kenchington et al. (2011).

Greenland

The poorly studied benthic invertebrate fauna off Greenland (i.e., the Greenlandic sector of Baffin Bay and Davis Strait, Denmark Strait and Greenland Sea) lacks historical data on basic ecosystem components necessary to document the state of the environment and potential future changes. However, recent research initiatives have been undertaken as a consequence of climate change, ongoing oil and mineral exploration, and an increasing market demand for environmental certification of industrial fisheries. On a species level, geographic and inter-annual differences in the growth of dominant coastal primary and secondary producers are related to variation in seasonal sea ice dynamics (Krause-Jensen et al., 2012). Similarly, the energy budget of commercially exploited scallops is negatively affected by increasing temperature (Blicher et al., 2010). Exploring such relationships (**Fig. 3.12**) is critical when considering direct economic implications of climate change. On a community level, data are too scarce to document such relationships, although a recent macrozoobenthic survey on a shallow bank in Davis Strait did not show any difference in species richness between 1976 and 2009. The recent studies in West Greenland documented the presence of highly diverse macrozoobenthic communities and also suggest that the benthos plays a key role in carbon flux in the regional shelf and coastal systems. Several organisms recovered during these surveys are potentially new to science.

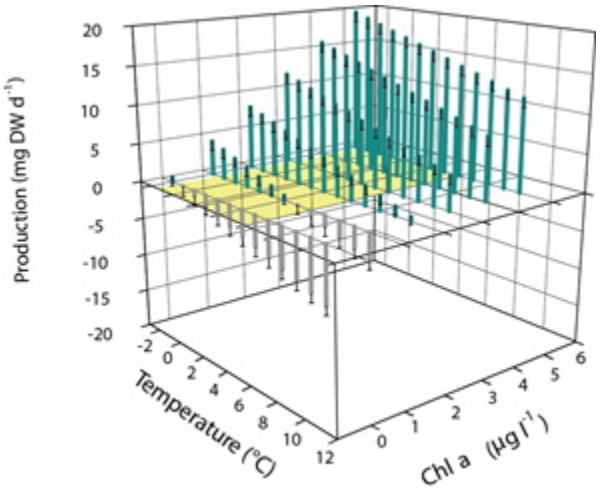

Fig. 3.12. Example of effect of environmental variables (temperature and chlorophyll a) on growth rate of the commercial bivalve *Chlamys islandica* in Greenland waters (Blicher et al., 2010). Red bars show negative effects of increasing C:N ratios (to 14). Yellow shade marks the range of values encountered in the field study.

Iceland

Within the 200 mile, 750,000 km^2 economic zone of Iceland the occurrence of over 1,900 benthic invertebrates species of all major phyla and classes has been recorded over the past few years as a result of the BIOICE (Benthic Invertebrates of Icelandic Waters) program. This area includes a central part of the Greenland-Scotland Ridge, which forms an isolating barrier between the abyssal plains of the North Atlantic and the Arctic oceans (Dauvin et al., 2012). Near-bottom water temperature and the number of benthic species vary greatly north and south of the ridge. Although by far the lowest species diversity occurred in the deeper parts of the Arctic Ocean (>600 m) north of the ridge, a significant portion of endemic species was found here, mostly confined to lower taxonomic levels (Briggs and Bowen, 2012). As a result of climate warming, near-bottom water temperature on the shelf around Iceland has been increasing in recent decades (Sólmundsson et al., 2007). Specifically, a ~2-3°C temperature increase on the shelf areas south and west of Iceland during the last three decades has affected benthic species distributions. An example is the angler fish, *Lophius piscatorius*, whose distribution has expanded in Icelandic waters.

Barents Sea

As an inflow shelf, the Barents Sea ecosystem is particularly strongly influenced by inter-annual and seasonal climate-driven variations, including factors such as ice cover and the strength of inflowing Atlantic water. Water temperatures have increased by 1.5°C since the 1970s, with the strongest increase in the northern Barents Sea. However, a decrease in Atlantic water temperature between 2006 and 2011 in the Barents Sea Opening is reported in the *Ocean* essay. Historical benthic data show that dominant boreal-arctic species have their temperature optimum close to the long-term temperature mean, and that any deviations from that mean will have negative impacts on abundance, reproductive success and change distribution range (Anisimova et al., 2011 and references therein). This negative effect is higher in temperatures above than below the long-term mean temperature. The average infaunal biomass in years

around the long-term mean temperature is 100-147 g wet weight/m^2. As in the Canadian Arctic, the design of Ecologically or Biologically Significant Marine Areas continues in the Barents Sea.

Kara and Laptev Seas

The Kara Sea region has one of the few long-term Arctic benthic time series. Here, infaunal community stability was evaluated for 1927-1945, 1975, 1993 and 2007 (Kozlovsky et al., 2011). The dominant species and infaunal biomass values were quite stable over time, with bivalve mollusks as the predominant taxon. The total number of species amounted to just over 200. Intense study effort has increased the number of known species in the Laptev Sea to almost 1800 (Sirenko and Vassilenko, 2009), relative to 500 in an inventory from 1963. The expected number of species (a diversity measure not biased by the research effort conducted) in the Laptev Sea approaches the same number as in the western Barents Sea. Besides increased investigative effort, a second reason for high species richness is likely the wide range of depths in the area, ranging from the shallows of the Novosibirsky Islands to the lower continental slope.

Arctic Basin

A recent compilation of existing literature documents 1125 taxa in the deep Arctic Basin, with the majority of taxa represented within the arthropods, foraminiferans, annelids and nematodes (Bluhm et al., 2011). Due to low overall sampling effort, this number is expected to increase with further studies of the Arctic deep sea. As known for other deep-sea basins, faunal abundance and biomass decrease with depth, but contrary to the typical mid-depth diversity peak known for other deep-sea regions, no such peak was observed in the analysis of polychaete and nematode diversity. In contrast, studies of ostracod and foraminiferan diversity detected mid-depth peaks, but at a shallower depth than in lower latitude basins (Yasuhara et al., 2012). While several major topographically complex ridge systems bisect the Arctic Ocean basin, they do not seem to present biogeographic barriers, as the fauna in the entire basin (with the exception of rare species) is mostly similar to today's Atlantic fauna owing to Fram Strait being the only deep-water connection to the Arctic Ocean. At HAUSGARTEN (in the eastern Fram Strait and the only Arctic long-term deep-sea observatory for detecting changes in abiotic and biotic parameters in a transition zone between the northern North Atlantic and the central Arctic Ocean; Soltwedel et al., 2005), photographic surveys conducted in 2002, 2004 and 2007 at ~2500 m depth documented significant decreases in megafauna densities, evenness and diversity measures over the study period or for the most recent sampling date (Bergmann et al., 2011). Changes in species abundances and feeding guild distribution coincided with observed increases in bottom water temperatures and changes in food availability related to changes in sea ice cover. The temperature and volume flux of Atlantic Water in Fram Strait are described in the *Ocean* essay.

References

Archambault, P., P. V. R. Snelgrove, J. A. D. Fisher, J. M. Gagnon, D. J. Garbary, M. Harvey, E. L. Kenchington, V. Lesage, M. Lévesque, C. Lovejoy, D. L. Mackas, C. W. McKindsey, J. R. Nelson, P. Pepin, L. Piché and M. Poulin. 2010. From sea to sea: Canada's three oceans of biodiversity. *PLoS ONE*, 5(8), e12182. doi:10.1371/journal.pone.0012182.

Anisimova, N. A, L. L. Jørgensen, P. Lubin and I. Manushin. 2011. Chapter 4.1.2. Benthos. *The Barents Sea. Ecosystem, Resources, Management. Half a Century of Russian-Norwegian Cooperation*, T. Jakobsen and V. K. Ozhigin (eds.), Tapir Academic Press, Trondheim, 315-328.

Bergmann, M., T. Soltwedel and M. Klages. 2011. The interannual variability of megafaunal assemblages in the Arctic deep sea: Preliminary results from the HAUSGARTEN observatory (79°N). *Deep-Sea Res. I*, 58, 711-723.

Blicher, M. E., S. Rysgaard and M. K. Sejr. 2010. Seasonal growth variation in *Chlamys islandica* (Bivalvia) from Sub-Arctic Greenland is linked to food availability and temperature. *Mar. Ecol. Prog. Ser.*, 407, 71-86.

Bluhm, B. A., W. G. Ambrose, Jr., M. Bergmann, L. M. Clough, A. V. Gebruk, C. Hasemann, K. Iken, M. Klages, I. R. MacDonald, P. E. Renaud, I. Schewe, T. Soltwedel and M. Włodarska-Kowalczuk. 2011. Diversity of the arctic deep-sea benthos. *Marine Biodiv.*, 41, 87-107.

Brown, T. A. and S. T. Belt, 2012. Identification of the sea ice diatom biomarker IP_{25} in Arctic benthic macrofauna: direct evidence for a sea ice diatom diet in Arctic heterotrophs. *Polar Biol.*, 35, 131-137.

Briggs, J. C. and B. W. Bowden. 2012. A realignment of marine biogeographic provinces with particular reference to fish distribution. *J. Biogeogr.*, 39, 12-30.

Dauvin, J. C., A. Sandrine, A. Weppe and G. Guðmundsson. 2012. Diversity and zoogeography of Icelandic deep-sea Ampeliscidae (Crustacea: Amphipoda). *Deep-Sea Res. I*, 68, 12-23.

Denisenko, S. G. 2007. Zoobenthos of the Barents Sea in the conditions of the variable climate and anthropogenic influence. *Dynamics of marine ecosystem and modern problem of conservation of biological resources of the Russian seas*, V. G. Tarasov (ed.), Dalnauka, Vladivostok, 418-511, in Russian.

Dunton, K. H., S. V. Schonberg and L. W. Cooper. 2012. Food web structure of the Alaskan nearshore shelf and estuarine lagoons of the Beaufort Sea. *Estuar. Coasts*, 35, 416-435.

Grebmeier, G. M. 2012. Shifting patterns of life in the Pacific Arctic and sub-Arctic Seas. *Ann. Rev. Mar. Sci.*, 4, 16.1-16.16.

Kenchington, E., H. Link, V. Roy, P. Archambault, T. Siferd, M. Treble and V. Wareham. 2011. Identification of Mega- and Macrobenthic Ecologically and Biologically Significant Areas (EBSAs) in the Hudson Bay Complex, the Western and Eastern Canadian Arctic. *DFO Can. Sci. Advis. Sec. Res. Doc.* 2011/071. vi + 52 p.

Kozlovskiy, V. V., Chikina, M. V., Kucheruk, N. V. and A. B. Basin. 2011. Structure of the macrozoobenthic communities in the southwestern Kara Sea. *Oceanology*, 51, 1012-1020, doi: 10.1134/S0001437011060087.

Krause-Jensen, D., N. Marbà, et al. 2012. Seasonal sea ice cover as principal driver of spatial and temporal variation in depth extension and annual production of kelp in Greenland. *Glob. Change Biol.*, 18, 2981-2994.

Link, H., P. Archambault, T. Tamelander, P. E. Renaud and D. Piepenburg. 2011. Spring-to-summer changes and regional variability of benthic processes in the western Canadian Arctic. *Polar Biol.*, 34, 2025-2038.

Rand, K. M. and E. A. Logerwell. 2011. The first demersal trawl survey of benthic fish and invertebrates in the Beaufort Sea since the late 1970s. *Polar Biol.*, 34, 475-488.

Sirenko, B. I. and S. V. Vassilenko. 2009. Fauna and zoogeography of benthos of the Chukchi Sea. *Explorations of the Fauna of the Seas*, 61(69), 1-230.

Sólmundsson, J., E. Jónsson and H. Björnsson. 2007. Recent changes in the distribution of anglerfish in Icelandic waters (*in Icelandic with English abstr.*). *Náttúrufræðingurinn*, 1, 13-20.

Soltwedel and seventeen others. 2005. HAUSGARTEN: multidisciplinary investigations at a deep-sea, long-term observatory in the Arctic Ocean. *Oceanography*, 18(3), 46-61.

Terrestrial Ecosystems Summary

Section Coordinator: Michael Svoboda

Canadian Wildlife Service, Environment Canada, Whitehorse, YT, Canada & CAFF/CBMP

December 4, 2012

The 2012 Terrestrial Ecosystem Section of the Arctic Report Card includes primary producers (vegetation), herbivores (lemmings & caribou and reindeer) and predators (Arctic fox). Another essay highlights changes in arctic migratory wader (shorebird) populations, which introduces and emphasizes the influence of southern stressors and drivers on Arctic wildlife. The five essays highlight meaningful detectable changes of regional, continental and global significance, suggest key factors responsible for the changes (be it climate, anthropogenic or both) and illustrate the connections between the Arctic marine and terrestrial ecosystems. An example is the direct link between increases in Arctic tundra vegetation productivity and earlier peak productivity in many parts of the Arctic on one hand, and the increasing duration of the open water season and decreasing summer sea ice extent in the Arctic Ocean on the other. Information from long-term, ground-based observations shows that, in addition to increasing air temperatures and loss of summer sea ice, widespread greening is also occurring in response to other factors. These include landslides and other geomorphological processes related to warming permafrost, tundra fires and increased human presence in the Arctic.

The impacts of increased biomass production in Arctic tundra ecosystems on arctic wildlife are unclear. Migratory caribou/reindeer appear to be within known ranges of natural variation, with many herds that have experienced declines in the past decade beginning to stabilize or increase. Like caribou, lemming abundance dramatically alters the composition of the tundra food web, the biomass and structure of vegetation, and the productivity of numerous other birds and mammals that depend on them as a food source. Lemming populations are cyclic, with the recovery to high populations after low density years most often associated with a period of successful breeding and recruitment of young under the winter snow. Regularity in cycle duration seems to be decaying, i.e., lengthening, in many Arctic regions, and cycle amplitude in some regions has collapsed to relatively low densities. Recent studies suggest a link between changes in the lemming population cycle and changes in the characteristics of the snow pack, e.g., duration and number of ice layers, and the subsequent impact on ground conditions, e.g., temperature and ice layers. One animal most directly affected by lemming population dynamics is the Arctic fox, which depends on them as a primary food source. In Europe, the Arctic fox population has not recovered from over-harvesting at the start of the 20th Century and the recent absence of lemming peaks; consequently, the Arctic fox has declined to near extinction in the European Arctic. In North America, the Arctic fox is abundant. In both regions, the Red fox has expanded northward into historic Arctic fox-only territories. The Red fox, twice the size of the Arctic fox with about twice the home range area, affects the Arctic fox via competition for resources and intra-guild predation.

At a more global scale, waders connect the Arctic to virtually all corners of the world, apart from Antarctica, via their migratory routes. This extensive range highlights the significance of extra-Arctic impacts on some populations that frequent the Arctic. Waders are by far the most numerous and species rich taxa among all Arctic waterbirds and serve as good indicators of the state of global coastal and inland wetlands. Current data suggest a profound and widespread decline in wader population abundance, due primarily to hunting and harvesting, pollution and habitat loss.

Waders (Shorebirds)

C. Zöckler[1], R. Lanctot[2], S. Brown[3], E. Syroechkovskiy[4]

[1]UNEP World Conservation Monitoring Centre, Cambridge, UK
[2]U.S. Fish & Wildlife Service, Division of Migratory Bird Management, Anchorage, AK, USA
[3]Manomet Center for Conservation Sciences, Plymouth, MA, USA
[4]BirdsRussia, Moscow, Russia

November 29, 2012

Highlights

- Migratory Arctic shorebirds link virtually all corners of the World, apart from Antarctica, through their migratory routes; consequently, some populations that frequent the Arctic are affected by factors outside the Arctic.
- Waders are by far the most numerous and species rich taxa among all Arctic waterbirds and serve as good indicators of the state of global coastal and inland wetlands.
- More than 40% of arctic wader populations are declining, while only 9% are showing increasing trends.
- The African-Eurasian Flyway is the most stable of the flyways, with only 25% of the 46 populations showing declining trends. In the East Asia Australasian flyway, 100% of the 11 populations with known trends are declining, whereas in North America 56% of the 34 populations with a known trend are declining. Only 3 of the 20 populations in central Asia have trends and all are thought to be stable.

Introduction

Migratory Arctic birds fly to virtually all corners of the world, apart from Antarctica, via their migratory routes. They migrate to almost all inland and coastal wetlands, and offshore waters are often utilised by Arctic breeding waders in winter. Most Arctic waders (also known as shorebirds), spend only two to three months on the Arctic breeding grounds during the brief summer.

Across the Arctic a total of eight flyways that connect geographic areas to the south have been described (Boere & Stroud, 2006). For this comparative analysis, the three American flyways have been combined into one and the Black Sea/Mediterranean has been combined with the African Eurasian, leaving four major flyways for discussing the status and trends of waders (**Fig. 4.11**). Trend data are primarily from Wetlands International (2012) and supplemented by published reports from selected representative key sites in the region to provide the best information available for analyses and discussion from an Arctic and flyway perspective.

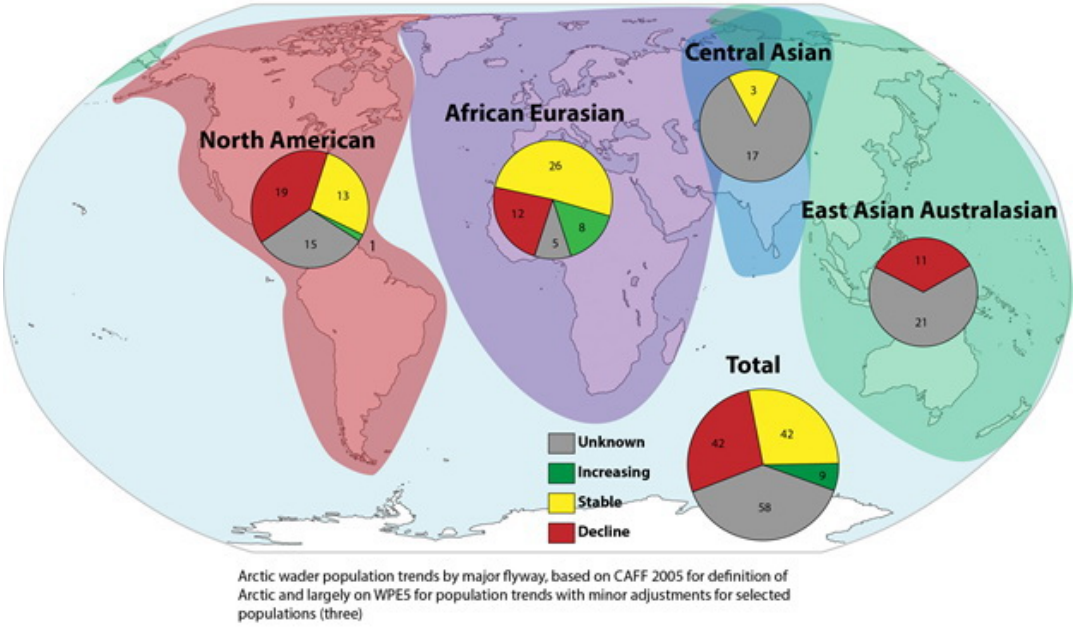

Fig. 4.11. Arctic wader population trends by major flyway, based on CAFF (2001) for definition of Arctic and largely on WPE5 for population trends, with minor adjustments for three selected populations. Numbers in the circle sectors are the number of populations with a particular trend (unknown, increasing, stable, decline).

Waders are by far the most numerous and species rich taxa among all Arctic waterbirds and serve as good indicators on the state of global coastal and inland wetlands, pointing to numerous pressures mostly in the non-breeding areas. Arctic waders include 71 species and 70 separate populations amounting to almost 50 million individuals which regularly undertake long-distance migrations to all corners of the globe (Zöckler, 2012).

Flyways

The status and trend data are available for 94 populations covering >60 species of Arctic waders or 61% of the 153 populations recognised for this analysis. Of these populations over 45% are declining while 8.5% show increasing trends. Although the available data vary considerably among the flyways, the results reveal declining trends in most flyways, apart from the central Asian Flyway, although WPE5 (World Population Estimates, Fifth Edition by Wetlands International, 2012) has not established trends for many populations due to the lack of data for the entire populations (**Fig. 4.11**, **Table 4.1**). Data from the central Asia Flyway are scarce and not available for most flyway populations; however, trend data assembled from key sites in India, reflecting a significant proportion for three species (Balachandran, 2006), do not point to a similar declining picture seen in other flyways (**Fig. 4.11**).

Table 4.1. Trends in Arctic waterbird population by family based on Delany and Scott (2006) plus updates for some goose populations from 2008 (Griffin, 2009; Mitchell, 2009; Colhoun, 2009) and waders by Balachandran (2006), Sitters and Tomkovich (2010) and Moores et al. (2008). Arctic population delineated as defined by CAFF (2001).

Family (number of species)	No of pop.	Known pop. Trends	No of pop. Increasing (%)	No of pop. Stable (%)	No. of pop. Decreasing (%)	Total pop. size (in 1000 ind.)
Divers (5)	13	5	-	3	2 (40)	2,195
Grebes (2)	5	2	-	2	-	200
Swans (3)	13	9	6	1	3 (33)	513
Geese (12)	49	45	19	14	12 (22)	17,139
Ducks (26)	70	45	2	25	18 (40)	26,337
Eider Ducks (4)	17	16	1	6	9 (55)	4,221
Cranes (2)	4	4	-	1	3 (75)	453
Waders*(71)	170	92	2	38	52 (56,5)	48,760
Gulls (20)	35	20	9	6	5 (20)	17,170
Terns (4)	7	4	-	2	2	5,680
Skuas (4)	-	-	-	-	-	500
Total (153)	**383**	**242**	**39 (16 %)**	**98 (40 %)**	**101 (42 %)**	**123 168 000**

*includes rough estimates of the Arctic proportion of semi-boreal species such as Common Snipe

African-Eurasian Flyway. For approximately 90% of the populations, trend information is available within the African-Eurasian Flyway (AEF). Considering the complexity of the flyway network sites and differing monitoring efforts across the region, continued updating of observations are encouraged. At the AEF level the results suggest that this flyway's wader populations are stable and mainly reflect European populations migrating to North Africa. Twenty-five percent of the populations are declining, which is the lowest number of declining populations compared to all other flyways.

Regular monitoring takes place at key stopover and wintering sites in the Dutch-German-Danish Wadden Sea areas (JMMB, 2011) and in the Langebaan lagoon in South Africa (Harebottle et al., 2006). Arctic waders have been monitored at these sites for over 23 years. Trends from both sites cannot be compared as they refer to different species and populations and illustrate also the difficulty in deriving reliable and accurate population estimates with mixing and shifting populations.

Trend data from 2006 for Langebaan Lagoon in South Africa are available for a period of 23 years, and show declining trends for Curlew Sandpiper, Sanderling, Turnstone, Grey Plover, Red Knot and increasing numbers for Bar-tailed Godwit and Whimbrel (Harebottle et al., 2006).

North American Flyway. In North America, there are 34 species with a total of 50 populations (**Fig. 4.11**). Across the North American Arctic, shorebird diversity is highest near the Bering Strait and northern Alaska, with fewer species in Canada and Greenland. Most information on population sizes of arctic shorebirds has recently been updated with information collected during the Program for Regional and International Shorebird Monitoring (PRISM) surveys (Bart and Johnston, 2012, see Arctic PRISM (Environment Canada). A first round of surveys conducted between 2001 and 2011 has provided population estimates for 26 shorebird species. The reliability of the population estimates varies by species, but will improve as remaining areas of the Arctic are surveyed and a greater understanding of habitat relationships, which are used to extrapolate densities, are developed. Based on this and other information (see Andres et al. 2012), most of the 50 populations known to breed in the North American Arctic number in the

tens of thousands (29) to millions (9). A small number (12) have populations below 25,000 (**Table 4.2**).

Table 4.2. Estimated population sizes in 2012 of North American shorebirds that breed in the High or Low Arctic (see map at http://www.arcticbiodiversity.is). Ranges of population estimates are reported as probability intervals or as expert opinion (estimated). If ranges are not available, a measure of certainty is provided as: (1) low - educated guess, perhaps in the same order of magnitude, wide variation among data sources; (2) moderate - restricted populations or behavior that allows somewhat reliable surveys, estimate comes from several reliable survey types with different methods or incomplete coverage; (3) high - dedicated survey or census of a population. Method denotes that estimates were generated from survey data (SD) or by expert opinion (EX). Trend categories are: significant decline (DEC), apparent decline (dec), possibly extinct (EXT?), apparent increase (inc), significant increase (INC), stable (STA), or unknown (UNK). Long-term refers to trends over the last 30+ years, short-term over the last decade. Excerpted from Andres et al. (2012); see this reference for additional information on methodology.

Common name	Species/subspecies (population)	Point Estimate	Certainty/range	Method	2012 trend long-term	2012 trend short-term
Black-bellied Plover	*Pluvialis squatarola squatarola*	262,700	95% = 134,000–391,500	SD	UNK	UNK
Black-bellied Plover	*P. s. cynosurae*	100,000	moderate	EX	DEC	STA
American Golden-Plover	*Pluvialis dominica*	500,000	95% = 294,200–705,800	SD	dec	UNK
Pacific Golden-Plover	*Pluvialis fulva*	42,500	estimated 35,000–50,000	EX	UNK	UNK
Common Ringed Plover	*Charadrius hiaticula psammodroma*	2,000	low	EX	UNK	dec
Semipalmated Plover	*Charadrius semipalmatus*	200,000	low	EX	INC	STA
Spotted Sandpiper	*Actitis macularius*	660,000	Low	EX	STA	STA
Solitary Sandpiper	*Tringa solitaria cinnamomea*	63,000	Low	EX	UNK	UNK
Wandering Tattler	*Heteroscelus incanus*	15,750	Estimated 10,000–25,000	EX	UNK	UNK
Eskimo Curlew	*Numenius borealis*	<50	low	EX	EXT?	EXT?
Whimbrel	*Numenius phaeopus hudsonicus*	40,000	low	SD	dec	dec
Whimbrel	*N. p. rufiventris*	40,000	moderate	SD	UNK	UNK
Whimbrel	*Numenius phaeopus* (both subspecies)	80,000	moderate	SD	dec	dec
Bristle-thighed Curlew	*Numenius tahitiensis*	10,000	high	SD	UNK	UNK
Hudsonian Godwit	*Limosa haemastica* (Alaska)	21,000	high	SD	STA	STA
Bar-tailed Godwit	*Limosa lapponica baueri*	90,000	estimated 80,000–120,000	SD	dec	dec
Marbled Godwit	*L. f. beringiae*	2,000	Estimated 2,000 – 3,000	EX	STA	STA
Ruddy Turnstone	*Arenaria interpres morinella*	180,000	moderate	EX	DEC	DEC
Ruddy Turnstone	*A. i. interpres* (Alaska)	20,000	moderate	EX	UNK	UNK
Ruddy Turnstone	*Arenaria i. interpres* (Canada)	45,000	moderate	EX	dec	dec
Black Turnstone	*Arenaria melanocephala*	95,000	approx. 95% = 76,000–114,000	SD	STA	STA
Surfbird	*Aphriza virgata*	70,000	Moderate	EX	STA	dec
Red Knot	*C. canutus islandica*	80,000	moderate	EX	dec	dec
Red Knot	*C. c. rufa*	42,000	high	SD	DEC	DEC
Red Knot	*C. c. roselaari*	17,000	13,700–20,200	SD	dec	dec
Sanderling	*Calidris alba*	300,000	low	EX	dec	dec
Semipalmated Sandpiper	*Calidris pusilla* (Eastern)	405,000	moderate	SD	DEC	dec
Semipalmated Sandpiper	*Calidris pusilla* (Central)	405,000	moderate	SD	DEC	STA
Semipalmated Sandpiper	*Calidris pusilla* (Western)	1,450,000	95% = 1,023,700– 1,876,300	SD	STA	STA
Semipalmated Sandpiper	*Calidris pusilla* (all populations)	2,260,000	95% = 1,728,400–2,791,600	SD	dec	dec
Western Sandpiper	*Calidris mauri*	3,500,000	moderate	EX	dec	dec
Least Sandpiper	*Calidris minutilla*	700,000	moderate	EX	STA	STA
White-rumped Sandpiper	*Calidris fuscicollis*	1,694,000	95% = 560,100–3,827,900	SD	STA	STA
Baird's Sandpiper	*Calidris bairdii*	300,000	low	EX	UNK	UNK
Pectoral Sandpiper	*Calidris melanotos*	1,600,000	95% = 1,129,600–2,070,400	SD	DEC	DEC
Purple Sandpiper	*Calidris maritima maritima*	10,000	moderate	EX	dec	dec
Purple Sandpiper	*C. m. belcheri*	15,000	moderate	EX	dec	dec
Purple Sandpiper	*C. m.* (both subspecies)	25,000	moderate	SD	dec	dec
Rock Sandpiper	*Calidris ptilocnemis ptilocnemis*	19,800	95%= 17,900–21,900	SD	UNK	UNK
Rock Sandpiper	*C. p. tschuktschorum*	50,000	low	EX	UNK	UNK
Rock Sandpiper	*C. p. couesi*	75,000	low	EX	UNK	UNK
Dunlin	*C. a. arctricola*	500,000	95% = 304,000–696,000	SD	DEC	DEC
Dunlin	*Calidris alpina pacifica*	550,000	low	EX	STA	STA
Dunlin	*C. a. hudsonia*	450,000	95% = 220,700–679,300	SD	STA	STA
Stilt Sandpiper	*Calidris himantopus*	1,243,700	95% = 418,800-2,068,600	SD	dec	STA
Buff-breasted Sandpiper	*Tryngites subruficollis*	56,000	estimated 35,000–78,000	SD	DEC	UNK
Long-billed Dowitcher	*Limnodromus scolopaceus*	500,000	moderate	EX	UNK	UNK
Wilson's Snipe	*Gallinago delicata*	2,000,000	low	EX	STA	STA
Red-necked Phalarope	*Phalaropus lobatus*	2,500,000	low	EX	DEC	UNK
Red Phalarope	*Phalaropus fulicarius*	1,620,000	95% = 1,143,700–2,096,300	SD	dec	UNK

Shorebird trend data come primarily from the International Shorebird Survey (ISS) and the Maritimes Shorebird Survey; both surveys began in 1974 and are focused on counting

shorebirds during migration along the east coast of North America (although the ISS also has data from the Midwestern United States; Bart et al., 2007). This information, as well as species-specific information derived from breeding and wintering areas, has been consolidated by Andres et al. (2012). Long-term trends (over the last >30 years) indicate that of the 50 populations, 24 have apparent or significant declines, 13 have unknown trends, 11 are stable, 1 is increasing, and 1 is likely extinct (**Table 4.2**). Short-term trends (over last decade) indicate that 19 have apparent or significant declines, 16 have unknown trends, 14 are stable, and 1 is likely extinct (**Table 4.2**). Repeated surveys in the Arctic, as outlined in the PRISM protocols (Bart and Johnston, 2012), will provide additional information on trend data from the breeding grounds when the second round of surveys is completed.

Shorebird populations on average appear to be declining more rapidly than other bird species groups in the Canadian Arctic (**Fig. 4.12**). Within the shorebird group, populations have declined by 60% overall and 10 species are in severe decline (North American Bird Conservation Initiative Canada, 2012). These declines are likely due to habitat alteration at breeding, migration and wintering areas, changes in the availability of prey, increases in predators, more frequent severe weather events, hunting, pesticides and increased natural resource exploration and extraction (North American Bird Conservation Initiative Canada, 2012).

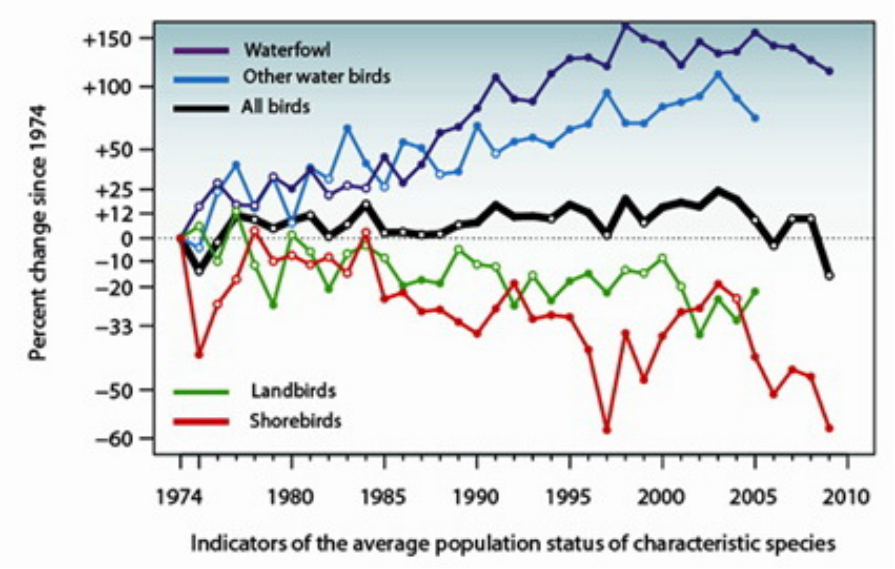

Fig. 4.12. National Bird Biodiversity Indicators from Canada show a strongly declining trend since 1974 for all waders (shorebirds; red line) compared to other bird types (North American Bird Conservation Initiative Canada, 2012).

Central Asian. The situation in central Asia remains largely unknown. Trend data are available only for 3 out of 20 populations and these three were considered stable (WPE5, Wetlands International, 2012). However, long term monitoring at Point Calimere in Southern India shows strong declining trends between 1980 and 2002 for Little Stint *Calidris minuta* (90%), Curlew sandpiper *C. ferruginea* (75%) and Ruff *Philomachus pugnax* (90%; Balachandran, 2006). All three species also declined by 50% between 1989 and 1999 at Lake Chilika (Balachandran, 2006). Further declines have occurred in Little Stints at the same location between 2001 and 2004; the population was estimated at only 30% of the 1988 population size. In contrast, peak counts between 2001 and 2004 for Curlew sandpiper seem to indicate a recovering population (Balachandran, 2006). Because these data are from only a portion of the central Asian population and WPE5 did not establish a trend assessment for these species (Wetlands

International, 2012), more monitoring is required to fully assess these and other species within the Central Asian flyway.

East Asian Australasian. Trend information for a large proportion (about 66%) of the 32 wader populations in the East Asian Australasian Flyway (EAAF) is unavailable. Of the few known population trends, all are declining. Although the flyway boasts the most species-rich complex, it has the least number of individuals. Many regions, mainly in Indonesia, Vietnam and China, remain devoid of migratory wader population data. It remains likely that the unknown populations are also declining and many recent data from Australia point to a continuing decline of many populations. Gosbell & Clemens (2006), for example, documented a long-term rapid decline in Curlew sandpipers *C. ferruginea* (see **Figs. 4.13** and **4.14**). Wilson et al. (2011) considered 22 migrant and 8 resident species with seven species of migrants to be declining significantly, and abundance of one species as significantly increasing. Declines of 43-79% in migrant abundance over 15 years were also observed. Among the declining species were ten Arctic waders, while two populations, Red-necked Stint and Sharp-tailed sandpiper, were increasing. With the exception of the Curlew sandpiper, it is not clear how representative these results are of the entire flyway.

The Far-Eastern Curlew and Great Knot have recently been classified as Vulnerable and added to the IUCN list of globally-threatened species, having experienced declines of 30-49% over the last 20-30 years (BirdLife International, 2012). Populations of Red Knots and Bar-tailed Godwits from Siberian and Alaskan breeding grounds are also declining; having lost over half of their individuals they have declined at a rate of 5-9% per year in last decade (Wilson et al., 2011). One of the key species under threat on the flyway is the Spoon-billed sandpiper (see the case study below).

The situation in the EAAF is of particular concern. The EAAF supports more migratory waterbird species and a higher proportion that is globally threatened than any other flyway in the World (MacKinnon et al., 2012; Amano et al., 2010). It also has the highest rate of loss of intertidal wetlands (as much as 50% in the last 30 years) (Barter, 2006; Yang et al., 2011) and only 5% of intertidal wetlands are protected.

Fig. 4.13. Curlew sandpiper trends monitored at seven sites in Australia (Gosbell & Clemens, 2006).

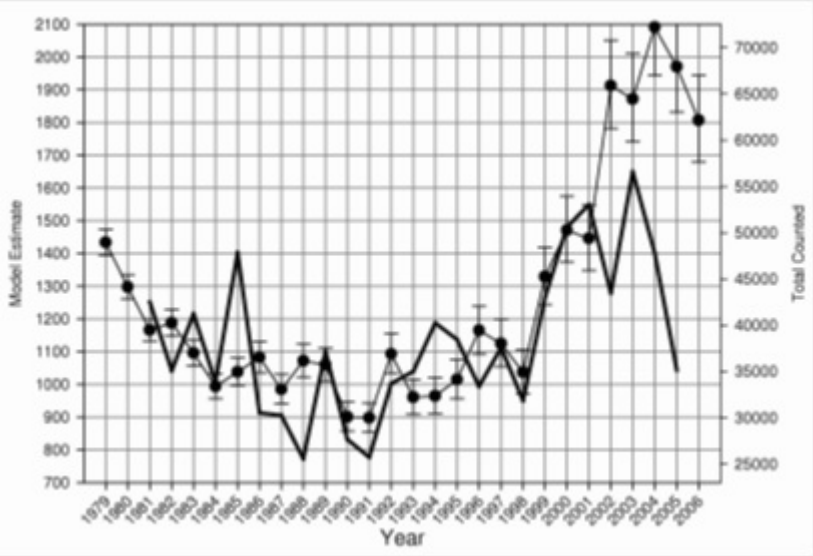

Fig. 4.14. Red-necked Stint population trends monitored at coastal wetlands in Victoria, Australia (Gosbell& Clemens, 2006).

Threats

Although the surveys above provide information on the status and trends of shorebirds breeding in the Arctic, they can be difficult to interpret as they often do not provide enough information to determine the mechanisms behind any declines or increases, the life stage when shorebird populations are likely to be limited (e.g., breeding, migration, non-breeding), or how climate conditions may influence recovery. To address some of these limitations, the Arctic Shorebird Demographics Network was established in 2010 to collect demographic data on shorebirds breeding in the Arctic (http://www.manomet.org/arctic-shorebird-demographics-network). The Network is composed of 14 field sites (2 in Russia, 7 in Alaska, 5 in Canada) that collect data to generate estimates of adult bird survival, nesting success, and reproductive effort. At each site environmental data that are sensitive to climate change are collected, and this information is used to help interpret changes in the demographic traits.

Although the breeding period is a very important and sensitive time for arctic waders, stressors and/or threats that occur outside the Arctic are often considered more important when trying to understand observed population trends of these global creatures.

Hunting and harvesting. Hunting of shorebirds is widespread across all major global flyways and could be a significant factor in the observed declines in all flyways (Zwarts et al., 2010; Zöckler et al., 2010a; Morrison et al., 2012; Balachandran, personal communication). Moreover, harvesting of food in critical migration feeding areas can also increase pressure on migrating populations (e.g., harvesting horseshoe crabs *Limulus polyphemus* in Delaware Bay, an area which reportedly sees the passage of approximately 60% of the total population of the Semipalmated Sandpiper *C. pusilla* during the spring migration) (Mizrahi et al., 2012).

Pollution. The use of pesticides in agricultural areas such as rice fields may affect shorebirds using those habitats directly, and drainage of pesticides into coastal areas and onto mudflats also has the potential to affect shorebirds (Morrison et al., 2012). Small-scale gold mining has increased considerably in the northern South American wintering range, and mercury, which is used in the extraction process and can reach the coast via the rivers, has the potential to affect

shorebirds in coastal areas (Morrison et al., 2012). Increasing frequency and severity of hurricanes during southbound migration may be causing increased mortality during this period (Morrison et al., 2012).

Habitat loss. Major projects are developing and rapidly altering the Asian coastlines. Intertidal mudflats are disappearing at a rate of 350,000-400,000 ha /decade in the Yellow Sea, a major stop over and key moulting area for several wader species in the EAAF (Murray et al., 2011; Yang et al. 2011; Ko et al., 2011).

Case Study: Spoon-billed sandpiper

The Spoon-billed Sandpiper *Eurynorhynchus pygmeus* (SBS), a wader with a remarkable and unique spatulate bill, is one of the world's rarest and most unusual birds. No other bird hatches with such an adaptation and no clear scientific explanation for such a bill shape has been found. It is the significant species of the East Asian Flyway, where tens of millions of migratory waterbirds share the limited grounds with 45% of the World's human population, and is heading towards extinction perhaps faster than any other bird species on Earth (Syroechkovskiy, 2005). It declined by more than 90% over the last 30 years and is now critically endangered. A realistic risk of extinction in 15-20 years has been predicted by modeling, when recent trends obtained mainly in Arctic breeding areas were projected into the future (Zöckler et al., 2010b). Recent population estimates of about 100 breeding pairs are based on evaluations in the intensively-studied breeding grounds. Of the 42 known main breeding locations, 28 were revisited in the last twelve years: 18 breeding population were extinct and ten populations showed extreme declines in numbers; no stable or increasing populations were discovered. In past five years, one key breeding population became extinct and another key population is considered nearly extinct. Only one breeding population seems to be stable, although on very low levels of about 20-30 breeding pairs only around Meinypilgyno, Chuktoka (Syroechkovskiy et al., unpublished).

Breeding on coastal tundra in Chukotka (Russian Far East) and wintering 5,000 km away on the tropical coasts of China and south-east Asia, the spoon-billed sandpiper faces many threats. The main threats are: (1) habitat reclamation in the non-breeding grounds, such as inter-tidal areas of East Asia for farming and development; (2) subsistence hunting pressure in Myanmar, Bangladesh and some other wintering grounds; and (3) very low breeding productivity in Chukotka. The situation is particularly difficult in China, where around 50% of intertidal areas are reclaimed, development is increasing and there is little conservation action. Spoon-billed sandpipers and millions of other waterbirds depend on large tidal areas, such as the Saemangeum in South Korea, to rest and refuel on migration. This reclamation project, reported to be the largest in the World, has added seriously to the decline of the species.

A project focusing on the conservation of the species started in 2000 in Russia. The effort focuses on the following activities: (1) conservation action to mitigate threats in wintering grounds in Myanmar, Bangladesh, Thailand, China and Vietnam; (2) inventories in the non-breeding range to discover remaining key sites; (3) captive breeding program led by WWT, with the goal of establishing the first ever captive population at Slimbridge, UK, so as to allow the re-introduction of the species to the Russian breeding grounds should the wild populations continue to decline; (4) "head starting", a project aimed at increasing the number of juveniles produced at the key breeding site in Chukotka, which holds around 30% of the world population (this involves taking eggs from incubating birds and raising chicks to fledging age at Meinopylgino, before releasing them back into the wild); (5) monitoring and guarding key breeding sites as well as further research on breeding ecology; and (6) advocacy and

awareness work along the whole flyway, with particular focus on governments and local communities.

References

Amano, T., T. Székely, K. Koyama, H. Amano and W. J. Sutherland. 2010. A framework for monitoring the status of populations: an example from 3 wader populations in the East Asian-Australasian flyway. *Biol. Conserv.*, 143, 2238-2247.

Andres, B. A., P. A. Smith, R. I. G. Morrison, C. L. Gratto-Trevor, S. C. Brown and C. A. Friis. 2012. Population estimates of North American shorebirds, 2012. *Wader Study Group Bull.*, in press.

Balachandran, S. 2006. The decline in wader populations along the east coast of India with special reference to Point Calimere, south-east India. In *Waterbirds around the World*, G. C. Boere, C. Galbraith and D. A. Stroud (eds), The Stationery Office, Edinburgh, UK, pp. 296-301.

Bart, J., S. Brown, B. Harrington and R. I. G. Morrison. 2007. Survey trends of North American shorebirds: population declines or shifting distributions. *J. Avian Biol.*, 38, 73-82.

Bart, J. and V. Johnston (eds.). 2012. Arctic shorebirds in North America: A Decade of Monitoring. *Studies in Avian Biology*, 44, University of California Press, 320 pp.

Blew, J., K. Günther, K. Laursen, M. van Roomen, P. Südbeck, K. Eskildsen and P. Potel. 2007. Trends of waterbird populations in the International Wadden Sea 1987-2004 - an update. In *Seriously Declining Trends in Migratory Waterbirds: Causes-Concerns-Consequences*, B. Reineking and P. Südbeck (eds.), Proc. of the International Workshop, 31 August 2006, Wilhelmshaven, Germany, Wadden Sea Ecosystem No. 23. Common Wadden Sea Secretariat, Wadden Sea National Park of Lower Saxony, Institute of Avian Research, Joint Monitoring Group of Breeding Birds in the Wadden Sea, Wilhelmshaven, Germany.

Boere, G. C. and D. A. Stroud. 2006. The flyway concept: What it is and what it isn't. In *Waterbirds around the World*, G. C. Boere, C. Galbraith and D. A. Stroud (eds,), The Stationery Office, Edinburgh, UK, pp. 40-47.

CAFF. 2001. *Arctic Flora and Fauna: Status and Conservation*. Conservation of Arctic Flora and Fauna (CAFF), Helsinki, Finland, 266 pp.

Harebottle, D. M and L. G. Underhill. 2006. The Arctic connection: Monitoring coastal waders in South Africa - a case study. In *Waterbirds around the World*, G. C. Boere, C. Galbraith and D. A. Stroud (eds,), The Stationery Office, Edinburgh, UK, pp. 138-139.

Joint Monitoring of Migratory Birds (JMMB). 2011. Trends of migratory and wintering waterbirds in the Wadden Sea 1987/88-2009/10. www.waddensea-secretariat.org, Wilhelmshaven Germany.

Gosbell, K. and R. Clemens. 2006. Population monitoring in Australia: Some insights after 25 years and future directions. *Stilt*, 50, 162-175.

Ko, Y., D. K. Schubert and R. T. Hester. 2011. A conflict of greens: Green development versus habitat preservation - the case of Incheon, South Korea. *Environment: Science & Policy for Sustainable Development*, 53, 3-17.

MacKinnon, J., Y. Verkuil and N. Murray. 2012. IUCN situation analysis on East and Southeast Asian intertidal habitats, with particular reference to the Yellow Sea (including the Bohai Sea). Occasional Paper of the IUCN Species Survival Commission No. 47. IUCN, Gland, Switzerland and Cambridge, UK. ii + 70pp. Also available at www.iucn.org/asiancoastalwetlands.

Morrison, R. I. G., B. J. McCaffery, R. E. Gill, S. K. Skagen, S. L. Jones, G. W. Page, C. L. Gratto-Trevor and B. A. Andres. 2006. Population estimates of North American shorebirds, 2006. *Wader Study Group Bull.*, 111, 67-85.

Morrison, R. I. G., D. S. Mizrahi, R. K. Ross, O. H. Ottema, N. de Pracontal and A. Narine. 2012. Dramatic declines of Semipalmated sandpipers on their major wintering areas in the Guianas, northern South America. *Waterbirds*, 35(1), 120-134.

Murray, N. J., R. S. Clemens and R. A. Fuller. 2011. Massive losses of East Asian intertidal habitats detected by remote sensing. International Congress on Conservation Biology. Auckland, New Zealand.

North American Bird Conservation Initiative Canada. 2012. The state of Canada's birds, 2012. Environment Canada, Ottawa, Canada 36pp.

Smith, P. A., C. L. Gratto-Trevor, B. T. Collins, S. D. Fellows, R. B. Lanctot, J. Liebezeit, B. J. McCaffery, D. Tracy, J. Rausch, S. Kendall, S. Zack and H. R. Gates. 2012. Trends in abundance of Semipalmated sandpipers: Evidence from the Arctic. *Waterbirds*, 35(1), 106-119.

Wetlands International. 2012. *Waterbird Population Estimates, Fifth Edition*. Retrieved from wpe.wetlands.org.

Yang, H.-Y. B. Chen, M. Barter, T. Piersma, C.-F. Zhou, F.-S. Li and Z.-W. Zhang. 2011 Impacts of tidal land reclamation in Bohai Bay, China: Ongoing losses of critical Yellow Sea waterbird staging and wintering sites. *Bird Conservation International*, 21, 241-259.

Zöckler, C., T. Htin Hla, N. Clark, E. Syroechkovskiy, N. Yakushev, S. Daengphayon and R. Robinson. 2010a. Hunting in Myanmar: A major cause of the decline of the Spoon-billed Sandpiper. *Wader Study Group Bull.*, 117, 1-8.

Zöckler, C., E. Syroechkovskiy and P. W. Atkinson. 2010b. Rapid and continued population decline in the Spoon-billed Sandpiper *Calidris pygmeus* indicates imminent extinction unless conservation action is taken. *Bird Conservation International*, 20,95-111.

Zöckler, C. 2012. Status Threat and Protection of Arctic Waterbirds. In *Protection of the Three Poles*, F. Huettmann (ed.), Springer, Tokyo, Japan, pp. 203-216.

Zwarts, L, R. G. Bijlsma , J. van der Kamp and E. Wymenga. 2009. *Living on the Edge: Wetlands and Birds in a Changing Sahel*. KNNV Publisher Zeist, The Netherlands, 564 pp.

Vegetation

H.E. Epstein[1], D.A. Walker[2], U.S. Bhatt[3], P. Bieniek[3], J. Comiso[4], J. Pinzon[5], M.K. Raynolds[2], C.J. Tucker[5], G.J. Jia[6], H. Zeng[6], I.H. Myers-Smith[7], B.C. Forbes[8], D. Blok[9], M.M. Loranty[10], P.S.A. Beck[11], S.J. Goetz[11], T.V. Callaghan[12], G.H.R. Henry[7], C.E. Tweedie[13], P.J. Webber[14], A.V. Rocha[15], G.R. Shaver[16], J.M. Welker[17]

[1]Department of Environmental Sciences, University of Virginia, Charlottesville, VA, USA
[2]Institute of Arctic Biology, University of Alaska Fairbanks, Fairbanks, AK, USA
[3]Geophysical Institute, University of Alaska Fairbanks, Fairbanks, AK, USA
[4]Cryospheric Sciences Branch, NASA Goddard Space Flight Center, Greenbelt, MD, USA
[5]Biospheric Science Branch, NASA Goddard Space Flight Center, Greenbelt, MD, USA
[6]Institute of Atmospheric Physics, Chinese Academy of Sciences, Beijing, China
[7]Department of Geography, University of British Columbia, Vancouver, BC, Canada
[8]Arctic Centre, University of Lapland, Rovaniemi, Finland
[9]Center for Permafrost, University of Copenhagen, Copenhagen, Denmark
[10]Department of Geography, Colgate University, Hamilton, NY, USA
[11]Woods Hole Research Center, Falmouth, MA, USA
[12]Department of Animal and Plant Sciences, University of Sheffield, Sheffield, UK
[13]Department of Biology, University of Texas - El Paso, El Paso, TX, USA
[14]Department of Plant Biology, Michigan State University, East Lancing, MI, USA
[15]Department of Biological Sciences, University of Notre Dame, Notre Dame, IN, USA
[16]The Ecosystems Center, Marine Biological Laboratory, Woods Hole, MA, USA
[17]Department of Biological Sciences, University of Alaska Anchorage, Anchorage, AK, USA

December 4, 2012

Highlights

- Over the past 30 years (1982-2011), the Normalized Difference Vegetation Index (NDVI), an index of green vegetation, has increased 15.5% in the North American Arctic and 8.2% in the Eurasian Arctic. In the more southern regions of Arctic tundra, the estimated aboveground plant biomass has increased 20-26%.
- Increasing shrub growth and range extension throughout the Low Arctic are related to winter and early growing season temperature increases. Growth of other tundra plant types, including graminoids and forbs, is increasing, while growth of mosses and lichens is decreasing.
- Increases in vegetation (including shrub tundra expansion) and thunderstorm activity, each a result of Arctic warming, have created conditions that favor a more active Arctic fire regime.

Introduction

Eighty percent of the non-alpine tundra biome in the Arctic lies within 100 km of the Arctic Ocean and adjacent seas, and its distribution is largely controlled by cold summer air masses associated with the pack ice. It is expected that if sea ice decline continues at recently observed rates (see the *Sea Ice* essay), the adjacent tundra areas will continue to become warmer during the summer (Lawrence et al., 2008), and the higher temperatures will increase tundra primary productivity and biomass, and alter species composition (Bhatt et al., 2010; Elmendorf et al.,

2012b; Callaghan et al., 2011; Epstein et al., 2012), with consequences for other tundra ecosystem components and processes. This essay reports on changes in tundra biomass and greenness, phenology, shrubs, non-native species and wildfires.

Long-term circumpolar change in tundra biomass and greenness

A very strong correlation (r^2 = 0.94, p< 0.001) has been established between above-ground plant biomass at the peak of the growing season and the NDVI (Normalized Difference Vegetation Index), an index of vegetation greenness, derived from Advanced Very High Resolution Radiometer (AVHRR) data, along Arctic transects in both North America and Eurasia (Raynolds et al., 2012). Using this relationship, Epstein et al. (2012) determined that above-ground tundra biomass at representative sites increased by 19.8% during the period of the NDVI record (1982-2010), with the greatest increases (20-26%) evident in the mid- to southern (Low Arctic) tundra. This has major implications for tundra ecosystem properties, including active layer depth, permafrost temperature and distribution, hydrology, wildlife and human use of Arctic landscapes. The active layer and permafrost temperature are described in the *Permafrost* essay.

Over the thirty years of AVHRR observations (1982-2011), area-averaged maximum (peak growing season) NDVI (**Fig. 4.1**, right side) has increased 15.5% in the North American Arctic, with a particularly sharp increase since 2005, and 8.2% in the Eurasian Arctic, although values there have been nearly constant since 2001 (Bhatt et al., 2010 updated to 2011). Summer land temperature trends (based on AVHRR radiative surface temperatures) in the tundra regions also show different geographic patterns (1982-2011), with the area-averaged Summer Warmth Index (SWI, the sum of mean monthly surface temperatures >0°C) increasing 10.1% for North America and decreasing 2.6% for Eurasia (**Fig. 4.1**, left side). Also see **Figs. 1.2** and **1.3** in the essay on *Air temperature, Atmospheric Circulation and Clouds* for information on change in air temperature over land.

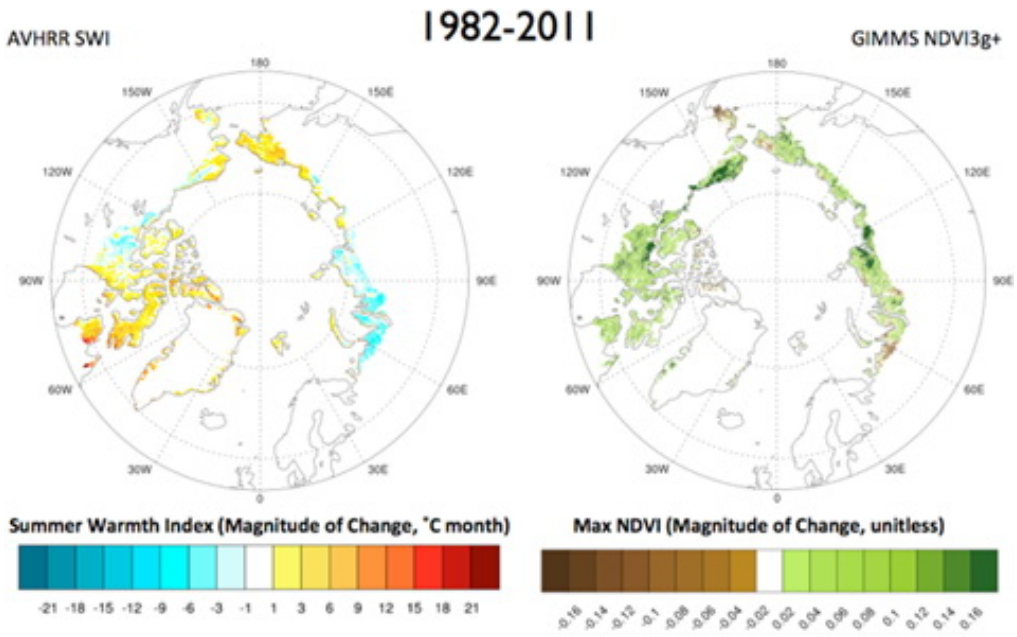

Fig. 4.1. Magnitude of changes in Summer Warmth Index for land area (left) and tundra MaxNDVI

(annual maximum NDVI, usually reached in early August) (right). Magnitude of change is the slope of the simple linear regression trend line multiplied by the number of years of record (30 y, 1982-2011). All of the above information was derived from AVHRR data and the Global Inventory, Modeling and Mapping Studies (GIMMS) data set. Figure updated from Bhatt et al. (2010).

Circumpolar phenology

During the period 2000-2010, based on Moderate Resolution Imaging Spectroradiometer (MODIS) NDVI, the growing season (SOS) began earlier while the end of the growing season (EOS) was delayed; consequently, the length of the growing season (LOS) increased over much of the high-latitude region (Zeng et al., 2011). Spring green-up in Eurasia occurred on average 15.2 days earlier than green-up in North America, and senescence in Eurasia occurred on average 13.6 days later than in North America. The date of peak NDVI has become earlier in Eurasia since 2000, with no substantial shifts in North America. The correlations between NDVI phenology parameters and monthly temperatures were generally strong, with higher temperatures in May and September likely contributing to the earlier SOS and delayed EOS, respectively.

Observations of shrub expansion

There are a growing number of observations of increasing shrubs at sites around the Arctic (**Fig. 4.2**, e.g. Naito and Cairns, 2011; Myers-Smith et al., 2011a). Circumpolar plot-based monitoring of vegetation changes indicates that shrub species have increased in canopy height and abundance at sites that have experienced recent summer warming, particularly in wetter versus drier conditions (Elmendorf et al., 2012b). Various studies have used measurements of radial and lateral stem growth to examine the factors controlling the expansion of tundra shrub species. Areas in Arctic Russia, sub-Arctic Sweden, western Canada and Alaska, and other sites in the High Arctic, show strong correlations between early growing season temperatures and the growth of shrub species (Forbes et al., 2010; Hallinger et al., 2010; Weijers et al., 2010; Rayback et al.. 2011; Blok et al., 2011a; Myers-Smith et al., 2011b). Some studies indicate that almost half of the variation in growth of certain shrub species can be explained by early summer temperatures alone (Forbes et al., 2010; Macias-Fauria et al., 2012). In addition, winter temperatures and snow were also found to correlate with shrub growth at some sites (Hallinger et al., 2010; Schmidt et al., 2010). Long-term snow addition and removal studies as part of the International Tundra Experiment (ITEX) found that deeper snow and the resultant winter soil warming led to increases in shrub growth (Rogers et al., 2011). See the *Snow* essay for more information about its changing distribution and characteristics.

A recent study in the northwest Eurasian Arctic (Macias-Fauria et al., 2012) showed that during the past half century, alder (*Alnus*) and willow (*Salix*) shrubs have responded over a >100,000 km^2 area to a rise in summer temperature of approximately 2°C. In the same region, there has been an increase in permafrost temperatures - see the *Permafrost* essay. Alder and willow are two of the three most abundant erect shrub genera (the other is *Betula*) north of the continental treeline. Analysis of annual growth in *Salix lanata* L. revealed remarkably high correlations with summer temperature across the tundra and taiga zones of west Siberia and Eastern Europe (Forbes et al., 2010). The data indicate that low shrub thickets can transform into taller shrublands, which suggests that rather than a coniferous treeline migrating northward, Low Arctic vegetation change might include structurally novel deciduous woodland (tall shrubland) ecosystems (Macias-Fauria et al., 2012).

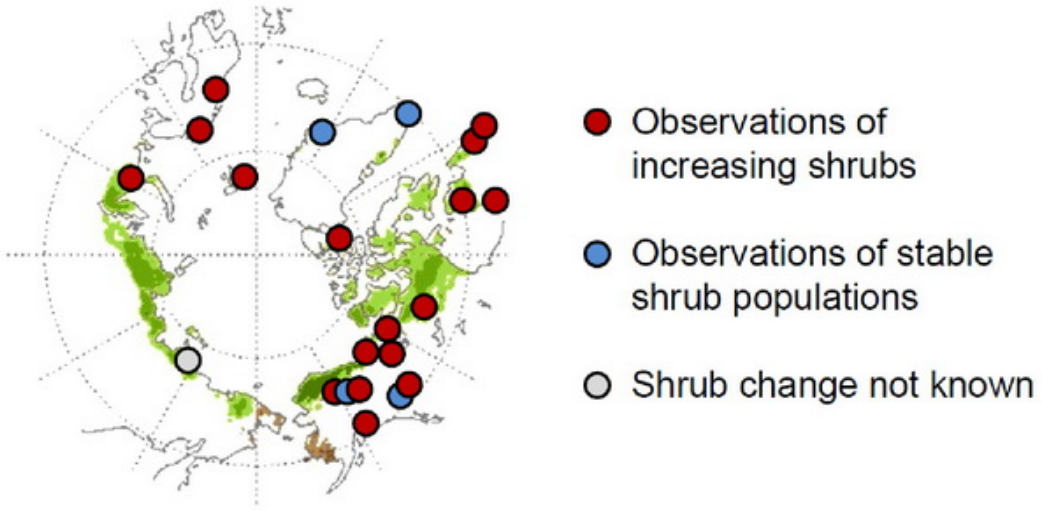

Fig. 4.2. Changes in shrub cover observed in recent studies. Figure from Myers-Smith et al. (2011a) on a map of maximum NDVI change (Bhatt et al., 2010).

Shrub expansion is, however, not uniform, and in Alaska it is becoming increasing clear from repeat photography that some shrub communities are expanding, while others are stagnant (Tape et al., 2012). Expanding patches of *Alnus viridis ssp. fruticosa* (Siberian alder) contained shrub stems with thicker growth rings than in stable patches. Also, growth in expanding patches showed strong correlation with spring and summer warming, whereas alder growth in stable patches showed little correlation with temperature. Shrub expansion also appeared to be related to the landscape position and soil conditions, often associated with floodplains, stream corridors, and rock outcrops. This indicates that existing soil properties predispose certain parts of the landscape to rapid vegetation responses to climate change.

The role of herbivores in affecting vegetation changes is becoming increasingly evident (Johnson et al., 2011; Cahoon et al., 2012). There is evidence from Fennoscandia that heavy grazing by reindeer may significantly check deciduous shrub growth (Kitti et al., 2009; Olofsson et al., 2009), and prevent the disappearance of shorter-statured tundra (Yu et al., 2011). In cases where erect shrubs are already above the reindeer browse line, ~1.8 m, their transformation into tree-size individuals is likely to correlate with warming temperatures rather than grazing intensity (Forbes et al., 2010). In ice-free regions of central west Greenland, the exclusion of caribou and muskoxen led to dramatic increases in shrub cover, leaf area, photosynthesis, and a nearly threefold increase in net carbon uptake by tundra ecosystems (for a more detailed description of potential changes in soil carbon uptake/release, see the *Carbon Dioxide and Methane* essay). These responses were accentuated by warming, but only in the absence of the herbivores (Cahoon et al., 2012). See the *Rangifer* essay for information about the status of caribou and reindeer in the Arctic.

Evidence for general tundra greening in addition to shrub expansion

Interestingly, the greening of Arctic tundra in response to warming does not appear to be confined to shrub vegetation. Beck and Goetz (2011, 2012) found increases in summer NDVI across the North Slope of Alaska since the mid-1990s regardless of shrub cover. This supports field-based observational and experimental results that other tundra plant types are responding to multi-year warming with increased growth (e.g. Walker et al. 2006, Callaghan et al. 2011, Elmendorf et al., 2012a, 2012b). Elmendorf et al. (2012b) analyzed repeated surveys of tundra

vegetation plot data between 1980 and 2010 at 46 locations and found biome-level trends of increased plant canopy height for most vascular plant growth forms. Increased abundances of shrub, forbs and rushes were related to summer warming. In a meta-analysis of 61 tundra warming experiments, most of which were part of the ITEX network (Elmendorf et al., 2012a), warming yielded significant increases in the heights of shrubs, graminoids and forbs, significant increases in shrub abundance, and significant declines in lichens and mosses. In a synthesis of studies that were part of the Back to the Future (BTF) project, Callaghan et al. (2011) presented several observations of tundra vegetation increases including, but not limited to, shrubs, as well as several plant community changes (e.g. Myers-Smith et al., 2011a; Hudson and Henry, 2009; Hill and Henry, 2011; Daniëls and de Molenaar, 2011; Madsen et al., 2011; Villarreal et al., 2012; Lin et al., 2012).

Non-native species

Non-native plant species are a minor vegetation component throughout the Arctic, composing less than 10% of the flora and almost entirely restricted to disturbed areas near human habitation (Hultén, 1968; Elven & Elvebakk, 1996; Panarctic Flora Project, 2000; Aiken et al., 2007; AKEPIC, 2012). The majority of these species are widespread ruderal (weedy) plants that do not reach high densities and are not considered to be a major threat to the ecology of the biome (Carlson et al., 2008; AKEPIC 2012). Greater diversity of non-native species is associated with sites with long histories of transportation of goods and materials (e.g., Hudson Bay Company posts in Nunavut), areas with more extensive use of livestock (e.g., Barentsburg, Spitsbergen) and, more recently, sites of deliberate introductions for gardens and landscaping (Elven and Elvebakk, 1996; Panarctic Flora Project, 2000; Aiken et al., 2007). Short growing seasons and low temperatures in the Arctic appear to restrict establishment, growth and reproduction of many non-native species. Sites with warm microclimates (e.g., Pilgrim Hot Springs in northwestern Alaska) often harbor many more non-native species than surrounding areas. More broadly across Alaska, the diversity of non-native species is strongly correlated with growing degree days (**Fig. 4.3**) in settlements of fewer than 10,000 people (AKEPIC, 2012). While non-native species are currently a small component of the diversity and biomass of the region, increasing propagule pressure, rising temperatures and high levels of disturbance, including the increase in natural resource development activities, suggest that the Arctic will likely face growing rates of non-native plant establishment, as we are already seeing spread throughout the sub-Arctic (Carlson and Shephard, 2007; Conn et al., 2008).

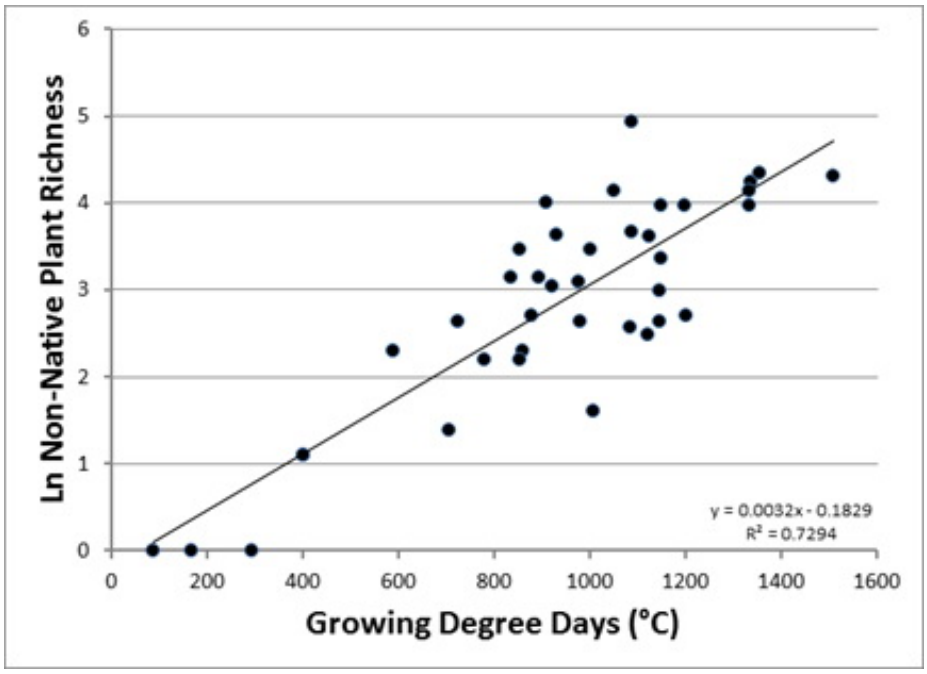

Fig. 4.3. Relationship between growing degree days (>4.4°C) and non-native plant species richness in settlements of fewer than 10,000 people across Alaska.

Tundra fires

New evidence suggests that Arctic warming may be influencing fire regimes both directly and indirectly. In the past, Arctic fires were rare and limited by low temperatures, fuel loads and ignition sources, resulting in fire return intervals in the hundreds to thousands of years (Wein, 1977). However, increases in vegetation (including shrub tundra expansion) and thunderstorm activity, each a result of Arctic warming, have created conditions that favor a more active Arctic fire regime (Higuera et al., 2008; Hu et al., 2010). Conditions over the last decade have been particularly favorable for Arctic fires in Alaska, with 37 fires burning ~400 km^2 in the Noatak region in 2010, and the single largest fire (the Anaktuvuk River fire) burning 1000 km^2 in 2007 (Higuera et al., 2011). These events have profound effects on land-atmosphere exchanges of carbon and energy. For example, the 2007 Anaktuvuk River fire resulted in a loss of 2.1 Tg C to the atmosphere (for a more detailed description of carbon in the atmosphere and land to atmosphere carbon flux, see the *Carbon Dioxide and Methane* essay), enough to offset the annual net carbon uptake of the entire biome (Mack et al. 2011); increased burn-severity led to reduced post-fire carbon sequestration, as well as increases in soil temperature and active layer thaw depth (Rocha and Shaver, 2011a, 2011b). For a circum-Arctic perspective on the active layer and permafrost temperature, see the *Permafrost* essay.

References

Aiken, S. G., M. J. Dallwitz, L. L. Consaul, C. L. McJannet, R. L. Boles, G. W. Argus, J. M. Gillett, P. J. Scott, R. Elven, M. C. LeBlanc, L. J. Gillespie, A. K. Brysting, H. Solstad, H. and J. G. Harris. 2007. Flora of the Canadian Arctic Archipelago: Descriptions, Illustrations, Identification, and Information Retrieval. *NRC Research Press*, National Research Council of Canada, Ottawa. http://nature.ca/aaflora/data, accessed on 25 September 2012.

AKEPIC. 2012. Alaska Exotic Plant Information Clearinghouse Database. *Alaska Natural Heritage Program*, University of Alaska Anchorage. http://aknhp.uaa.alaska.edu/maps/akepic/, accessed on 25 September 2012.

Beck, P. S. A. and S. J. Goetz. 2011. Satellite observations of high northern latitude vegetation productivity changes between 1982 and 2008: Ecological variability and regional differences. *Environ. Res. Lett.*, 6, 045501.

Beck P. S. A. and S. J. Goetz. 2012. Corrigendum: Satellite observations of high northern latitude vegetation productivity changes between 1982 and 2008: ecological variability and regional differences. *Environ. Res. Lett.*, 7, 029501.

Bhatt, U. S., D. A. Walker, M. K. Raynolds, J. C. Comiso, H. E. Epstein, J. Gensuo, R. Gens, J. E. Pinzon, C. J. Tucker, C. E. Tweedie and P. J. Webber. 2010. Circumpolar Arctic tundra vegetation change is linked to sea-ice decline. *Earth Interactions*, 14, 1-20.

Blok, D., U. Sass-Klaassen, G. Schaepman-Strub, M. M. P. D. Heijmans, P. Sauren and F. Berendse. 2011. What are the main climate drivers for shrub growth in Northeastern Siberian tundra? *Biogeosci.*, 8, 169-1179.

Cahoon, S. M. P., P. F. Sullivan, E. Post and J. M. Welker. 2012. Large herbivores limit CO_2 uptake and suppress carbon cycle responses to warming in West Greenland. *Glob. Change Biol.*,18, 469-479.

Callaghan, T. V., C. E. Tweedie, J. Åkerman, C. Andrews, J. Bergstedt, M. G. Butler, T. R. Christensen, D. Cooley, U. Dahlberg, R. K. Danby, F. J. A. Daniëls, J. G. de Molenaar, J. Dick, C. E. Mortensen, D. Ebert-May, U. Emanuelsson, H. Eriksson, H. Hedenås, G. H. R. Henry, D. S. Hik, J. E. Hobbie, E. J. Jantze, C. Jaspers, C. Johansson, M. Johansson, D. R. Johnson, J. F. Johnstone, C. Jonasson, C. Kennedy, A. J. Kenney, F. Keuper, S. Koh, C. J. Krebs, H. Lantuit, M. J. Lara, D. Lin, V. L. Lougheed, J. Madsen, N. Matveyeva, D. C. McEwen, I. H. Myers-Smith, Y. K. Narozhniy, H. Olsson, V. A. Pohjola, L. W. Price, F. Rigét, S. Rundqvist, A. Sandström, M. Tamstorf, R. V. Bogaert, S. Villarreal, P. J. Webber and V. A. Zemtsov. 2011. Multi-decadal changes in tundra environments and ecosystems: Synthesis of the International Polar Year Back to the Future Project (IPY-BTF). *Ambio* 40, 705-716.

Carlson, M. L., I. V. Lapina, M. Shephard, J. S. Conn, R. Densmore, P. Spencer, J. Heys, J. Riley and J. Nielsen. 2008. Invasiveness ranking system for non-native plants of Alaska. *USDA, Forest Service, Gen. Tech. Rep.* R10, R10-TP-143. 218 pp.

Carlson, M. L. and M. Shephard. 2007. The spread of invasive exotic plants in Alaska: Is establishment of exotics accelerating? Harrington, T. B. and S. H. Reichard (eds.). Meeting the Challenge: Invasive Plants in Pacific Northwestern Ecosystems. *USDA Forest Service, Pacific Northwest Research Station, Gen. Tech. Rep.* PNW-GTR-694.

Conn, J., K. Beattie, M. Shephard, M. L. Carlson, I. V. Lapina, M. Hebert, R. Gronquist and M. Rasy. 2008. Alaska *Melilotus* (Fabaceae) invasions: Distribution, origin and susceptibility of plant communities. *Arctic, Antarct. Alpine Res.*, 40, 298-308.
Daniëls, F. J. A. and J. G. de Molenaar. 2011. Flora and vegetation of Tasiilaq, Formerly Angmagssalik, Southeast Greenland - a comparison of data from between around 1900 and 2007. *Ambio* doi:10.1007/s13280-011-0171-3.

Elmendorf, S. C., G. H. R. Henry, R. D. Hollister, R. G. Bjork, A. D. Bjorkman, T. B. Callaghan, L. S. Collier, E. J. Cooper, J. H. C. Cornelissen, T. A. Day, A. M. Fosaa, W. A. Gould, J. Gretarsdottir, J. Harte, L. Hermanutz, D. S. Hik, A. Hofgaard, F. Jarrad, I. S. Jonsdottir, F. Keuper, K. Klanderud, J. S. Klein, S. Koh, G. Kudo, S. L. Land, V. Loewen, J. L. May, J. Mercado, A. Michelsen, U. Molau, I. H. Myers-Smith, S. F. Oberbauer, S. Pieper, E. Post, C. Rixen, C. H. Robinson, N. M. Schmidt, G. R. Shaver, A. Stenstrom, A. Tolvanen, O. Totland, T. Troxler, C. H. Wahren, P. J. Webber, J. M. Welker and P. A. Wookey. 2011a. Global assessment of experimental climate warming on tundra vegetation: heterogeneity over space and time. *Ecol. Lett.*, 15, 164-175.

Elmendorf, S. C., G. H. R. Henry, R. D. Hollister, R. G. Bjork, N. Boulanger-Lapointe, E. J. Cooper, J. H. C. Cornelissen, T. A. Day, E. Dorrepaal, T. G. Elumeeva, M. Gill, W. A. Gould, J., Harte, D. S. Hik, A. Hofgaard, D. R. Johnson, J.F. Johnstone, I. S. Jonsdottir, J. C. Jorgenson, K. Klanderud, J. S. Klein, S. Koh, G. Kudo, M. Lara, E. Levesque, B. Magnusson, J. L. May, J. Mercado-Diaz, A. Michelsen, U. Molau, I. H. Myers-Smith, S. F. Oberbauer, V. G. Onipchenko, C. Rixen, N. M. Schmidt, G. R. Shaver, M. J. Spasojevic, P. E. Porhallsdottir, A. Tolvanen, T. Troxler, C. E. Tweedie, S. Villarreal, C. H. Wahren, X. Walker, P. J. Webber, J. M. Welker and S. Wipf. 2011b: Plot-scale evidence of tundra vegetation change and links to recent summer warming. *Nature Climate Change*, 2, 453-457.

Elven, R. and A. Elvebakk. 2006. Part 1. Vascular plants. In *Catalogue of Svalbard Plants, Fungi, Algae, and Cyanobacteria*, A. Elvebakk and P. Prestrud, A. *Norsk Polaristitutt. Skrifter* 198. Oslo, Norway.

Epstein, H. E., D. A. Walker, M. K. Raynolds, U. Bhatt, C. J. Tucker and J. E. Pinzon. 2012. Dynamics of aboveground phytomass of the circumpolar arctic tundra during the past three decades. *Environ. Res. Lett.*, 7, 015506.

Forbes, B. C., M. M. Fauria and P. Zetterberg. 2010. Russian arctic warming and 'greening' are closely tracked by tundra shrub willows. *Glob. Change Biol.*, 16, 1542-1554. doi: 10.1111/j.1365-2486.2009.02047.x.

Hallinger, M., M. Manthey and M. Wilmking. 2010. Establishing a missing link: warm summers and winter snow cover promote shrub expansion into alpine tundra in Scandinavia. *New Phytologist* 186, 890-899. doi: 10.1111/j.1469-8137.2010.03223.x.

Higuera, P. E., L. B. Brubaker, P. M. Anderson, T. A. Brown, A. T. Kennedy and F. S. Hu. 2008. Frequent fires in ancient shrub tundra: implications of paleorecords for arctic change. *PLOS ONE*, 3, e0001744.

Higuera, P. E., M. L. Chipman, J. L. Barnes, M. A. Urban and F.S. Hu. 2011. Variability of tundra fire regimes in Arctic Alaska: millennial-scale patterns and ecological implications, *Ecol. Applic.*, 21, 3211-3226.

Hill, G. B. and G. H. R. Henry. 2011. Responses of high Arctic wet sedge tundra to climate warming since 1980. *Glob. Change Biol.*, 17, 276-287.

Hu, F. S., P. E. Higuera, J. E. Walsh, W. L. Chapman, P. A. Duffy, L. B. Brubaker, M. L. Chipman. 2010. Tundra burning in Alaska: Linkages to climatic change and sea ice retreat. *J. Geophys. Res. - Biogeosci.*, 115, G04002.

Hudon, J. M. G. and G. H. R. Henry. 2009. Increased plant biomass in a high Arctic heath community from 1981-2008. *Ecology*, 90, 2657-2663.

Hultén, E. 1968. Flora of Alaska and Neighboring Territories. Stanford University Press, Stanford, California.

Johnson, D. R., M. J. Lara, G. R. Shaver, G. O. Batzli, J. D. Shaw and C. E. Tweedie. 2011. Exclusion of brown lemmings reduces vascular plant cover and biomass in Arctic coastal tundra: Resampling of a 50+ year herbivore exclosure experiment near Barrow, *Alaska. Environ. Res. Lett.*, 6, 045507.

Kitti, H., B. C. Forbes and J. Oksanen. 2009. Long- and short-term effects of reindeer grazing on tundra wetland vegetation. *Polar Biol.*, 32, 253-261.

Lantz, T. C., P. Marsh, S. V. Kokelj. 2012. Recent shrub proliferation in the Mackenzie Delta uplands and microclimate implications. *Ecosystems* doi: 10.1007/s10021-012-9595-2.

Lawrence, D. M., A. G. Slater, R. A. Tomas, M. M. Holland and C. Deser. 2008. Accelerated Arctic land warming and permafrost degradation during rapid sea ice loss. *Geophys. Res. Lett.*, 35, L11506.

Lin, D. H., D. R. Johnson, C. Andresen and C. E. Tweedie. 2012. High spatial resolution decade-time scale land cover change at multiple locations in the Beringian Arctic (1948-2000s). *Environ. Res. Lett.*, 7, 025502.

Macias-Fauria, M., B. C. Forbes, P. Zetterberg and T. Kumpula. 2012. Eurasian Arctic greening reveals teleconnections and the potential for structurally novel ecosystems. *Nature Climate Change*, 2, 613-618.

Mack, M. C., S. Bret-Harte, T. N. Hollingsworth, R. R. Jandt, E. A. G. Schuur, G. R. Shaver and D. L. Verbyla. 2011. Carbon loss from an unprecedented Arctic tundra wildfire. *Nature*, 475, 489-492.

Madsen, J., C. Jaspers, M. Tamstorf, C. E. Mortensen and F. Rigét. 2011. Long-term effects of grazing and global warming on the composition and carrying capacity of graminoid marshes for moulting geese in East Greenland. *Ambio* doi:10.1007/x13280-011-0170-4.

Myers-Smith, I. H., B. C. Forbes, M. Wilmking, M. Hallinger, T. Lantz, D. Blok, K. D. Tape, M. Macias-Fauria, U. Sass-Klaassen, E. Lévesque, S. Boudreau, P. Ropars, L. Hermanutz, A. Trant, L. S. Collier, S. Weijers, J. Rozema, S. A. Rayback, N. M. Schmidt, G. Schaepman-Strub, S. Wipf, C. Rixen, C. B. Ménard, S. Venn, S. Goetz, L. Andreu-Hayles, S. Elmendorf, V. Ravolainen, J. Welker, P. Grogan, H. E. Epstein and D. S. Hik. 2011a. Shrub expansion in tundra ecosystems: dynamics, impacts and research priorities. *Environ. Res. Lett.*, 6, 045509. doi: 10.1088/1748-9326/6/4/045509.

Myers-Smith, I. H., D. S. Hik, C. Kennedy, D. Cooley, J. F. Johnstone, A. J. Kennedy and C. J. Krebs. 2011b. Expansion of canopy-forming willows over the twentieth century on Herschel Island, Yukon Territory, Canada. *Ambio*, 40, 610-623.

Naito, A. T. and D. M. Cairns. 2011. Patterns and processes of global shrub expansion. *Progr. Phys. Geogr.*, 35, 423 -442. doi: 10.1177/0309133311403538.

Olofsson, J., L. Oksanen, T. Callaghan, P.E. Hulme, T. Oksanen and O. Suominen. 2009. Herbivores inhibit climate-driven shrub expansion on the tundra. *Glob. Change Biol.*, 15, 2681-2693.

Panarctic Flora Project. 2000-2008. Analysis of vascular plant diversity circumpolar Arctic. Botanical Institute. V. L. Komarova RAS. http://www.binran.ru/projects/paf/diversity.htm#Вместо, accessed on 26 September 2012.

Rayback, S. A., A. Lini and G. H. Henry. 2011. Spatial variability of the dominant climate signal in Cassiope tetragona from sites in arctic Canada. *Arctic*, 64, 98-114.

Raynolds, M. K., D. A. Walker, H. E. Epstein, J. E. Pinzon and C. J. Tucker. 2012. A new estimate of tundra-biome phytomass from trans-Arctic field data and AVHRR NDVI. *Remote Sens. Lett.*, 3, 403-411.

Rocha, A. V. and G. R. Shaver. 2011a. Burn severity influences postfire CO_2 exchange in arctic tundra. *Ecol. Applic.*, 21, 477-489.

Rocha, A. V. and G. R. Shaver. 2011b. Postfire energy exchange in arctic tundra: The importance and climatic implications of burn severity. *Glob. Change Biol.*, 17, 2831-2841.

Rogers, M. C., P. F. Sullivan and J. M Welker. 2011. Evidence of nonlinearity in the response of net ecosystem CO_2 exchange to increasing levels of winter snow depth in the High Arctic of northwest Greenland. *Arctic Antarct. Alpine Res.*, 43, 95-106.

Schmidt, N. M., C. Baittinger, J. Kollmann, and M. C. Forchhammer. 2010. Consistent dendrochronological response of the dioecious Salix arctica to variation in local snow precipitation across gender and vegetation types. *Arctic Antarct. Alpine Res.*, 42, 471-475. doi: 10.1657/1938-4246-42.4.471.

Tape, K. D., M. Hallinger, J. M. Welker and R. W. Ruess. 2012. Landscape heterogeneity of shrub expansion in Arctic Alaska. *Ecosystems* doi:10.1007/s10021-012-9540-4.

Villarreal, S., R. D. Hollister, D. R. Johnson, M. J. Lara, P. J. Webber and C. E. Tweedie. 2012. Tundra vegetation change near Barrow, Alaska (1972-2010). *Environ. Res. Lett.*, 7, 015508.

Walker, M. D., C. H. Wahren, R. D. Hollister, G. H. R. Henry, L. E. Ahlquist, J. M. Alatalo, M. S. Bret-Harte, M. P. Calef, T. V. Callaghan, A. B. Carroll, H. E. Epstein, I. S. Jonsdottir, J. A. Klein, B. Magnusson, U. Molau, S. F. Oberbauer, S. P. Rewa, C. H. Robinson, G. R. Shaver, K. N. Suding, C. C. Thompson, A. Tolvanen, O. Totland, P. L. Turner, C. E. Tweedie, P. J. Webber and P.A. Wookey. 2006. Plant community responses to experimental warming across the tundra biome. *Proc. Nat. Acad. Sci. USA.*, 103, 1342-1346.

Weijers, S., R. Broekman and J. Rozema. 2010. Dendrochronology in the High Arctic: July air temperatures reconstructed from annual shoot length growth of the circumarctic dwarf shrub Cassiope tetragona. *Quat. Sci. Rev.*, 29, 3831-3842. doi: 10.1016/j.quascirev.2010.09.003.

Wein, R. W. 1977: Frequency and characteristics of arctic tundra fires. *Arctic*, 29, 213-222.

Yu, Q., H. E. Epstein, D. A. Walker, G. V. Frost and B. C. Forbes. 2011: Modeling dynamics of tundra plant communities on the Yamal Peninsula, Russia, in response to climate change and grazing pressure. *Environ. Res. Lett.*, 6, 045505.

Zeng, H., G. Jia and H. Epstein, 2011: Recent changes in phenology over the northern high-latitudes detected from multi-satellite data. *Environ. Res. Lett.*, 6, 045508.

Lemmings (*Lemmus* and *Dicrostonyx* spp.)

D.G. Reid[1], R.A. Ims[2], N.M. Schmidt[3], G. Gauthier[4], D. Ehrich[2]

[1]Wildlife Conservation Society, Whitehorse, Canada
[2]Department of Arctic and Marine Biology, University of Tromsø, Norway
[3]Department of Biosciences - Arctic Environment, Aarhus University, Denmark
[4]Department of Biology, Laval University, Canada

November 7, 2012

Highlights

- Changes in lemming abundance dramatically alter the composition of the tundra food web, the biomass and structure of vegetation, and the productivity of numerous other birds and mammals.
- Recovery of lemmings to high populations after low density years is most often associated with a period of successful breeding and recruitment of young under the winter snow.
- Regularity in cycle duration seems to be decaying in many Arctic regions, and cycle amplitude in some regions has collapsed to relatively low densities. More monitoring is required to clarify these patterns.
- Future field investigations and modeling are required to identify the primary factors influencing the lengthening period between cycle peaks, and the apparent disappearance of strong population increases to peak densities, because understanding and predicting future Arctic food web dynamics depends on our understanding of lemming abundance.

Lemming Population Dynamics

Brown lemmings (*Lemmus* spp.) and collared lemmings (*Dicrostonyx* spp.) are the only small rodents with natural distributions in high Arctic regions. They are also found throughout the low Arctic, often in conjunction with various vole species (genera *Microtus* and *Myodes*). The exact number of recognized species varies depending on interpretations of genetic data, especially from island populations (e.g., Wrangel Island). Species composition differs considerably between the Palearctic (Europe and Asia) and the Nearctic (North America and Greenland). Based on Jarrell and Fredga (1993), there are at least three *Lemmus* species in the Palearctic: the Siberian brown lemming *L. sibiricus*, the Norway lemming *L. lemmus*, and even the Nearctic brown lemming *L. trimucronatus* ranging into Siberia. Also, the Palearctic collared lemming, *Dicrostonyx torquatus*, is widespread through Eurasia. In the Nearctic, *Lemmus* is represented by only one species (*L. trimucronatus*), but *Dicrostonyx* by at least two species: the Nearctic collared lemming *Dicrostonyx groenlandicus*, and the Ungava collared lemming *Dicrostonyx hudsonius*.

Lemmings are of particular interest and ecological importance because they are prey for the majority of Arctic predators, and in many Arctic regions their populations follow multiannual population fluctuations of considerable amplitude (Stenseth and Ims, 1993). Lemmings can also affect the species composition and dynamics of tundra vegetation (Olofsson et al., 2011) - see

the *Vegetation* essay for further information on tundra vegetation. When abundant, lemmings attract nomadic and migratory predators, support high reproductive success in these and resident predators, and indirectly influence the population dynamics of various alternative prey such as nesting shorebirds (see the *Waders (Shorebirds)* essay) and waterfowl (Gauthier et al., 2004; Ims and Fuglei, 2005; Gilg et al., 2006). Grazing impacts of lemmings during population peaks are so profound that they can be detected from satellite images (Olofsson et al., 2012). Changes in lemming abundance dramatically alter the composition of the tundra food web, and the productivity of numerous other birds and mammals, from year to year; see the *Arctic Fox* essay, for example.

The population fluctuations in lemmings have been characterized as cycles because peak (high density) populations often recur every three to five years (Stenseth and Ims, 1993). Peak populations generally last no longer than a year, suffering heavy mortality from the various predators they attract, especially during the Arctic summer. Their death rate exceeds production of young and the population declines into a period of low density that can last one or two years. During this low phase, the predators that specialize in lemmings (such as Snowy Owl *Bubo scandiacus*, and the stoat *Mustela erminea*, and least weasel *M. nivalis*) move elsewhere, become scarce, or suffer reduced reproduction of their own (MacLean et al., 1974; Gilg et al. 2006). Recovery of lemmings to high populations densities (the increase phase of the cycle) most often includes a period of successful breeding and recruitment of young under the winter snow (Ims et al., 2011), often in conjunction with a dearth of predators (Stenseth and Ims, 1993). Snow conditions seem particularly influential in this winter breeding because early and deep snow provides maximal insulation for the lemmings living in their winter nests on the ground surface (Duchesne et al., 2011; Reid et al., 2011). See the *Snow* essay for additional information on snow distribution and other characteristics.

Lemming abundance is monitored at Arctic sites using density of their winter nests, mark-recapture live trapping, or snap trapping. Although considerable variability in the amplitude and duration (period) of lemming cycles has been noted from site to site, including some regions with no strong cycles (e.g., western North American mainland, Krebs et al., 1995, 2002) or irregular outbreaks (e.g., low-arctic Fennoscandia; Ims et al., 2011), limited long-term data sets have often indicated remarkable regularity in duration within a site, with variable amplitude. For example, on Bylot Island, Nunavut, Canada, Nearctic collared lemmings and Nearctic brown lemmings fluctuate fairly synchronously, with much lower amplitude in the collared lemmings. The brown lemmings exhibit outbreaks, with highly variable amplitude, every 3 to 4 years (**Fig. 4.4**; Gruyer et al., 2008; G. Gauthier unpublished data), but there is little evidence of substantive shift in duration or amplitude during the past two decades. Although peaks in abundance tended to be lower from 2001 to 2009 than during the previous decade, the most recent peak (2011) was very high.

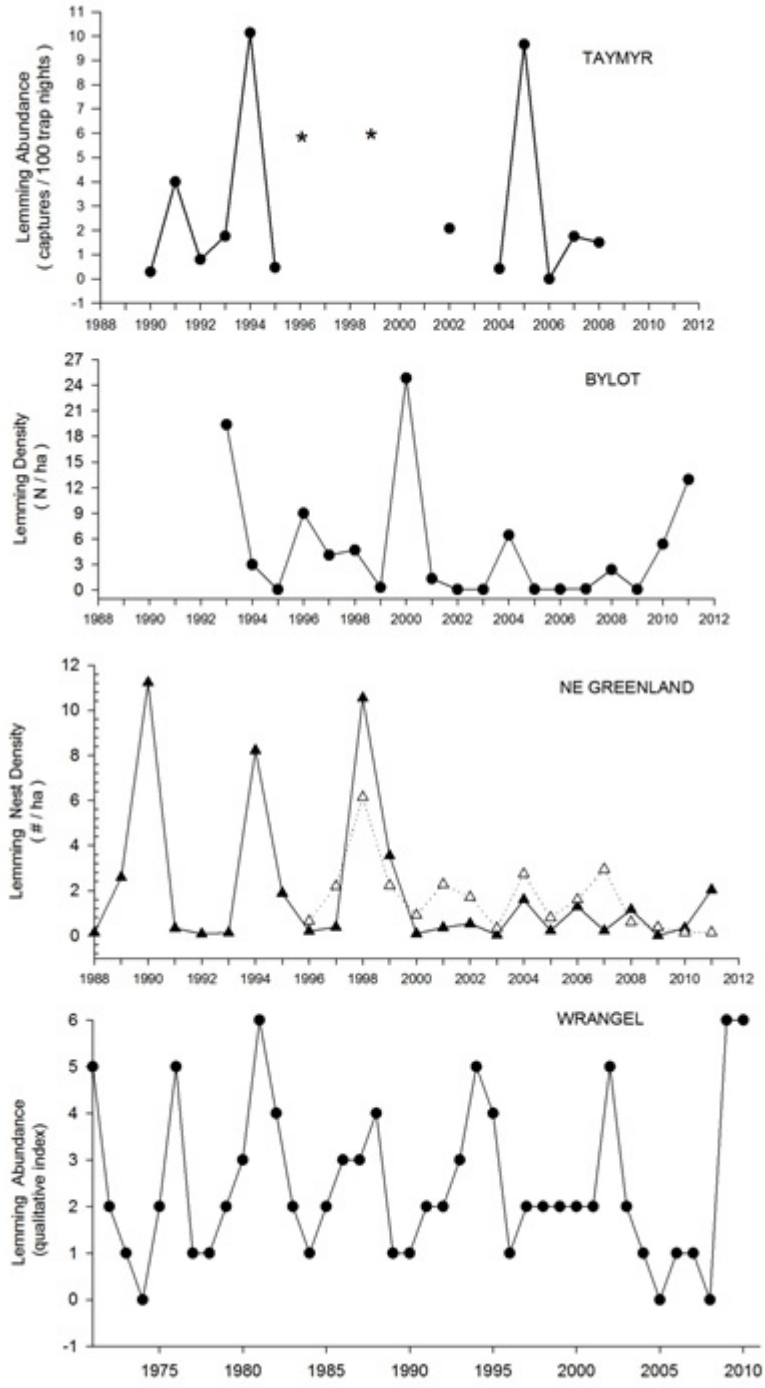

Fig. 4.4. Temporal changes in lemming abundance at various circumpolar sites: Taymyr Peninsula, Russia (Siberian brown lemming, stars are years with unquantified high densities; data courtesy of B. Ebbinge & I. Popov); Bylot Island, Canada (Nearctic brown lemming; data courtesy G. Gauthier); northeast Greenland (Nearctic collared lemming at Traill Island (black triangles) and Zackenberg (open triangles); data courtesy B. Sittler and N. M. Schmidt); Wrangel Island, Russia (Siberian brown lemming and Wrangel Island collared lemming combined; data courtesy I. Menyushina; note different x-axis).

In some regions, however, the cyclic pattern is changing, especially the cycle duration. On Wrangel Island, northeast Russia, the period between years with peak densities has increased from five years in the 1970s to close to eight years in the 1990s and 2000s (**Fig. 4.4**; Menyushina et al., 2012). In Greenland, Nearctic collared lemming abundance is tracked using winter nest counts at Traill Island (~72°N) and Zackenberg (~74°N), both in high Arctic northeast Greenland. Until 2000, lemming dynamics on Traill Island were characterized by regular cycles of approximately 4 years (**Fig. 4.4**; Gilg et al., 2003; Schmidt et al., 2012). Given the high degree of correlation in abundance between the two localities (Schmidt et al., 2008), the dynamics at Zackenberg were most likely similar to those on Traill Island prior to 1996. Around 2000, the population dynamics changed simultaneously at both localities, and regular cycles were replaced by irregular, lower amplitude fluctuations at low densities, especially at Traill Island (**Fig. 4.4**; Schmidt et al., 2012). On southern Banks Island, in the western Canadian archipelago, outbreaks of Nearctic collared lemmings and Nearctic brown lemmings occurred every 3 to 4 years in the 1960s and 1990s (Maher, 1967; Larter, 1998). Further north on the island, the cyclic period seems to have increased to 5 years since the late 1990s (Parks Canada, 2009).

In some other regions the data are less clear, partly because of more intermittent monitoring. On the Taymyr Peninsula of north-central Russia, Siberian brown lemmings cycled with outbreaks every 3 to 4 years from the 1960s to 1990s (Kokorev & Kuksov, 2002). More recent monitoring suggests a more variable period (**Fig. 4.4**; Ebbinge & Mazurov, 2005; Popov 2009). In this region collared lemmings are less numerous but fluctuate in synchrony.

Interpretations of these trends towards longer cycle duration and cycles with noticeably lower amplitude are driven by correlations and models, and specifically those involving changes in snow conditions associated with a warming Arctic climate (Ims and Fuglei, 2005) - see the *Snow* essay for additional information on changing snow conditions. The idea that winter snow conditions could have a dramatic effect on dynamics by influencing winter reproduction was proposed by MacLean et al. (1974). Reduced cyclic amplitude suggests constraints on the winter breeding necessary for rapid population growth. Gilg et al. (2009) have modelled the effects of longer snow-free periods (earlier melt and later onset) and more thaw and freeze events in winter, and found them sufficient to explain the changing amplitudes in the Greenland data. Prolonged cycle duration could also result from a changing snow pack, including more frequent thaw-refreeze events causing ground icing and limiting food availability for winter reproduction, as suggested by Menyushina et al. (2012) for Wrangel Island. Also, recent studies on the Norwegian lemming from low-Arctic and sub-Arctic Fennoscandia provide a connection between dampened cycles and milder winters during which snow melt creates ice layers, which make it more difficult for lemmings to reach their food plants (Kausrud et al., 2008; Ims et al., 2011).

The processes described in the previous paragraph require further investigation, including attempts to refute alternative hypotheses for these changing dynamics, such as changing food quality or availability, changing temporal distributions of predators (e.g., the Arctic fox - see the *Arctic Fox* essay) associated with changing marine ice distribution and duration, and shifts in long-term climate phases such as the North Atlantic Oscillation (NAO) - see the essays on *Air Temperature, Atmospheric Circulation and Clouds*, *Snow* and *Greenland Ice Sheet* for information about the influence on the NAO on the physical environment. More monitoring, at a greater diversity of sites, is also required to search for replicable patterns. However, there is growing concern that changing winter conditions in the Arctic may be altering lemming population dynamics, with numerous, often dramatic and unpredictable direct and indirect effects on predators and alternative prey in the same food web (Schmidt et al. 2012). Moreover,

the future fate of the lemming cycle may have dramatic implications for the development of tundra vegetation, in particular the rate of expansion of shrubs under climatic warming (Olofsson et al., 2009) - see the *Vegetation* essay for information on tundra vegetation and changing shrubs.

References

Duchesne, D., Gauthier. G. and Berteaux, D. 2011. Habitat selection, reproduction and predation of wintering lemmings in the Arctic. *Oecologia*, 167, 967-980.

Ebbinge, B. S. and Y. L. Masurov. 2005. Pristine wilderness of the Taimyr Peninsula: 2004 report. Heritage Institute, Moscow.

Gauthier, G., J. Bêty, J. F. Giroux, J.F. and L. Rochefort. 2004. Trophic interactions in a high Arctic Snow Goose colony. *Integrative and Comparative Biol.*, 44, 119-129.

Gilg, O., I. Hanski I. and B. Sittler. 2003. Cyclic dynamics in a simple vertebrate predator-prey community. *Science*, 302, 866-868.

Gilg, O., B. Sittler, B. Sabard, A. Hurstel, R. Sané, P. Delattre and I. Hanski. 2006. Functional and numerical responses of four lemming predators in high Arctic Greenland. *Oikos*, 113,193-216.

Gilg, O., B. Sittler and I. Hanski. 2009. Climate change and cyclic predator-prey population dynamics in the high Arctic. *Glob. Change Biol.*, 15, 2634-2652.

Gruyer, N., G. Gauthier and D. Berteaux. 2008. Cyclic dynamics of sympatric lemming populations on Bylot Island, Nunavut, Canada. *Can. J. Zool.*, 86, 910-917.

Ims, R. A. and E. Fuglei. 2005. Trophic interaction cycles in tundra ecosystems and the impact of climate change. *BioSci.*, 55, 311-322.

Ims, R. A., N. G. Yoccoz and S. Killengreen. 2011. Determinants of lemming outbreaks. *Proc. Nat. Acad. Sci.*, 108, 1970-1974.

Jarrell, G. H. and K Fredga. 1993. How many kinds of lemmings? A taxonomic overview. In *The Biology of Lemmings*, N. C. Stenseth and R. A. Ims (eds.), pp 45-57, Linnean Society Symposium Series No. 15. Academic Press, London.

Johnson, D. R., M. J. Lara, G. R. Shaver, G. O. Batzli, J. D. Shaw and C. E. Tweedie. 2011. Exclusion of brown lemmings reduces vascular plant cover and biomass in Arctic coastal tundra: resampling of a 50+ year herbivore exclosure experiment near Barrow, Alaska. *Environ. Res. Lett.*, 6, doi:10.1088/1748-9326/6/4/045507.

Kokorev, Y. I. and V. A. Kuksov. 2002. Population dynamics of lemmings, *Lemmus sibiricus* and *Dicrostonyx torquatus*, and Arctic fox *Alopex lagopus* on the Taimyr Peninsula, Siberia, 1960-2001. *Ornis Svecica*, 12, 139-143.

Krebs, C. J., R. Boonstra and A. J. Kenney. 1995. Population dynamics of the collared lemming and the tundra vole at Pearce Point, Northwest Territories, Canada. *Oecologia*, 103, 481-489.

Krebs, C. J., A. J. Kenney, S. Gilbert, K. Danell, A. Angerbjörn, S. Erlinge, R. G. Bromley, C. Shank and S. Carrière. 2002. Synchrony in lemming and vole populations in the Canadian Arctic. *Can. J. Zool.*, 80, 1323-1333.

Larter, N. C. 1998. Collared lemming abundance, diet and morphometrics on Banks Island, 1993-1996. Manuscript Report No. 107. Department of Environment and Natural Resources, Government of Northwest Territories, Inuvik.

MacLean, S. F., B. M. Fitzgerald and F. A. Pitelka. 1974. Population cycles in Arctic lemmings: winter preproduction and predation by weasels. *Arct. Alpine Res.*, 6, 1-12.

Maher, W. J. 1967. Predation by weasels on a winter population of lemmings, Banks Island, Northwest Territories. *Can. Field-Naturalist*, 81, 248-250.

Menyushina, I. E., D. E. Ehrich, J.-A. Henden, R. A. Ims and N. G. Ovsyanikov. 2012. The nature of lemming cycles on Wrangel: an island without small mustelids. *Oecologia*, doi: 10.1007/s00442-012-2319-7.

Olofsson, J., L. Oksanen, T. Callaghan, P. E. Hulme, T. Oksanen and O. Suominen. 2009. Herbivores inhibit climate-driven shrub expansion on the tundra. *Glob. Change Biol.*, 15, 2681-2693.

Olofsson, J., H. Tømmervik and T. V. Callaghan. 2012. Vole and lemming activity observed from space. *Nature Climate Change*, 1, 220-223.

Parks Canada. 2009. Aulavik National Park monitoring program: Lemming winter nest surveys. Western Arctic Field Unit, Parks Canada Agency, Inuvik.

Popov, I. Y. 2009. Some characteristics of lemming inhabitance in western Taimyr: problems of animals study and protection in the north. In *Proceedings of All-Russian Scientific Conference*, A. Taskaev (ed.), pp 194-196. Komi Science Centre, Institute of Biology and Ministry of Komi Republic on Natural Resources and Environmental Protection, Syktyvkar. [In Russian].

Reid, D. G., F. Bilodeau, C. J. Krebs, G. Gauthier, A. J. Kenney, S. Gilbert, M. C. Leung, D. Duchesne and E. Hofer. 2011. Lemming winter habitat choice: A snow-fencing experiment. *Oecologia*, doi 10.1007/s00442-011-2167-x.

Schmidt, N. M., T. B. Berg, M. C. Forschhammer, D. K. Hendrichsen, L. A. Kyhn, H. Meltofte H. and T. T. Høye. 2008. Vertebrate predator-prey interactions in a seasonal environment. *Adv.Ecol. Res.*, 40, 345-370.

Schmidt, N. M., R. A. Ims, T. T. Høye, O. Gilg, L. H. Hansen, J. Hansen, M. Lund, E. Fuglei, M. C. Forchhammer and B. Sittler. 2012. Response of an Arctic predator guild to collapsing lemming cycles. *Proc. Roy. Soc. B*, doi:10.1098/rspb.2012.1490.

Stenseth, N. C. and R. A. Ims. 1993. Population dynamics of lemmings: temporal and spatial variation - an introduction. In *The Biology of Lemmings*, N. C. Stenseth and R.A. Ims (eds.), pp 61-96, Linnean Society Symposium Series No. 15, Academic Press, London.

Arctic Fox (*Vulpes lagopus*)

A. Angerbjörn[1], D. Berteaux[2], R. Ims[3]

[1]Department of Zoology, Stockholm University
[2]Département de Biologie, Université du Québec à Rimouski
[3]Department of Biology, University of Tromsø, Norway

November 10, 2012

Highlights

- The current population of Arctic fox in Fennoscandia is estimated to be less than 200 individuals compared to over 15,000 in the mid-19th century.
- Arctic fox depend on lemmings as a primary food source; consequently fox population trends reflect changes in the lemming population cycle. Thus, for example, in Fennoscandia, Arctic fox reproductive peaks in 2011 were followed by reproductive failure in 2012, closely following lemming population trends.
- In North America over the last century, the Red fox has been expanding northward into historically arctic fox-only territories.
- Long term monitoring at Bylot Island, Nunavut, Canada, has shown relatively stable arctic fox populations and reproductive rates despite the presence of red foxes with low population density.

Introduction

The Arctic fox *Vulpes lagopus* (syn. *Alopex*) is a small circumpolar canid and opportunist predator inhabiting the arctic tundra. In many Arctic areas, it is the most abundant mammalian predator, affecting breeding success of migrating birds and possibly also lemming cycles (see the *Lemming* essay for more information about the lemming cycle and other topics). Where lemmings (*Lemmus* sp.) are present (Fennoscandia, Siberia, North America and parts of Greenland) the Arctic fox relies heavily on this prey, but also on other rodents (*Microtus* sp., *Myodes* sp.), ptarmigan, passerines and carcasses. Where lemmings are absent (Iceland, Svalbard and western Greenland), they live on other resources such as sea birds, seal carcasses and fish. Some populations switch between lemmings, migratory birds and marine resources depending on intra- and interannual variations in prey availability.

Lemming numbers fluctuate drastically, but normally with a regularity in a cycle with peaks every 3-5 years (lemming years). This variation in food availability is a key determinant of Arctic fox reproductive success. During a lemming population peak phase, an Arctic fox female can give birth to as many as 20 cubs (Tannerfeldt and Angerbjörn, 1998), while most females fail to reproduce during a low lemming phase, and those that do have only a few cubs. Arctic fox mortality is also dependent on the lemming cycle, with a higher survival in years with high density of lemmings. Juvenile mortality can be as high as 90% (due to starvation and predation) during their first year when lemming abundance is low.

The Arctic fox may also depend on remains of carrion left by larger predators such as the polar bear (*Ursus maritimus*), arctic wolf (*Canis lupus*), wolverine (*Gulo gulo*) and humans where seal

hunting is common. Present low numbers of these predators in some areas may have reduced the amount of winter food available for Arctic foxes to scavenge (Angerbjörn et al., 2004). It is itself a victim of predation, mainly from *Vulpes vulpes*, *Gulo gulo*, *Aquila chrysaëtos*, and humans.

Arctic fox dens are usually situated in frost-free ground, often in low mounds or eskers (long winding ridges of stratified sand and gravel) on the open tundra. The dens have 4-250 entrances and a system of tunnels, which covers up to 1000 square meters (Dalerum et al., 2002). Some dens have been used for centuries by generations of foxes. Arctic foxes can start breeding in their first year of life and are considered to be essentially monogamous, although extra-pair paternity is frequent and they can increase group size at high population densities (Cameron et al., 2011; Norén et al., 2012). Territories are maintained by pairs during the breeding season or sometimes all year round, with size and shape determined by food availability. Foxes sometimes wander hundreds of kilometres from their territories during winter, both on land and on sea ice. Young foxes can sometimes stay in their parent's home range but are usually not allowed to breed. Mating usually occurs in April-May, and the young are born after a gestation of 52 days. At the age of three to four weeks the young start to appear outside the den and weaning takes place at the age of 5 to 9 weeks. The young gradually become independent during the following month. Some cubs may leave the den in their sixth week of life while others stay until early spring before they disperse. The average life span for animals that reach adulthood is around three years.

The Artic fox has developed many physical attributes that have allowed them to adapt to the Arctic environment and they do not hibernate during the winter months. The winter fur of the Arctic fox has the best insulative properties among all mammals. They further conserve body heat by having fur on the soles of their feet (Linnaeus named it *lagopus*, hare-foot), small ears, a short nose, and a well-developed ability to reduce blood flow to peripheral regions of the body. In autumn, they can put on more than 50% of their body weight as fat for insulation and as energy reserves. Arctic foxes change between summer and winter pelage and thereby adjust insulating properties and enhance camouflage.

Most information about population status and the ecology of the species is from Europe (in particular Fennoscandia) and North America.

Europe

In mainland Europe, the Arctic fox is found above the alpine tree line in the mountain tundra of Fennoscandia (Sweden, Finland, Norway) and north of the arctic tree-line in north-eastern Norway and north-western Russia. Today, the Fennoscandian Arctic foxes are distributed in four geographically separate areas (**Fig. 4.5**). Between these populations, the migration rate is very low or absent (Dalén et al., 2006). The present population status and its historical development is best known from mountain tundra of Fennoscandia located in the north-western regions of the Swedish counties (**Fig. 4.5**) of Jämtland (C), Västerbotten and Norrbotten (A) and in the northern regions of Finnish Lapland (Dalén et al., 2006). In Norway, it is found in the eastern, south-central and northern region.

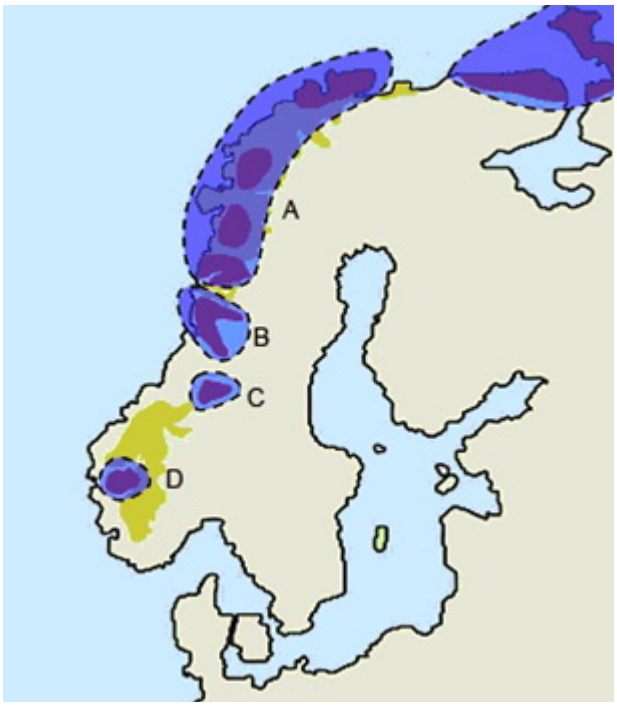

Fig. 4.5. Distribution of Fennoscandian Arctic foxes. Four distinct populations occur in northern Fennoscandia (A, which includes all mountain tundra areas north of Vindelfjällen up to Finnmark), Borgafjäll/Børgefjell (B), Helagsfjällen/Dovre (C) and Hardangervidda, Norway (D).

The Arctic fox was one of the first mammal species to colonize Fennoscandia after the last ice age and is well known for its fluctuating population size due to the lemming cycle. Historically, the Arctic fox was an abundant species, with breeding populations reaching at least 15,000 individuals in lemming peak years during the mid-19th Century. However, fox numbers suffered a drastic decline due to over-harvesting by the fur industry at the beginning of the 20th Century. Despite legal protection, the population has remained at a low density for over 80 years. The situation deteriorated further in the 1980s and 1990s because of an absence of lemming peaks. In 2000, only 3 Arctic fox litters were found in Sweden, Finland and Norway, indicating that the population was close to extinction. It is a priority species according to the European Commission Habitats Directive.

At the present population size of less than 200 individuals in mainland Europe, even a small change in demographic parameters or pure "accidents" can dramatically affect the risk of extinction. As a rule of thumb, vertebrate populations smaller than 500 individuals are considered to be at considerable risk of extinction (Thomas, 1990), although considerably larger populations might be required to secure long-term persistence (Traill et al., 2007). Many young Arctic foxes have little chance of finding a non-related partner. The species is highly dependent on a regular pattern of population cycles of small rodents. The main threat is the small population size constrained by low food availability due to disruptions of the rodent cycle. The Red fox (*Vulpes vulpes*) poses an additional threat to the Arctic fox; this is discussed in more detail below.

More recently, in 2011, Fennoscandia experienced a peak lemming year, which favoured Arctic fox reproduction. Sweden observed about 65 Arctic fox litters that same year (**Fig. 4.6**). This was the most productive summer since 1970. However, lemming populations crashed in 2012

and resulted in complete reproductive failure in Sweden and Norway (Angerbjörn et al., unpublished). This is a clear demonstration of the current vulnerable state of the species in this part of Europe and how strongly Arctic foxes depend on lemming abundance.

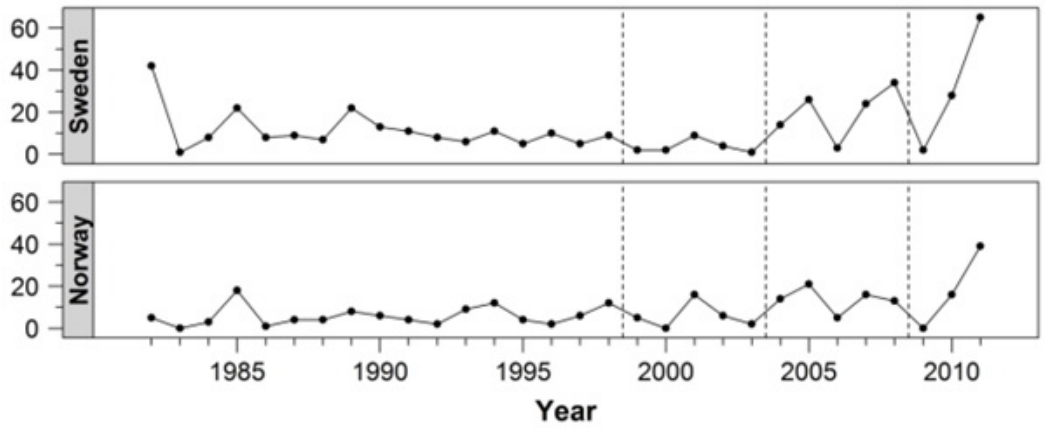

Fig. 4.6. Number of Arctic fox litters observed in Sweden and Norway between 1982 and 2011. In 2012, no fox litters were observed in Sweden, and only one litter was observed in Norway.

It is believed that climate change has decreased snow cover, and increased growing season and primary productivity in northern Fennoscandia - see the *Snow* essay for more information on snow cover change, and the *Vegetation* essay for more information about changing growing season and primary productivity. Connected to this warming and possibly also land use change in tundra areas (Killengreen et al., 2011) is the impact of the Red fox. It is twice the size of the Arctic fox and has about twice the home range area. The Red fox is a dominant competitor, a predator on juveniles and adults, and is currently increasing its range above the tree line, taking over dens and excluding Arctic foxes from parts of their breeding range (Tannerfeldt et al., 2002) and carrion food resources during the winter (Killengreen et al., 2012). Consequently, the Arctic fox is forced to retreat to higher altitudes during summer to reduce the risk of Red fox predation on their cubs. Regarding the food niche, Red fox has a broader range of alternative prey sources that are less accessible to Arctic foxes during low lemming phases.

Projects such as Save the Endangered Fennoscanidan Alopex, SEFALO and SEFALO+ have successfully used a combination of supplemental feeding and Red fox control to increase the number of Arctic foxes. However, earlier conservation attempts did not reach major parts of the distribution area. For example, SEFALO+ only reached the B and C sub-populations, and the situation is still critical in the larger parts of the distribution range A (**Fig. 4.5**).

North America

In North America the Arctic fox is abundant and the overall population probably ranges in the tens of thousands of individuals (ABA unpublished). From the 1920s to the mid 1970s, Arctic fox fur represented the most important asset traded by Inuit in Canada to secure cash and other valuable goods (Sawtell, 2005). Currently, trapping is no longer a major economic activity and only a few hunters still trap foxes. The effects on populations of the heavy trapping period followed by a virtual cessation of trapping are unknown.

Over the last century, a northward expansion in the distribution of the Red fox has been observed in North America (Macpherson, 1964). For example, according to pelt records, Red

foxes were observed for the first time in 1918 in southern Baffin Island, Nunavut, Canada, and continued their expansion northward to reach Pond Inlet and Arctic Bay in the late 1940s (Macpherson, 1964). Nowadays, Red foxes breed in the High Canadian Arctic, e.g., on Bylot Island, Nunavut. Coinciding with this northward spread of the Red fox, the Arctic fox abundance appears to have declined in some places, as documented through local traditional knowledge (Gagnon and Berteaux, 2009). There is now an extensive zone of overlap in the distribution of both species.

Detailed long-term monitoring of an Arctic fox population on Bylot Island began in 1993. The monitoring was first opportunistic but became systematic in 2003. About 100 dens covering approximately 600 km^2 are now surveyed annually (Cameron et al., 2011). About 20-35 adults and 10-60 cubs are trapped and marked every year. The monitoring also involves automatic cameras placed at dens, systematic analysis of feeding regime through stable isotopes, and year-round monitoring of space use through satellite telemetry. The reproductive population varies greatly between years and is strongly dependent on the local lemming cycle. No long-term trend in abundance was observed in the last decade (**Fig. 4.7**). The Red fox breeds in the study area where it competes with and predates on arctic foxes, but the number of reproductive individuals is stable at 0-2 per year.

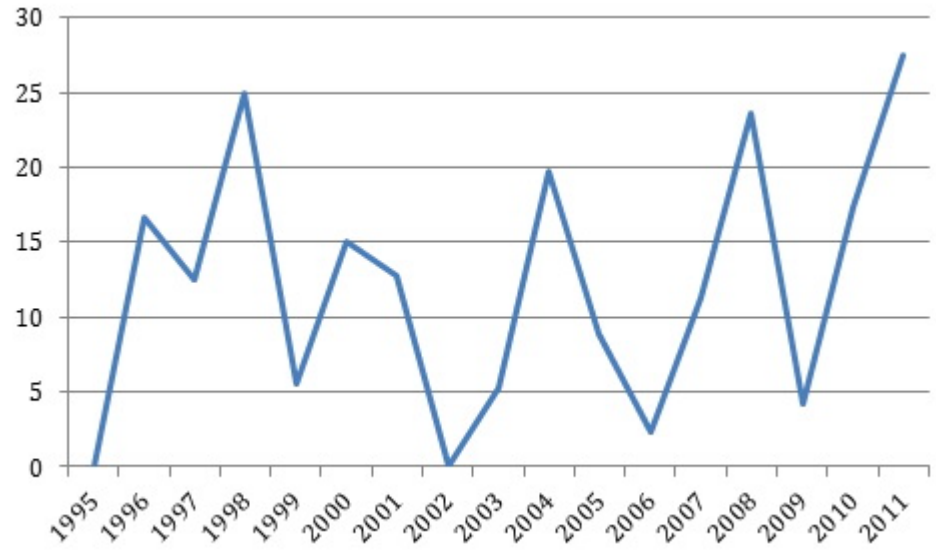

Fig. 4.7. Percentage of dens where pairs of Arctic foxes raised litters on Bylot Island, Nunavut, from 1995 to 2011. The number of surveyed dens increased from 30 to 100 during the study period. Figure after Cadieux et al. (2008).

Arctic fox and Red fox distributions also overlap in western North America. Aerial surveys were conducted at Herschel Island, Yukon, Canada, and the coastal mainland to investigate the relative abundance of Red and Arctic foxes over the last 40 years. Although these areas have experienced intense climate warming trends in recent decades, little change in the relative abundance of the two species was observed (Gallant et al., 2012). Fox dens in northern Yukon are mostly occupied by Arctic fox, with active Red fox dens occurring sympatrically, i.e., the latter live in the same territory without interbreeding with Arctic fox. Although vegetation changes have been reported, there is no indication that secondary productivity and food abundance for foxes have increased, which may explain the population stability. Thus, as indicated for northernmost Fennoscandia, the expansion of Red fox at the expense of the Arctic

fox may be related to other phenomena causing increased secondary productivity and resources to expanding Red fox populations (Killengreen et al., 2011).

References

ABA. Unpublished. Arctic Biodiversity Synthesis and Recommendations. CAFF International Secretariat, Akureiri, Iceland, scheduled for publication in 2013.

Angerbjörn A., P. Hersteinsson and M. Tannerfeldt. 2004. Arctic fox (*Alopex lagopus*). In *Canids: Foxes, Wolves, Jackals and Dogs - Status Survey and Conservation Action Plan*. D. W. Macdonald and C. Sillero-Zubiri (eds), 117-123, IUCN, Gland.

Cadieux, M.-C., G. Gauthier, C.-A. Gagnon, E. Lévesque, J. Bêty and D. Berteaux. 2008. Monitoring the environmental and ecological impacts of climate change on Bylot Island, Sirmilik National Park. 2004-2008 Final Report. Université Laval. 113 pp.

Cameron, C., D. Berteaux and F. Dufresne. 2011. Spatial variation in food availability predicts extrapair paternity in the arctic fox. *Behavioral Ecol.*, 22, 1364-1373.

Dalén, L., K. Kvaløy J. D. C. Linnell, B. Elmhagen, O. Strand, M. Tannerfeldt, H. Henttonen, E. Fuglei, A. Landa and A. Angerbjörn. 2006. Population structure, genetic variation and dispersal in a critically endangered arctic fox population. *Mol. Ecol.*, 15, 2809-2819.

Dalerum, F., M. Tannerfeldt, B. Elmhagen., D. Becker and A. Angerbjörn. 2002. Distribution, morphology and use of arctic fox dens in Sweden. *Wildlife Biol.*, 8, 187-194.

Gagnon, C. A. and D. Berteaux. 2009. Integrating traditional ecological knowledge and ecological science: A question of scale. *Ecol. Soc.*, 14, 19.

Gallant, D., B. G. Slough, D. G. Reid and D. Berteaux. 2012. Arctic fox versus red fox in the warming Arctic: four decades of den surveys in north Yukon. *Polar Biol.*, doi 10.1007/s00300-012-1181-8.

Killengreen, S. T., N. Lecomte, D. Ehrich, T. Schott, N. G. Yoccoz and R. A. Ims. 2011. The importance of marine vs. human induced subsidies in the maintenance of an expanding mesocarnivore in the Arctic tundra. *J. Anim. Ecol.*, 80, 1049-1060.

Killengreen, S.T., E. Strømseng, N. G. Yoccoz and R. A. Ims. 2012. How ecological neighbourhoods influence the structure of the scavenger guild in low arctic tundra. *Diversity & Distributions*, 18, 563-574.

MacPherson, A. H. 1964. A Northward Range Extension of the Red Fox in the Eastern Canadian Arctic. *J. Mammal.*, 45(1), 138-140.

Norén, K., P. Hersteinsson, G. Samelius, N. E. Eide, E. Fuglei, B. Elmhagen, L. Dalén, T. Meijer and A. Angerbjörn. 2012. From monogamy to complexity: Social organization of arctic foxes (*Vulpes lagopus*) in contrasting ecosystems. *Can J. Zool.*, 90, 1102-1116.

Sawtell, S. 2005. Pond Inlet. In *Encyclopedia of the Arctic*, M. Nuttall (Ed.), pp. 1682. New York: Routledge.

Tannerfeldt, M., B. Elmhagen and A. Angerbjörn. 2002. Exclusion by interference competition? The relationship between red and arctic foxes. *Oecologia*, 132:213-220.

Tannerfeldt, M. and A. Angerbjörn. 1998. Fluctuating resources and the evolution of litter size in the arctic fox. *Oikos*, 83(3), 545-559.

Thomas, C. D. 1990. What do real population dynamics tell us about minimum viable population sizes? *Conserv. Biol.*, 4(3), 324-327.

Traill, L. W., J. A. Bradshaw and B. W. Brook. 2007. Minimum viable population size: A meta-analysis of 30 years of published estimates. *Biol. Conserv.*, 139(1-2), 159-166.

Caribou and Reindeer (Rangifer)

D. Russell[1] and A. Gunn[2]

[1]Yukon College, Box 10038 Whitehorse YT, Canada Y1A 7A1
[2]368 Roland Road, Salt Spring Island, BC, Canada V8K 1V1

November 10, 2012

Highlights

- The total, pan-Arctic population of Arctic reindeer and caribou (Rangifer) may have ceased to decline, thus ending a ~40-year cycle.
- There is strong regional variation in Rangifer populations; some are declining, but most are either increasing or stable.

Geographic Variation of Rangifer Population Trends

The most recent population estimates for migratory tundra reindeer and caribou herds indicate that while some herds are either increasing or stable at high numbers (Porcupine, Central Arctic, Teshekpuk Lake, Bluenose East, Kangerlussuaq-Sisimiut), other herds are stable but at low numbers (Cape Bathurst, Bluenose West, Bathurst, Leaf River, Lena-Olenyk) and some herds are starting or continuing to decline (Taimyr, Akia-Maniitsoq, Western Arctic). The current status of the 23 herds, updated by the CircumArctic Monitoring and Assessment (CARMA) Network, is illustrated in **Fig. 4.8**.

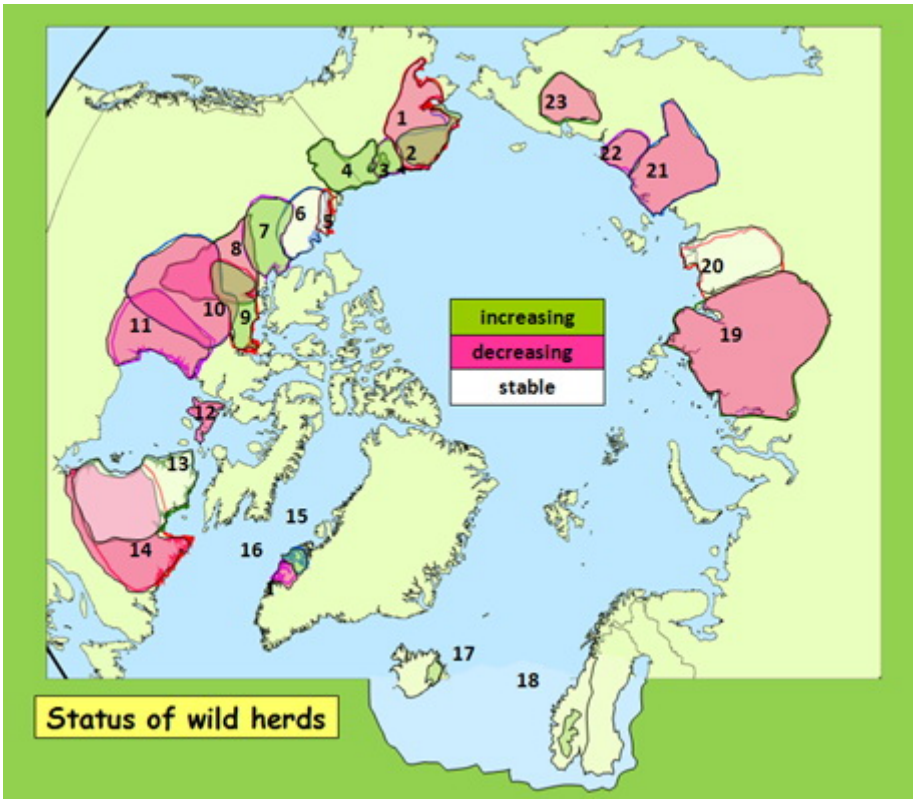

Fig. 4.8. Current status of the world's migratory tundra reindeer and caribou herds. 1: Western Arctic; 2: Teshekpuk Lake; 3: Central Arctic; 4: Porcupine; 5: Cape Bathurst; 6: Bluenose West; 7: Bluenose East; 8: Bathurst; 9: Ahiak; 10: Beverly; 11: Qamanirjuaq; 12: Southampton; 13: Leaf River; 14: George River; 15: Kangerlussuaq-Sisimiut; 16: Akia-Maniitsoq; 17: Snoefells; 18: Norwegian; 19: Taimyr; 20: Lena-Olenyk; 21: Yana-Indigurka; 22: Sundrunskya; 23: Chokotka. Descriptions of the herds in the text are cross-referenced to the numbers above.

Temporal Variation in Migratory Tundra Rangifer

Local and traditional knowledge has indicated that caribou go through periods of abundance and scarcity every 40-60 years. However, relatively objective population estimates have only been employed since the late 1960s and early 1970s. These estimates have shown one single "cycle" over the last 40 years. This cycle is "somewhat" synchronous around the Arctic, although there is a lot of individual herd variation (**Figs. 4.9 and 4.10**).

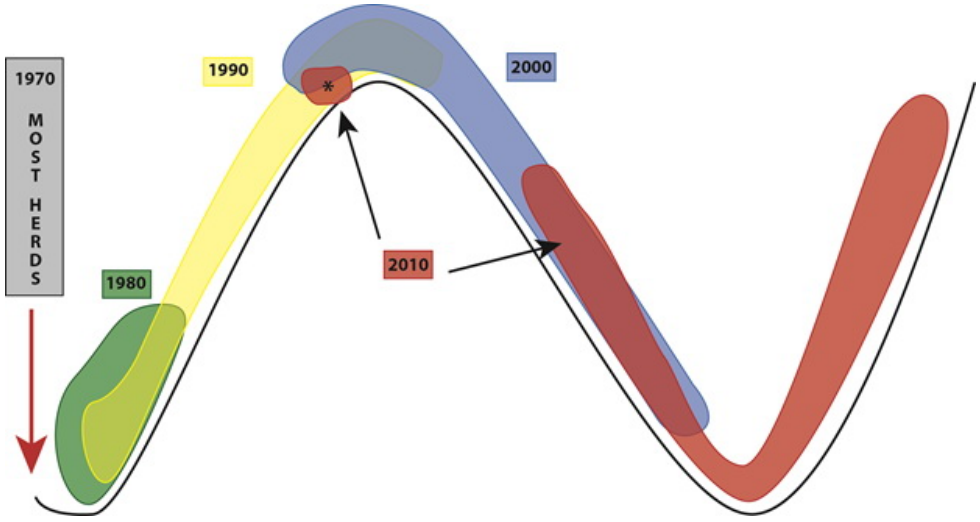

Fig. 4.9. Diagram of herd status between the 1970s and the present. The coloured polygons represent the relative status of herd population cycles in 1970, 1980, 1990, 2000 and 2010. For example, in 2010, herds were either still declining, stabilized, increasing again or still increasing. Note that the asterisk (*) denotes two herds on the Alaska Coastal Plain that, as of 2010, have never declined since initial estimates in the early 1970s. The x-axis represents time and the y-axis represents herd status.

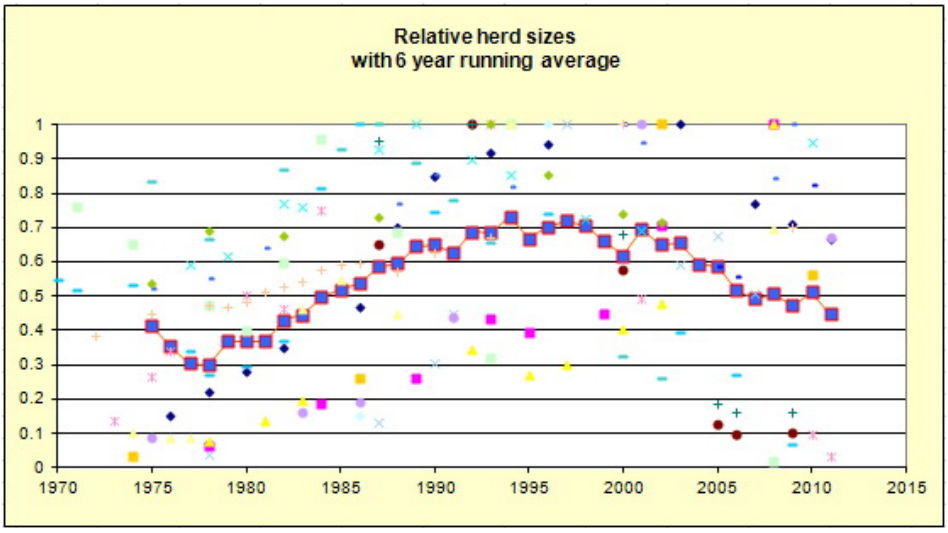

Fig. 4.10. The relative population size (proportion of maximum estimate) for migratory tundra Rangifer herds (1970-2011). The red line through purple squares is a 6-year running average. Data are from the CARMA Web site www.carmanetwork.com).

In the last 20-30 years, methods of counting have become more standardized, which improves the statistical reliability of trend information. Herd size is estimated from photographs taken either when the cows aggregate on the calving ground, or during summer when the insect harassment drives the animals into aggregations. In Russia, the methods include photography of summer aggregations, but did not include the use of radio- or satellite-collared individuals to ensure that all aggregations are found. Since 1970, for the 23 circum-Arctic herds whose size is tracked through aerial surveys, the numbers of caribou and wild reindeer have declined from a recorded peak of about 5.5 million to 2.7 million (CARMA, 2011).

In the last 3 years, population estimates indicate that we may now be seeing a halt to the declines, and recovery of some herds, particularly in western Canada (**Fig. 4.8**). These changes are likely the results of co-management boards taking strong steps to reduce harvest levels. Increased development, more efficient harvesting methods and regional climate trends, however, are still a concern that may affect speed, timing and magnitude of the recovery (Gunn et al., 2010). At the same time, herds that have not declined since estimates began have started to decline.

In Alaska, the Western Arctic herd (No. 1 in **Fig. 4.8**) was at a low (75,000) in the mid 1970s, then increased during the 1980s and 1990s, and reached a peak of 490,000 in 2003. The herd then declined to 325,000 caribou in 2011 (Dau, personal communication 2012). Both the Teshekpuk Lake (2) and Central Arctic (3) herds were recognized as distinct herds in the 1970s, and were estimated to number 4000-5000. Both herds increased, and continued to increase, during the 1990s. By 2008, the Teshekpuk Lake herd had reached 64,107 and the Central Arctic herd 67,000 (Parrett, 2009; Lenart, 2009). The Porcupine herd (4) reached a peak in 1989 (178,000), declined to 123,000 by 2001, before recovering and increasing to 169,000 by 2010 (Alaska Department of Fish and Game, 2011b).

In Canada, there is considerable variation in the timing of increases and decreases, and changes in survey techniques likely contributed to differences in estimated herd size. All Canadian herds have declined since peak sizes, although surveys and estimates after 1994 limited in number for the Ahiak (9) and Beverly herds (10). The Beverly herd likely peaked at 276,000 in 1994, but then numbers of breeding cows declined sharply and essentially had disappeared from the traditional calving grounds by 2011. There are two explanations for this: (1) cows moved to the coastal calving range of the unmonitored Ahiak herd in the mid 1990s (Nagy et al., 2011, 2012), or (2) Beverly numbers declined severely after 1994 and the remaining few cows migrated with Ahiak cows to the higher calving densities to maintain the advantages of gregarious calving (Gunn et al., 2012a, 2012b).

The Qamanirjuaq (11) was estimated to have decreased from 496,000 in 1994 to 345,000 in 2008 (Campbell et al. 2011). However, these estimates were not significantly different and, because there were 14 years between counts, any intervening trends could not be determined. The Cape Bathurst (5) and Bluenose-West (6) herds stabilized between 2006 and 2009 after sharp declines (Davison, personal communication 2010; CARMA, 2011). The 2010 census of the Bluenose-East (7) showed that the herd increased from 66,700 in 2006 to 98,600 in 2010 (Government of NWT, 2010). Caribou were re-introduced on Southampton Island (12) in 1967, following the extirpation of caribou on the island. The initial re-introduction increased to a peak of 30,381 animals in 1997. Brucellosis has been implicated in the subsequent decline of the herd to a 2009 estimate of 13,953 (Campbell et al., in press). Strict harvest limits were imposed after 2011 estimates indicated that the herd numbered 7,800 animals (Nunatsiaq News, 2012).

The George River herd (14) increased from about 5000 animals in the 1950s to 750,000 in the mid-1990s (Couturier et al. 2004). The herd then declined to about 385,000 individuals in 2001, and declined further to 74,131 based on the 2010 post-calving photo-census (Ressources naturelles et Faune, 2010). Current estimates indicate the herd is likely about 26,000 animals (Brodeur, personal communication 2012). The Leaf River Herd also declined from a peak of 680,000 to current estimates of 420,000, which is considered stable over the last few years (Brodeur, personal communication 2012).

There are two major herds in Greenland. Recent surveys indicate that the largest herd, the Kangerlussuaq-Sisimiut (15) has increased from under 60,000 in 2001 to 98,000 in 2010. In

contrast, the smaller Akia-Maniitsoq (16) herd declined from 46,000 in 2001 to 31,000 in 2010 (Cuyler, 2007; CARMA, 2011).

Reindeer were introduced to Iceland (17) in the late 1700s (Thórisson, 1984). In the absence of predators and with active harvesting the number was estimated at approximately 6,500 animals in fall 2009 (Thorarinsdottir, personal communication 2010; CARMA, 2011).

Wild mountain reindeer in Norway (18) consist of 23 separate herds that, in 2004, numbered from 22,000 to 29,000 animals. Herds are largely regulated by hunting and the degree of infrastructure, range fragmentation and forage conditions largely determine individual herd status (Lund, 2004).

In Russia, the Taimyr Herd (19) is one of the largest in the world. Between the 1950s and 1970s, the herd increased from 110,000 to 450,000. Commercial hunting increased and held the herd at about 625,000 animals in 1990. Then, subsidies to commercial hunters were removed in 1991, hunting declined and the herd grew rapidly to 1 million animals by 2000. Currently, the herd is assumed to be declining, although the population has not been estimated since 2000 (Klovov, 2004; Kolpashikov et al., in press). East of the Taimyr, in the central Siberian region of Yakutia, there are three large herds of migratory tundra wild reindeer. In 2009, the Lena-Olenek herd (20) numbered over 95,000 reindeer, a slight increase from 90,000 estimated in 2001. The Yana-Indigirka (21) population declined from 130,000 reindeer in 1987 to 34,000 by 2002. The Sundrun (22) population declined from about 40,000 reindeer in 1993 to about 28,500 by 2002. East of Yakutia, the Chukotka herd (23) increased following the collapse of the domestic reindeer industry.

The domestic reindeer industry in Russia collapsed rapidly from 587,000 in 1971 to about 92,000 by 2001 (Klokov, 2004). Consequently, the wild reindeer recovered and numbered 32,200 individuals by 1986, 120,000-130,000 in 2002, then declined to less than 70,000 by 2009. Typically, when wild reindeer migrate through the range of domestic reindeer, the domestic animals become part of the wild herd, thus augmenting the perceived number of wild reindeer. When reindeer husbandry was no longer economical, herders were less likely to protect their domestic stock from migrating wild reindeer. Hence the increase in wild herd size as the domestic reindeer industry collapsed.

References

Alaska Department of Fish and Game. 2011a. Press release - Western Arctic caribou Herd count revised. http://www.adfg.alaska.gov/index.cfm?adfg=pressreleases.pr03242011.

Alaska Department of Fish and Game. 2011b. Press release - Porcupine Caribou Herd shows growth. http://www.adfg.alaska.gov/index.cfm?adfg=pressreleases.pr03022011.

Campbell, M., J. Boulanger and D. Lee. Demographic Effects of an Outbreak of Brucella suis On Island Bound Barren-Ground Caribou (Rangifer tarandus groenlandicus) Southampton Island Nunavut. Presented at the 13th Arctic Ungulate Conference, Yellowknife, Northwest Territories, Canada, August, 2011, in press.

Campbell, M., J. Nishi and J. Boulanger. 2010. A calving ground photo survey of the Qamanirjuaq migratory barren-ground caribou (Rangifer tarandus groenlandicus) population -- June 2008. Technical Report Series 2010 No. 1-10. Government of Nunavut. 129 p.

CARMA. 2011. Circumarctic Monitoring and Assessment (CARMA) Network Web site www.carmanetwork.com.

Couturier, S., D. Jean, R. Otto and S. Rivard. 2004. Demography of the migratory tundra caribou (Rangifer tarandus) of the Nord-du-québec region and Labrador. Ministère des Ressources Naturelles, de la Faune et des Parcs, Québec, and Direction de la recherche sur la faune. Québec. 68 p.

Cuyler, C. 2007. West Greenland caribou explosion: What happened? What about the future? Proceedings of the 11th North American Caribou Workshop, Jasper, Alberta, Canada, 23-27 April 2006. *Rangifer*, Special Issue, 17, 219-226.

Government of NWT. 2010. Press release - Survey results of Bluenose East caribou herd released. Website: http://www.enr.gov.nt.ca/_live/documents/content/Survey_Results_Bluenose-East_Caribou_Herd.pdf.

Gunn, A., K. G. Poole and J. S. Nishi. 2012a. A conceptual model for migratory tundra caribou to explain and predict why shifts in spatial fidelity of breeding cows to their calving grounds are infrequent. *Rangifer*, Special Issue, 20, 259-267.

Gunn, A., K. G. Poole, J. Wierzchowski , J. S. Nishi, J. Adamczewski, D. Russell and A. D'Hont. 2012b. The influence of geography and abundance on the Ahiak caribou calving grounds, Nunavut, Canada. Presentation at 2012 Arctic Ungulate Conference and submitted to *Rangifer*.

Gunn, A. and D. R. Russell. 2011. Northern Caribou Population Trends. Canadian Biodiversity: Ecosystem Status and Trends, 2010 Technical Thematic Report Series No. 10. Canadian Councils of Resource Ministers. Ottawa, iv+55 p.

Gunn A., D. R. Russell, R. White and G. Kofinas. 2009. Facing a future of change: Migratory caribou and reindeer. *Arctic*, 62(3), 3-4.

Klokov, K. 2004. Russia. Chapter Family-Based Reindeer Herding and Hunting Economies, and the Status and Management of Wild Reindeer/Caribou Populations. Sustainable Development Program, Arctic Council, Published by Centre for Saami Studies, University of Tromsø.

Kolpashikov, L., V. Makhailov and D. Russell. In press. The role of harvest in the dynamics of the Taimyr wild reindeer herd: Lessons for North America.

Lenart, E. A. 2009. Units 26B and 26C caribou. Pages 299-325 in P. Harper. Editor. Caribou Management report of survey and inventory activities 1 July 2006 - 30 June 2008. Alaska Department of Fish and game. Project 3.0 Juneau, Alaska, USA.

Lund, E. 2004. Wild reindeer in Norway. In *Family-Based Reindeer Herding and Hunting Economies, and the Status and Management of Wild Reindeer/Caribou Populations*, B. Ulvevadet and K. Klokov (eds.). Sustainable Development Program, Arctic Council, Published by Centre for Saami Studies, University of Tromsø.

Nagy, J. A, D. H. Johnson, M. W. Campbell, A. Kelly, N. C. Larter and A. E. Derocher. 2010. The Beverly barren-ground caribou herd has not disappeared: It just changed calving grounds.

Unpublished abstract, 25-28 October 2010, 13th North American Caribou Workshop, Winnipeg, Manitoba.

Nagy, J. A., D. L. Johnson, N. C. Larter, M. W. Campbell, A. E. Derocher, A. Kelly, M. Dumond, D. Allaire, D. and B. Croft. 2011. Subpopulation structure of caribou (*Rangifer tarandus L.)* in Arctic and sub-Arctic Canada. *Ecol. Applic.*, 21, 2334-2348.

Nunatsiaq News. 2012. Nunavut orders strict caribou quota for Southampton Island. http://www.nunatsiaqonline.ca/stories/article/65674nunavut_orders_strict_caribou_quota_for_southampton_island/.

Parrett, L. S. 2009. Unit 26A. Teshekpuk caribou herd. In *Caribou Management Report of Survey and Inventory Activities, 1 July 2006 - 30 June 2008*, P. Harper (ed.), 271-298. Alaska Department of Fish and Game. Project 3.0, Juneau, Alaska, USA.

Ressources naturelles et Faune. 2010. Results of the George River Caribou Herd census [online]. Government of Quebec. http://www.mrn.gouv.qc.ca/english/press/press-release-detail.jsp?id=8713 (accessed 23 December, 2010). Press release.

Thórisson, S. 1984. The history of reindeer in Iceland and reindeer study 1979-1981. *Rangifer*, 4(2), 22-38.

Terrestrial Cryosphere Summary

Section Coordinator: Marco Tedesco

City College of New York, New York, NY, USA

November 15, 2012

In 2012, several terrestrial cryosphere records were set. New minimum snow cover extent values occurred over the Northern hemisphere in June, when snow still covers most of the Arctic region, and over Eurasia in May. The rate of loss of June snow cover extent, -17.6%/decade during the period of satellite observation (1979-2012), was a new record relative to the 1979-2000 mean value, and greater than that of September sea ice extent (-13.0%/decade) during the same period. Snow cover duration was the second shortest on record. New record high temperatures at 20 m depth were measured at most permafrost observatories on the North Slope of Alaska and in the Brooks Range, Alaska, where measurements began in the late 1970s. In Greenland, melting at the surface set a new record and in some locations lasted up to ~2 months longer than the average for the period of 1979-2011. An exceptional event was recorded in July 2012, when melting occurred over ~97% of the Greenland ice sheet. Albedo (reflectivity) estimated from satellite measurements (2000-2012) and mass losses measured in situ at high elevations also set new records in Greenland. Outside Greenland, nineteen of twenty Arctic glaciers reported by the World Glacier Monitoring Service had a negative mass balance for the 2009-2010 balance year, and, in the 2010-2011 balance year the mass losses from the four Canadian Arctic glaciers were the greatest on record. Consistent with the in situ measurements, the GRACE satellite-derived mass loss in 2010-11 from all the glaciers and ice caps in the Canadian Arctic Islands was the largest for this region since GRACE observations began in 2002.

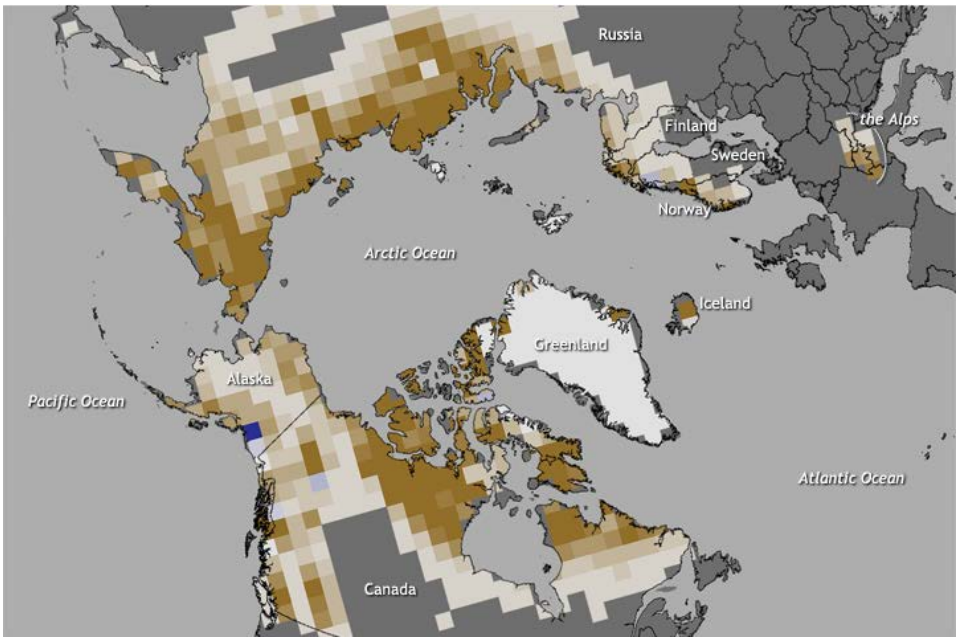

June 2012 snow extent anomaly. Brown colors indicate areas of greatest loss compared to the average snow extent. Large snow map available from NOAA Climate.gov.

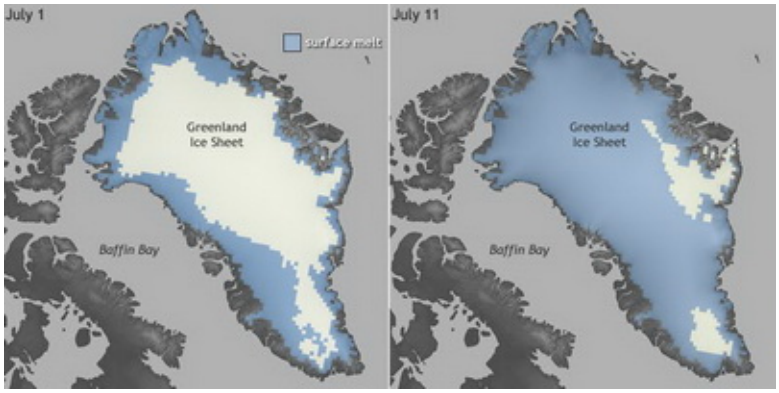

Greenland surface melt extent on July 1 & 11, 2012, based on SSM/I data provided by Tom Mote. Blue color indicates area of surface melt. Large surface melt maps available from NOAA Climate.gov.

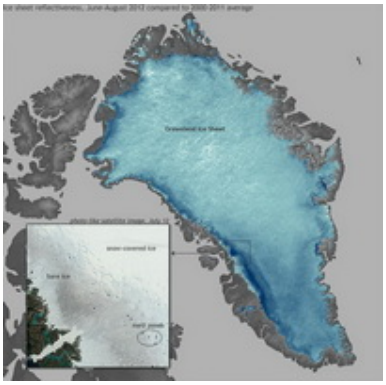

Summer (JJA) albedo anomaly in 2012. Darker blue colors show areas with lower reflectivity relative to the 2000-2011 reference period. Based on data derived from MODIS observations. (Hunter) Large reflectivity map available from NOAA Climate.gov.

Snow

C. Derksen and R. Brown

Climate Research Division, Environment Canada

November 7, 2012

Highlights

- A new record low June snow cover extent (SCE) for the Northern Hemisphere (when snow cover is mainly located over the Arctic) was set in 2012. A new record low May SCE was also established over Eurasia.
- 2012 spring snow cover duration was the second shortest on record for both the North American and Eurasian sectors of the Arctic because of earlier than normal snow melt.
- The rate of loss of June snow cover extent between 1979 and 2012 (-17.6% per decade relative to the 1979-2000 mean) is greater than the loss of September sea ice extent (-13.0% per decade) over the same period.

Snow covers the high latitude land surface for up to nine months of the year, and thereby plays a major role in the energy and freshwater budgets of the Arctic. Variability and change in snow cover extent (SCE) and snow cover duration (SCD) are of primary climatological importance, while estimates of the amount of water stored by the snowpack (snow depth or snow water equivalent) are important for hydrological purposes. While interannual variability in SCE and SCD during the snow melt period are controlled largely by surface temperature (warmer temperatures melt snow earlier), climate controls on the timing of snow cover onset in autumn and the seasonal accumulation of snow depth are more complicated, as they include influences by both temperature and precipitation. Recent reductions in Arctic spring snow cover have direct effects on many components of the Arctic physical environment, including the length of the growing season, the timing and dynamics of spring river runoff, the ground thermal regime, and wildlife population dynamics (Callaghan et al., 2011).

Northern Hemisphere spring SCE anomalies (relative to a 1988-2007 reference period) computed from the weekly NOAA snow chart Climate Data Record (CDR; maintained at Rutgers University and described in Brown and Robinson, 2011) for months when snow cover is confined largely to the Arctic showed a continued reduction from the historical mean during the spring 2012 (**Fig. 5.1**). New record lows for both May and June SCE were established over Eurasia in 2012 — the fifth consecutive year that a new record low June SCE was established for this region. Spring 2012 marked the third time in the past five years that a new record low June SCE was set for North America. The rate of snow cover loss over Northern Hemisphere land areas in June between 1979 and 2012 is -17.6% per decade (relative to the 1979-2000 mean), which exceeds the rate of September sea ice loss over the same time period (-13.0% per decade; Derksen and Brown, 2012). The rate of reduction in Arctic June SCE over the period of the NOAA data record exceeds the CMIP5 (Coupled Model Intercomparison Project Phase 5) model ensemble simulated and projected (historical + scenario rcp8.5 [rcp" representative concentration pathway of radiative forcing due to increasing greenhouse gas concentration) rate of decrease by more than a factor of three (Derksen and Brown, 2012).

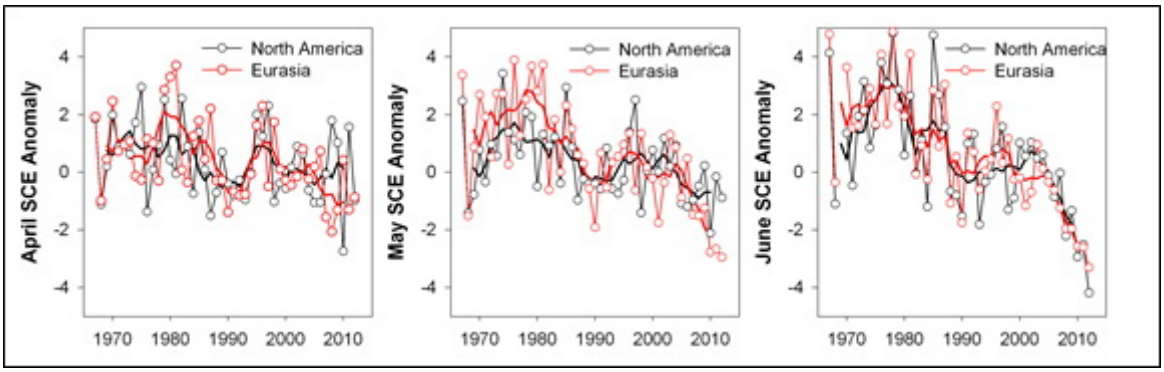

Fig. 5.1. Monthly Arctic snow cover extent (SCE) standardized (and thus unitless) anomaly time series (with respect to 1988-2007) from the NOAA snow chart CDR for (a) April (b) May and (c) June. Solid black and red lines depict 5-yr running means for North America and Eurasia, respectively.

Spatial patterns of fall and spring SCD departures derived from the NOAA daily IMS snow cover product for 2011/12 show no fall SCD anomalies over the Canadian Arctic, earlier than normal snow onset across the eastern Siberian Arctic, and later than normal snow onset over northern Europe (**Fig. 5.2a**). There is an almost complete absence of longer than normal SCD during the Arctic spring, with the earliest snow melt departures occurring over the central Canadian Arctic and coastal regions across the Eurasian Arctic (**Fig. 5.2b**).

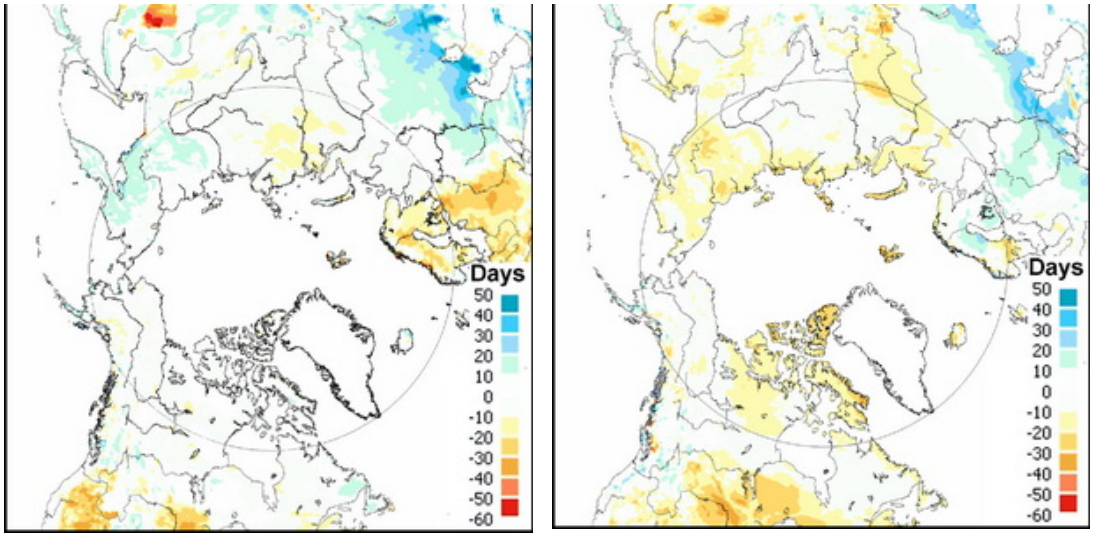

Fig. 5.2. Snow cover duration (SCD) departures (days; with respect to 1998-2010) from the NOAA IMS data record for the 2011-12 snow year: (a) fall; and (b) spring. Latitude circle denotes 60ºN.

During spring 2012 Arctic snow melt season was characterized by a strongly negative North Atlantic Oscillation (NAO) which reached a low of -2.25 in June (see also the essays on *Air Temperature, Atmospheric Circulation and Clouds*, and *Greenland Ice Sheet*). A negative NAO is associated with enhanced southerly air flow into the Arctic which contributes to warm temperature anomalies and rapid ablation of the snowpack. The only other year since 1950 to have a June NAO value lower than -2.0 was 1998, during which warm temperature anomalies were also present across Arctic land areas. The strongly negative NAO also played a key role in the extensive melting and mass losses observed in summer 2012 on the Greenland Ice Sheet (see the *Greenland Ice Sheet* essay).

A striking feature in the SCD anomaly time series (also computed from the NOAA snow chart CDR using a 1988-2007 reference period) is the seasonal asymmetry of the trends through the data record (**Fig. 5.3**). In contrast to the trend towards less snow in the spring period (as a result of earlier melt), the start date of snow cover over the Arctic appears to be unchanged during the satellite era. This is surprising because the *in situ* based air temperature record (CRUtem3v, Brohan et al., 2006) identifies significant warming trends over Arctic land areas (since 1980) in both the snow onset and melt periods. The seasonal asymmetry is consistent with a weaker coupling between snow cover and air temperatures in the autumn compared to the spring. The potential impact of increased Arctic atmospheric moisture availability (Serreze et al., 2012) on Arctic snow cover (e.g. snow onset date, annual maximum SWE, snow albedo) remains to be determined.

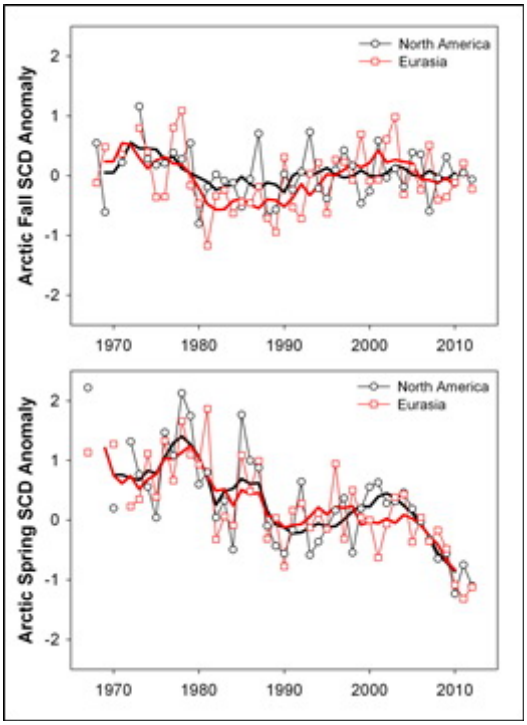

Fig. 5.3. Arctic seasonal snow cover duration (SCD) standardized (and thus unitless) anomaly time series (with respect to 1988-2007) from the NOAA record for (a) the first (fall) and (b) second (spring) halves of the snow season. Solid black and red lines depict 5-yr running means for North America and Eurasia, respectively.

Mean April snow depth from the Canadian Meteorological Centre (CMC) daily gridded global snow depth analysis (Brasnett, 1999) shows large regions of positive April snow depth anomalies over both the North American and Eurasian Arctic (**Fig. 5.4**). This means the record setting loss of spring snow cover in 2012 was driven more by rapid ablation rather than an anomalously low snow accumulation.

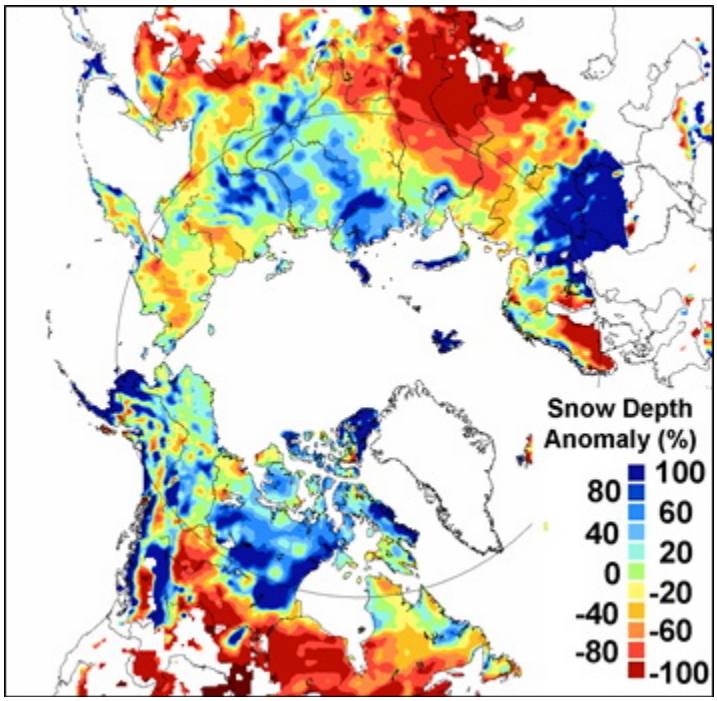

Fig. 5.4. April 2012 snow depth anomaly (% of 1999-2010 average) from the CMC snow depth analysis. Latitude circle denotes 60ºN.

References

Brasnett, B. 1999. A global analysis of snow depth for numerical weather prediction. *J. Appl. Meteorol.*, 38, 726-740.

Brohan, P., J. J. Kennedy, I. Harris, S. F. B. Tett and P. D. Jones. 2006. Uncertainty estimates in regional and global observed temperature changes: A new data set from 1850. *J. Geophys. Res.*,111: D12106, doi:10.1029/2005JD006548.

Brown, R. and D. Robinson. 2011 Northern Hemisphere spring snow cover variability and change over 1922-2010 including an assessment of uncertainty. *The Cryosphere*, 5, 219-229.

Callaghan, T., M. Johansson, R. Brown, P. Groisman, N. Labba, V. Radionov, R. Barry, O. Bulygina, R. Essery, D Frolov, V. Golubev, T. Grenfell, M. Petrushina, V. Razuvaev, D. Robinson, P. Romanov, D. Shindell, A. Shmakin, S. Sokratov, S. Warren and D. Yang. 2011. The changing face of Arctic snow cover: A synthesis of observed and projected changes. *Ambio*, 40, 17-31.

Derksen, C. and R. Brown. 2012. Spring snow cover extent reductions in the 2008-2012 period exceeding climate model projections. *Geophys. Res. Lett.*, doi:10.1029/2012GL053387 (in press).

Serreze, M., A. Barrett and J. Stroeve. 2012. Recent changes in tropospheric water vapor over the Arctic as assessed from radiosondes and atmospheric reanalyses. *J. Geophys. Res.*, 117: D10104, doi:10.1029/2011JD017421.

Mountain Glaciers and Ice Caps (Outside Greenland)

M. Sharp[1], G. Wolken[2], M.-L. Geai[1], D. Burgess[3]

[1]University of Alberta, Department of Earth and Atmospheric Sciences
[2]Alaska Division of Geological & Geophysical Surveys
[3]Geological Survey of Canada, National Glaciology Program

With data contribution from J.G. Cogley

November 9, 2012

Highlights

- In 2009-2010, the most recent balance year for which data are available for the twenty Arctic glaciers reported by the World Glacier Monitoring Service (WGMS), nineteen glaciers had a negative mass balance.
- In the 2010-2011 balance year, the mass losses from the four Canadian Arctic glaciers reported by the WGMS were the greatest in records that are between 49 and 52 years long.
- The GRACE-derived mass loss (96±49 Gt) in 2010-11 from all the glaciers and ice caps in the Canadian Arctic Islands was the largest for this region since GRACE observations began in 2002.

Mountain glaciers and ice caps in the Arctic, with an area of over 400,000 km^2, contribute significantly to global sea level change (Meier et al., 2007; Gardner et al., 2011; Jacob et al., 2012). They lose mass by iceberg calving, and by surface melt and runoff. The climatic mass balance (B_{clim}, the difference between annual snow accumulation and runoff) is an index of how they respond to climate change and variability. Note that B_{clim} is a new term (Cogley et al., 2011) synonymous with net mass balance (B_n) used in previous Arctic Report Cards (e.g., Sharp and Wolken, 2011).

Measurements of B_{clim} of 27 Arctic glaciers have been published for 2009-2010 (World Glacier Monitoring Service, 2012). These are located in Alaska (three), Arctic Canada (four), Iceland (nine), Svalbard (four), Norway (two) and Sweden (5) (**Fig. 5.5**, **Table 5.1**). All but one of these glaciers (Kongsvegen in Svalbard) had a negative annual balance. Mass balances of glaciers in Iceland, Gulkana Glacier in interior Alaska, and several glaciers in northern Scandinavia were extremely negative in 2009-2010. In the Canadian Arctic, the 2009-2010 balances of the Devon and Melville Island South ice caps were the 4th and 3rd most negative within the 51- and 49-year records, respectively (**Table 5.1**).

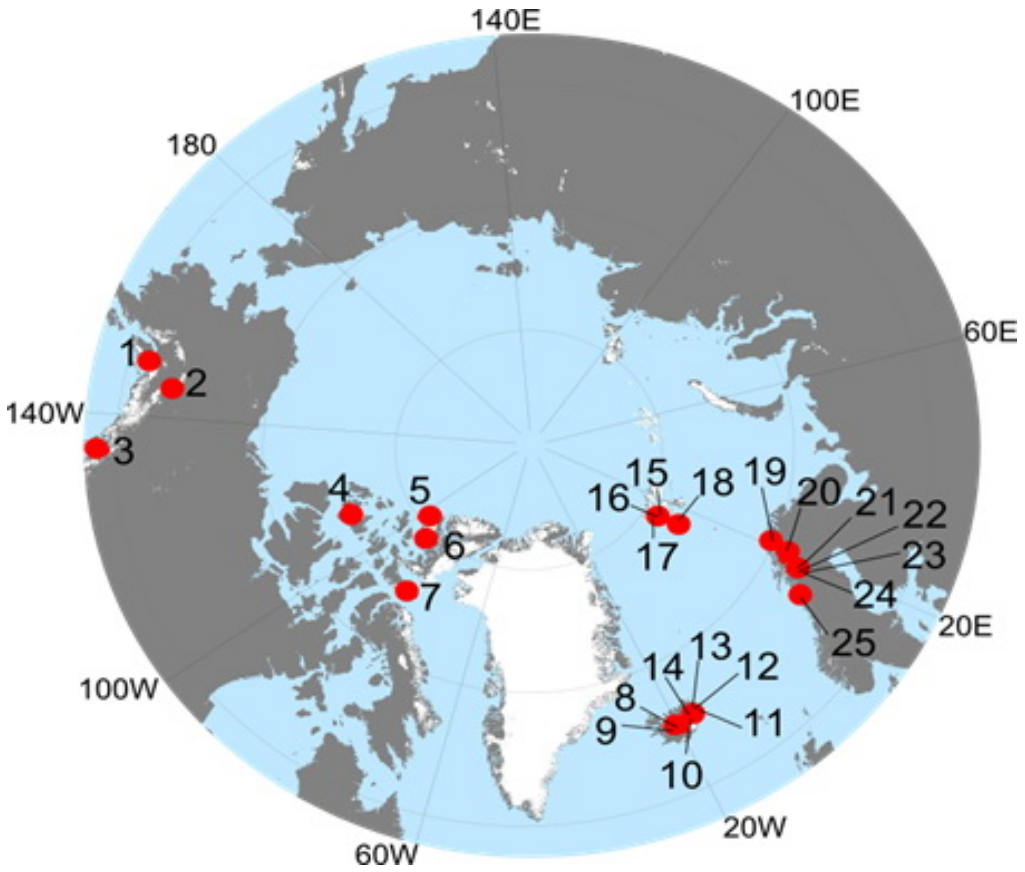

Fig. 5.5. Locations of Arctic glaciers for which long-term records of climatic mass balance (B_{clim}) are available and for which recent data are reported here. 1. Wolverine; 2. Gulkana; 3. Lemon Creek; 4. Melville South Ice Cap; 5. Meighen Ice Cap; 6. White Glacier; 7. Devon Ice Cap; 8. Hofsjökull; 9. Langjökull; 10. Tungnaarjökull; 11. Eayjabakkajökull; 12. Bruarjökull; 13. Dyngjujökull; 14. Koeldukvislarjökull; 15. Kongsvegen ; 16. Austre Broggerbreen; 17. Midtre Lovenbreen; 18. Hansbreen; 19. Lanfjordjoekelen; 20. Marmaglaciaren; 21. Riukojietna; 22. Rabots Glaciar; 23. Storglaciaren; 24. Tarfalaglaciaren; 25. Engabreen.

Table 5.1. Measured annual net surface mass balances of glaciers in Alaska, Arctic Canada, Iceland, Svalbard, Norway and Sweden for 2009-2010, and Arctic Canada for 2010-11. Data for glaciers in Alaska, Iceland, Svalbard, Norway and Sweden are from the World Glacier Monitoring Service (2012). (Data for Arctic Canada were supplied by D. Burgess and J. G. Cogley).

Region	Glacier	Net Balance 2009-10 (kg m^{-2} yr^{-1})	Net Balance 2010-11 (kg m^{-2} yr^{-1})
Alaska	Wolverine	-85	
	Lemon Creek	-580	
	Gulkana	-1832	
Arctic Canada	Devon Ice Cap	-417	-683
	Meighen Ice Cap	-387	-1310
	Melville S. Ice Cap	-939	-1339
	White	-188	-983
Iceland	Langjökull S. Dome	-3800	
	Hofsjökull E	-2830	
	Hofsjökull N	-2400	
	Hofsjökull SW	-3490	
	Köldukvislarjökull	-2870	
	Tungnaarjökull	-3551	
	Dyngjujökull	-1540	
	Brúarjökull	-1570	
	Eyjabakkajökull	-1750	
Svalbard	Midre Lovenbreen	-200	
	Austre Broggerbreen	-440	
	Kongsvegen	+130	
	Hansbreen	-14	
Norway	Engabreen	-520	
	LangfjordjØkulen	-760	
Sweden	Marmaglaciaren	-500	
	Rabots Glaciar	-1080	
	Riukojietna	-960	
	Storglaciaren	-690	
	Tarfalaglaciaren	-1060	

B_{clim} data for 2010-2011 are only available for the four glaciers in the Canadian High Arctic (**Table 5.1**). That year, B_{clim} values were the most negative on record for all four glaciers. In the Canadian Arctic, between 5 and 9 of the most negative mass balance years in the 49-52 year record have occurred since 2000. The mean annual mass balance for the period 2000-2011 is between 3 (Melville South Ice Cap) and 8 (Meighen Ice Cap) times as negative as the 1963-1999 average for each ice cap. This is a result of strong summer warming over the region that began around 1987 (Gardner and Sharp, 2007) and accelerated significantly after 2005 (Sharp et al. 2011). This trend is clearly evident in all the mass balance records shown in **Fig. 5.6**. The scale of the accelerating mass loss seen in **Fig. 5.6** is illustrated by a comparison of the mean loss for the four glaciers in three periods of the record: -575.3 kg m^{-2} a^{-1} in 2005-2011; -218.8 kg m^{-2} a^{-1} in 1995-2002; -184.9 kg m^{-2} a^{-1} in 1989-1994.

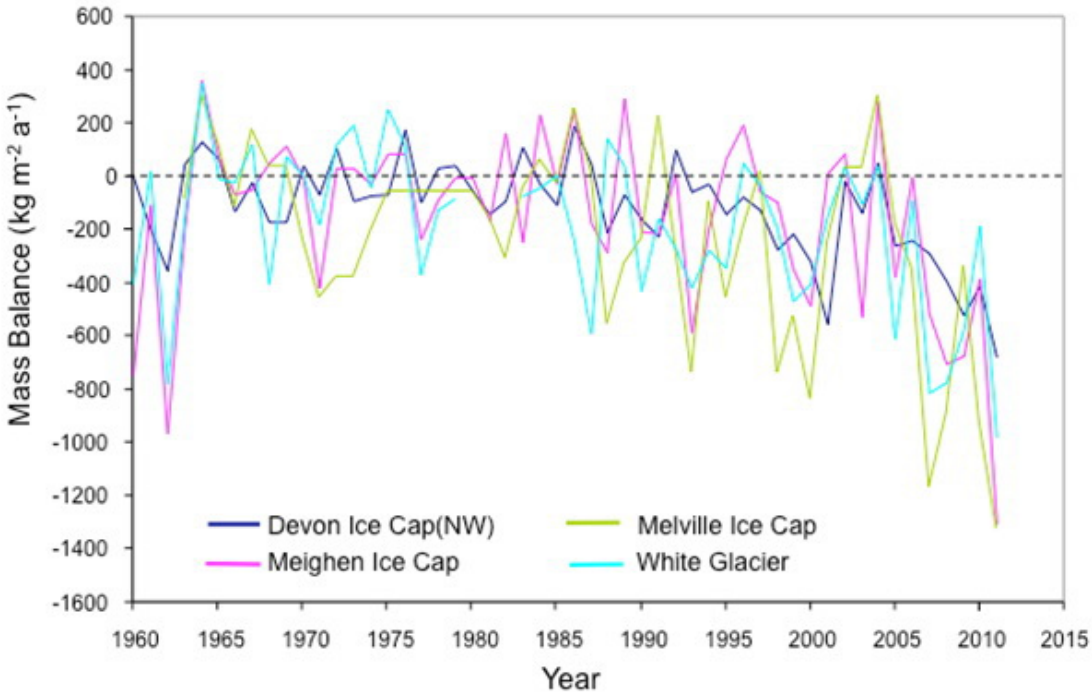

Fig. 5.6. Annual net surface mass balance since 1960 of four glaciers in the Queen Elizabeth Islands, Nunavut, Canada, showing the sharp acceleration in mass loss rate since 2005 and the record mass loss in 2010-11. Data are from the World Glacier Monitoring Service.

In 2010-11, the estimated mass loss from all the glaciers and ice caps in the Canadian Arctic Islands was -96±49 Gt (Sharp and Wolken, 2012). Derived using GRACE satellite gravimetry, this estimate of the complete mass balance, ΔM, which includes mass losses by iceberg calving, was the most negative value for this region during the GRACE observation period, 2002-2011. In the previous balance year, 2009-2010, the GRACE-derived ΔM estimate for this region was -73±55 Gt, and the mean annual value for the period 2004-2009 was -63 Gt (Sharp and Wolken, 2012). The large B_{clim} values reported in the previous paragraph are consistent with the increasing GRACE-derived ΔM estimates, which confirm the growing importance of glaciers and ice caps in the Canadian Arctic Islands as contributors to global sea level rise (Gardner et al., 2011).

Variability in mean summer temperature accounts for much of the inter-annual variability in B_{clim} in cold, dry regions like the Canadian high Arctic while, in more maritime regions, like Iceland

and southern Alaska, variability in winter precipitation is also a factor. Land surface temperature (LST) over ice in summer is likely closely related to B_{clim}. **Fig. 5.7** shows moderate to large LST anomalies over glaciers and ice caps throughout the Arctic, particularly in summers 2011 and 2012 in the Canadian high Arctic (northern Ellesmere, Agassiz, Axel Heiberg, Prince of Wales). More generally in 2011 (and 2012), glacier mass balance in the Canadian high Arctic was affected by the same atmospheric circulation and advection of warm air into the region that caused significant melting on the Greenland ice sheet (Sharp and Wolken, 2011; Tedesco et al., 2012).

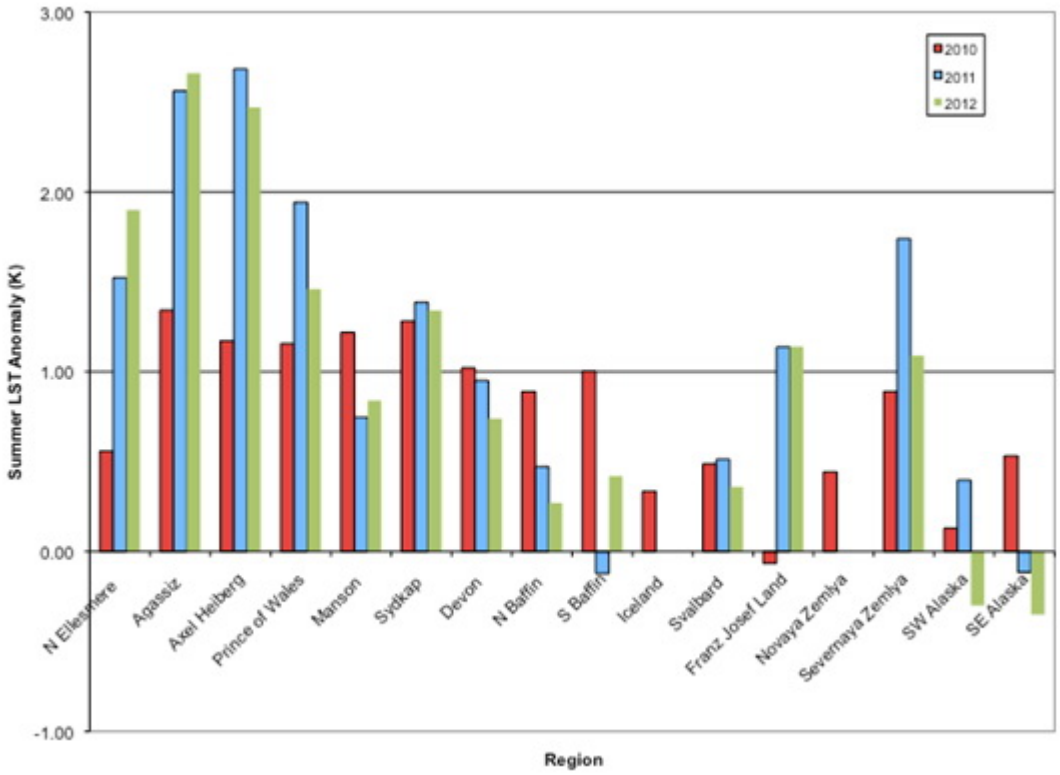

Fig. 5.7. Comparison of 2010, 2011 and 2012 summer mean land surface temperature (LST) anomalies (relative to 2000 to 2010 climatology) for 16 glaciated regions of the Arctic based on the MODIS MOD11A2 LST product.

References

Cogley, J. G., R. Hock, L. A. Rasmussen, A. A. Arendt, A. Bauder, R. J. Braithwaite, P. Jansson, G. Kaser, M. Möller, L. Nicholson and M. Zemp, 2011, *Glossary of Glacier Mass Balance and Related Terms*, IHP-VII Technical Documents in Hydrology No. 86, IACS Contribution No. 2, UNESCO-IHP, Paris.

Gardner, A. S. and M. Sharp. 2007. Influence of the Arctic circumpolar vortex on the mass balance of Canadian high Arctic glaciers. *J. Climate*, 20, 4586-4598.

Gardner, A. S., G. Moholdt, B. Wouters, G. J. Wolken, J. G. Cogley, D. O. Burgess, M. J. Sharp, C. Braun and C. Labine, 2011. Sharply increased mass loss from glaciers and ice caps in the Canadian Arctic Archipelago. *Nature*, 473, 357-360.

Jacob, T., J. Wahr, W. T. Pfeffer and S. Swenson. 2012. Recent contributions of glaciers and ice caps to sea level rise. *Nature*, 482, 514-518.

Meier, M. F., M. B. Dyurgerov, U. K. Rick, S. O'Neel, W. T. Pfeffer, R. S. Anderson, S. P. Anderson and A. F. Glazovsky. 2007. Glaciers dominate eustatic sea level rise in the 21st century. *Science*, 317, 1064-1067.

Sharp, M. and G. Wolken. 2011. Glaciers and Ice Caps (Outside Greenland). In *Arctic Report Card 2011*, http://www.arctic.noaa.gov/reportcard.

Sharp, M. and G. Wolken. 2012. Glaciers and Ice Caps (Outside Greenland). [in State of the Climate in 2011], *Bull. Amer. Meteorol. Soc.*, 93(7), S149-S150.

Sharp, M., D. O. Burgess, J. G. Cogley, M. Ecclestone, C. Labine and G. J. Wolken. 2011. Extreme melt on Canada's Arctic ice caps in the 21st century. *Geophys. Res. Lett.*, 38, L11501, doi:10.1029/2011GL047381.

Tedesco, M., J. E. Box, J. Cappellen, T. Mote, R. S. W. van der Wal and J. Wahr. 2012. Greenland Ice Sheet. [in State of the Climate in 2011], *Bull. Amer. Meteorol. Soc.*, 93(7), S150-S153.

World Glacier Monitoring Service. 2012. Preliminary glacier mass balance data 2009 and 2010. http://www.geo.uzh.ch/microsite/wgms/mbb/sum10.html. Accessed September 29, 2012.

Greenland Ice Sheet

J.E. Box[1], J. Cappelen[2], C. Chen[1], D. Decker[1], X. Fettweis[3], E. Hanna[4], N.T. Knudsen[5], T. Mote[6], K. Steffen[7], M. Tedesco[8], R.S.W. van de Wal[9], J. Wahr[10]

[1]Byrd Polar Research Center, The Ohio State University, Columbus, OH, USA
[2]Danish Meteorological Institute, Copenhagen, Denmark
[3]Department of Geography, University of Liège, Liège, Belgium
[4]Department of Geography, University of Sheffield, UK
[5]Department of Geology, Aarhus University, Aarhus, Denmark
[6]Department of Geography, University of Georgia, Athens, Georgia, USA
[7]Swiss Federal Research Institute WSL, Birmensdorf, Switzerland
[8]City College of New York, New York, NY, USA
[9]Institute for Marine and Atmospheric Research Utrecht, Utrecht University, Utrecht, The Netherlands
[10]CIRES, University of Colorado, Boulder, CO, USA

November 28, 2012

Highlights

- The duration of melting at the surface of the ice sheet in summer 2012 was the longest since satellite observations began in 1979, and a rare, near-ice sheet-wide surface melt event was recorded by satellites for the first time.
- The lowest surface albedo observed in 13 years of satellite observations (2000-2012) was a consequence of a persistent and compounding feedback of enhanced surface melting and below normal summer snowfall.
- Field measurements along a transect (the K-Transect) on the western slope of the ice sheet revealed record-setting mass losses at high elevations.
- A persistent and strong negative North Atlantic Oscillation (NAO) index caused southerly air flow into western Greenland, anomalously warm weather and the spatially and temporally extensive melting, low albedo and mass losses observed in summer 2012.

Surface Melting and Albedo

In 2012, ice sheet surface melting set two new, satellite era records - melt extent and melt index - according to passive microwave observations made since 1979 (e.g., Tedesco, 2007, 2009). Melt extent is the fractional area (in %) of the surface of the ice sheet where melting was detected. The melt index (MI) is the number of days on which melting occurred multiplied by the area where melting was detected.

Melt extent over the Greenland ice sheet reached record values during 11-12 July, covering as much as ~97% of the ice sheet on a single day (**Figs. 5.8** and **5.9**, and, e.g., Nghiem et al., 2012). Confirmed by different methods for analyzing passive microwave observations (e.g., Mote and Anderson, 1995; Tedesco, 2009), the almost 100% melt extent is nearly four times greater than the ~ 25% average melt extent that occurred in 1981-2010.

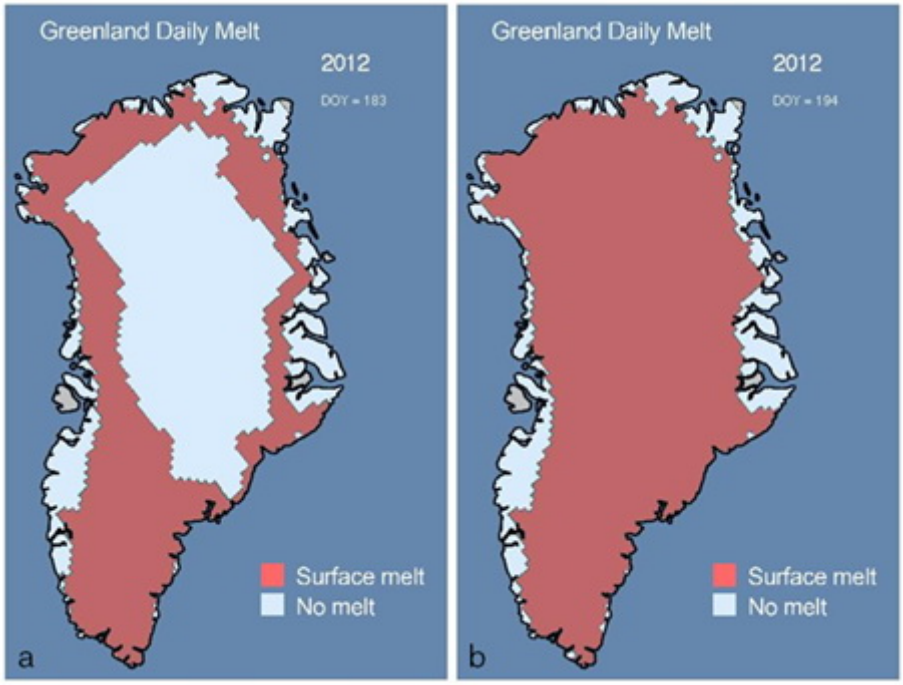

Fig. 5.8. Surface melt extent on the Greenland Ice Sheet on 1 July 2012 (a) and 12 July 2012 (b) detected by the SSM/I passive microwave sensor. Figure is after Tedesco et al. (2007).

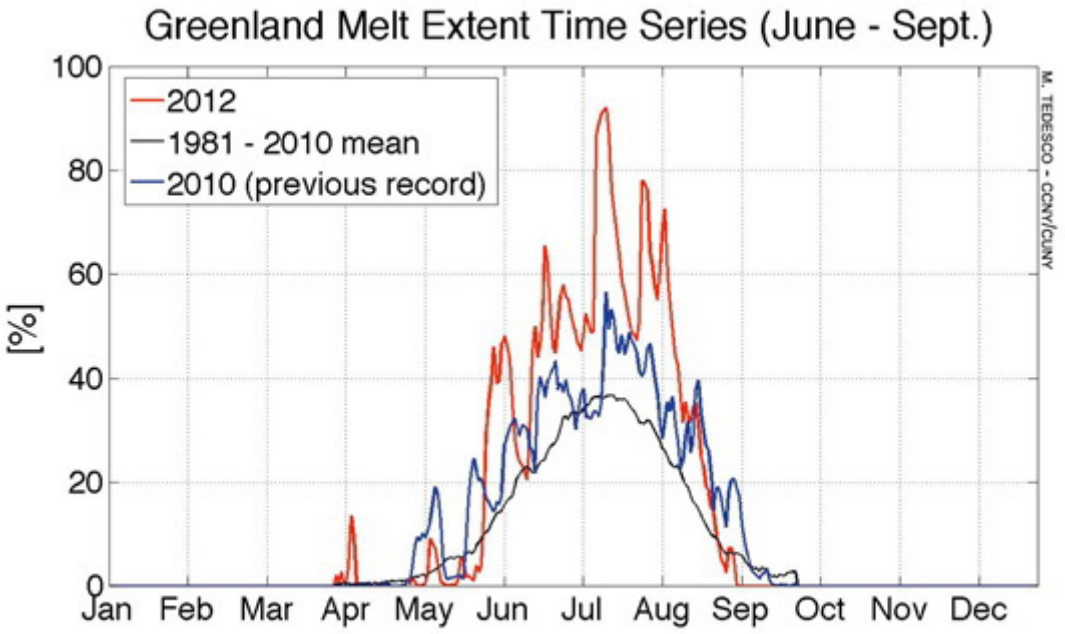

Fig. 5.9. Surface melt extent on the Greenland Ice Sheet detected by the SSM/I passive microwave sensor. Figure is after Tedesco et al. (2007).

The standardized melt index (SMI) for 2012 was about +2.4, almost twice the previous record of about +1.3 in 2010 (**Fig. 5.10**). Melting in 2012 began about two weeks earlier than average at low elevations and, for a given elevation, was sustained longer than the previous record year

(2010) for most of June through mid-August. Melting lasted up to 140 days (20-40 days greater than the mean value) at low elevations in some areas of southwest Greenland. The 2012 anomaly for the number of melting days (i.e., number of melting days in 2012 minus the 1980-2010 average) exceeded 27 days in the south and 45 days in the northwest. Some areas in northwest Greenland between 1400 and 2000 m a.s.l. had nearly two months more melt than during the 1981-2010 reference period.

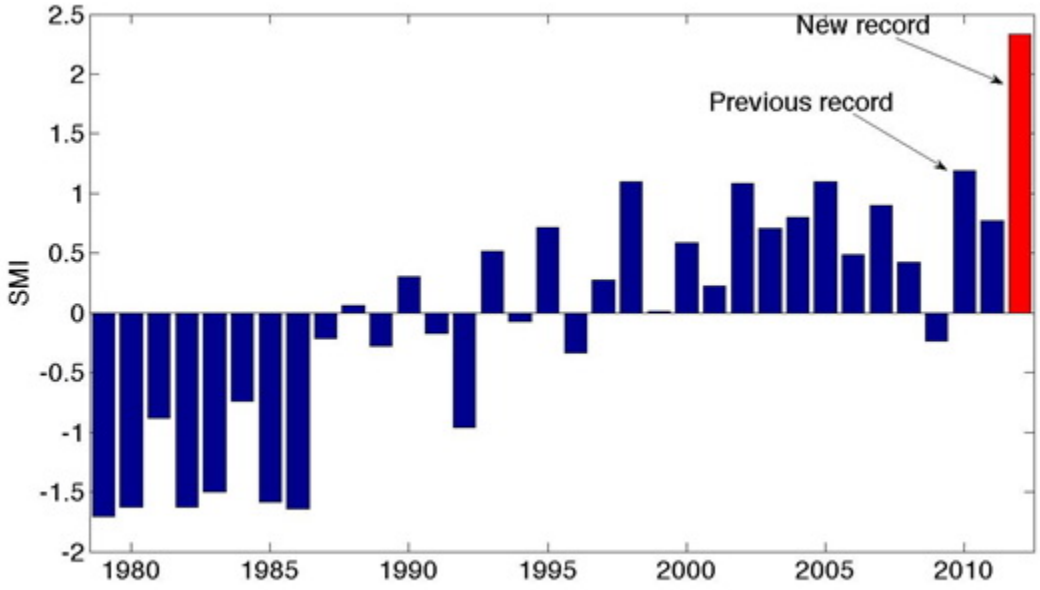

Fig. 5.10. Greenland ice sheet standardized melting index (SMI). The index is calculated by subtracting the melt index (MI) from the 1979 - 2012 average and dividing by its standard deviation (Tedesco, 2007). MI is the number of days on which melting occurred multiplied by the area where melting was detected.

The regions of extended melt duration coincide with areas of anomalously low albedo (or reflectivity, where a surface with low albedo/reflectivity will absorb more solar radiation and warm more than a surface with high albedo/reflectivity). The albedo anomalies across the ice sheet in June-August 2012, when solar irradiance is highest and the albedo is lowest in magnitude, are illustrated in **Fig. 5.11**. Negative albedo anomalies were widespread across the ice sheet, but were particularly low along the western and northwestern margins in areas where darker bare ice was exposed after the previous winter's snow accumulation had melted completely away. The low albedo was compounded by a persistent feedback of enhanced surface melting due to relatively warm air temperatures and below normal summer snowfall.

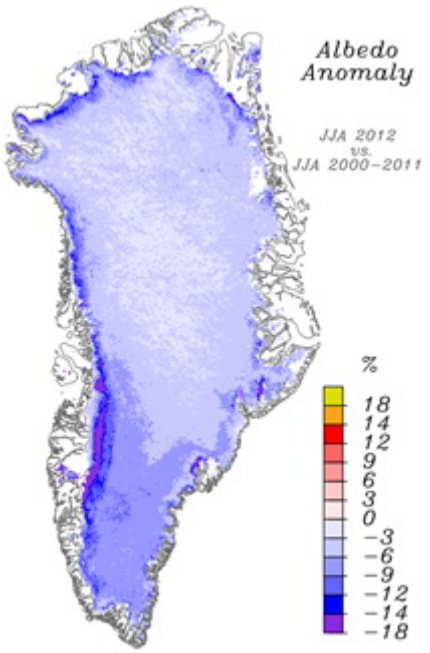

Fig. 5.11. Summer (JJA) albedo (reflectivity) anomaly in 2012 relative to the 2000-2011 reference period. Data were derived from MODIS (Moderate Resolution Imaging Spectroradiometer) observations. Figure is after Box et al. (2012).

While **Fig. 5.11** shows that there is strong spatial variation in albedo, **Fig. 5.12** shows that the area-averaged albedo of the entire ice sheet has continued to decline during the period of MODIS observations (2000-2012). The area-averaged albedo for 2012 was a new record low, and occurred only one year after the previous record of 2011.

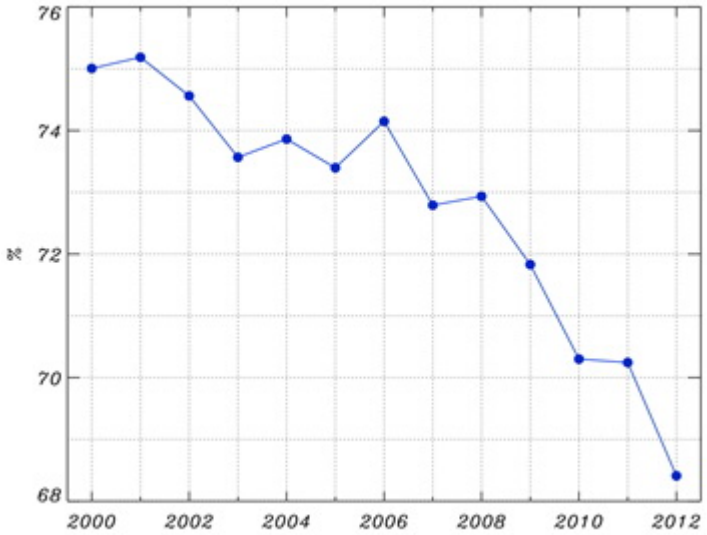

Fig. 5.12. Area-averaged albedo of the Greenland ice sheet during June-August each year of the period 2000-2012. Data are derived from MODIS MOD10A1 observations. Figure is after Box et al. (2012).

Equilibrium Line Altitude Along the K-Transect

The 150 km long K-Transect is located near Kangerlussuaq at 67°N between 340 m and 1500 m above sea level (a.s.l.) on the western flank of the ice sheet (van de Wal et al., 2005). The equilibrium line altitude (ELA), the highest altitude at which winter snow survives, is a convenient indicator of the competing effects of surface mass loss from melting and surface mass gain from snow accumulation. The mass balance measurements along the K-transect in 2012 confirm the extensive surface melting observed by satellite (see the previous section on Surface Melting and Albedo).

In 2012, estimates from ground observations placed the ELA far above the height of the ice sheet topographic divide near this latitude (2687 m a.s.l.) and an unprecedented 3.7 times the standard deviation above the 21-year mean ELA value (**Fig. 5.13**). The satellite-derived snowline, a close proxy of ELA, at the end of the K-transect melt season also occurred at a record high elevation according to MODIS observations made since 2000 (**Fig. 5.13**) (Box et al., 2009a; van de Wal et al., 2012).

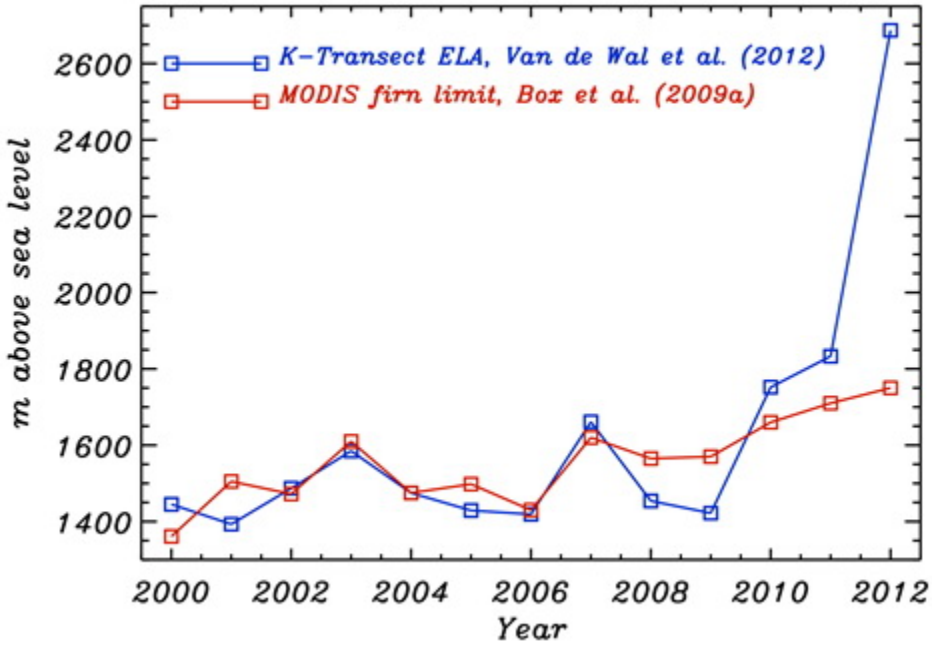

Fig. 5.13. The equilibrium line altitude (ELA), the highest altitude at which winter snow survives, from ground observations (solid line) and the firn line (a proxy for ELA) from MODIS observations (broken line) along the K-transect. It is located near Kangerlussuaq on the western flank of the ice sheet at 67°N between 340 m and 1500 m above sea level (a.s.l.). The difference between the ground and satellite observations in 2012 is because MODIS is not as sensitive to the ELA as it is to the firn line. ELA data are from van der Wal et al. (2012). MODIS data are from Box et al. (2009a).

B_{clim} (the difference between annual snow accumulation and runoff - see also the *Glaciers and Ice Caps* essay) during 2011-2012 along the K-transect was characterized by exceptional melt at high elevations. At the highest elevation site (S10, elevation 1847 m, almost 350 m higher than the previous ELA of 1500 m) the surface mass balance was estimated to be -74 cm w.e. (water equivalent). Relatively low winter snow accumulation at high elevation resulted in

relatively low albedo, which, coupled with high air temperatures, compounded high melt rates after melt onset. Below 1500 m elevation, surface mass balance values decreased gradually to normal values near the ice margin (**Fig. 5.14**).

Figure 5.14 suggests that the mass balance along the transect in 2012 was the second lowest since measurements began in 1991. However, a weighted mass balance that includes the S10 site, which is above the former ELA of 1500 m, indicates that the 2011-2012 mass balance year was the most negative in 22 years.

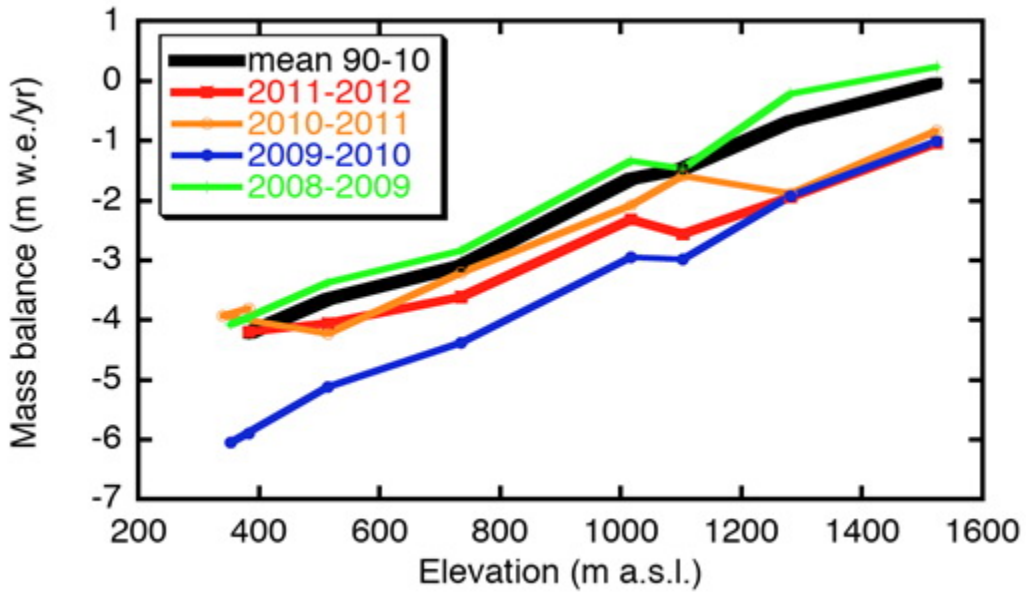

Fig. 5.14. Surface mass balance as a function of elevation below 1500 m along the K-transect since 2008-2009. The 20-year (1990-2010) average is also shown. The 2012 record does not include the highest elevation site, S10, which was measured for the first time in summer 2012. Figure is updated from Box et al. (2011).

Atmospheric Circulation and Air Temperature as they Relate to Melting, Albedo and ELA

The large melt extent and high melt index, low albedo and negative mass balance in 2012 were a consequence of the atmospheric circulation and high air temperatures.

Summer 2012 was characterized by a negative North Atlantic Oscillation (NAO) index for the entire season; a -2.4 standard deviation anomaly relative to the NAO average for June-August during 1981-2010. Consequently, sea level pressure was anomalously high over the ice sheet (see **Fig. 1.6** in the essay on *Air Temperature, Atmospheric Circulation and Clouds*) and atmospheric circulation was characterized by warm air advection from the south into western Greenland (**Fig. 5.15**). This same circulation pattern has occurred each summer since 2007 (Box et al., 2012). It is noteworthy that a very negative NAO in spring 2012 had a significant negative impact on circum-Arctic snow cover extent (see the *Snow* essay).

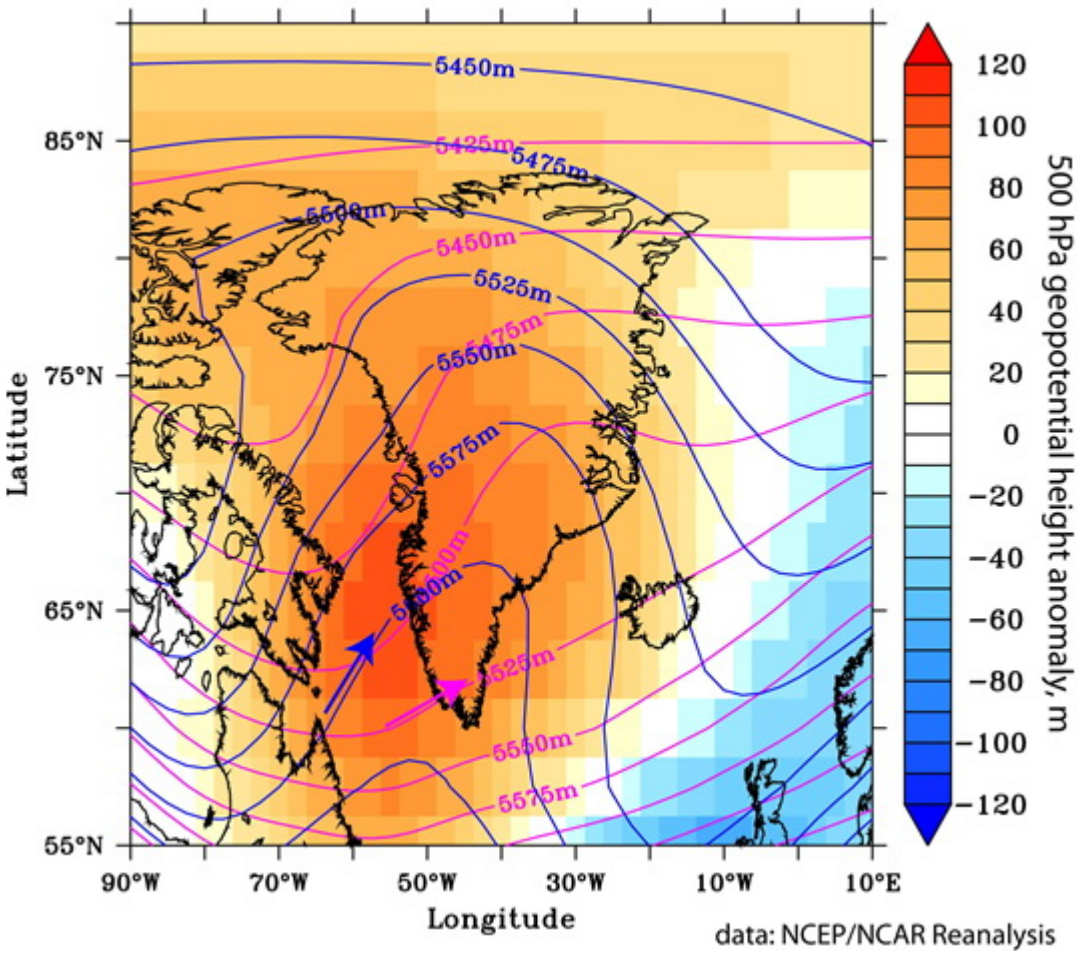

Fig. 5.15. Geopotential height (500 hPa) anomalies for June-August, 2012 (blue lines) referenced to the 1981-2010 mean (magenta lines). The arrow in the lower left quadrant shows that the prevailing upper air flow from the south advected warm air into Greenland. Data source: NCEP/NCAR Reanalysis version R1.

As a consequence of the atmospheric circulation pattern (**Fig. 5.15**), surface air temperatures at long-term meteorological stations in Greenland were characterized by record-setting warm summer months (not illustrated), particularly in the west and south of the island and at high elevations. For example, the Greenland Climate Network (GC-Net) automatic weather station at Summit (3199 m above sea level) measured hourly-mean air temperatures above the freezing point for the first time since measurements began in 1996 (**Fig. 5.16**).

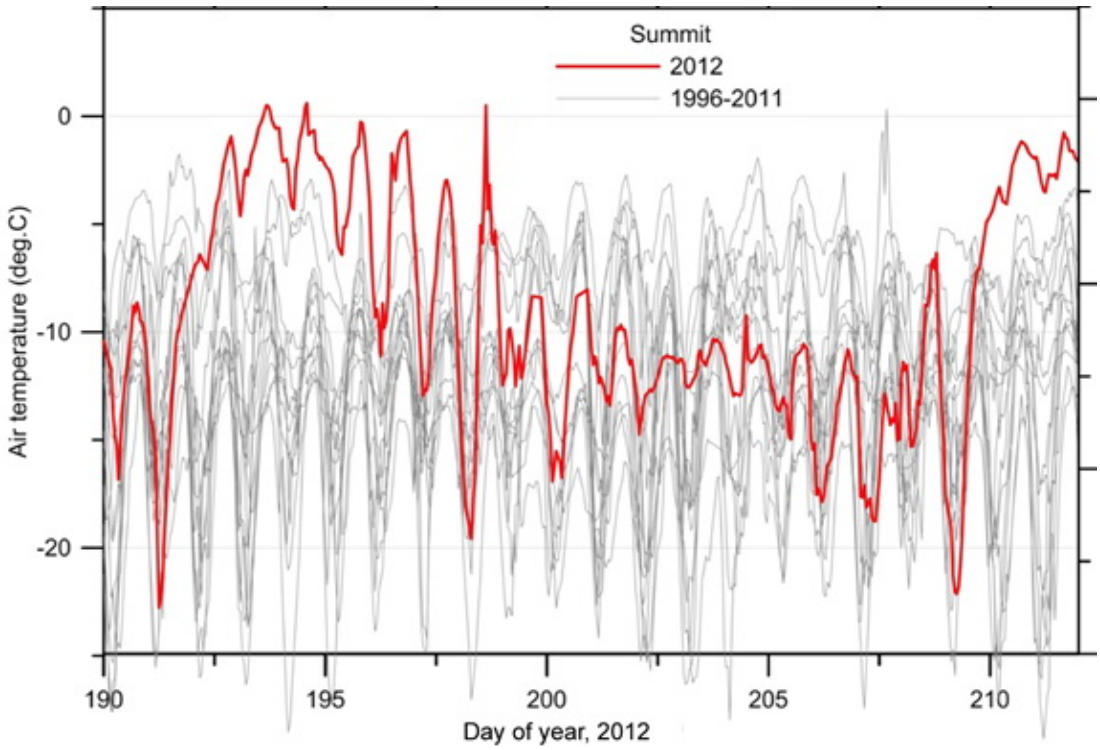

Fig. 5.16. Hourly mean air temperature at Summit (elevation 3199 m above sea level) from 9 July through 2 August 2012 (red) and for 1996-2011 (grey). Unpublished data from K. Steffen.

Seasonally-averaged upper air temperature data available from twice-daily radiosonde observations show anomalous warmth throughout the troposphere in summer 2012 (**Fig. 5.17**). Similar upper air temperature profiles were observed in 2011 (Box et al., 2011). The overall warm pattern near the surface between 850 and 1000 hPa is consistent with a warming trend evident in the period of reliable records beginning in 1964, and most pronounced since the mid-1980s (Box and Cohen, 2006). This recent warming trend is seen in the long-term air temperature reconstruction for the ice sheet, which also shows that mean annual air temperatures in all seasons are now higher than they have been since 1840 (**Fig. 5.18**).

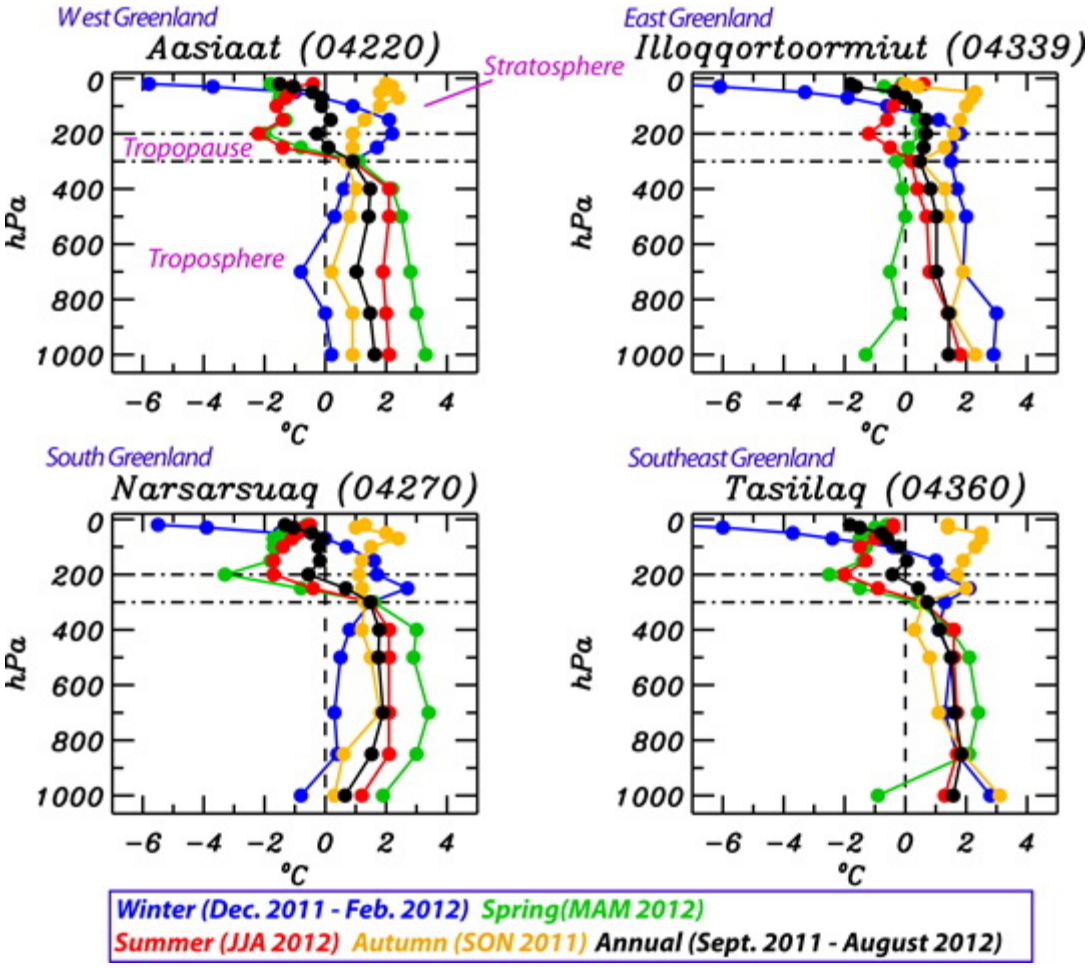

Fig. 5.17. Upper air temperature anomalies relative to the 1981-2010 reference period in winter, spring and summer of 2012 at four coastal locations in Greenland. The winter season includes data for December 2011. Data are from twice-daily radiosonde observations available at the Integrated Global Radiosonde Archive (http://www.ncdc.noaa.gov/oa/climate/igra/). WMO station numbers are in parentheses.

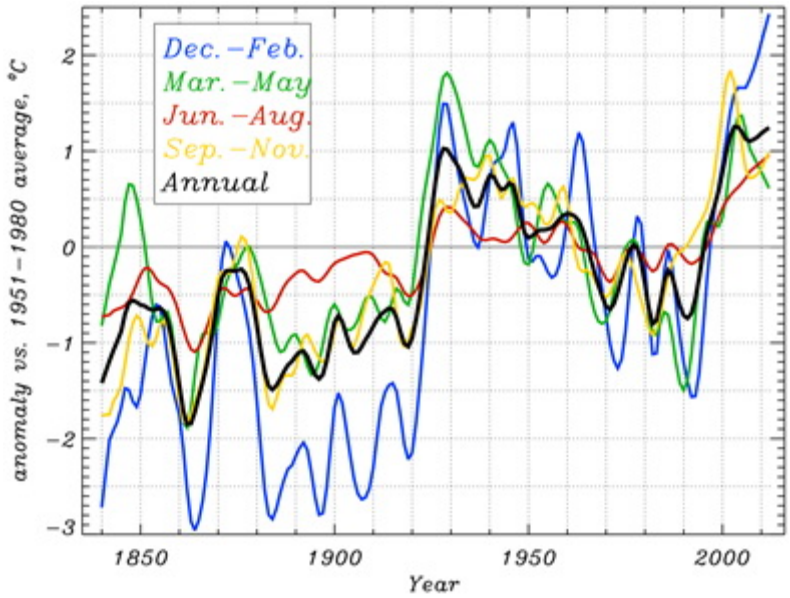

Fig. 5.18. Seasonally-averaged, near-surface air temperature reconstruction for the entire Greenland ice sheet, 1840 to August 2012 (after Box et al., 2009b).

Greenland Mass Changes from GRACE

GRACE satellite gravity solutions computed according to Velicogna and Wahr (2006) are used to estimate monthly changes in the total mass of the Greenland ice sheet (**Fig. 5.19**). The data show that the ice sheet continues to lose mass and has contributed +8.0 mm to globally-averaged sea level rise since 2002. The rate of mass loss has accelerated during the period of observation, the mass loss of 367 Gt/y between September 2008 and September 2012 being almost twice that for the period June 2002-July 2006 (193 Gt/y). GRACE data also show that significant mass loss has occurred from glaciers and ice caps in the Canadian Arctic (see the *Glaciers and Ice Caps* essay).

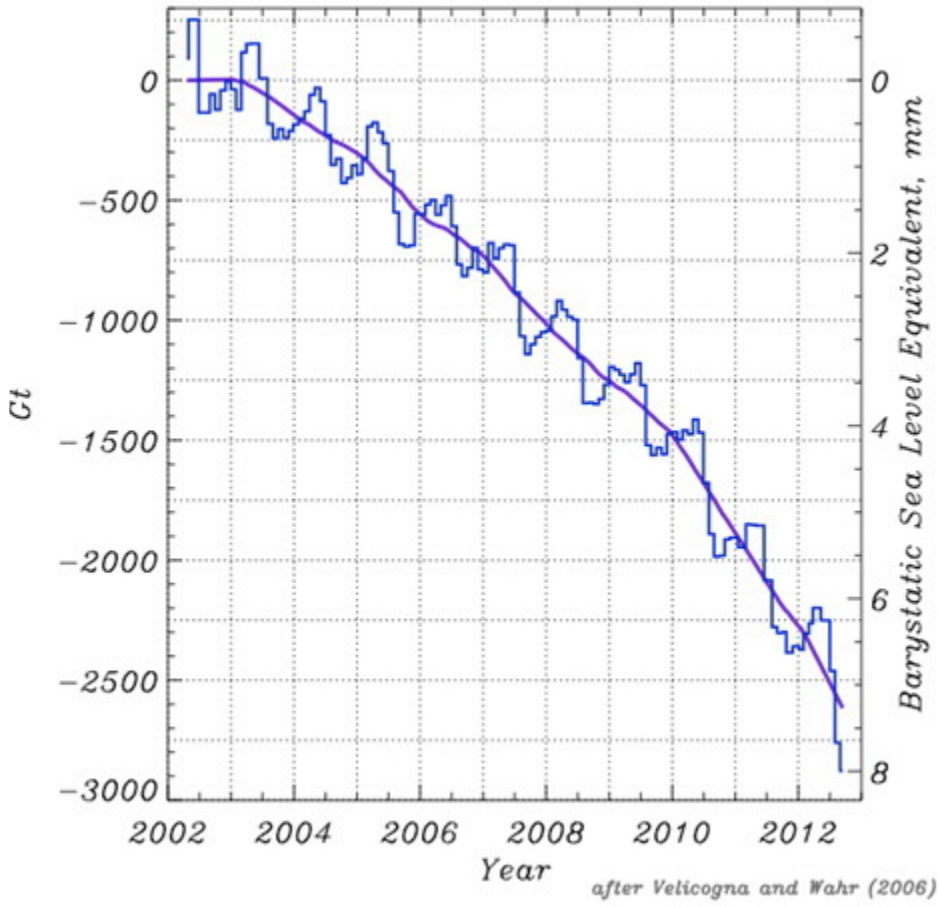

Fig. 5.19. Monthly smoothed (purple) and unsmoothed (blue) values of the total mass (in Gigatons, Gt), of the Greenland ice sheet from GRACE March 2002-September 2012. The barystatic ("bary" refers to weight) effect on local sea level change is the volume of freshwater added or removed divided by the ocean surface area. It does not include the effects of water thermal expansion, salinity or the associated changes to the gravity field. Figure is after Velicogna and Wahr (2006).

Marine-terminating Glacier Area Changes

Marine-terminating glaciers are the outlets through which the inland ice can flow most rapidly and in the largest quantities to the ocean. Iceberg calving and retreat of the glaciers leads to flow acceleration and inland ice sheet mass loss, which contributes to sea level rise.

Daily surveys using cloud-free MODIS visible imagery (Box and Decker, 2011; http://bprc.osu.edu/MODIS/) indicate that in the year prior to end of the 2012 melt season the marine-terminating glaciers collectively lost an area of 297 km^2. This is 174 km^2 greater than the average annual loss rate of the previous 11 years (132 km^2 yr^{-1}) (**Fig. 5.20**) and also greater than losses in the 1980s and 1990s (Howat and Eddy, 2011).

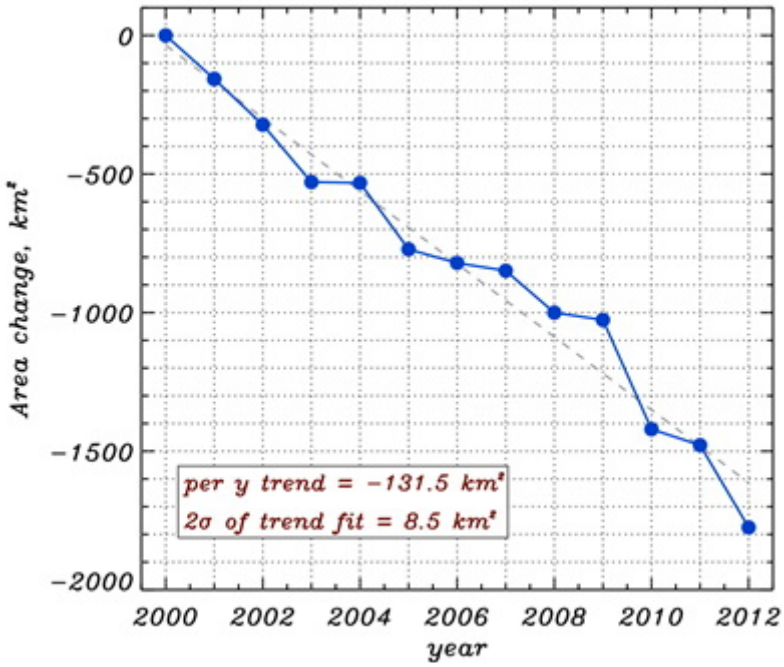

Fig. 5.20. Cumulative net annual area change at the 40 widest marine-terminating glaciers of the Greenland Ice Sheet (after Box and Decker, 2011). The dashed line is a least-squares regression fit with a slope of 131.5 km^2 of area loss per year since 2000.

Since 2000, the net area change of the forty widest marine-terminating glaciers is -1775 km^2 (**Fig. 5.20**), ten times the area of Washington, DC. Glaciers in northernmost Greenland contributed to half of the net area change. In 2012, the six glaciers with the largest net area loss were Petermann (-141 km^2), 79 glacier (-27 km^2), Zachariae (-26 km^2), Steenstrup (-19 km^2), Steensby (-16 km^2, the greatest retreat since observations began in 2000) and Jakobshavn (-13 km^2). While the total area change was negative in 2012, four of forty glaciers did grow in area relative to the end of the 2011 melt season.

References

Box, J. E. and A. E. Cohen. 2006. Upper-air temperatures around Greenland: 1964-2005. *Geophys. Res. Lett.*, 33, L12706, doi:10.1029/2006GL025723.

Box, J. E., R. J., Benson, D. Decker and D. H. Bromwich. 2009a. Greenland ice sheet snow line variations 2000-2008, Association of American Geographers Annual Meeting, Las Vegas, NV, 22-27 March, 2009.

Box, J. E., L. Yang, D.H. Browmich and L-S. Bai. 2009b. Greenland ice sheet surface air temperature variability: 1840-2007. *J. Climate*, 22(14), 4029-4049, doi:10.1175/2009jcli2816.1.

Box, J. E. and D. T. Decker. 2011. Greenland marine-terminating glacier area changes: 2000-2010. *Ann. Glaciol.*, 52(59) 91-98.

Box, J. E. and fifteen others. 2011. Greenland Ice Sheet. In *Arctic Report Card 2011*, http://www.arctic.noaa.gov/reportcard.

Box, J. E., X. Fettweis, J. C. Stroeve, M. Tedesco, D. K. Hall and K. Steffen. Greenland ice sheet albedo feedback: thermodynamics and atmospheric drivers. *The Cryosphere*, 6, 821-839, doi:10.5194/tc-6-821-2012, 2012.

Howat, I. M. and A. Eddy. 2011. Multidecadal retreat of Greenland's marine-terminating glaciers. *J. Glaciol.*, 57(203), 389-396.

Mote, T. L. and M. R. Anderson. 1995. Variations in melt on the Greenland ice sheet based on passive microwave measurements. *J. Glaciol.*, 41, 51-60.

Nghiem, S. V., D. K. Hall, T. L. Mote, M. Tedesco, M. R. Albert, K. Keegan, C. A. Shuman, N. E. DiGirolamo and G. Neuman. 2012. The extreme melt across the Greenland Ice Sheet in 2012. *Geophys. Res. Lett.*, 39, L20502, doi:10.1029/2012GL053611.

Tedesco, M. 2007. Snowmelt detection over the Greenland ice sheet from SSM/I brightness temperature daily variations. *Geophys. Res. Lett.*, 34, L02504, doi:10.1029/2006GL028466.

Tedesco, M. 2009. Assessment and development of snowmelt retrieval algorithms over Antarctica from K-band spaceborne brightness temperature (1979-2008). *Remote Sens. Environ.*, 113(2009), 979-997.

Velicogna, I. and J. Wahr. 2006. Acceleration of Greenland ice mass loss in spring 2004. *Nature*, 443(7109), 329-331. doi:10.1038/Nature05168.

van de Wal, R. S. W., W. Greuell, M. R. van den Broeke, C.H. Reijmer and J. Oerlemans. 2005. Surface mass-balance observations and automatic weather station data along a transect near Kangerlussuaq, West Greenland. *Ann. Glaciol.*, 42, 311-316.

van de Wal, R. S. W., W. Boot, C. J. P. P. Smeets, H. Snellen, M. R. van den Broeke and J. Oerlemans. 2012. Twenty-one years of mass balance observations along the K-transect, West Greenland. *Earth Sys. Sci. Data*, 5, 351-363, doi:10.5194/essdd-5-351-2012.

Permafrost

V.E. Romanovsky[1], S.L. Smith[2], H.H. Christiansen[3], N.I. Shiklomanov[4], D.A. Streletskiy[4], D.S. Drozdov[5], N.G. Oberman[6], A.L. Kholodov[1], S.S. Marchenko[1]

[1]Geophysical Institute, University of Alaska Fairbanks, Fairbanks, Alaska, USA
[2]Geological Survey of Canada, Natural Resources Canada, Ottawa, Ontario, Canada
[3]Geology Department, University Centre in Svalbard, UNIS, Norway
and Institute of Geography and Geology, University of Copenhagen, Denmark
[4]Department of Geography, George Washington University, Washington, DC, USA
[5]Earth Cryosphere Institute, Tyumen, Russia
[6]MIRECO Mining Company, Syktyvkar, Russia

November 9, 2012

Highlights

- In 2012, new record high temperatures at 20 m depth were measured at most permafrost observatories on the North Slope of Alaska and in the Brooks Range, where measurements began in the late 1970s. Only two coastal sites show exactly the same temperatures as in 2011.
- A common feature at Alaskan, Canadian and Russian sites is greater warming in relatively cold permafrost than in warm permafrost in the same geographical area.
- During the last fifteen years, active-layer thickness has increased in the Russian European North, the region north of East Siberia, Chukotka, Svalbard and Greenland.
- Active-layer thickness on the Alaskan North Slope and in the western Canadian Arctic was relatively stable during 1995-2011.

The most direct indicators of permafrost stability and changes in permafrost state are the permafrost temperature and the active layer thickness (ALT). The ALT is the top layer of soil and/or rock that thaws during the summer and freezing again during the fall, i.e., it is not permafrost. Permafrost temperature measured at a depth where seasonal variations in ground temperature cease to occur is the best indicator of long-term change. This depth varies from a few meters in warm, ice-rich permafrost to 20 m and more in cold permafrost and in bedrock (Smith et al., 2010; Romanovsky et al., 2010a). However, if continuous year-round temperature measurements are available, the mean annual ground temperature (MAGT) at any depth within the upper 15 m can be used for detection of changing conditions. International Polar Year (IPY 2007-2009) resulted in significant enhancement of the permafrost observing system in the Arctic, where there are now ~600 boreholes (**Fig. 5.20**; Brown et al., 2010; Romanovsky et al., 2010a). A borehole inventory, including mean annual ground temperatures for most of these boreholes, is available online (http://nsidc.org/data/g02190.html).

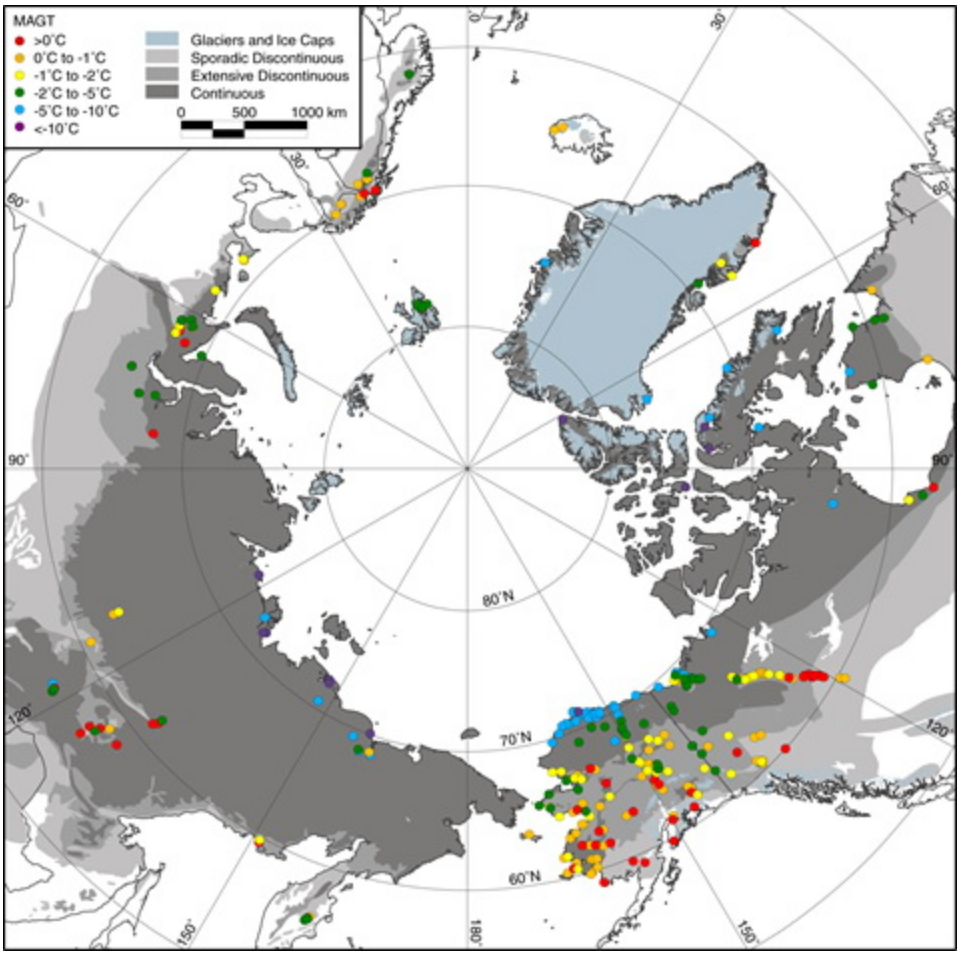

Fig. 5.21. Circum-Arctic view of mean annual ground temperature (MAGT) in permafrost during the International Polar Year (IPY 2007-2009; from Romanovsky et al., 2010).

Permafrost temperatures in the Arctic and sub-Arctic lowlands generally decrease from south to north. Higher ground temperatures are found in the southern discontinuous zone, where MAGT is above 0°C at many locations (**Fig. 5.21**). The temperature of warm permafrost in the discontinuous zone generally falls within a narrow range, with MAGT at most sites being >-2°C (Christiansen et al., 2010; Romanovsky et al., 2010a; Smith et al., 2010) (**Fig. 5.21**). Temperatures as low as -3°C, or even -4°C, however, may be observed in some specific ecological or topographic conditions (Jorgenson et al., 2010). A greater MAGT range occurs within the continuous permafrost zone, from >-1°C at some locations to as low as -15°C at others (Christiansen et al., 2010; Romanovsky et al., 2010a; Romanovsky et al., 2010b; Smith et al., 2010). MAGT >0°C is observed at some locations near the southern boundary of the continuous zone (**Fig. 5.21**), which may indicate that this boundary is shifting northward (Romanovsky et al., 2010b). Permafrost temperatures <-10°C are presently found only in the Canadian Arctic Archipelago (Smith et al., 2010) and near the Arctic coast in Siberia.

Our understanding of the thermal state of mountain permafrost in northwestern Canada (Yukon) has improved in recent years (e.g. Lewkowicz et al., 2012). In the sporadic permafrost zone of southern Yukon, warm, thin permafrost formed under earlier, colder conditions persists in organic soils in valley floors (Lewkowicz et al., 2011). Recent research also indicates that air temperature inversions are an important factor influencing mountain permafrost distribution

(Lewkowicz and Bonnaventure, 2011; Lewkowicz et al. 2012). Thus, permafrost may be less extensive at higher elevations than suggested by predictions based on air temperatures measured at standard weather stations located in valley floors (Smith et al., 2010).

Systematic observations of permafrost temperature in Alaska, Canada and Russia since the middle of the 20th Century provide several decades of continuous data from several sites. The records allow assessment of changes in permafrost temperatures on a decadal time scale. A general increase in permafrost temperatures is observed during the last several decades in Alaska (Osterkamp, 2008; Smith et al., 2010; Romanovsky et al., 2010a), northwest Canada (Smith et al., 2010) and Siberia (Oberman, 2008; Romanovsky et al., 2010b). At most Alaskan permafrost observatories there was substantial warming during the 1980s and especially in the 1990s (**Fig. 5.22**). The magnitude and nature of the warming varies between locations, but is typically from 0.5°C to 2°C at the depth of zero seasonal temperature variations over this 20 year period (Osterkamp, 2008). At the beginning of the 2000s, permafrost temperature was relatively stable on the North Slope of Alaska (Smith et al., 2010) (**Fig. 5.22**), and there was even a slight decrease (from 0.1°C to 0.3°C) in Interior Alaska during the last four years (**Fig. 5.22**), but the permafrost warming has resumed since 2007. This warming trend is initially evident at the Arctic coastal sites and then propagates into the northern foothills of the Brooks Range (**Fig. 5.22b**), where a noticeable warming in the upper 20 m of permafrost has become evident since 2008 (Romanovsky et al., 2011).

In 2012, new record high temperatures at 20 m depth were measured at most permafrost observatories on the North Slope of Alaska, i.e., north of the Brooks Range, where measurements began in the late 1970s (**Fig. 5.22b**). The exceptions were West Dock and Deadhorse, where temperatures in 2012 were the same as the record-high temperatures observed in 2011. Record high temperatures were also observed in 2012 in the Brooks Range (Chandalar Shelf) and in its southern foothills (Coldfoot). These distinct patterns of permafrost warming on the North Slope and a slight cooling in the Alaska Interior in 2010-2011 are in good agreement with air temperature patterns observed in the Arctic and the sub-Arctic (see the essay on *Air Temperature, Atmospheric Circulation and Clouds*) and might also be a result of snow distribution variations (see the *Snow* essay for more information on changing snow cover).

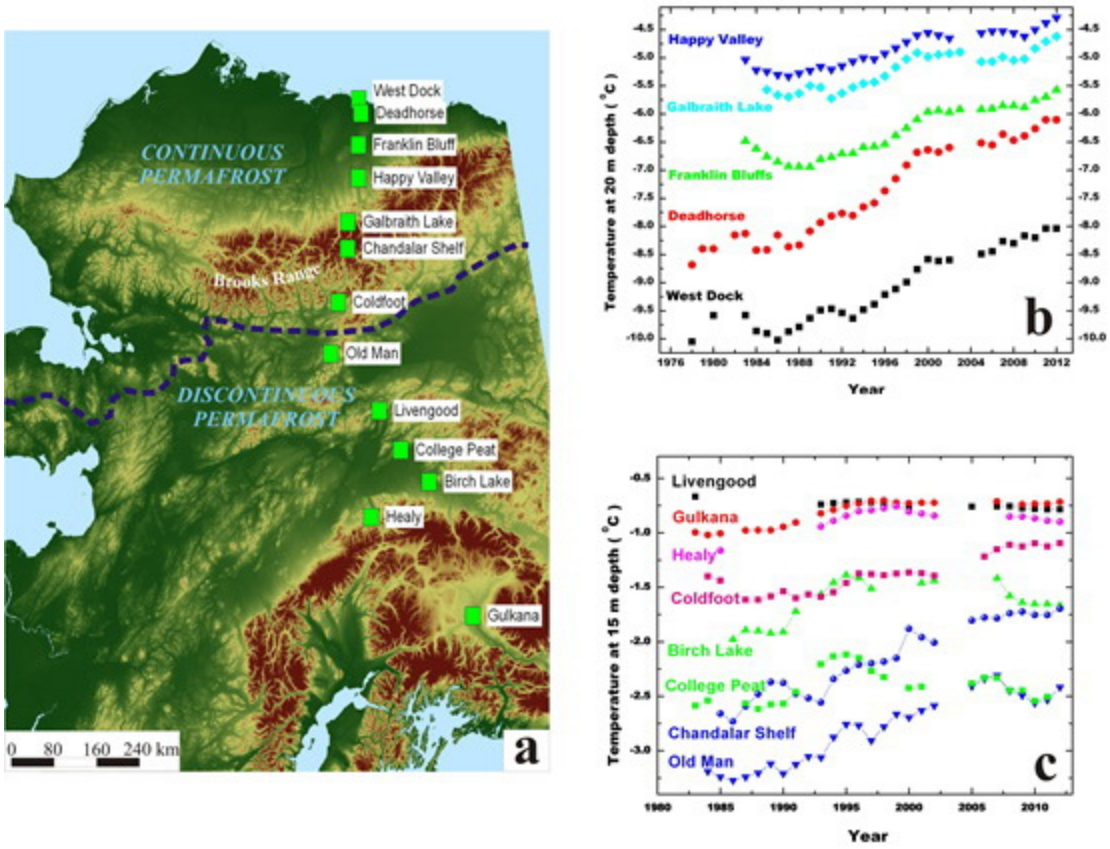

Fig. 5.22. Time series of annual permafrost temperatures (b and c) measured from north to south across Alaska (a) in the continuous and discontinuous permafrost zones.

A similar temperature increase in colder permafrost during the last 40 years in northwest Canada was determined by comparison of measurements made between 2003 and 2007 with those made in the late 1960s and early 1970s (Burn and Kokelj, 2009). In the discontinuous zone of western Canada, the increase in permafrost temperature continues to be small, e.g., not exceeding 0.2°C per decade in the central and southern Mackenzie Valley (**Fig. 5.23**, Norman Wells and Wrigley) (Smith et al., 2010; Derksen et al. 2012). In the eastern and high Canadian Arctic, greater warming has been observed, and since 2000 there has continued to be a steady increase in permafrost temperature (**Fig. 5.23**, Alert). Significant increases in winter air temperature appear to be largely responsible for the recent increases in permafrost temperature in northern Canada, particularly at polar desert sites where snow cover is minimal (Smith et al., 2012). These changes in permafrost conditions are consistent with the recent observed reduction in spatial extent and mass of the cryosphere across the Canadian Arctic (Derksen et al., 2012).

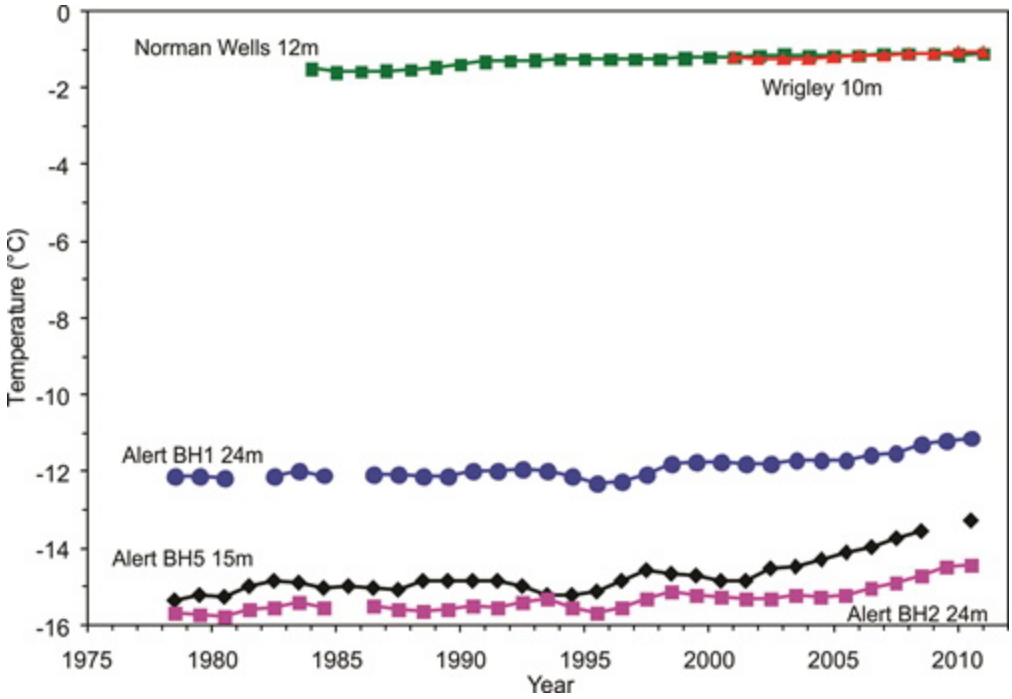

Fig. 5.23. Time series of mean annual permafrost temperature at 12 m depth at Norman Wells and Wrigley in the discontinuous permafrost zone of the central Mackenzie Valley, Northwest Territories, Canada and at 15 m and 24 m depth at CFS Alert, Nunavut, Canada (updated from Smith et al., 2010, 2012). The method described in Smith et al. (2012) was used to address gaps in the data record and produce a standardized record of mean annual ground temperature. Note the large temperature difference between the low (a) and high (b) latitude sites.

Permafrost temperature has increased by 1°C to 2°C in northern Russia during the last 30 to 35 years (Oberman, 2008; Romanovsky et al., 2010b; Drozdov et al., 2012). An especially noticeable temperature increase was observed during the late 2000s in the Russian Arctic, where the mean annual temperature at 15 m depth increased by >0.35°C in the Tiksi area and by 0.3°C at 10 m depth in the north of European Russia during 2006-2009. However, relatively low air temperatures during summer 2009 and the following winter of 2009-2010 interrupted the warming trend at many locations in the Russian Arctic, especially in the western sector. Nevertheless, many sites in East Siberia show continuous increase in permafrost temperatures at 15 to 25 m depth (**Fig. 5.24**; Kholodov et al., 2012).

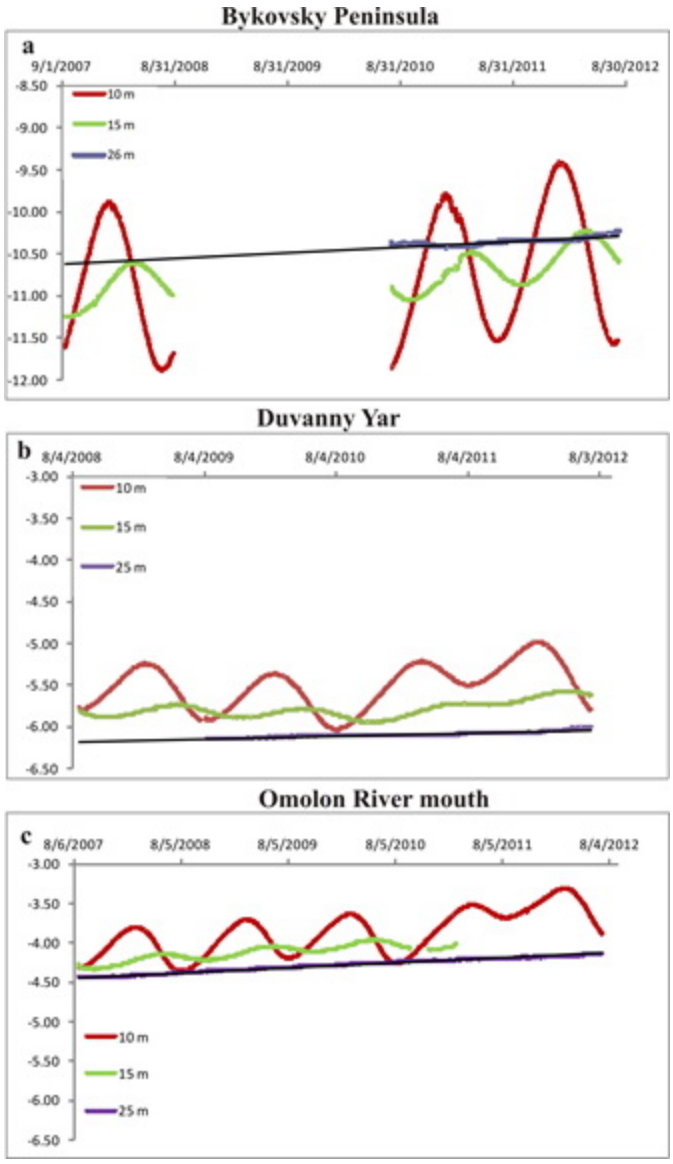

Fig. 5.24. Time series of permafrost temperatures at observation sites located in tundra (a) and boreal forest (b and c) eco-zones in East Siberia. Note that the temperature range on the y-axis of (b) and c) is the same and narrower than (a). Figure updated from Kholodov et al. (2012).

A common feature at Alaskan, Canadian and Russian sites is greater warming in relatively cold permafrost than in warm permafrost in the same geographical area (Romanovsky et al., 2010a). With a long-term warming at the ground surface, more constituent ice in fine-grained frozen sediment turns into water in the upper 5 to 15 m of permafrost, with little effect on permafrost temperature (Romanovsky and Osterkamp, 2000). In contrast, temperatures in colder permafrost are much more responsive to changes in temperature at the ground surface. This difference in the rate of permafrost warming is responsible for the fact that permafrost temperatures at such distant sites in Alaska as Chandalar Shelf in the Brooks Range and Birch Lake in Interior Alaska, which are 445 km apart, now have exactly the same permafrost temperatures. Another such example is the Old Man and College Peat sites, which are 225 km apart (**Fig. 5.22**).

In the Nordic area, including Greenland, most permafrost temperature monitoring sites were established during IPY 2007-2009 (Christiansen et al., 2010). There are only a few sites with moderately long records dating back to the late 1990s. The latter also show a recent decadal warming, of 0.04 to 0.07ºC/yr, in the highlands of southern Norway, northern Sweden and Svalbard, with the largest warming in Svalbard and in northern Scandinavia (Isaksen et al, 2011; Christiansen et al., 2010).

Long-term observations of changes in active-layer thickness (ALT) are less conclusive. Thaw depth observations exhibit substantial inter-annual fluctuations, primarily in response to variations in summer air temperature (e.g., Smith et al. 2009; Popova and Shmakin, 2009). Decadal trends in ALT vary by region. (Shiklomanov et al., 2012).

A progressive increase in ALT has been observed in some Nordic countries, e.g., in the Abisko area of Sweden since the 1970s, with a faster rate after 1995 that resulted in disappearance of permafrost in several mire landscapes (e.g., Åkerman and Johansson, 2008; Callaghan et al., 2010). This increase in thaw propagation ceased during 2007-2010, coincident with drier summer conditions (Christiansen et al., 2010). Increases in ALT since the late 1990s have been observed on Svalbard and Greenland, but these are not spatially and temporarily uniform (Christiansen et al., 2010).

Increase in ALT during the last fifteen years has been observed in the north of European Russia (Drozdov et al., 2012; Kaverin et al., 2012), in the north of East Siberia (Fyodorov-Davydov et al., 2008) and in Chukotka (Zamolodchikov, 2008), but ALT was relatively stable in the northern regions of West Siberia (**Fig. 5.25**).

Active-layer trends are different for North American sites, where a progressive increase of ALT is evident only at sites in Interior Alaska; there, the maximum ALT for the 18-year observation period occurred in 2007 (**Fig. 5.25**). Active-layer thickness on the North Slope of Alaska is relatively stable, without pronounced trends during 1995-2008 (Streletskiy et al., 2008; Shiklomanov et al., 2010). Similar results are reported from the western Canadian Arctic. Smith et al. (2009) found no definite trend in the Mackenzie Valley during the last 15 years, with some decrease in ALT following a maximum in 1998. Although an 8 cm increase in thaw depth was observed between 1983 and 2008 in the northern Mackenzie region, shallower thaw has been observed since 1998 (Burn and Kokelj, 2009). In the eastern Canadian Arctic, ALT has increased since the mid-1990s, with the largest increase occurring in bedrock of the discontinuous permafrost zone (Smith et al., 2010).

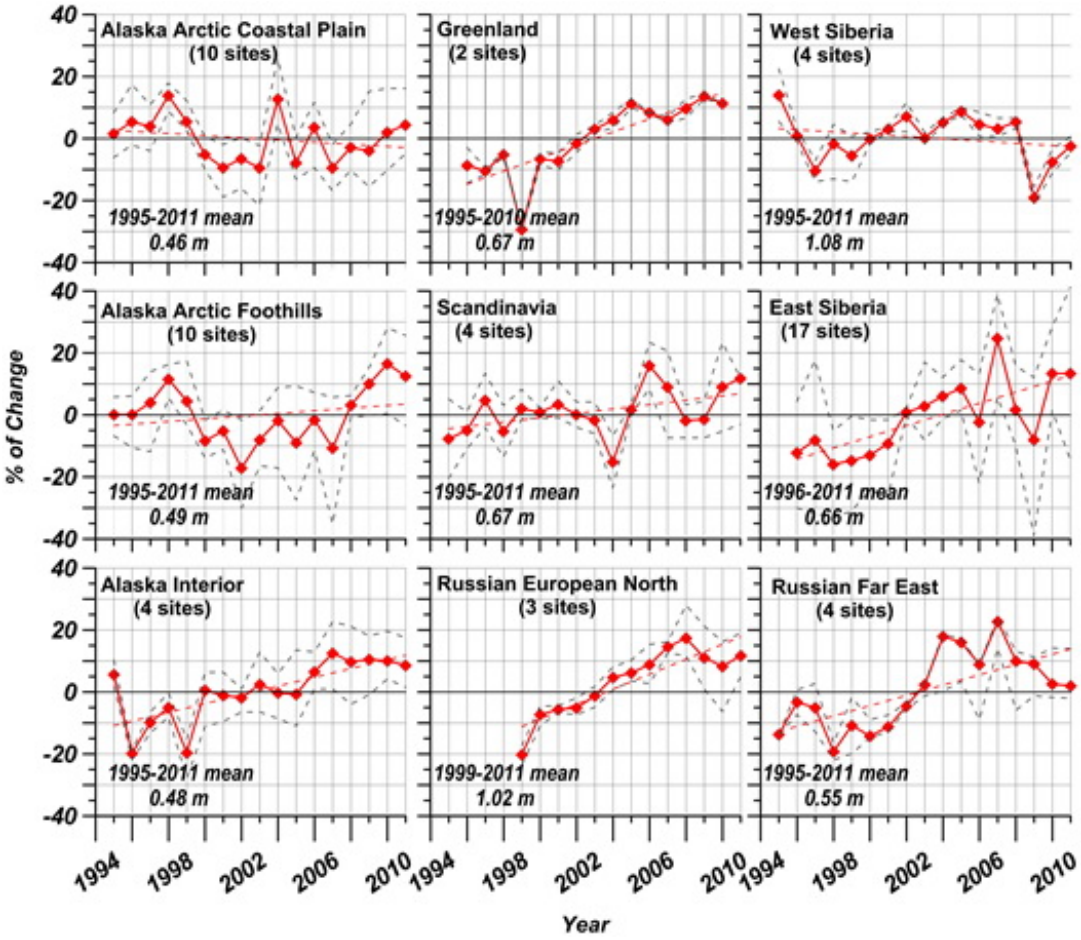

Fig. 5.25. Active-layer change in nine different Arctic regions according to the Circumpolar Active Layer Monitoring (CALM) program. The data are presented as annual percentage deviations from the mean value for the period of observations (indicated in each graph). Solid red lines show mean values. Dashed grey lines represent maximum and minimum values. Thaw depth observations from the end of the thawing season were used. Availability of at least ten years of continuous thaw depth observations through to the 2011 thawing season was the only criterion for site selection. For Greenland sites, 2011 data are not available. The number of CALM sites within each region varies and is indicated in each graph. Figure updated from Shiklomanov et al. (2012).

The last 30 years of ground warming have resulted in the thawing of permafrost in areas of discontinuous permafrost in Russia (Oberman, 2008; Romanovsky et al., 2010b). This is evidenced by changes in the depth and number of taliks (a sub-surface layer of year-round unfrozen ground within permafrost), especially in sandy and sandy loam sediments compared to clay. A massive development of new closed taliks in the southern continuous permafrost zone, resulting from increased snow cover and warming permafrost, was responsible for the observed northward movement by several tens of kilometers of the boundary between continuous and discontinuous permafrost (Oberman and Shesler, 2009; Romanovsky et al., 2010b). The frequently-reported long-term permafrost thawing in the Central Yakutian area around the city of Yakutsk is directly related to natural (forest fire) or anthropogenic (agricultural activities, construction sites) disturbances (Fedorov and Konstantinov, 2008) and are not significantly correlated with climate (Romanovsky et al., 2010b).

References

Åkerman, H. J. and M. Johansson. 2008. Thawing permafrost and thicker active layers in sub-arctic Sweden. *Permafr. Periglac. Process.*, 19, 279-292. doi:10.1002/ppp.626.

Brown J., A. Kholodov V. Romanovsky K. Yoshikawa S. Smith H. Christiansen, G. Viera and J. Noetzli. 2010. The Thermal State of Permafrost: the IPY-IPA snapshot (2007-2009). In *Proceedings of the 63rd Canadian Geotechnical Conference & 6th Canadian Permafrost Conference*, Calgary, Canada, September 2010, 12-16, 6 pp.

Burn C. R. and S. V. Kokelj. 2009. The environment and permafrost of the Mackenzie Delta area. *Permafr. Periglac. Process.*, 20(2), 83-105, doi: 10.1002/ppp.655.

Callaghan, T. V., F. Bergholm, T. R. Christensen, C. Jonasson, U. Kokfelt and M. Johansson. 2010. A new climate era in the sub-Arctic: Accelerating climate changes and multiple impacts. *Geophys. Res. Lett.*, 37, L14705, doi:10.1029/2009GL042064.

Christiansen, H. H., B. Etzelmüller, K. Isaksen, H. Juliussen, H. Farbrot, O. Humlum, M. Johansson, T. Ingeman-Nielsen, L. Kristensen, J. Hjort, P. Holmlund, A. B. K. Sannel, C. Sigsgaard, H. J. Åkerman, N. Foged, L. H. Blikra, M. A. Pernosky and R. Ødegård. 2010. The Thermal State of Permafrost in the Nordic area during the International Polar Year. *Permafr. Periglac. Process.*, 21, 156-181, doi: 10.1002/ppp.687.

Derksen, C., S. L. Smith, M. Sharp, L. Brown, S. Howell, L. Copland, D. R. Mueller, Y. Gauthier, C. Fletcher, A. Tivy, M. Bernier, J. Bourgeois, R. Brown, C. R. Burn, C. Duguay, P. Kushner, A. Langlois, A. G. Lewkowicz, A. Royer and A. Walker. 2012. Variability and change in the Canadian cryosphere. *Climatic Change*, 115, 59-88. doi:10.1007/s10584-012-0470-0.

Drozdov, D. S., G. V. Malkova, N. G. Ukraintseva and Yu. V. Korostelev. 2012, Permafrost Monitoring of Southern Tundra Landscapes in the Russian European North and West Siberia. *Proceedings of the 10th International Conference on Permafrost, Salekhard, Russia, June 25 - 29, 2012*, Vol. 2, 65-70.

Fedorov A. N, and P. Y. Konstantinov. 2008. Recent changes in ground temperature and the effect on permafrost landscapes in Central Yakutia. *Proceedings of the 9th International Conference on Permafrost*, D. L. Kane and K. M. Hinkel (eds), June 29-July 3, Fairbanks, Alaska, Institute of Northern Engineering, University of Alaska Fairbanks, vol. 1, 433-438.

Fyodorov-Davydov, D. G., A. L. Kholodov, V. E. Ostroumov, G. N. Kraev, V. A. Sorokovikov, S. P. Davydov and A. A. Merekalova. 2008. Seasonal Thaw of Soils in the North Yakutian Ecosystems. *Proceedings of the 9th International Conference on Permafrost*, D. L. Kane and K. M. Hinkel (eds), June 29-July 3, Fairbanks, Alaska, Institute of Northern Engineering, University of Alaska Fairbanks, vol. 1, 481-486.

Isaksen, K., R. S. Oedegård, B. Etzelmüller, C. Hilbich, C. Hauck, H. Farbrot, T. Eiken, H.O. Hygen and T. F. Hipp. 2011. Degrading mountain permafrost in southern Norway: spatial and temporal variability of mean ground temperatures, 1999-2009. *Permafr. Periglac. Process.*, 22(4), 361-377, doi: 10.1002/ppp.728.

Jorgenson, M. T, V. E. Romanovsky, J. Harden, Y. L. Shur, J. O'Donnell, T. Schuur and M. Kanevskiy. 2010. Resilience and vulnerability of permafrost to climate change. *Can. J. Forest Res.*, 40, 1219-1236, doi:10.1139/X10-060.

Kaverin, D., G. Mazhitova, A. Pastukhov and F. Rivkin. 2012. The Transition Layer in Permafrost-Affected Soils, Northeast European Russia. *Proceedings of the 10th International Conference on Permafrost*, K. M. Hinkel (ed.), Salekhard, Yamal-Nenets Autonomous District, Russia. The Northern Publisher Salekhard, vol. 2, 145-148.

Kholodov, A., D. Gilichinsky, V. Ostroumov, V. Sorokovikov, A. Abramov, S. Davydov and V. Romanovsky. 2012. Regional and local variability of modern natural changes in permafrost temperature in the Yakutia coastal lowlands, northeastern Siberia. *Proceedings of the 10th International Conference on Permafrost*, K. M. Hinkel (ed.), Salekhard, Yamal-Nenets Autonomous District, Russia. The Northern Publisher Salekhard, vol. 1, pp. 203-208.

Lewkowicz, A. G., P. P. Bonnaventure, S. L. Smith and Z. Kuntz. 2012. Spatial and thermal characteristics of mountain permafrost, northwest Canada. *Geogr. Annaler, Series A Physical Geography*, 94, 195-215, doi: 10.1111/j.1468-0459.2012.00462.x.

Lewkowicz, A. G., B. Etzelmüller and S. L Smith. 2011. Characteristics of discontinuous permafrost from ground temperature measurements and electrical resistivity tomography, southern Yukon, Canada. *Permafr. Periglac. Process.*, 22(4), 320-342, doi: 10.1002/ppp.703.

Lewkowicz, A. G. and P. P. Bonnaventure. 2011. Equivalent elevation: A new method to incorporate variable surface lapse rates into mountain permafrost modelling. *Permafr. Periglac. Process.*, 22(4), 153-162, doi: 10.1002/ppp.720.

Oberman, N. G. 2008. Contemporary permafrost degradation of northern European Russia. *Proceedings of the 9th International Conference on Permafrost*, D. L. Kane and K. M. Hinkel (eds.), June 29-July 3, Fairbanks, Alaska, Institute of Northern Engineering, University of Alaska Fairbanks, vol. 2, 1305-1310.

Oberman, N. G. and I. G. Shesler, 2009. Observed and projected changes in permafrost conditions within the European north-east of the Russian Federation. Problemy Severa I Arctiki Rossiiskoy Federacii (Problems and Challenges of the North and the Arctic of the Russian Federation), vol. 9, 96-106 (in Russian).

Osterkamp, T. E. 2008. Thermal state of permafrost in Alaska during the fourth quarter of the Twentieth Century (Plenary Paper). *Proceedings of the 9th International Conference on Permafrost*, D. L. Kane and K. M. Hinkel (eds.), June 29-July 3, Fairbanks, Alaska, Institute of Northern Engineering, University of Alaska Fairbanks, vol. 2, 1333-1338.

Popova, V. V. and A. B. Shmakin. 2009. The influence of seasonal climatic parameters on the permafrost thermal regime, West Siberia, Russia. *Permafr. Periglac. Process.*, 20, 41-56, doi:10.1002/ppp.640.

Romanovsky, V. E. and T. E. Osterkamp. 2000. Effects of unfrozen water on heat and mass transport processes in the active layer and permafrost. *Permafr. Periglac. Process.*, 11, 219-239.

Romanovsky, V. E., S. L. Smith and H. H. Christiansen. 2010a. Permafrost thermal state in the polar Northern Hemisphere during the International Polar Year 2007-2009: A synthesis. *Permafr. Periglac. Process.*, 21,106-116, doi: 10.1002/ppp.689.

Romanovsky, V. E., D. S. Drozdov, N. G. Oberman, G. V. Malkova, A. L. Kholodov, S. S. Marchenko, N. G. Moskalenko, D. O. Sergeev, N. G. Ukraintseva, A. A. Abramov, D. A. Gilichinsky and A. A. Vasiliev. 2010b. Thermal state of permafrost in Russia. *Permafr. Periglac. Process.*, 21,136-155, doi: 10.1002/ppp.683.

Romanovsky, V., N. Oberman, D. Drozdov, G. Malkova , A. Kholodov and S. Marchenko. 2011. Permafrost [in "State of the Climate in 2010"]. *Bull. Amer. Meteor. Soc.*, 92(6), S152-S153.

Shiklomanov, N. I., D. A. Streletskiy, F. E. Nelson, R. D. Hollister, V. E. Romanovsky, C. E. Tweedie, J. G. Bockheim and J. Brown. 2010. Decadal variations of active-layer thickness in moisture-controlled landscapes, Barrow, Alaska. *J. Geophys. Res.*, 115, G00I04, doi:10.1029/2009JG001248.

Shiklomanov N. I., D. A. Streletskiy and F. E. Nelson. 2012. Northern Hemisphere component of the global Circumpolar Active Layer Monitoring (CALM) Program. *Proceedings of the 10th International Conference on Permafrost*, K. M. Hinkel (ed.), Salekhard, Yamal-Nenets Autonomous District, Russia. The Northern Publisher Salekhard, vol. 1, 377-382.

Smith, S. L., S. A. Wolfe, D. W. Riseborough and F. M. Nixon. 2009. Active-layer characteristics and summer climatic indices, Mackenzie Valley, Northwest Territories, Canada. *Permafr. Periglac. Process.*, 20, 201-220, doi:10.1002/ppp.651.

Smith, S. L., V. E. Romanovsky, A. G. Lewkowicz, C. R. Burn, M. Allard, G. D. Clow, K. Yoshikawa and J. Throop. 2010. Thermal state of permafrost in North America - A contribution to the International Polar Year. *Permafr. Periglac. Process.*, 21,117-135.

Smith, S.L., J. Throop and A. G. Lewkowicz. 2012. Recent changes in climate and permafrost temperatures at forested and polar desert sites in northern Canada. *Can. J. Earth Sci.*, 49, 914-924, doi:10.1139/e2012-019.

Streletskiy D. A, N. I. Shiklomanov, F. E. Nelson and A. E. Klene. 2008. 13 years of observations at Alaskan CALM sites: Long-term active layer and ground surface temperature trends. *Proceedings of the 9th International Conference on Permafrost*, D. L. Kane and K. M. Hinkel (eds.), June 29-July 3, Fairbanks, Alaska, Institute of Northern Engineering, University of Alaska Fairbanks, vol. 2, 1727-1732.

Zamolodchikov, D. 2008. Recent climate and active layer changes in northeast Russia: Regional output of Circumpolar Active Layer Monitoring (CALM). *Proceedings of the 9th International Conference on Permafrost*, D. L. Kane and K. M. Hinkel (eds.), June 29-July 3, Fairbanks, Alaska, Institute of Northern Engineering, University of Alaska Fairbanks, vol. 2, 2021-2027.